Hot Topics in Acute Care Sugery and Trauma

Fausto Catena
Salomone Di Saverio
Luca Ansaloni
Federico Coccolini
Massimo Sartelli *Editors*

CT Scan in Abdominal Emergency Surgery

Springer

Hot Topics in Acute Care Surgery and Trauma

This series covers the most debate dissues in acute care and trauma surgery, from perioperative management to organizational and health policy issues. Since 2011, the founder members ofthe World Society of Emergency Surgery's (WSES) Acute Care and Trauma Surgeons group, who endorse the series, realized the need to provide more educational tools for young surgeons in training and for general physicians and other specialists new to this discipline: WSES is currently developing a systematic scientific and educational program founded on evidence-based medicine and objective experience. Covering the complex management of acute trauma and non-trauma surgical patients, this series makes a significant contribution to this program and is a valuable resource for both trainees and practitioners in acute care surgery.

More information about this series at http://www.springer.com/series/15718

Fausto Catena • Salomone Di Saverio
Luca Ansaloni • Federico Coccolini
Massimo Sartelli
Editors

CT Scan in Abdominal Emergency Surgery

Springer

Editors
Fausto Catena
Emergency and Trauma Surgery
Ospedale Maggiore di Parma Emergency and Trauma Surgery
Parma, Parma, Italy

Luca Ansaloni
General, Emergency and Trauma Surgery
Department Bufalini Hospital
Cesena, Italy

Massimo Sartelli
Department of Surgery Macerata Hospital
Macerata, Italy

Salomone Di Saverio
Cambridge Colorectal Unit
Cambridge University Hospitals NHS Foundation Trust
Addenbrooke's Hospital
Cambridge, UK

Federico Coccolini
General, Emergency and Trauma Surgery
Department
Bufalini Hospital
Cesena, Italy

ISSN 2520-8284 ISSN 2520-8292 (electronic)
Hot Topics in Acute Care Surgery and Trauma
ISBN 978-3-319-48346-7 ISBN 978-3-319-48347-4 (eBook)
https://doi.org/10.1007/978-3-319-48347-4

Library of Congress Control Number: 2017960211

Printed on acid-free paper

This Springer imprint is published by the registered company Springer International Publishing AG part of Springer Nature
The registered company address is: Gewerbestrasse 11, 6330 Cham, Switzerland

To my wife Rita and to my sons Guglielmo and Lodovico for the time stolen from them and devoted to work

Foreword to the Series

Since 2011, the founding members of the World Society of Emergency Surgery's (WSES) Acute Care and Trauma Surgeons group, in collaboration with the American Association for the Surgery for Trauma (AAST), endorse the development and publication of the "Hot Topics in Acute Care Surgery and Trauma," realizing the need to provide more educational tools for young surgeons in training and for general physicians and other surgical specialists new to this discipline. These new forthcoming titles have been selected and prepared with this philosophy in mind. In particular, *CT Scan in Abdominal Emergency Surgery* focuses on the diagnostic impact of CT scans in severe abdominal trauma and in nontraumatic acute abdomen, the two clinical entities that constitute the main reasons for referrals to this imaging technique in emergency. The concept behind this practical book is that emergency surgeons and physicians not only need the clinical knowledge to manage the different acute pathological conditions but they must also have a full understanding of diagnostic imaging modalities. Each chapter includes a description of a specific acute abdominal disorder: in addition to the clinical presentation and to the diagnosis and management guidelines, the readers will find a special focus on imaging studies with clear and concise descriptions. This book is a useful tool to achieve a strong background to understand CT scans and to perform right diagnosis with proper conservative or surgical treatments.

Cesena, Italy — Federico Coccolini
Riverside, CA — Raul Coimbra
Calgary, AB, Canada — Andrew W. Kirkpatrick
Cambridge, UK — Salomone Di Saverio

Preface

In the past era, the science of emergency surgery was a completely different one without CT scans. We used to perform a good number of diagnostic laparotomies, and plain abdomen X-ray was the most used diagnostic test. Nowadays, plain abdomen X-ray is seldom used, and diagnostic laparoscopy has taken the place of diagnostic laparotomy.

CT scan is the "king" of emergency surgery diagnosis and the only barrier between clinical examination and diagnostic laparoscopy—as a matter of fact, CT scan is the fundamental tool in emergency surgery. According to the WSES Guidelines, CT scan is the test with the highest sensitivity and specificity in intra-abdominal infections. It is therefore mandatory for any surgeon/physician dealing with emergency surgery patients to have a specific expertise to read CT images.

This book focuses on the diagnostic impact of CT scans in severe abdominal trauma and in nontraumatic acute abdomen, the two clinical entities that constitute the main reasons for referrals to this imaging technique in emergency. The concept behind this practical book is that emergency surgeons and physicians not only need the clinical knowledge to manage the different acute pathological conditions but they must also have a full understanding of diagnostic imaging modalities.

To this end, each chapter includes a description of a specific acute abdominal disorder: in addition to the clinical presentation and to the diagnosis and management guidelines, the readers will find a special focus on imaging studies with clear and concise descriptions. Evolution and grading scales will also be included for the interpretation and high-quality images.

This easy-to-read book is not only an ideal source of practical information for acute care surgeons, radiologists, physicians, and for all the members of the emergency team, but also a useful tool to understand CT scans and to perform right diagnosis with proper conservative or surgical treatments.

Enjoy the reading …

Parma, Italy — Fausto Catena
Cambridge, UK — Salomone Di Saverio
Cesena, Italy — Luca Ansaloni
Cesena, Italy — Federico Coccolini
Macerata, Italy — Massimo Sartelli

Contents

Diagnostic Tools in ACS: CT Scan, Diagnostic Laparoscopy, and Exploratory Laparotomy

1

Ning Lu and Walter L. Biffl

1.1 Introduction

The abdomen is a black box of diagnostic uncertainty. There is an old surgical adage that goes "never let the skin come between you and the diagnosis." However, it is just that: an old adage. The surgeon has many alternatives to employ in situations in which the clinical diagnoses, or decision to operate, are not straightforward. In this chapter, three primary modalities are discussed: computed tomography (CT) scanning, diagnostic laparoscopy (DL), and exploratory laparotomy (LAP).

1.2 CT Scanning

The CT scan is an exceedingly valuable tool for the diagnosis of essentially any abdominal surgical problem. A CT scan can quickly and accurately demonstrate any number of pathologies while ruling out others, allowing the surgeon to narrow the list of differential diagnoses and plan definitive management strategies. It is noninvasive, rapid, and nearly universally available and has been insinuated into myriad clinical care guidelines for surgical problems. The ability to grade the severity of pathology prior to operating allows the surgeon to tailor the approach to the situation and to counsel the patient regarding expectations more accurately.

N. Lu, M.D.
Hawaii Residency Program in General Surgery, Honolulu, HI, USA

W.L. Biffl, M.D. (✉)
Acute Care Surgery, The Queen's Medical Center, Honolulu, HI, USA

Department of Surgery, John A. Burns School of Medicine, University of Hawaii—Manoa, Honolulu, HI, USA
e-mail: walt@biffl.com

F. Catena et al. (eds.), *CT Scan in Abdominal Emergency Surgery*, Hot Topics in Acute Care Surgery and Trauma, https://doi.org/10.1007/978-3-319-48347-4_1

1.2.1 Perforated Gastroduodenal Ulcers

CT is 95% sensitive and 93% specific for diagnosing gastroduodenal perforation. In addition to identifying free air, signs of peri-duodenal fat stranding, wall defect/ulcer, and wall thickening can be seen 72–89% of the time [1]. However, these other signs may not be visible before at least 6 h of symptomatology [2].

1.2.2 Cholecystitis

Ultrasonography is the accepted standard for detecting cholelithiasis and diagnosing acute calculous cholecystitis. CT can detect gallstones only 50% of the time, but in patients with equivocal ultrasounds, CT can demonstrate wall thickening, pericholecystic stranding, and pericholecystic fluid [3–5]. CT is also valuable in identifying complications of cholecystitis, including emphysematous, hemorrhagic, or perforated cholecystitis [6].

1.2.3 Choledocholithiasis

CT has a diagnostic sensitivity ranging from 56.5 to 81% and a specificity ranging from 72.8% to 96%. Thus, it is not the initial imaging study of choice for patients suspected of choledocholithiasis [7, 8]. On the other hand, CT can accurately and reliably identify common bile duct dilation.

1.2.4 Pancreatitis

CT has a 92% sensitivity and 100% specificity in identifying acute pancreatitis. It is 80–90% accurate with a 90% sensitivity and 33% specificity in identifying pancreatic necrosis [9–11]. In addition, CT imaging allows classification of pancreatitis per Atlanta and revised Atlanta Classification [12, 13].

1.2.5 Small Bowel Obstruction

CT is able to diagnose complete bowel obstruction with a sensitivity of 92% (81–100%) and a specificity of 93% (68–100%). CT is able to diagnose intestinal ischemia with 83% (63–100%) sensitivity and 92% (61–100%) specificity [14, 15]. CT has great value in patients with inconclusive plain films and can be helpful in determining the likely etiology of the obstruction, whether it is due to hernias, adhesions, or malignancy [16].

1.2.6 Mesenteric Ischemia

CT angiography is rapid and noninvasive for diagnosis of acute mesenteric ischemia and its multiple etiologies (arterial thrombosis, arterial embolism, mesenteric vein thrombosis, and nonocclusive ischemia), with a sensitivity and specificity of 96% and 94%, respectively [17]. CT angiography in nonocclusive mesenteric ischemia will demonstrate no signs of arterial or venous occlusion, may demonstrate vascular spasm, and may demonstrate more diffuse nonconsecutive segments of bowel with signs of ischemia. However, after ruling out vascular occlusive disease, diagnosing nonocclusive mesenteric ischemia still requires a high clinical suspicion [18]. The ability to differentiate the multiple etiologies of mesenteric ischemia is critical as the treatment for each can vary.

1.2.7 Appendicitis

CT is 91% sensitive and 90% specific for diagnosing acute appendicitis. For those suspected of having appendicitis, there is clear benefit to the use of IV, but not oral contrast [19]. In addition, CT can grade the severity of appendicitis (inflamed, perforated with localized free fluid, perforated with regional abscess, perforated with diffuse peritonitis) [20]. The grading of appendicitis can allow for appropriate treatment plans, which may be operative or via IR drainage.

1.2.7.1 Diverticulitis

CT is 94% sensitive and 99% specific in the diagnosis of acute diverticulitis [21]. In addition to identifying the absence or presence of perforation, CT allows for Hinchey classification of perforated diverticulitis. This facilitates determination of whether hospitalization is required and selection of patients for medical vs. surgical therapy [22] (Table 1.1).

Table 1.1 Summary of CT in diagnosing intra-abdominal pathologies

Pathology	Sensitivity	Specificity	Grading/classification capability
Perforated gastroduodenal ulcers	95%	93%	
Cholecystitis	–	–	
Choledocholithiasis	56.5–81%	72.8–96%	
Pancreatitis	92%	100%	X
Pancreatic necrosis	90%	33%	
Small bowel obstruction	92% (81–100%)	93% (68–100%)	
Intestinal ischemia	83% (63–100%)	92% (61–100%)	
Mesenteric ischemia	96%	94%	X
Appendicitis	91%	90%	X
Diverticulitis	94%	99%	X

CT is, of course, not without risks. The average CT abdomen/pelvis with contrast has an estimated radiation dose of 10–30 and 3–10 mSv in pediatric patients. The average CT angiogram of the abdomen has an estimated radiation dose of 1–10 and 0.3–3 mSv in pediatric patients. When possible, the risks of radiation exposure are minimized in the pregnant and pediatric populations. Depending on the pathology, ultrasound and MRI are viable options with similar accuracy. In the pediatric population, ultrasound approaches the accuracy of CT in diagnosing appendicitis with a sensitivity of 88% and specificity of 94% [23]. In the pregnant population suspected of appendicitis, MRI has a sensitivity of 97% and specificity of 95% [24].

Most non-trauma patients are candidates for CT for diagnosis. It is not recommended for patients who are unstable and in extremis. For those with renal dysfunction, exposure to contrast agents should be minimized. There is a well-known risk of contrast-induced nephropathy.

1.3 Diagnostic Laparoscopy

Laparoscopy is increasingly used in the diagnosis and treatment of many intra-abdominal pathologies. Traditionally, patients admitted with acute abdominal pain of unclear origin are managed with observation (serial abdominal exams, laboratory tests, and/or repeat imaging), progressing to surgery only if signs of peritonitis develop. However, this can lead to delays in diagnosis. In certain populations (immunocompromised, morbidly obese, paraplegic/quadriplegic, sedated, comatose), the abdominal exam is not always reliable. In patients with a suspected acute abdomen or unexplained unrelenting acute abdominal pain, especially those with an unreliable exam, diagnostic laparoscopy may be invaluable. The diagnostic accuracy of laparoscopy is 90%–99.5% [25–30].

After a diagnosis is made, treatment can also be achieved laparoscopically in many instances with safety and efficacy. By avoiding laparotomy, the relatively higher morbidity can be avoided as well. In cases of acute cholecystitis and acute appendicitis, laparoscopic cholecystectomy and appendectomy are safe and effective, now becoming the standard of care (level I). For patients with Hinchey I–IV perforated diverticulitis, when colectomy is performed, laparoscopic colectomy (with or without Hartmann's procedure) has been performed successfully by expert laparoscopic groups. For patients with Hinchey III perforated diverticulitis, laparoscopic exploration with peritoneal lavage and drainage is an emerging therapeutic modality. Current recommendation for laparoscopic management of diverticulitis is level 3. For gastroduodenal perforations, laparoscopic management has been demonstrated to be safe and effective (level 1) [31]. In the case of adhesive small bowel obstruction, laparoscopy is an emerging therapy, which may be successful in hands of an experienced laparoscopic surgeon on a hemodynamically stable patient, in the absence of peritonitis or severe intra-abdominal sepsis, in patients with localized distension on imaging, in the absence of severe abdominal distention, in an anticipated single band, and in a low peritoneal adhesion index. The etiology of the obstruction can be determined with 96.9% accuracy, and treatment can be provided

without conversion to laparotomy in more than 50% of patients [16, 32, 33]. Minimally invasive necrosectomy is an emerging therapeutic option with less morbidity and mortality than open necrosectomy in the hands of experienced laparoscopic surgeons [34, 35].

Laparoscopy is contraindicated with patients known to have a "frozen abdomen," massive bowel distention, inability to tolerate pneumoperitoneum, uncorrectable coagulopathy, uncorrectable hypercapnia >50 torr, or hemodynamic instability [36]. Historically, laparoscopy was delayed until the second trimester to reduce the likelihood of complications including spontaneous abortions and preterm labor. However, recent studies show that it may be safe to perform laparoscopy during any trimester of pregnancy without increased risk to the mother or fetus. However, data on long-term effects to children is lacking [37].

Given the safety, efficacy, and accuracy of diagnostic laparoscopy, with the added ability to treat most diagnosed pathologies, laparoscopy should be considered in the majority of patients with an acute abdomen.

1.4 Exploratory Laparotomy

For those with suspected intra-abdominal pathologies, and certainly those with evidence of peritonitis, laparotomy is still the gold standard. Patients with an acute abdomen and a contraindication to laparoscopy require laparotomy. Especially critical in the decompensating patient, laparotomy has the ability to diagnose with absolute certainty and provide treatment of the disease. However, exploratory laparotomy has significantly higher morbidity (5–22%), compared to diagnostic laparoscopy. Thus, in stable patients without contraindications, a minimally invasive approach should be considered.

Conclusions

The three modalities—CT, DL, and LAP—are individually very accurate and thus frequently employed. Rather than consider them competitive, they are complementary tests that have major roles in acute care surgery.

References

1. Lee D, Park MH, Shin BS, Jeon GS. Multidetector CT diagnosis of non-traumatic gastroduodenal perforation. J Med Imaging Radiat Oncol. 2015;60(2):182–6.
2. Grassi R, Romagno S, Pinto A, Romano L. Gastro-duodenal perforations: conventional plain film, US and CT findings in 166 consecutive patients. Eur J Radiol. 2004;50(1):30–6.
3. Fidler J, Paulson EK. Layfield l. CT evaluation of acute cholecystitis: findings and usefulness in diagnosis. AJR Am J Roentgenol. 1996;166(5):1085.
4. Paulson EK. Acute cholecystitis: CT findings. Semin Ultrasound CT MR. 2000;21(1):56.
5. Bennett GL, Balthazar EJ. Ultrasound and CT evaluation of emergent gallbladder pathology. Radiol Clin North Am. 2003;41(6):1203–16.
6. Yarmish GM, Smith MP, Rosen MP, Baker ME, Blake MA, Cash BD, Hindman NM, Kamel IR, Kaur H, Nelson RC, Piorkowski RJ, Qayyum A, Tulchinsky M. ACR appropriateness criteria right upper quadrant pain. J Am Coll Radiol. 2014;11(3):316–22.

7. Tseng CW, Chen CC, Chen TS, Chang FY, Lin HC, Lee SD. Can computed tomography with coronal reconstruction improve the diagnosis of choledocholithiasis? J Gastroenterol Hepatol. 2008;23(10):1586.
8. Singh A, Mann HS, Thukral CL, Singh NR. Diagnostic accuracy of MRCP as compared to Ultrasound/CT in patients with obstructive jaundice. J Clin Diagn Res. 2014;8(3):103–7.
9. Balthazar EJ, Robinson DL, Megibow AJ, Ranson JH. Acute pancreatitis: value of CT in establishing prognosis. Radiology. 1990;174(2):331–6.
10. Clavien PA, Hauser H, Meyer P, Rohner A. Value of contrast-enhanced computerized tomography in the early diagnosis and prognosis of acute pancreatitis. A prospective study of 202 patients. Am J Surg. 1988;155(3):457–66.
11. Block S, Maier W, Bittner R, et al. Identification of pancreas necrosis in severe acute pancreatitis: imaging procedures versus clinical staging. Gut. 1986;27(9):1035–42.
12. Thoeni RF. The revised Atlanta classification of acute pancreatitis: its importance for the radiologist and its effect on treatment. Radiology. 2012;262(3):751–64.
13. Banks PA, Bollen TL, Dervenis C, Gooszen HG, Johnson CD, Sarr MG, Tsiotos GG, Vege SS, Acute Pancreatitis Classification Working Group. Classification of acute pancreatitis—2012: revision of the Atlanta classification and definitions by international consensus. Gut. 2013;62(1):102–11.
14. Zalcman M, Sy M, Donckier V, Closset J, Gansbeke DV. Helical CT signs in the diagnosis of intestinal ischemia in small-bowel obstruction. AJR Am J Roentgenol. 2000;175(6):1601–7.
15. Mallo RD, Salem L, Lalani T, Flum DR. Computed tomography diagnosis of ischemia and complete obstruction in small bowel obstruction: a systematic review. J Gastrointest Surg. 2005;9(5):690–4.
16. Di S, S CF, Galati M, Smerieri N, Biffl WL, Ansaloni L, Tugnoli G, Velmahos GC, Sartelli M, Bendinelli C, Fraga GP, Kelly MD, Moore FA, Mandalà V, Mandalà S, Masetti M, Jovine E, Pinna AD, Peitzman AB, Leppaniemi A, Sugarbaker PH, Goor HV, Moore EE, Jeekel J, Catena F. Bologna guidelines for diagnosis and management of adhesive small bowel obstruction (ASBO): 2013 update of the evidence-based guidelines from the World Society of Emergency Surgery ASBO Working Group. World J Emerg Surg. 2013;8(1):42.
17. Oliva IB, Davarpanah AH, Rybicki FJ, Desjardins B, Flamm SD, Francois CJ, Gerhard-Herman MD, Kalva SP, Ashraf Mansour M, Mohler ER 3rd, Schenker MP, Weiss C, Dill KE. ACR Appropriateness Criteria® imaging of mesenteric ischemia. Abdom Imaging. 2013;38(4):714–9.
18. R W, Nishimaki H, Fujii K, Kakita S, Hayakawa K. Usefulness of multidetector-row CT (MDCT) for the diagnosis of non-occlusive mesenteric ischemia (NOMI): assessment of morphology and diameter of the superior mesenteric artery (SMA) on multi-planar reconstructed (MPR) images. Eur J Radiol. 2010;76(1):96–102.
19. Garst GC, Moore EE, Banerjee MN, Leopold DK, Burlew CC, Bensard DD, Biffl WL, Barnett CC, Johnson JL, Sauaia A. Acute appendicitis: a disease severity score for the acute care surgeon. J Trauma Acute Care Surg. 2013;74(1):32–6.
20. Smith MP, Katz DS, Lalani T, Carucci LR, Cash BD, Kim DH, Piorkowski RJ, Small WC, Spottswood SE, Tulchinsky M, Yaghmai V, Yee J, Rosen MP. ACR Appropriateness Criteria® right lower quadrant pain—suspected appendicitis. Ultrasound Q. 2015;31:85–91.
21. Laméris W, van Randen A, Bipat S, Bossuyt PM, Boermeester MA, Stoker J. Graded compression ultrasonography and computed tomography in acute colonic diverticulitis: meta-analysis of test accuracy. Eur Radiol. 2008;18(11):2498–511.
22. Balfe DM, Levine MS, Ralls PW, Bree RL, DJ DS, Glick SN, Megibow AJ, Saini S, Shuman WP, Greene FL, Laine LA, Lillemoe K. Evaluation of left lower quadrant pain. American College of Radiology. ACR Appropriateness Criteria. Radiology. 2000;215 Suppl:167–71.
23. Doria AS, Moineddin R, Kellenberger CJ, et al. US or CT for diagnosis of appendicitis in children and adults? A meta-analysis. Radiology. 2006;241:83–94.
24. Barger RL Jr, Nandalur KR. Diagnostic performance of magnetic resonance imaging in the detection of appendicitis in adults: a meta-analysis. Acad Radiol. 2010;17(10):1211–6.

25. Gaitán HG, Reveiz L, Farquhar C, Elias VM. Laparoscopy for the management of acute lower abdominal pain in women of childbearing age. Cochrane Database Syst Rev. 2014;5:CD007683.
26. Schietroma M, Cappelli S, Carlei F, Pescosolido A, Lygidakis NJ, Amicucci G. "Acute abdomen": early laparoscopy or active laparotomic-laparoscopic observation? Hepatogastroenterology. 2007;54(76):1137–41.
27. Ates M, Coban S, Sevil S, Terzi A. The efficacy of laparoscopic surgery in patients with peritonitis. Surg Laparosc Endosc Percutan Tech. 2008;18(5):453–6.
28. Karamanakos SN, Sdralis E, Panagiotopoulos S, Kehagias I. Laparoscopy in the emergency setting: a retrospective review of 540 patients with acute abdominal pain. Surg Laparosc Endosc Percutan Tech. 2010;20(2):119–24.
29. Golash V, Willson PD. Early laparoscopy as a routine procedure in the management of acute abdominal pain: a review of 1,320 patients. Surg Endosc. 2005;19(7):882–5.
30. Kirshtein B, Roy-Shapira A, Lantsberg L, Mandel S, Avinoach E, Mizrahi S. The use of laparoscopy in abdominal emergencies. Surg Endosc. 2003;17(7):1118–24.
31. Coccolini F, Tranà C, Sartelli M, Catena F, Di Saverio S, Manfredi R, Montori G, Ceresoli M, Falcone C, Ansaloni L. Laparoscopic management of intra-abdominal infections: systematic review of the literature. World J Gastrointest Surg. 2015;7(8):160–9.
32. Coccolini F, Ansaloni L, Manfredi R, Campanati L, Poiasina E, Bertoli P, Capponi MG, Sartelli M, Di Saverio S, Cucchi M, Lazzareschi D, Pisano M, Catena F. Peritoneal adhesion index (PAI): proposal of a score for the "ignored iceberg" of medicine and surgery. World J Emerg Surg. 2013;8(1):6.
33. Kirshtein B, Roy-Shapira A, Lantsberg L, Avinoach E, Mizrahi S. Laparoscopic management of acute small bowel obstruction. Surg Endosc. 2005;19(4):464–7.
34. Babu BI, Siriwardena AK. Current status of minimally invasive necrosectomy for post-inflammatory pancreatic necrosis. HPB (Oxford). 2009;11(2):96–102.
35. Butcher P, Pugin F, Morel P. Minimally invasive necrosectomy for infected necrotizing pancreatitis. Pancreas. 2008;36(2):113–9.
36. Hori Y, SAGES Guidelines Committee. Diagnostic laparoscopy guidelines: This guideline was prepared by the SAGES Guidelines Committee and reviewed and approved by the Board of Governors of the Society of American Gastrointestinal and Endoscopic Surgeons (SAGES), November 2007. Surg Endosc. 2008;22(5):1353–83.
37. Pearl J, Price R, Richardson W, Fanelli R, Society of American Gastrointestinal Endoscopic Surgeons. Guidelines for diagnosis, treatment, and use of laparoscopy for surgical problems during pregnancy. Surg Endosc. 2011;25(11):3479–92.

Hepatic Trauma

2

James L. Patrick, Juliana Tobler, Andrew B. Peitzman, and Biatta Sholosh

2.1 Introduction

Injury to the liver is one of the leading causes of death from abdominal trauma and is responsible for 5% of all trauma admissions [1]. The liver's relatively large size, fixed attachment points to the surrounding tissues, and friable parenchyma make it an easily injured organ in deceleration events such as motor vehicle accidents [2]. Because the liver occupies most of the right upper quadrant, it can be easily injured in direct blunt-force trauma or penetrating injury. The right lobe is more commonly injured because it represents most of the hepatic parenchyma, and because of its close proximity to the surrounding ribs and spine. Left hepatic lobe injuries are less common and are more likely the result of a direct blow to that region. The approximate ratio of blunt force to penetrating hepatic trauma is 3.5:1 [3].

Over the past 20 years, nonoperative management has become the treatment of choice for blunt force trauma in hemodynamically stable patients [4]. Many factors have improved the success of nonoperative management. More sophisticated imaging capabilities have played a significant role in patient management and clinical outcome. The purpose of this chapter is to discuss the current imaging modalities used in diagnosis and treatment of hepatic trauma with a focus on computed tomography (CT).

J.L. Patrick, M.D. • J. Tobler, M.D. • B. Sholosh, M.D.
Abdominal Imaging Section, Department of Radiology, University of Pittsburgh School of Medicine, Pittsburgh, PA, USA

A.B. Peitzman (✉)
Department of Surgery, University of Pittsburgh School of Medicine, Pittsburgh, PA, USA
e-mail: peitzmanab@msx.upmc.edu

F. Catena et al. (eds.), *CT Scan in Abdominal Emergency Surgery*, Hot Topics in Acute Care Surgery and Trauma, https://doi.org/10.1007/978-3-319-48347-4_2

2.2 Diagnostic Imaging in Liver Trauma

2.2.1 FAST

Focused assessment with sonography for trauma (FAST) is a focused ultrasound examination performed solely to identifying the presence of free fluid indicating potentially life-threatening intra-abdominal hemorrhage or pericardial tamponade. FAST consists of ultrasound evaluation of 5 spaces in the supine position: pericardial, perihepatic, perisplenic, Morrison's pouch, and retrovesicular space. The advantages of ultrasound are that it is quick and repeatable with a high sensitivity and specificity (80–85% and 97–100%, respectively). The limitations of the study include operator dependence, and it may be difficult to perform in patients who are obese or have overlying bowel gas or subcutaneous emphysema [5]. Ultrasound will detect 400 mL or more of intraperitoneal fluid, and a positive FAST is invaluable in the triage of an unstable patient [5].

2.3 Noncontrast CT

Evaluation for overt visceral trauma is possible with noncontrast CT when hemoperitoneum or pneumoperitoneum are identified. Additionally, a high-density clot or "sentinel clot" may be demonstrated, suggesting the underlying source of hemorrhage. While noncontrast CT provides some information, intravenous contrast-enhanced CT is necessary to evaluate for vascular injury; identify infarcted or devascularized hepatic tissue and is more sensitive to determine extent of visceral injury. Noncontrast CT is not recommended for patients who can receive IV contrast because of its lack of sensitivity [5].

2.4 Contrast-Enhanced CT

In the past 20 years, multidetector contrast-enhanced CT has become the imaging modality of choice for the evaluation of visceral injury in the abdomen and pelvis. CT is noninvasive with a high sensitivity (99%) and specificity (96.8%) in the detection of traumatic liver lesions [6]. At large trauma facilities, a biphasic technique is generally employed in which an arterial phase of the chest and upper abdomen are obtained with an overlapping CT portal venous phase of the abdomen and pelvis. Biphasic technique has been demonstrated to be superior to a single portal venous phase for the detection of blunt force trauma [7]. Water soluble oral contrast is not generally administered in the trauma setting, but it may be utilized on a follow up CT obtained 6–12 h later if the initial CT was suspicious for gastrointestinal injury [8].

2.5 Acute Imaging Findings on Contrast-Enhanced CT

Hepatic parenchymal injury includes hepatic contusions, lacerations, and infarction. In addition, there are several vascular injuries that can occur within the liver. These include posttraumatic pseudoaneurysm and post-traumatic arteriovenous fistula, which represent contained vascular injury. It is important to differentiate these entities from active arterial or uncontained vascular injury more commonly referred to as "active extravasation" discussed later in the chapter.

2.6 Contusions

Hepatic contusions are common in the context of liver injury but are not included in the AAST liver grading system. On contrast-enhanced CT, they appear as low-density areas compared to the surrounding liver parenchyma and can be irregular in shape and size (Fig. 2.1). Small contusions can be difficult to differentiate from small lacerations, although this is not clinically significant. Contusions can either represent a crush injury or a deceleration shearing injury.

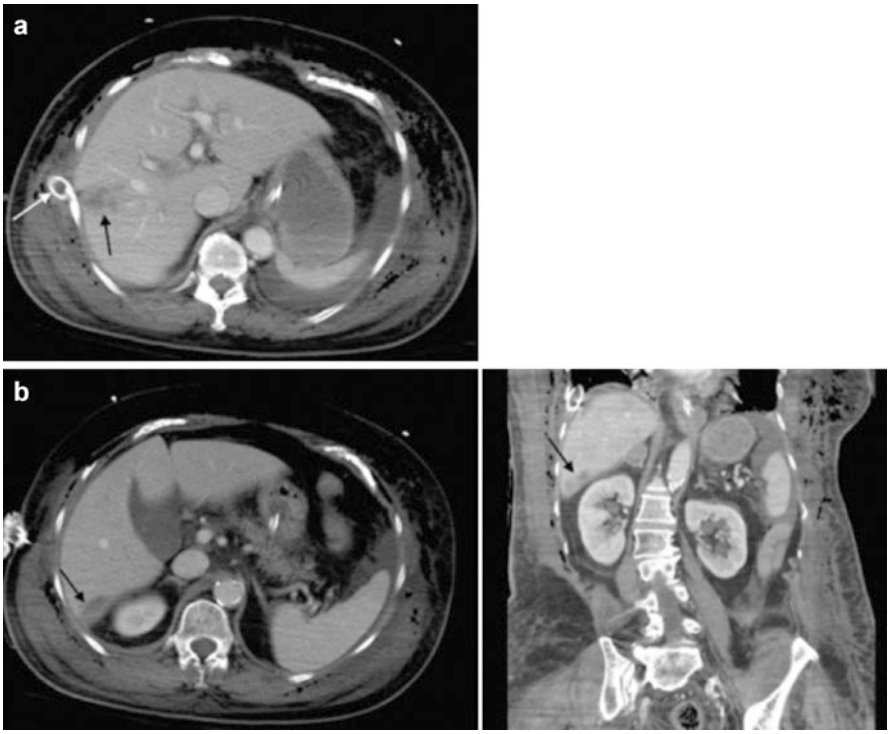

Fig. 2.1 A 72-year-old female involved in a motor vehicle accident. (**a**) There is a laceration of the right hepatic lobe (*black arrow*) which was not identified on the initial study and may be iatrogenic from the chest tube (*white arrow*) placement. (**b**) Hepatic contusion in the posterior right lobe adjacent to the right kidney (*black arrow*)

2.7 Lacerations

Lacerations are the most common traumatic liver injury. They are generally linear or branching, low-attenuation regions within the liver (Figs. 2.1a and 2.2). If a laceration extends to the liver capsule, careful inspection for extrahepatic hemorrhage should be performed (Fig. 2.3). Lacerations that extend into the liver hilum are more likely to be associated with biliary injury [9]. Lacerations that extend into the bare area of the liver, in the posterior right hepatic dome, can be present with isolated retroperitoneal hematomas [10]. On ultrasound, acute lacerations appear echogenic or heterogenous in linear or oblong areas. In the subacute phase, the laceration becomes more hypoechoic (Fig. 2.4).

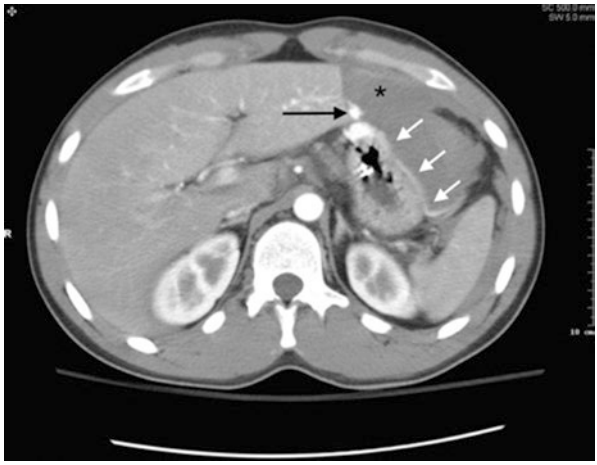

Fig. 2.2 A 22-year-old male stabbed in the left upper quadrant. There is complete transection of a portion of the left hepatic lobe, with active extravasation of contrast (*black arrow*) and hemoperitoneum. Note the contrast layering over the anterior aspect of the stomach (*white arrows*) and a small devascularized segment of the liver (*asterisk*)

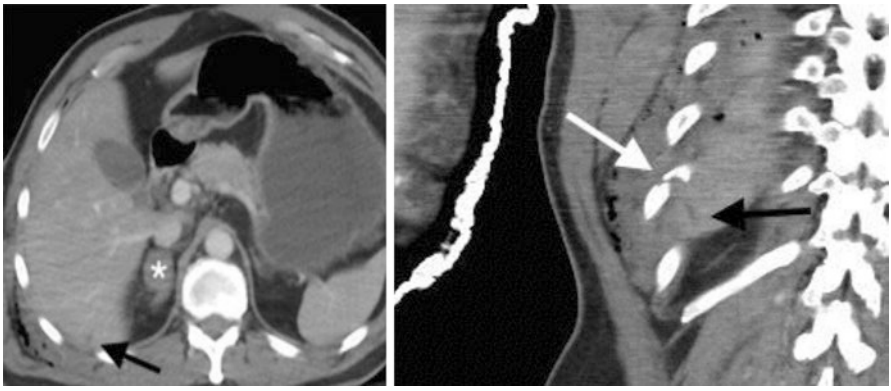

Fig. 2.3 Grade I liver laceration and adrenal hematoma. Male who sustained polytrauma from an ATV accident. Contrast-enhanced CT showed a grade I small peripheral segment VI liver laceration extending to the capsule (*black arrow*). The laceration is adjacent to a displaced right rib fracture (*white arrow*) and a right adrenal hematoma (*asterisk*)

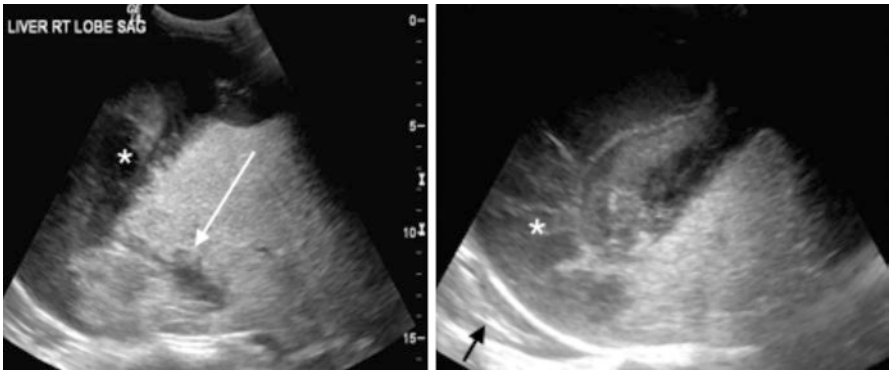

Fig. 2.4 Posterior right hepatic lobe laceration (*white arrow*) with a large subcapsular hematoma (*asterisk*) compressing the liver. A small right pleural effusion is incidental (*black arrow*)

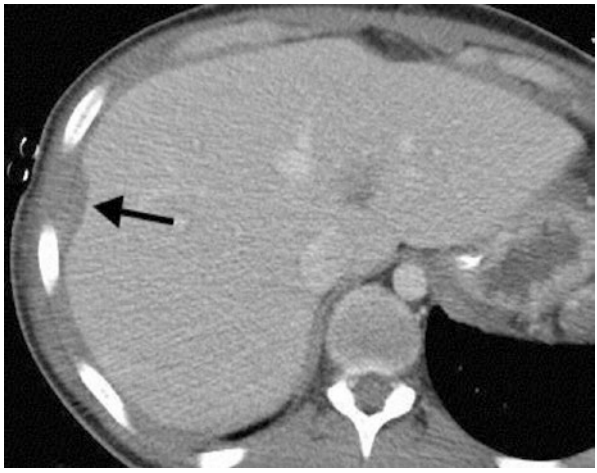

Fig. 2.5 Small right hepatic lobe subcapsular hematoma in a 24-year-old male status post MVC with pickup truck (*arrow*). The patient also sustained polytrauma with liver laceration, splenic laceration, status post splenectomy, and a left femur fracture (*not shown*)

2.8 Hematoma

Traumatic liver hematomas can be intrahepatic, perihepatic, or subcapsular. A hematoma will appear hyperdense relative to unenhanced liver parenchyma but appear hypodense compared to the enhanced liver (Fig. 2.5). According to the most widely used liver injury grading system from AAST, the intrahepatic hematomas are graded by size, presence of expansion, rupture, and active bleeding. Subcapsular hematomas are graded based on the percent of the liver surface they involve. Subcapsular blood in the liver results in adjacent parenchymal compression, similar to other encapsulated abdominal organs, whereas perihepatic blood does not (Figs. 2.6 and 2.7). On ultrasound, as hematomas evolve, they become better demarcated and more hypoechoic (Fig. 2.3).

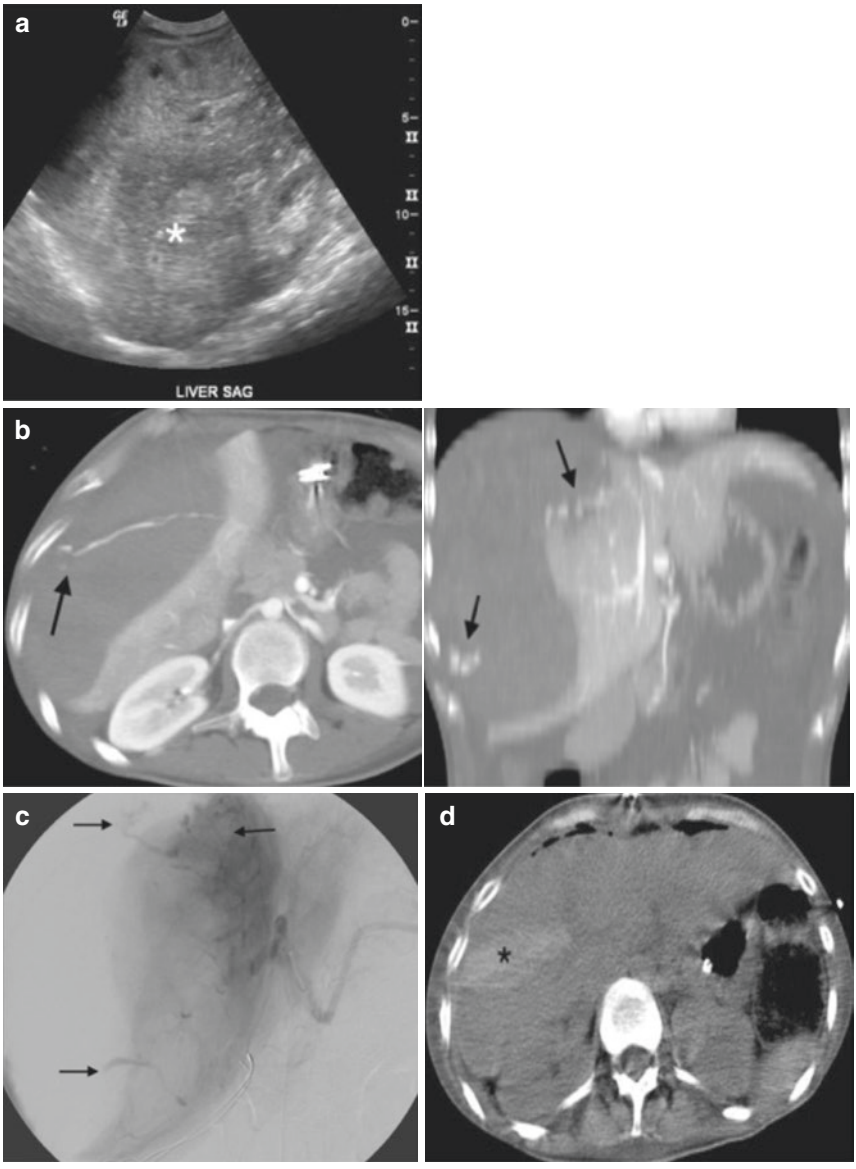

Fig. 2.6 A 27-year-old woman with hypotension after transjugular biopsy. Large subcapsular hematoma with active contrast extravasation. (**a**) Emergent ultrasound shows partial replacement of the right lobe by mixed echogenicity acute clot (*asterisk*). (**b**) Portal venous phase CT revealed a massive right lobe subcapsular hematoma with large hemoperitoneum. Note the acute hematoma is hypodense relative to the contrast-enhanced liver. Oblique coronal and oblique axial reconstructions reveal multiple foci of uncontained active contrast extravasation into the subcapsular hematoma (*black arrows*). (**c**) Digital subtraction image during emergent angiogram performed 45 min later confirmed multiple sites of active contrast extravasation indicating active bleeding (*black arrows*). These were successfully embolized with Gelfoam. Other sites of bleeding from the left lobe were detected and were also embolized (*not shown*). (**d**) Noncontrast CT following surgical clot evacuation demonstrates re-expansion of the liver with a hyperdense central right lobe hematoma (*asterisk*)

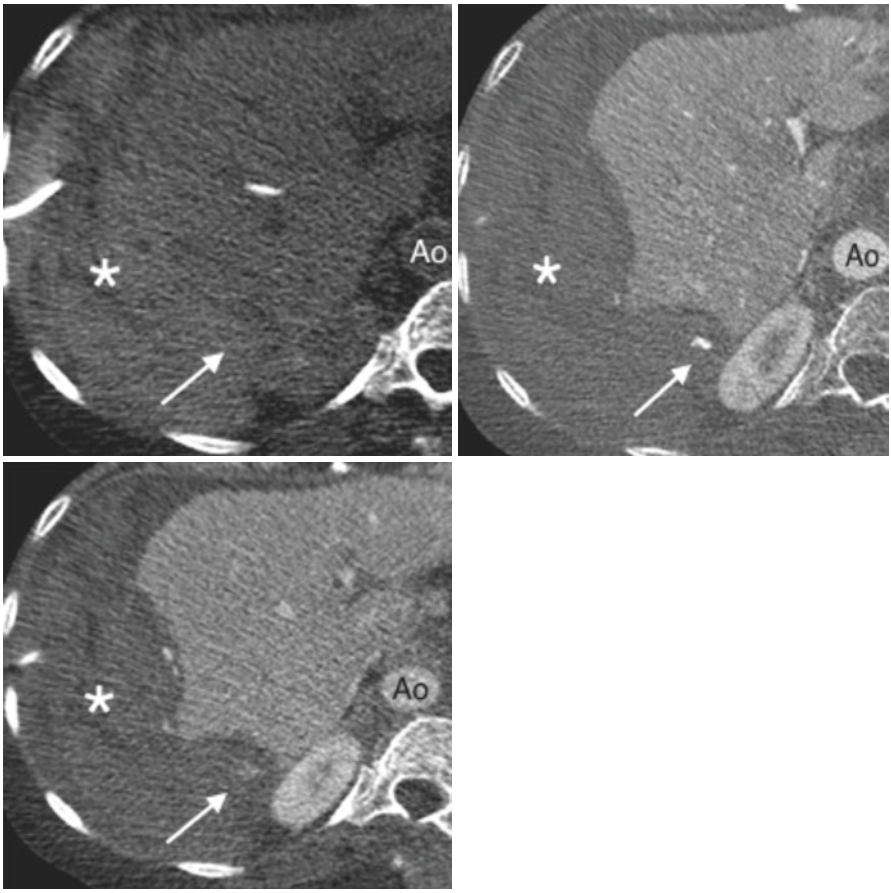

Fig. 2.7 Active contrast extravasation into a subcapsular hematoma. Penetrating liver trauma from percutaneous transhepatic cholangiography (PTC) resulting in a large subcapsular and perihepatic hematoma with active contrast extravasation (*arrow*). Non-contrast narrow window images show acute hyperdense subcapsular and perihepatic hematoma (*asterisk*). Arterial phase images show a small arterial focus of contrast extravasation (*arrow*) which enlarges on the portal venous phase (*arrow*). The density of the extravascular contrast blush on both post contrast phases is the same density as the contrast in the aorta (*Ao*)

2.9 Infarct

The liver maintains a dual blood supply from the hepatic artery and the portal venous system, making hepatic infarct/devascularization uncommon. However, posttraumatic infarcts are possible by the isolation and disruption of liver parenchyma from its blood supply (Fig. 2.2) or vascular occlusion in high-grade blunt injuries. Infarcts typically appear as a peripheral, wedge-shaped areas of decreased (in the case of ischemia) or absent enhancement on contrast-enhanced CT or decreased attenuation relative to normal liver on noncontrast CT.

Hepatic vascular injuries can involve the hepatic arteries, portal venous veins, or hepatic veins. The appearance of vascular injuries in the liver may be complex due to the dual blood supply. When portal venous flows interrupted, the affected parenchyma will be hyperenhanced during the hepatic arterial phase due to compensatory hepatic arterial flow. Subsequently, the segment becomes hypodense on portal venous phase due to the portal vein injury. This perfusional alteration is termed transient hepatic attenuation difference [11]. It can be difficult—although very important—to differentiate between contained and uncontained vascular injuries, which are indicated by extravasation of contrast outside of the normal contour of a vessel [2]. Determining whether a vascular injury is contained or noncontained will change clinical management. Included below are instructions on how to differentiate between a contained vascular injury and uncontained vascular injury.

2.10 Contained Vascular Injuries

Posttraumatic pseudoaneurysms and arteriovenous fistulas (AV) represent contained vascular injuries. Post-traumatic pseudoaneurysms variable in size, but the "blush" tends to be rounded or lobular with a curvilinear edge, and their enhancement parallels the density of the aorta on all phases. The pseudoaneurysm becomes less conspicuous on the portal venous phase (because it is still in communication with the intravascular space), whereas active contrast extravasation slowly expands on the portal venous phase (Fig. 2.8). A posttraumatic AV fistula represents a new communication between the arterial and venous sides of the circulation. In an AV fistula, contrast-enhanced blood quickly flows from a high-pressure hepatic artery into a lower-pressure vein resulting in early enhancement of the involved hepatic or portal vein branch during the hepatic arterial phase compared to the other veins (Fig. 2.8).

2.11 Uncontained Vascular Injuries

Uncontained arterial vascular injury needs to be differentiated from a pseudoaneurysm or AV fistula. With uncontained arterial vascular injuries, the "blush" of contrast during the arterial phase tends to be irregular and may have an indistinct border. During the portal venous phase, the contrast will persist and will change in size and morphology, generally becoming larger, although it may be diluted by the surrounding noncontrast blood (Fig. 2.7). During a single portal venous phase scan, it may be difficult to differentiate between contained and uncontained vascular injuries, although extravasation beyond the liver capsule represents an uncontained vascular injury [2].

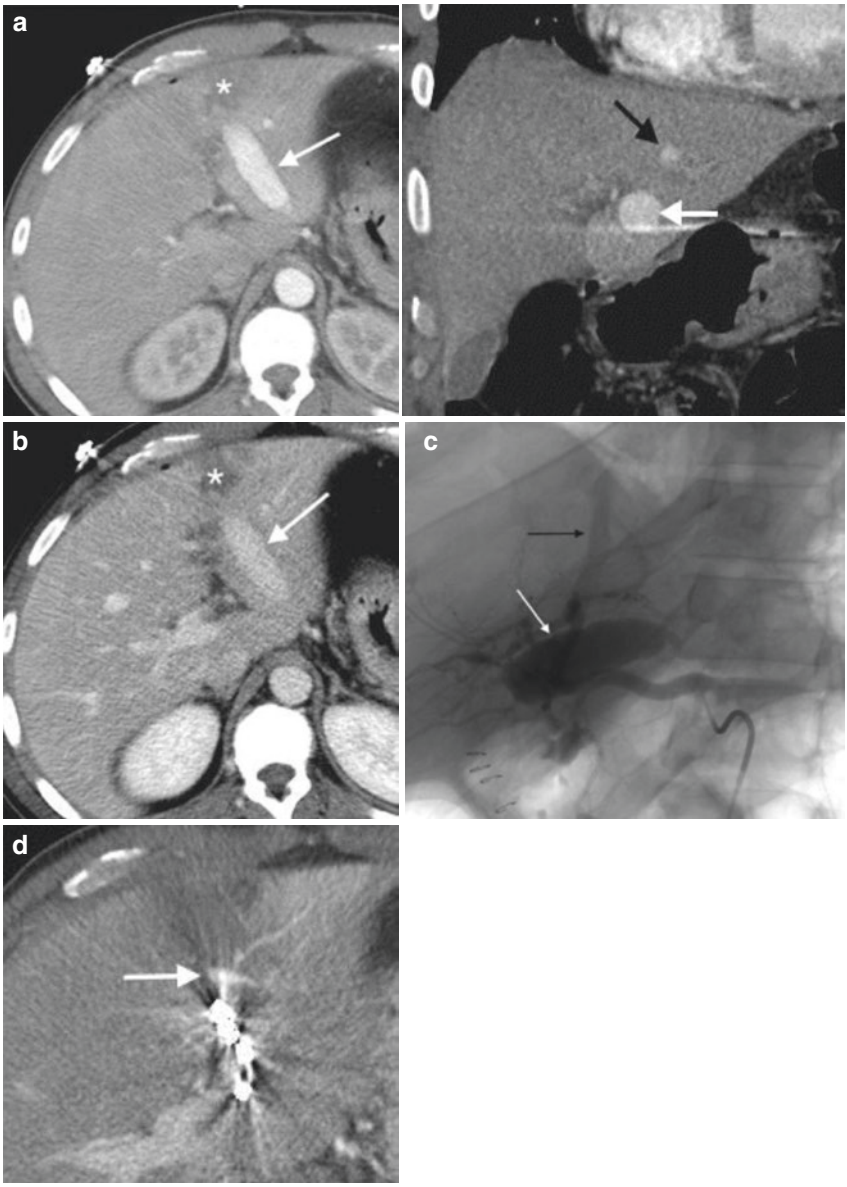

Fig. 2.8 Large traumatic pseudoaneurysm with AV fistula. (**a**) Arterial phase of a biphasic contrast-enhanced CT after stab wound to the left lateral segment showed an elongated 5.7-cm long left hepatic arterial pseudoaneurysm conforming to the shape of a knife blade (*white arrow*). Early opacification of the left hepatic vein (*black arrow*) on the corresponding coronal reconstruction represents an arterialvenous fistula (AVF). (**b**) A hypodense anterior wedge-shaped hepatic laceration is present (*asterisk*) with persistent contrast pooling in the pseudoaneursym. (**c**) Injection into the left hepatic artery during angiography confirmed the arterial LHA pseudoaneurysm with early opacification of the left hepatic vein indicating AVF. The pseudoanerysm was embolized during left hepatic vein occlusion. (**d**) Repeat CT 3 days later showed a small residual pseudoaneurysm with resolved AVF prompting a left hepatectomy. (**e**) The gross pathology specimen demonstrates a linear capsular stab wound and clot in the intrahepatic pseudoaneurysm

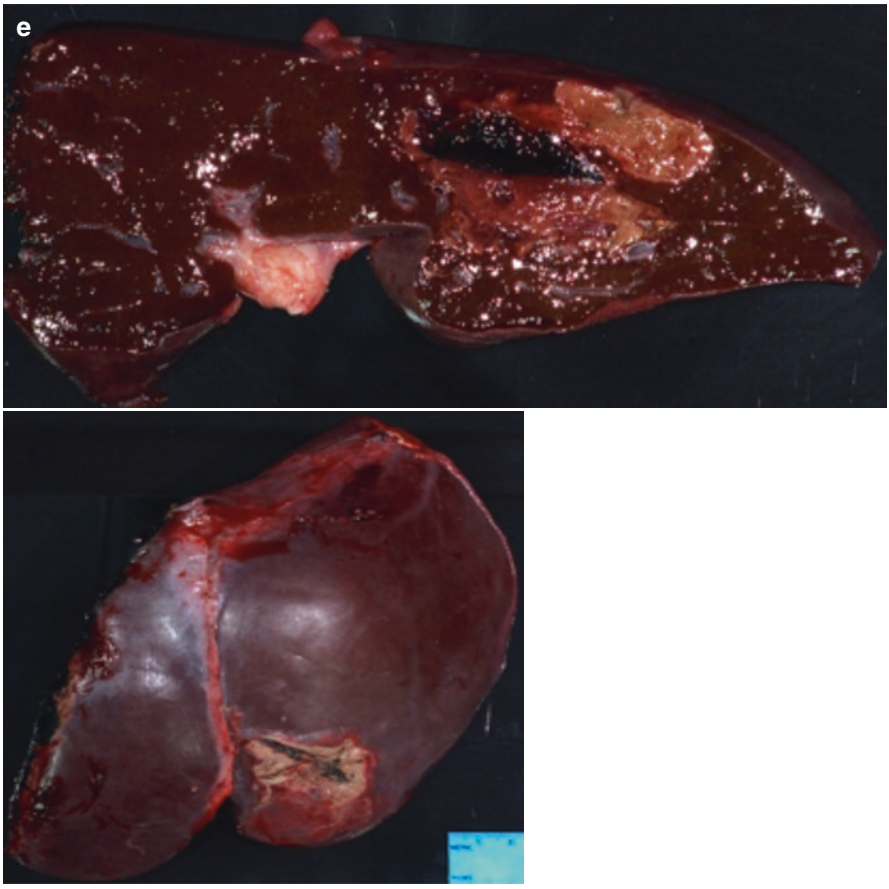

Fig. 2.8 (continued)

2.12 Liver Injury Scoring

A few liver injury classification systems have been created, with the most widely utilized being the 1994 revision of the American Association for the Surgery of Trauma (AAST) scoring scale for liver injury (Table 2.1) [12] . A CT-modified grading scale was created by Mirvis et al. in 1989 (Table 2.2) [13]. Both systems use the size and extent of the parenchymal hematoma or laceration to score the injuries. On the AAST and Mirvis grading scales, vascular injury is described as juxta-hepatic vascular injury or avulsion (AAST system) or devascularization of one or both hepatic lobes [13]. However, neither scoring systems includes findings such as active contrast extravasation or pseudoaneurysm, which are being increasingly treated with selective arterial embolization in hemodynamically stable patients. The CT-based grading system may underestimate injury seen at the time of surgery [14].

Table 2.1 AAST Liver Injury Grading Scale

Grade	Hematoma	Laceration	Vascular
1	*Subcapsular* < 1 cm	<1 cm depth	
II	*Subcapsular* 10–50% surface area *Intraparencymal* < 10 cm diameter	1–3 cm depth, or <10 cm length	
III	*Subcapsular* > 50% surface area, or ruptured capsule *Intraparencymal* > 10 cm diameter or expanding	>3 cm depth	
IV		Parenchymal disruption involving 25–75% of a lobe or 1–3 Couinaud's segments	
V		Parenchymal disruption involving >75% of a lobe or >3 Couinaud's segments in a single lobe	Juxtahepatic venous injuries
VI			Hepatic avulsion

Modified from http://www.aast.org/Libary/TraumaTools/InjuryScoringScales.aspx#liver

Table 2.2 Mirvis CT Modified Grading Scale

Grade	Hematoma	Laceration	Vascular
1	<1 cm thick		
2	1–3 cm thick		
3	*Intraparenchymal:* <3 cm diameter *Subcapsular* > 3 cm thick		
4		Lobar maceration	Lobar devascularization
5		Bilobar maceration	Bilobar devascularization

Derived from Mirvis S.E., et al. Blunt hepatic trauma in adults CT-based classification and correlation with prognosis and treatment. Radiology 1989 171:1, 27–32

2.13 Pitfalls Associated with CT Imaging

Several pitfalls need to be considered when evaluating the liver in a trauma patient. Normal anatomical structures such as the slips of the diaphragm and accessory hepatic fissures can mimic hepatic lacerations (Fig. 2.9). The configuration of geographic fat deposition in the liver can have variable appearances including a linear or wedge-shaped configuration mimicking laceration and infarct (Fig. 2.10). Nontraumatic liver lesions such as hemangiomas may occasionally be difficult to distinguish from hepatic injury (Fig. 2.9). Identification of the lesion on prior studies excludes acute traumatic cause. Artifacts can degrade image quality and negatively affect evaluation of the liver. A common artifact is beam hardening, which can result from the patient's arms being down by their sides, orthopedic hardware in the spine, or metallic foreign bodies including ballistic fragments or embolization coils.

Fig. 2.9 Pitfall. Fluid in an accessory fissure (*black arrow*). Linear fluid in the right inferior hepatic fissure can simulate a liver laceration. This becomes accentuated by hepatic edema, in the early phase after liver transplant (*as in this case*). Anasarca and perihepatic drain are present

Beam hardening can cause streaky linear hypodensities that can mimic laceration, but their typical appearance and lack of other traumatic findings will suggest an artifact (Fig. 2.12). In cases of more severe hepatic injury, normal islands of enhancing liver parenchyma located between intrahepatic hematoma or complex laceration could be mistaken for small islands of focal contrast extravasation. The periportal halo sign, manifested by interstitial low density surrounding the portal vein, can represent edema in patients who receive rapid fluid resuscitation but can also be caused by periportal blood tracking in the setting of liver injury. The periportal halo can make it difficult to depict small hepatic lacerations.

2.14 Delayed Complications of Liver Injury

The paradigm shift toward nonoperative management of hepatic injuries has increased the importance of accurate diagnosis of early and delayed complications (those occurring more than 10 days after liver injury). Such complications include delayed hemorrhage, abscess, posttraumatic pseudoaneurysm, hemobilia, and biliary complications such as biloma and bile peritonitis. Not only are most minor liver injuries (grade I or II) safely observed, but up to one-third of higher-grade injuries (grades III, IV, and V) are successfully treated without surgery. Although more patients with blunt liver trauma are being treated nonoperatively, in one study, up to

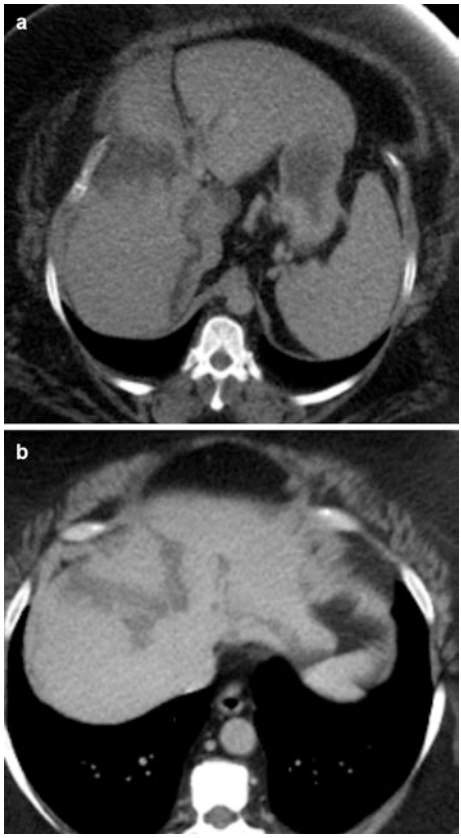

Fig. 2.10 Pitfall. Geographic hepatic steatosis mimicking liver laceration and infarct. (**a**) 45-year-old woman referred to a surgeon with a clinical history of "liver laceration." Geographic hepatic steatosis in a linear and wedge-shaped distribution simulates a liver laceration and hepatic infarct, respectively, in a morbidly obese patient without trauma. Note the lack of intraperitoneal hemorrhage. (**b**) CT performed 5 months later on the same patient from a more superior section of the liver shows the geographic steatosis is stable

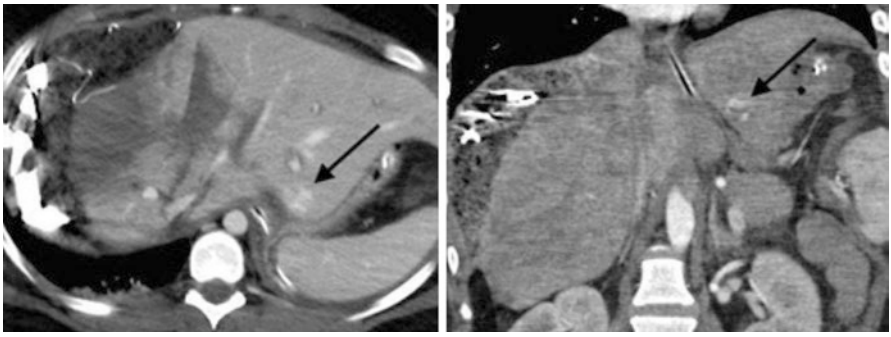

Fig. 2.11 Pitfall. Liver hemangioma. Coronal hepatic arterial phase and axial portal venous phase images from the same patient as above who has a 2 cm vascular lesion in segment II of the liver with peripheral discontinuous nodular enhancement matching the attenuation of the blood pool on all phases diagnostic of a cavernous hemangioma. Hemangiomas are a potential pitfall in the acute trauma patient as they could be confused with contained active bleeding

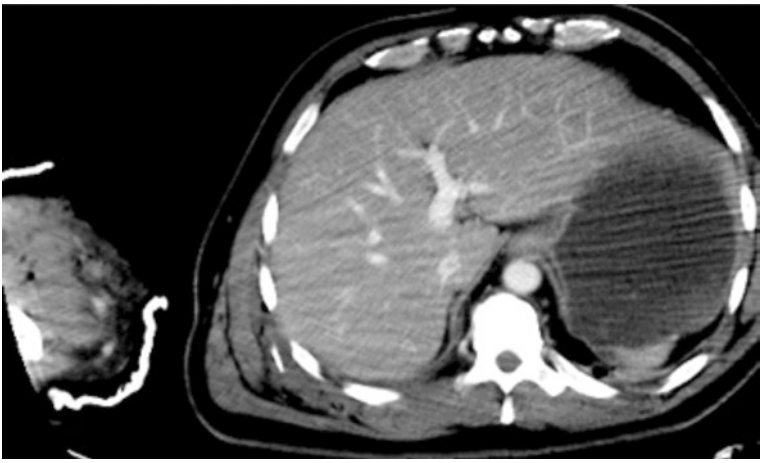

Fig. 2.12 Pitfall. Streak artifact. Multiple faint linear streaks through the liver parenchyma related to beam hardening from the ribs and the splinted right upper extremity. The patient was unable to raise the right arm for CT due to severe right scapula and right humerus fractures

24% of this cohort still required additional interventional procedures such as angiography, percutaneous drainage, or endoscopic retrograde cholangiography (ERC) with sphincterotomy and biliary stenting with a high (85%) success rate [15]. The rate of delayed complications and the need for these minimally invasive procedures primarily affects patients with higher-grade (grades IV and V) injuries.

2.15 Late Hemorrhage

"Late" bleeding generally occurs within 72 h after injury with an incidence of 2.8–3.5% [16]. In nonoperatively managed patients, delayed hemorrhage is the most common complication and cause of death. Some causes of late hemorrhage include rupture of a pseudoaneurysm or rupture of a subcapsular hematoma. Angiography (with selective catheter embolization) is useful if recurrent arterial bleeding occurs in a hemodynamically stable patient, with surgical treatment reserved if embolization is unsuccessful.

2.16 Abscess

Intra- or perihepatic abscess has a low incidence (0–7%). They present with clinical signs of infection and are more common in patients treated operatively. On CT, they appear as loculated fluid collections, in or near the liver, and may contain new gas bubbles or air-fluid levels (Fig. 2.13). Rim enhancement can be seen after intravenous contrast administration. Abscesses can be treated with image-guided percutaneous drain placement [17].

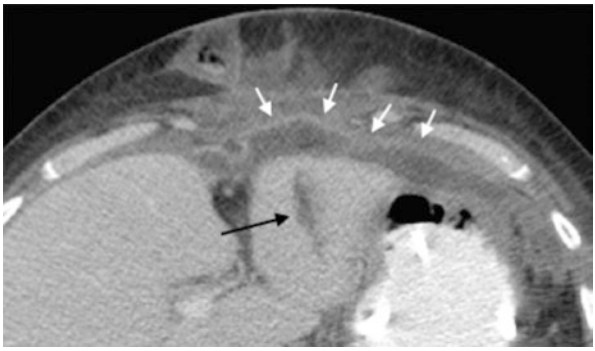

Fig. 2.13 Perihepatic abscess after penetrating liver injury. A 47-year-old female stab victim to the left lateral hepatic segment (*black arrow*). Anterior rim enhancing perihepatic abscess following liver hepatorrhaphy (*white arrows*). The patient also sustained gastric and pancreatic transection complicated by pancreatic duct leak (*not shown*)

2.17 Biliary Complications

The spectrum of biliary complications resulting from traumatic injury includes common findings such as biloma, bile leak, and bile peritonitis and less commonly biliary fistula, hemobilia, and bilhemia. A biloma results from disruption of the intrahepatic biliary ducts forming a contained bile collection in the parenchyma. It should be suspected on CT or ultrasound when an enlarging well-defined water-attenuation fluid collection pools in the area of liver injury (Fig. 2.14). ERCP (endoscopic retrograde cholangiopancreatography) is useful to diagnose bilomas by documenting extravasation of contrast from the injured bile ducts (Fig. 2.15). When bilomas are symptomatic, large, superinfected, or obstructing, treatment can be achieved by a combination of internal biliary stent placement to allow biliary duct healing and percutaneous drainage.

Biliary leaks occur in 4–23% of patients after major liver injury [18]. Bile leaks are suspected when a water density perihepatic fluid collection develops. Extra biliary-enteric pooling of the radiotracer during hepatobiliary scintigraphy is diagnostic of an active bile leak. While minor bile leak from hepatic lacerations is common, most cases are transient and self-limited. In about one-third of patients, ERCP and biliary stenting with percutaneous drainage are necessary for major biliary leaks [15, 17]. Bile peritonitis in liver trauma patients should be considered when there is persistent abdominal pain, distention, leukocytosis, and tenderness. On CT, rim enhancement around a biloma is typically observed.

A biliary fistula can occur spontaneously if bile leaks through a skin defect formed from penetrating trauma or a drain site. A biliary-pleural fistula may develop from transdiaphragmatic communication. Another uncommon complication is hemobilia, which develops when a communication between a vessel, usually an

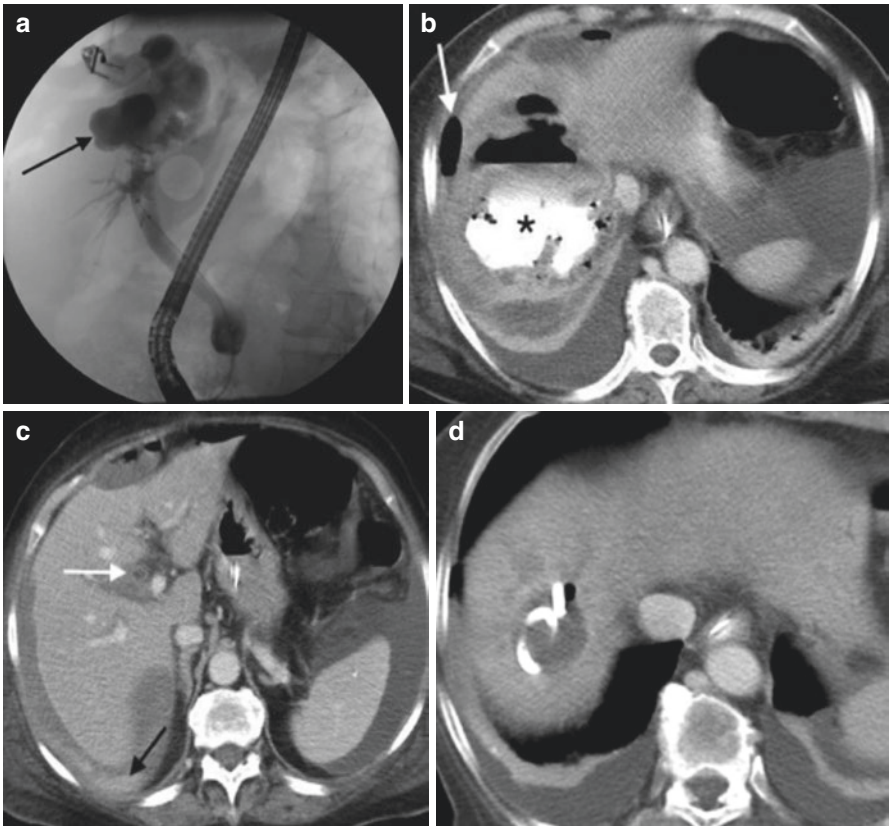

Fig. 2.14 (**a**) Intrahepatic biloma. Retrograde contrast injection during ERCP reveals a large irregular contrast collection in the liver dome communicating with biliary ductal system (*black arrow*). Purulent drainage from the bile duct at ERCP indicated an infected biloma. Biloma treated with biliary stent. (**b**) Contrast-enhanced CT performed 1 day later on the same patient revealed retained extravasated contrast injected during ERCP in the biloma (*asterisk*) with free air (*white arrow*). (**c**) An image more caudally revealed diluted dependent contrast (*black arrow*) and free fluid in the subhepatic space collection from a biliary leak. Bile duct wall enhancement represents cholangitis (*white arrow*). (**d**) Seven weeks after percutaneous drain placement, the biliary abscess has almost resolved

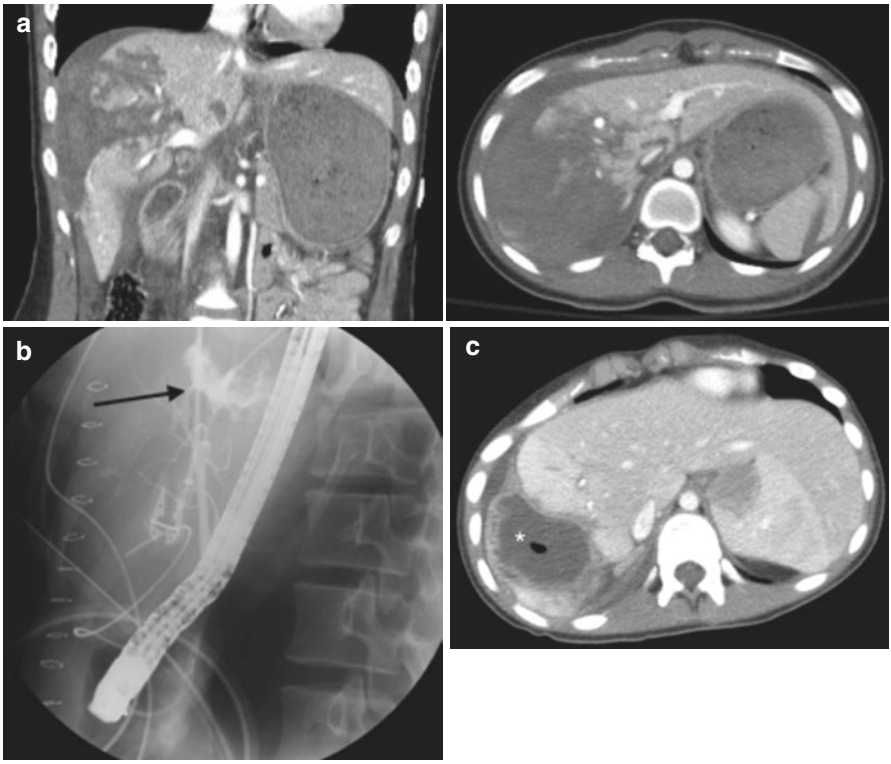

Fig. 2.15 An 18-year-old female status post motor vehicle collision. (**a**) AAST grade V liver laceration with extension to the hilum. (**b**) ERCP image demonstrates extravasation of contrast injected into the bile duct. (**c**) CT obtained 1 month later demonstrates an organized, rim enhancing infected biloma containing a locule of gas

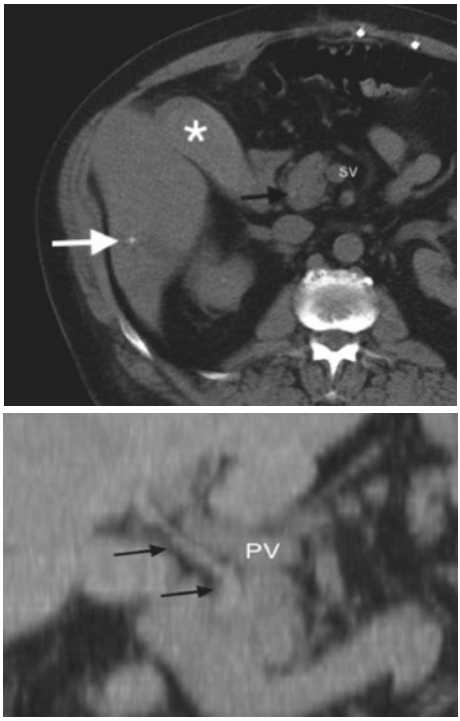

Fig. 2.16 Hemobilia. Noncontrast CT demonstrating hyperdense clot in the gallbladder (*asterisk*) and the bile duct (*black arrows*). Note the density of the bile duct is slighter higher than the adjacent superior mesenteric vein (*SV*) on the axial image and the adjacent portal vein on the coronal reconstruction (*PV*). This patient presented with hematochezia after right portal vein embolization prior to planned right hepatectomy for resection of colon cancer metastasis. Note the embolization coil in the right lobe (*white arrow*)

artery, drains into the lower-pressure biliary tree (Fig. 2.16). Patients present with upper gastrointestinal bleeding, and right upper quadrant pain with jaundice if a clot obstructs the biliary tree (Fig. 2.17). Angiography and embolization will stop the bleeding. Endoscopic treatment with biliary sphincterotomy and stenting can relieve biliary clots. Bilhemia is another rare but serious complication in which a traumatic fistula between the biliary ducts and hepatic veins results in serum hyperbilirubinemia [18].

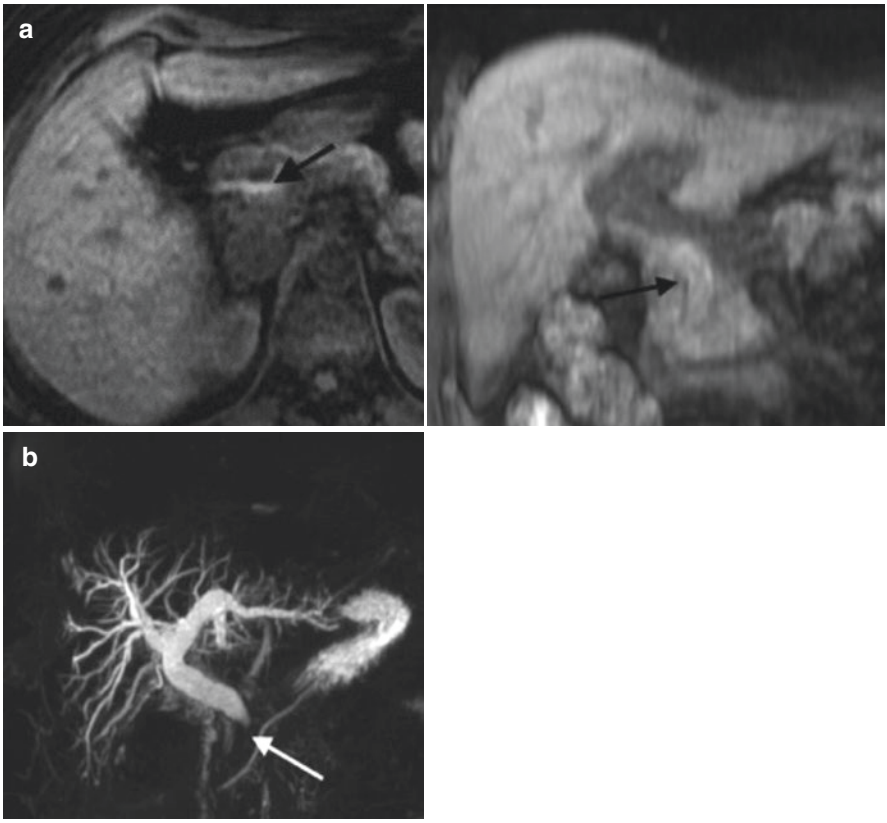

Fig. 2.17 Iatrogenic hemobilia. A 33-year-old woman who developed elevated liver function tests and abdominal pain after a random left lobe liver biopsy. (**a**) Axial and coronal fat suppressed T1 gradient echo images reveal layering T1 hyperintense filling defect in the extrahepatic duct (*black arrow*) compatible with hemobilia confirmed on subsequent ERCP (endoscopic retrograde cholangiopancreatography). (**b**) MIP images from a 3D MRCP showed biliary dilation due to biliary obstruction by the clot resulting in CBD cutoff (*white arrow*). The patient was treated with sphincterotomy and clot extraction. She recovered uneventfully

2.18 Ischemic Segments of Liver

Ischemic or devascularized segments of liver are more common with higher-grade injury (Fig. 2.18). Hepatic ischemia or necrosis can develop during the inciting injury, particularly when associated with major vessel disruption. Hepatic-related morbidity is also common after catheter hepatic embolization [19]. In one retrospective study, up to 19% (6 out of 31) of patients who required hepatic catheter angiography with embolization for their injuries developed hepatic infarction [20].

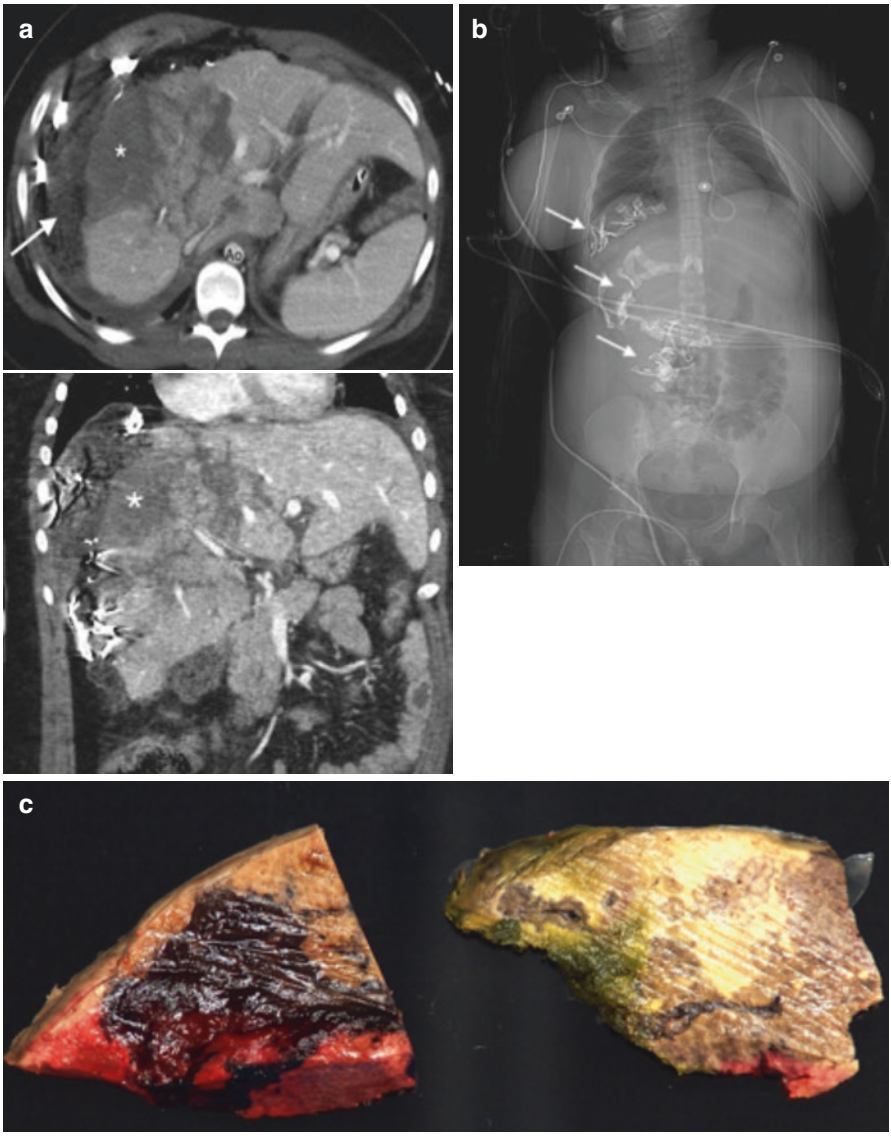

Fig. 2.18 Grade V liver laceration. 21-year-old female sustained a high speed MVA presented with positive FAST scan, and hemorrhagic shock was immediately managed surgically. Severe, bleeding right lobe liver laceration was treated with superficial right lobe hepatorrhaphy and packing with lap sponges. (**a**) Postoperative contrast-enhanced trauma CT showed a severe grade 5 liver injury with deep complex lacerations to segments I, IV and V–VIII. Segment VIII also sustained hemorrhagic infarction (*asterisk*). (**b**) Scout image from the post-operative CT scan demonstrates surgical packing material (*arrows*). (**c**) Gross pathologic specimen from the right hepatectomy performed 3 days later confirmed traumatic lacerations and a focal infarct with patchy hepatic and biliary necrosis

2.19 Other Clinical Complications

Clinical complications encountered after operative management of liver injury include hyperpyrexia (defined by maximal daily temperature >38° for the first three consecutive postoperative days), coagulopathy requiring blood transfusions, and hypoglycemia (serum glucose <80 mg/dL) during the first 24 hours.

2.20 Hepatic Arterial Embolization

Hepatic arterial embolization is increasingly utilized as an adjunct to surgery or in hemodynamically stable patients with a vascular injury detected on CT (Fig. 2.5). The dual blood supply of the liver allows embolization anywhere along the course of the hepatic artery as long as normal hepatopetal flow is present in the portal vein. This can be established with a portal venogram performed prior to embolization, if the clinical situation permits. The absence of normal hepatopetal portal venous flow significantly increases the risk of hepatic necrosis. The dual blood supply of the liver also results in challenges to achieving hemostasis. Ideally, embolization should be performed proximal and distal to the injured vessel to prevent continued supply by collateral vessels. Embolization should be achieved distal to the cystic artery as gallbladder necrosis carries significant morbidity.

Embolization material selection depends on the size of the vessel, location, and desire for permanent or temporary occlusion. The options include Gelfoam, coils, particles, and liquid sclerosants. Gelfoam provides inexpensive and temporary embolization that will recanalize in 2–3 weeks. Coils offer more precise control for placement, which is valuable when addressing arteriovenous fistulas or pseudoaneurysms. Particles can be used to target more diffuse bleeding; the material courses through the arteries until they finally occlude vessels of a smaller diameter than the particles themselves. Sclerosants are rapid and permanent and generally have limited utility except for in situations where the target organ can be sacrificed. In addition, when using particles, Gelfoam slurry, or liquid sclerosants, prevention of refluxed material is key to avoid nontarget embolization [21, 22].

References

1. Croce MA, et al. Nonoperative Management of Blunt Hepatic Trauma is the treatment of choice for hemodynamically stable patients results of a prospective trial. Ann Surg. 1995;221(6):744–55.
2. Mirvis, S.E. et al., 2014. Problem solving in Emergency Radiology., Elsevier Health Sciences.
3. Richardson JD, et al. Evolution in the Management of Hepatic Trauma: a 25-year perspective. Ann Surg. 2000;232(3):324–30.
4. Ward J, Alarcon L, Peitzman AB. Management of blunt liver injury: what is new? Eur J Trauma Emerg Surg. 2015;41(3):229–37.
5. Coccolini F, et al. Liver trauma: WSES position paper. World J Emerg Surg. 2015;10(1):1–10.

6. Kinnunen J, et al. Emergency CT in blunt abdominal trauma of multiple injury patients. Acta Radiol. 1994;35(4):319–22.
7. Boscak AR, Shanmuganathan K, Mrivis SE, et al. Optimizing trauma multidetector CT protocol for blunt splenic injury: need for arterial and venous phase scans. Radiology. 2013;268:79–88.
8. Dreizin D, Munera F. Blunt polytrauma: evaluation with 64-section whole-body CT angiography. Radiographics. 2012;32(3):609–31.
9. Yoon W, et al. CT in Blunt Liver Trauma. Radiographics. 2005;25(1):87–104.
10. Miele V, Andreoli C, Cicco DM, et al. Hemoretroperitoneum associated with liver bare area injuries: CT evaluation. Eur Radiol. 2002;12:765–9.
11. Chen WP, et al. Spectrum of transient hepatic attenuation differences in biphasic helical CT. Am J Roentgenol. 1999;172(2):419–24.
12. Moore EE, Cogbill TH, Jurkovich GJ, et al. Organ injury scaling: spleen and liver (1994 revision). J Trauma Acute Care Surg. 1995;38:323–4.
13. Mirvis SE, et al. Blunt hepatic trauma in adults: CT-based classification and correlation with prognosis and treatment. Radiology. 1989;171(1):27–32.
14. Becker CD, et al. Blunt hepatic trauma in adults: correlation of CT injury grading with outcome. Radiology. 1996;201(1):215–20.
15. Carrillo EH, et al. Interventional techniques are useful adjuncts in nonoperative management of hepatic injuries. J Trauma. 1999;46(4):619–24.
16. Stassen NA, et al. Nonoperative management of blunt hepatic injury. J Trauma Acute Care Surg. 2012;73:S288–93.
17. Zhang M. Bilhemia: a rare complication of transjugular intraheptic portosytemic shunt. ACG Case Rep J. 2015;3(1):60–2.
18. Hommes M, et al. Management of biliary complications in 412 patients with liver injuries. J Trauma Acute Care Surg. 2014;77(3):448–51.
19. Mohr AM, et al. Angiographic embolization for liver injuries: low mortality, high morbidity. J Trauma Acute Care Surg. 2003;55:1077–82.
20. Misselbeck TS, et al. Hepatic Angioembolization in trauma patients: indications and complications. J Trauma. 2009;67(4):769–73.
21. Bauer JR, Ray CE. Transcatheter arterial embolization in the trauma patient: a review. Semin Interv Radiol. 2004;21(01):11–22.
22. Lopera J. Embolization in trauma: principles and techniques. Semin Interv Radiol. 2010;27(01):014–28.

CT Imaging of the Injured Spleen

3

Eric M. Campion and Ernest E. Moore

3.1 Introduction

The spleen is one of the most commonly injured organs in the abdomen with up to 45% of patients with blunt abdominal injuries having a splenic injury [1]. Historically, the spleen was not recognized to have any significant function and was removed with impunity after trauma. It was eventually noted that patients had a higher rate of sepsis and severe infection after splenectomy, especially with encapsulated organisms.

Significant investigation led to the understanding of physiologic splenic function. The spleen is histologically made up of a network of vascular sinusoids ("red pulp"). The red pulp functions to eliminate senescent red blood cells. It also has a filtering function which can trap antigens and bacteria and present it to the lymphatic follicules and reticuloendothelial cells ("white pulp") that surround the red pulp. After these antigens are presented, immunoglobulins are produced, as well as important immune products such as opsonin. It is now recognized that this immune function plays an important role in the body's ability to respond to infection, especially with encapsulated organisms.

Asplenic patients are at risk for a specific clinical entity often referred to as "overwhelming post-splenectomy infection syndrome" or OPSI. As its name suggests, OPSI manifests itself as a severe, often life-threatening infection in asplenic patients. This includes patients with functional or surgical splenectomies from any cause, but patients with hematologic malignancies appear to be at higher risk than

E.M. Campion, M.D. (✉) • E.E. Moore, M.D.
Denver Health Medical Center, University of Colorado, Anschutz Medical Campus, Denver, CO, USA
e-mail: Eric.campion@dhha.org

F. Catena et al. (eds.), *CT Scan in Abdominal Emergency Surgery*, Hot Topics in Acute Care Surgery and Trauma, https://doi.org/10.1007/978-3-319-48347-4_3

patients whose spleen was removed for injury [2]. The lifetime incidence of OPSI is estimated at 5% for splenectomized patients [3]. Asplenic patients appear to be at increased risk of sepsis from all types of bacteria but are at a particularly high risk for infection with encapsulated organisms. The encapsulated bacteria *Streptococcus pneumoniae*, *Haemophilus influenzae*, and *Neisseria meningitidis* are classically associated with this syndrome, with *S. pneumoniae* being the most commonly found organism in OPSI [3]. The reported mortality rate is wide ranging but is quite high, 48% in one case series [4]. Vaccinations against these pathogens are critically important in helping to prevent this syndrome and must be given at regular intervals for the remainder of the individual's lifetime.

The understanding of the important functions of the spleen, along with the complications associated with laparotomy and OPSI, has led to an emphasis on splenic preservation when feasible. This is of particular emphasis in the pediatric population.

3.2 Anatomy

The spleen lives in the posterior left upper quadrant of the abdomen in close relationship to the stomach, tail of pancreas, and left kidney (Fig. 3.1a). The splenic hilum (artery and vein) enter the spleen anteromedially. The splenic artery is often quite tortuous and has a widely variable number of branches as it enters the spleen (Fig. 3.1b). The spleen also receives some of its blood supply from the short gastric vessels off of the left gastroepiploic artery. The splenic vein lies at the superior border of the pancreas and tends to take a more direct course into the splenic hilum (Fig. 3.1c). The spleen has several soft tissue "ligaments" that extend from the spleen to the surrounding organs. The gastrosplenic (spleen to stomach) and splenorenal (spleen to kidney) ligaments are the most prominent and surgically important. The gastrosplenic ligament contains the short gastric vessels, while the splenorenal is relatively avascular.

3.3 CT Imaging Protocols

The normal spleen, on a non-contrasted CT imaging study, has homogenous attenuation of 40–60 Hounsfield units [5]. The spleen is most commonly imaged in the portal venous phase of the contrast bolus on CT imaging. During the arterial contrast phase and early portal venous phase, the spleen appears mottled, becoming

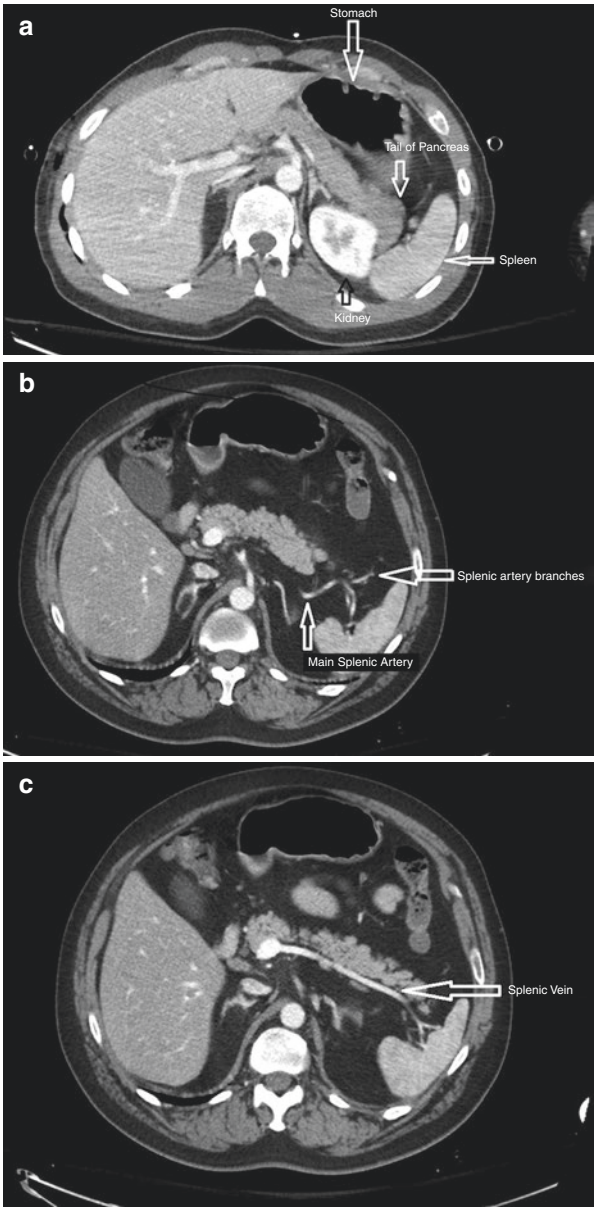

Fig. 3.1 (**a**) Anatomic relationships of the spleen with the surrounding organs. (**b**) Splenic artery with branches. (**c**) Splenic vein

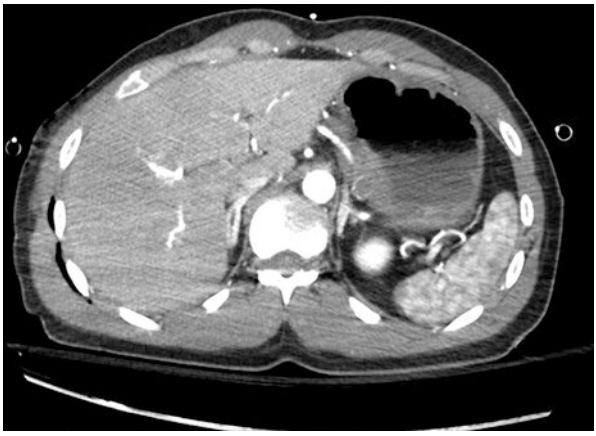

Fig. 3.2 Normal spleen during arterial phase. Notice the mottled appearance

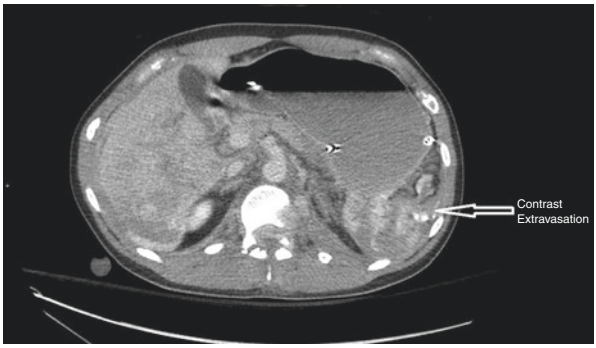

Fig. 3.3 Delayed phase imaging of the spleen with contrast extravasation

more homogenous during the middle and later portal venous phases (Fig. 3.2) [5]. The most common protocol for imaging the spleen for abdominal trauma is during the portal venous phase on imaging. This phase is best able to identify active bleeding and parenchymal injury (Fig. 3.1a) [6]. This can then be followed by a delayed phase 5 min later to further elucidate whether active extravasation is ongoing versus a contained injury (Fig. 3.3). However, recent data have suggested that the arterial phase imaging of the spleen is better able to identify contained vascular injury, such as pseudoaneurysms [6, 7]. The clinical relevance of these findings is unclear with at least one study determining that routine use of dual phase (arterial and portal venous) imaging would drastically increase the radiation dose without changing clinical outcome [8].

Given the uncertainty surrounding the need for arterial imaging of the spleen, many trauma centers routinely obtain arterial phase images of the spleen and liver only when a contrasted CT of the chest is being performed in conjunction with abdominal CT. Once arterial phase images are completed through the chest, liver, and spleen, the portal venous phase images of the abdomen are obtained using that same contrast bolus or the bolus is split to accommodate the different phases.

Delayed images during the renal excretory phase are obtained routinely by some trauma centers, while others perform delayed imaging selectively.

Follow-up surveillance imaging for high-grade blunt splenic injuries is somewhat controversial. In a recent study, 6% of patients developed delayed pseudoaneurysm or arterial extravasation on surveillance CT at 48 h. The number of delayed pseudoaneurysms identified on imaging in this study increased with increasing grade, but 20% of those identified were still in grade 1 or 2 injuries [9]. The clinical significance of these findings isn't entirely clear, although these lesions are implicated in failure of nonoperative management and delayed splenic bleeding. There is no clear consensus on the need for and timing of obtaining follow-up imaging and local practices vary.

3.4 Imaging Findings in Trauma

Traumatic injuries to the spleen produce a spectrum of injuries. A splenic laceration appears as a linear area of hypodensity within the spleen (see Fig. 3.1). The depth of laceration and involvement with trabecular vessels determines the severity on grading. A subcapsular hematoma is an area of hypodensity around the spleen that indents and distorts the parenchyma of the spleen (Fig. 3.4). The size relative to the spleen affects is grade. Lacerations involving parenchymal and trabecular vessels can devascularize portions or all of the spleen. This is seen as a hypodense area of the spleen without distortion of parenchyma.

A contrast "blush" is an area of contrast enhancement, with Hounsfield units >80, within the spleen or around the splenic vessels. When enlarging on delayed imaging, this can represent active bleeding either into the splenic parenchyma or the peritoneum (Fig. 3.3). When a contrast blush is unchanged on delayed imaging, it often represents a traumatic pseudoaneurysm or AV fistula.

Free blood around the spleen or throughout the abdomen is frequently seen with splenic injuries and increases with grade of injury. While the quantity of hemoperitoneum is associated with failure of nonoperative management, it has not been shown to be an independent predictor of failure [10].

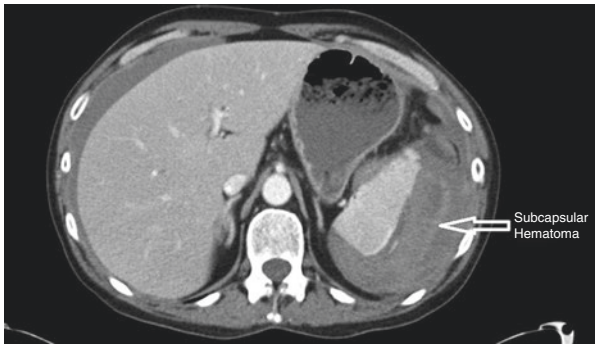

Fig. 3.4 Large subcapsular hematoma (note how splenic parenchyma is indented by hematoma)

Table 3.1 Spleen injury scale (1994 revision).

Grade	Injury type	Description of injury
1	Hematoma	Subcapsular, <10% surface area
	Laceration	Capsular tear, <1 cm
		Parenchymal depth
2	Hematoma	Subcapsular, 10–50% surface area
		Intraparenchymal, <5 cm in diameter
	Laceration	Capsular tear, 1–3 cm parenchymal depth that does not
		Involve a trabecular vessel
3	Hematoma	Subcapsular, >50% surface area or expanding; ruptured
		Subcapsular or parenchymal hematoma; intraparenchymal
		Hematoma ≥5 cm or expanding
	Laceration	>3 cm parenchymal depth or involving trabecular vessels
4	Laceration	Laceration involving segmental or hilar vessels producing
		Major devascularization (>25% of spleen)
5	Laceration	Completely shattered spleen
	Vascular	Hilar vascular injury with devascularized spleen

[a]Advance 1 grade for multiple injuries up to grade 3
From Moore et al. [11], with permission

Splenic injuries are most commonly graded by severity according to the AAST grading system (Table 3.1) [11]. Increasing splenic injury grade is associated with an increased risk of failure of nonoperative management and need for intervention.

Another blunt splenic injury grading system was developed out of Baltimore, which purports to show an improved correlation to failure of nonoperative management [12, 13]. Ongoing prospective study is being performed on this grading system, but it has not, as of yet, gained widespread utilization.

An interesting delayed finding after splenic injury or splenectomy is the presence of splenosis. Splenic tissue can autoimplant into other areas of the peritoneum and grow into defined nodules. This is typically clinically irrelevant but can be confused with neoplastic processes seen on imaging.

3.5 Interventions Based on Imaging Findings

The decision to intervene on splenic injuries is first based on the patient's hemodynamic factors. Patients that are hemodynamically unstable should proceed to the operating room without delay for management of their injuries. CT imaging should only be obtained in patients that arrive to the emergency department stable or are stabilized with resuscitation. In patients that are hemodynamically stable, the grade of splenic injury on CT imaging influences decisions in management. Nonoperative management is appropriate for the majority of stable patients with splenic injuries. Observation alone is the most common management strategy for patients with grade 1–3 injuries without active extravasation [14] (Figs. 3.5 and 3.6).

Patients with a splenic injury grade of 4 or 5 with normal hemodynamics warrant consideration for angiography as well as patients with active arterial

Fig. 3.5 Grade 1 splenic injury. Laceration of <1 cm

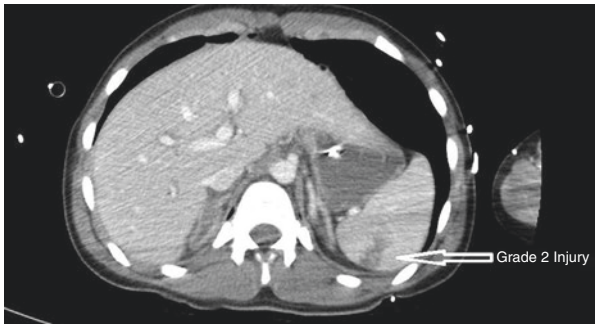

Fig. 3.6 Grade 2 splenic injury. Laceration of <3 cm not involving a trabecular vessel

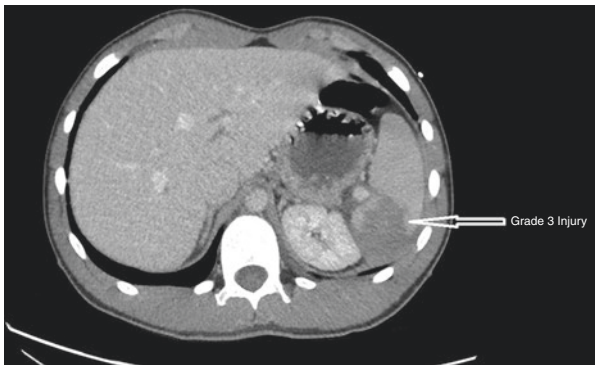

Fig. 3.7 Grade 3 splenic injury. Laceration >3 cm

extravasation or evidence of ongoing bleeding [15]. Routine angiography for patients with grade 3 injuries is under investigation, but is not currently routinely recommended. As with all traumatic injuries, there are many patient-specific factors that can affect management and the decisions surrounding splenic injury management need to be individualized to the specific clinical situation (Figs. 3.7, 3.8, and 3.9).

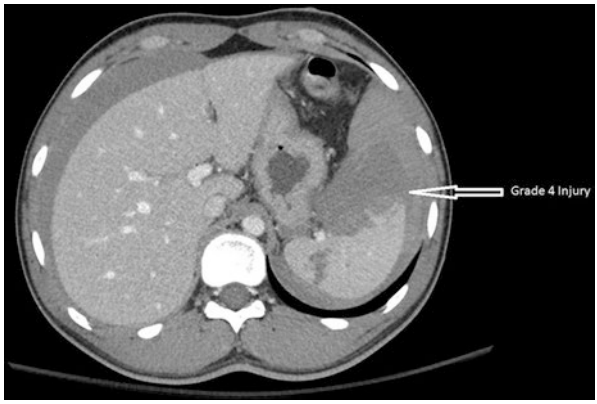

Fig. 3.8 Grade 4 splenic injury. Note the large area of devascularization (>25%)

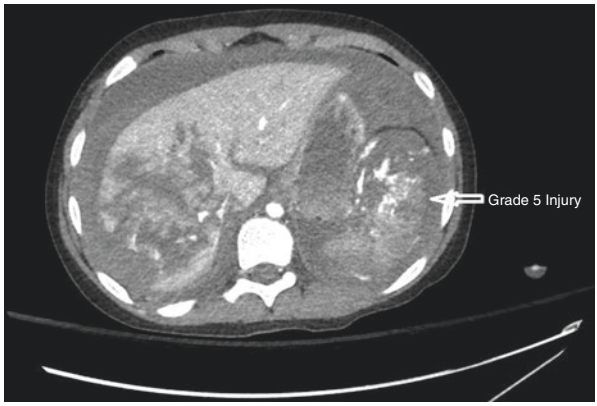

Fig. 3.9 Grade 5 splenic injury. Shattered spleen with multiple areas of contrast extravasation. Patient also has significant liver injury

References

1. Hildebrand DR, Ben-Sassi A, Ross NP, Macvicar R, Frizelle FA, Watson AJ. Modern management of splenic trauma. BMJ. 2014;348:g1864.
2. Sinwar PD. Overwhelming post splenectomy infection syndrome—review study. Int J Surg. 2014;12(12):1314–6.
3. Davidson RN, Wall RA. Prevention and management of infections in patients without a spleen. Clin Microbiol Infect. 2001;7(12):657–60.
4. Waghorn DJ. Overwhelming infection in asplenic patients: current best practice preventive measures are not being followed. J Clin Pathol. 2001;54(3):214–8.
5. Vancauwenberghe T, Snoeckx A, Vanbeckevoort D, Dymarkowski S, Vanhoenacker FM. Imaging of the spleen: what the clinician needs to know. Singapore Med J. 2015;56(3):133–44.
6. Boscak AR, Shanmuganathan K, Mirvis SE, Fleiter TR, Miller LA, Sliker CW, et al. Optimizing trauma multidetector CT protocol for blunt splenic injury: need for arterial and portal venous phase scans. Radiology. 2013;268(1):79–88.
7. Melikian R, Goldberg S, Strife BJ, Halvorsen RA. Comparison of MDCT protocols in trauma patients with suspected splenic injury: superior results with protocol that includes arterial and portal venous phase imaging. Diagn Interv Radiol. 2016;22(5):395–9.

8. Corwin MT, Fananapazir G, Lamba R, Salcedo ES, Holmes JF. Arterial phase CT for the detection of splenic injuries in blunt trauma: would it improve clinical outcomes? Clin Imaging. 2016;40(2):212–6.
9. Leeper WR, Leeper TJ, Ouellette D, Moffat B, Sivakumaran T, Charyk-Stewart T, et al. Delayed hemorrhagic complications in the nonoperative management of blunt splenic trauma: early screening leads to a decrease in failure rate. J Trauma Acute Care Surg. 2014;76(6):1349–53.
10. Watson GA, Hoffman MK, Peitzman AB. Nonoperative management of blunt splenic injury: what is new? Eur J Trauma Emerg Surg. 2015;41(3):219–28.
11. Moore EE, Cogbill TH, Jurkovich GJ, Shackford SR, Malangoni MA, Champion HR. Organ injury scaling: spleen and liver (1994 revision). J Trauma. 1995;38(3):323–4.
12. Marmery H, Shanmuganathan K, Alexander MT, Mirvis SE. Optimization of selection for nonoperative management of blunt splenic injury: comparison of MDCT grading systems. AJR Am J Roentgenol. 2007;189(6):1421–7.
13. Saksobhavivat N, Shanmuganathan K, Chen HH, DuBose JJ, Richard H, Khan MA, et al. Blunt splenic injury: use of a multidetector CT-based splenic injury grading system and clinical parameters for triage of patients at admission. Radiology. 2015;274(3):702–11.
14. Zarzaur BL, Kozar RA, Fabian TC, Coimbra R. A survey of American Association for the Surgery of Trauma member practices in the management of blunt splenic injury. J Trauma. 2011;70(5):1026–31.
15. Stassen NA, Bhullar I, Cheng JD, Crandall ML, Friese RS, Guillamondegui OD, et al. Selective nonoperative management of blunt splenic injury: an Eastern Association for the Surgery of Trauma practice management guideline. J Trauma Acute Care Surg. 2012;73(5 Suppl 4):S294–300.

Computed Tomography in Pancreatic and Duodenal Injuries

4

Ari Leppäniemi and Eila Lantto

4.1 Introduction

Pancreatic and duodenal injuries are quite rare, and their detection can be challenging both at the initial stage during diagnostic workup of an abdominal trauma patient and during explorative laparotomy. Their protected location in the retroperitoneum can give subtle symptoms and signs in isolated injuries leading to delayed diagnosis and management. The aim of this chapter is to describe the computed tomography (CT) findings of pancreatic and duodenal injuries.

4.2 Diagnostic Workup of Pancreatic and Duodenal Injuries

The majority of pancreatic and duodenal injuries are caused by blunt trauma, most commonly following a direct blow or compression injury to the upper abdomen. The mechanism of injury in penetrating trauma is direct violation of the pancreatic gland or duodenal wall by the wounding agent. A special type of injury is the intramural duodenal hematoma which presents most often with signs of progressive high intestinal obstruction (Fig. 4.1).

Depending on the institutional practice guidelines on managing penetrating and blunt abdominal injuries, the indications for operative exploration vary. However, in general, hemodynamically unstable patients with obvious abdominal injuries

A. Leppäniemi, M.D., Ph.D. (✉)
Meilahti Hospital, Abdominal Center, Helsinki University Hospital,
Haartmaninkatu 4, 00029 Helsinki, HUS, Finland
e-mail: ari.leppaniemi@hus.fi

E. Lantto, M.D., Ph.D.
Meilahti Hospital, Department of Radiology, Helsinki University Hospital,
Haartmaninkatu 4, 00029 Helsinki, HUS, Finland

F. Catena et al. (eds.), *CT Scan in Abdominal Emergency Surgery*, Hot Topics in Acute Care Surgery and Trauma, https://doi.org/10.1007/978-3-319-48347-4_4

Fig. 4.1 CT of an intramural duodenal hematoma

usually undergo prompt laparotomy, whereas stable patients will be evaluated clinically and radiologically.

In pancreatic injuries, CT is the primary diagnostic tool, although in rare cases, the initial CT image may be misleading and not show the presence of a pancreatic disruption. Sometimes a repeat CT a couple of days later may reveal the true extent of the injury. Other diagnostic options include magnetic resonance cholangiopancreatography (MRCP or MR) or endoscopic retrograde cholangiopancreatography (ERCP), and their roles are discussed later on.

Extraluminal air seen on CT in the peritoneal cavity of the retroperitoneum suggests the presence of a bowel perforation, but the exact location can be difficult to determine. Retroperitoneal or periduodenal air can point to the injury site, and sometimes oral contrast can be used to demonstrate the perforation site.

4.3 Grading of Organ Injuries and Management Principles

The American Association for the Surgery of Trauma has published the most commonly used scales for grading individual organ injuries. The injuries are graded from I to V with increasing severity. Although useful in determining the management strategy for pancreatic injuries, its role in managing duodenal injuries is less important.

In grade I and II pancreatic injuries, the main pancreatic duct is intact, and these patients can often be managed nonoperatively provided that no other injuries requiring surgical repair are present and that an injury to the major pancreatic duct has been excluded. Occasionally, a minor leak or a side fistula of the pancreatic duct can be managed with an endoscopically placed stent.

The disruption of the main pancreatic duct left to the superior mesenteric vein (grade III) usually requires operative management and removal of the pancreatic tail, with or without splenectomy. Grade IV injuries (transection to the right of the superior mesenteric vein but intact papilla of Vater) are very usually operated upon and can be very challenging. Sometimes a mere drainage is the best policy, although under favorable circumstances, a more complex repair with pancreaticojejunal anastomosis can be performed.

Major lacerations in the head of the pancreas with ductal involvement (grade V), devascularizing lesions of the duodenum, or duodenal lacerations with destruction of the ampulla and distal common duct usually undergo urgent surgery due to the

bleeding from adjacent vascular injuries. In very rare cases, these patients present in stable conditions and undergo diagnostic imaging.

Most duodenal perforations cause generalized peritonitis and require surgical management. The duodenal perforation, however, can sometimes give subtle signs, and therefore the timely diagnosis of duodenal perforation is crucial. A delay of more than 24 h in managing duodenal perforation is one of the major risk factors for poor outcome including failed duodenal repair and fistula formation. Asymptomatic duodenal perforations limited to the retroperitoneum can sometimes be managed nonoperatively including a percutaneously placed drain, but these patients require careful observation. Sometimes early surgery with duodenal repair is the safest option.

The treatment of an intramural duodenal hematoma is nonoperative consisting of nasogastric suction and parenteral fluid administration. Prolonged obstruction may require parenteral nutrition and even operative treatment if the obstruction persists for more than 2 weeks.

4.4 Complications

CT is useful in detecting postoperative pancreatitis, pseudocyst formation, and pancreatic fistulas. Definitive treatment of these complications requires usually advanced radiological and endoscopic techniques, and surgery is often the last option.

A controlled duodenal leak into a drain with good general condition of the patient can be managed expectantly, whereas progressive sepsis and uncontrolled leakage of the duodenal content outside the confined area of drainage require a reoperation, diversion of the duodenal content, luminal decompression, and insertion of a feeding jejunostomy, if not placed at the primary operation.

4.5 CT Imaging Technique

Conventional multidetector CT protocol for trauma patients includes arterial and portal venous phase imaging of the abdomen and pelvis, acquired 25–30 and 65–70 s after the beginning of intravenous contrast material administration. With biphasic contrast medium injection (split bolus technique), a single acquisition with simultaneous arterial and venous phase scanning provides comparable results and minimizes radiation dose. Thin axial, sagittal, and coronal images are routinely viewed on workstations. Additional curved MPR images can be used as problem-solving means in equivocal cases, i.e., to analyze the depth of parenchymal injury and disruption of pancreatic duct. Routinely administered oral contrast material is not used in emergency setting.

4.6 Imaging Findings in Pancreatic Injuries

Pancreatic trauma can be difficult to recognize because of coexisting injuries to other abdominal organs. Imaging findings of pancreatic injuries may range from normal appearance to complete transection of the pancreas.

Pancreatic injuries are commonly graded according to the American Association for the Surgery of Trauma classification described above. The major factors that influence the grade of injury include the location and severity of the parenchymal injury and the integrity of the main pancreatic duct. Specific and nonspecific signs of pancreatic injury on CT are presented in Table 4.1.

Pancreatic contusion causes frequently only subtle findings on imaging and may present as focal or diffuse nonlinear areas of low attenuation, inhomogeneous enhancement of pancreatic parenchyma, or focal pancreatic enlargement (Fig. 4.2).

Hematoma is seen as a hyperattenuating area within the pancreatic parenchyma and is a specific sign on pancreatic injury. Laceration is a linear hypodense or nonenhancing region perpendicular to the long axis of the pancreas. It may be superficial or extend through the entire pancreas, resulting in a transection (Figs. 4.3, 4.4, 4.5, and 4.6). Although CT may not always demonstrate the ductal disruption, it can be suggested based on the degree of the parenchymal injury. Laceration of more than 50% of the thickness of the parenchyma usually causes ductal injury (Figs. 4.4, 4.5, and 4.6).

Table 4.1 Specific and nonspecific signs of pancreatic injury

Specific signs	Nonspecific signs
Pancreatic fracture	Peripancreatic fat stranding or fluid
Pancreatic laceration	
Diffuse or focal pancreatic enlargement	Fluid separating the splenic vein from posterior aspect of the pancreas
Heterogenous enhancement	Thickening of the left anterior pararenal fascia
Pancreatic hematoma	Injuries to adjacent organs or vessels

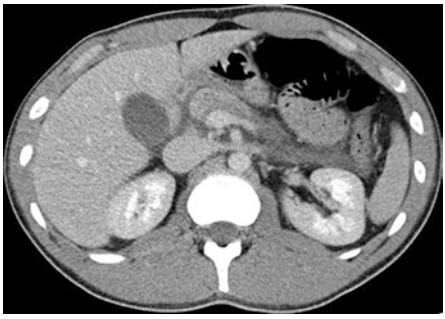

Fig. 4.2 Grade I pancreatic injury after a fist punch to the abdomen. Axial CT image demonstrates pancreatic contusion as inhomogeneous enhancement of the neck of the pancreas. Secondary signs of trauma include increased density of the peripancreatic fat, thickening of the left anterior pararenal fascia, and fluid between the splenic vein and pancreas

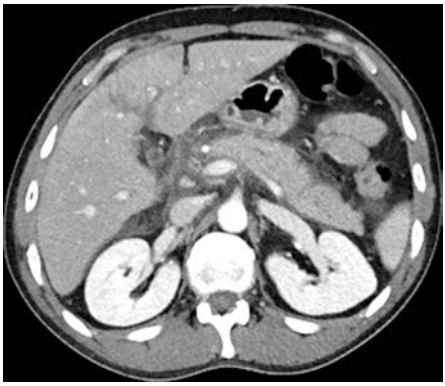

Fig. 4.3 Grade II pancreatic injury. CT shows a linear laceration across the distal body of the pancreas without ductal injury. There is also peripancreatic fluid and edema and laceration in the liver

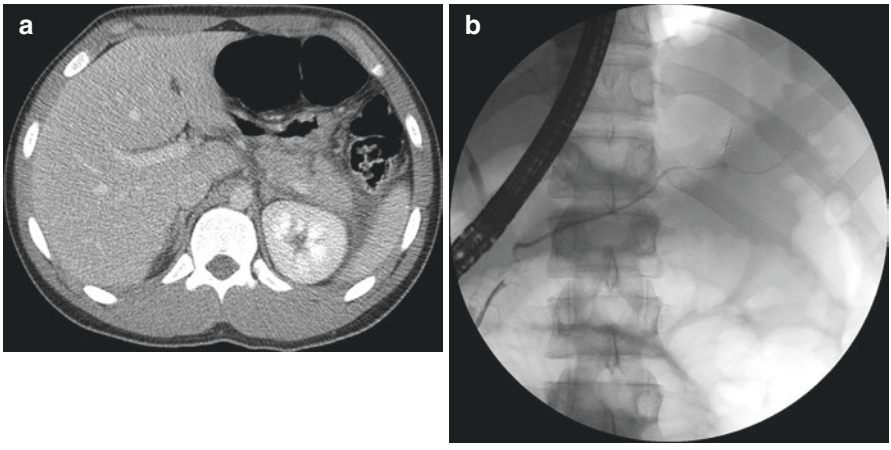

Fig. 4.4 (**a**, **b**) Grade III pancreatic injury. (**a**) Deep laceration in distal pancreatic parenchyma suggesting ductal injury after motorbike accident of a teenage boy. There is also peripancreatic fluid. (**b**) Ductal disruption was confirmed on ERCP

Fig. 4.5 Transection throughout the pancreatic body after bicycle accident with ductal injury. A fluid collection is communicating with the pancreas at the site of transection

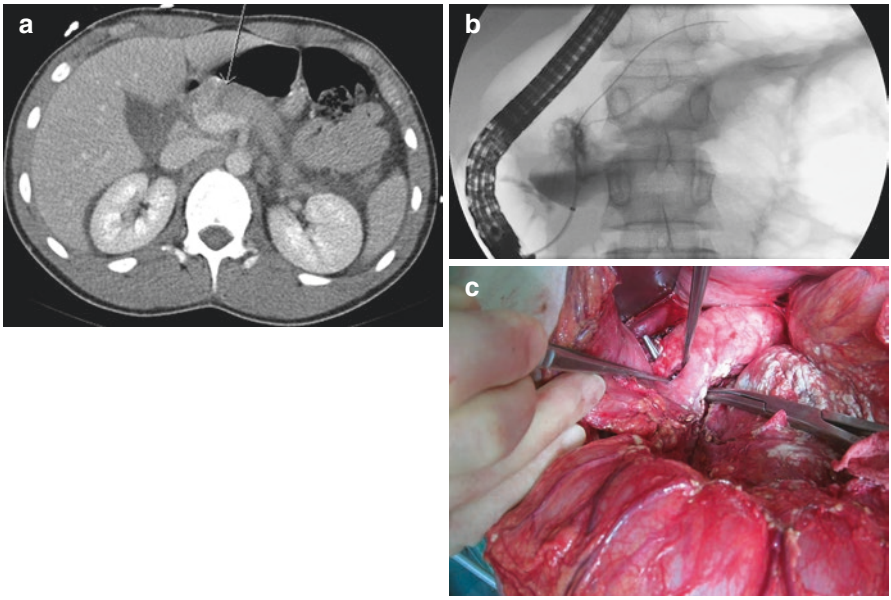

Fig. 4.6 (**a**–**c**) Grade IV pancreatic injury. (**a**) Transection of the pancreatic neck with some retro- and intraperitoneal fluid. (**b**) ERCP shows extravasation of contrast material confirming the ductal injury. (**c**) Transected pancreas at operation demonstrating the central pancreatic injury with ductal transection at the level of the superior mesenteric vein

Lacerations tend to occur at the junction of the body and tail due to shearing injuries with compression against the spine. Pancreatic fracture is diagnosed if there is a clear separation of fragments across the long axis of the pancreas (Figs. 4.7 and 4.8).

Secondary signs to look for are peripancreatic fat stranding and fluid collections and thickening of the left anterior pararenal fascia (Figs. 4.2, 4.3, and 4.4). Fluid between the splenic vein and pancreas is a nonspecific sign, but it may suggest pancreatic injury in a patient with blunt abdominal trauma.

Complications after pancreatic injury are traumatic pancreatitis, pseudocyst formation, abscesses, and fistulas (Figs. 4.7 and 4.8). The presence of focal peripancreatic fluid collections after trauma implies ductal injury. Posttraumatic strictures of the pancreatic duct and pseudoaneurysm formation of adjacent vascular structures have also been reported.

The most important pitfall in the early phase after injury is that CT findings may be absent or only subtle and nonspecific. The severity of pancreatic injury may be underestimated because of the difficulty in early detection of ductal integrity.

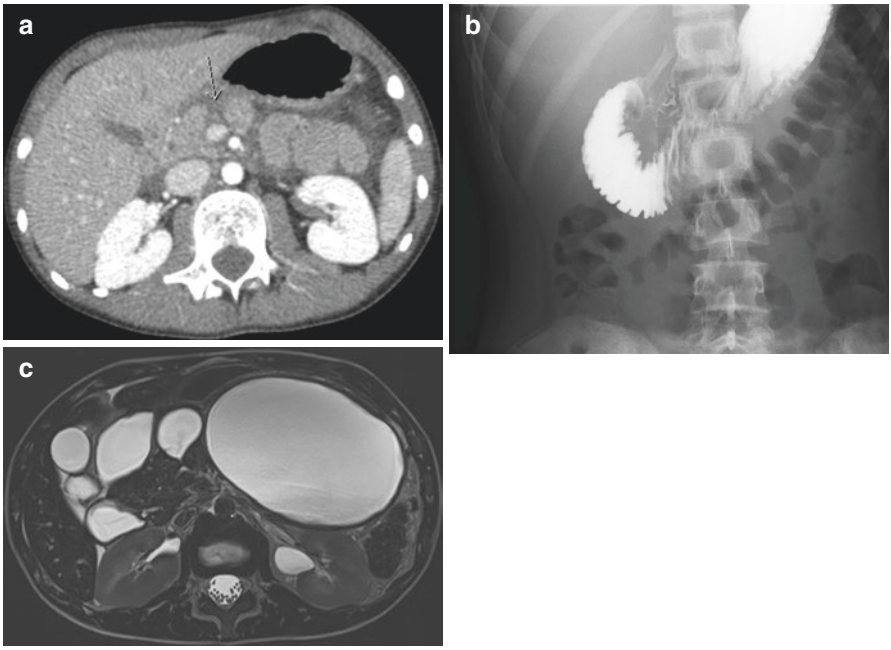

Fig. 4.7 (**a**–**c**) Grade III pancreatic injury. (**a**) Proximal fracture of the pancreatic neck in a child with bicycle handlebar injury. There is also fluid and edema in peripancreatic area. (**b**) Duodenography did not show duodenal injury. (**c**) MR demonstrates two pseudocysts anterior to the pancreas 3 weeks later. Pseudocyst on the right side communicates with the injured duct

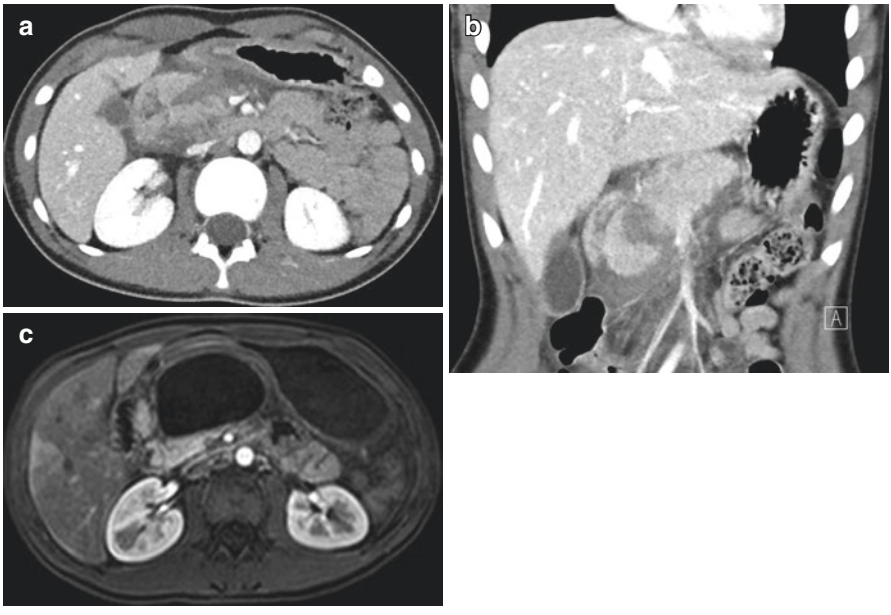

Fig. 4.8 (**a**–**c**) Grade IV injury. Extensive fracture of the pancreatic neck and head involving the ampulla with surrounding edema and fluid in (**a**) axial and (**b**) coronal CT images. (**c**) Three weeks later, MR shows a large pseudocyst communicating with the injured proximal duct

Fig. 4.9 CT image of a young woman with a gunshot wound in the upper abdomen. Image shows bullet track extending through hepatic segment III and pancreatic body to the anterior aspect of the spine. In operation, a laceration without ductal involvement was found in the pancreas

Peripancreatic fluid may be related also to aggressive resuscitation or injuries to adjacent organs. In contrast, sometimes the true extent of the pancreatic injury is only revealed at surgery (Fig. 4.9).

4.7 Role of MRCP and ERCP

Since difficulties in detecting pancreatic ductal injuries arise, magnetic resonance cholangiopancreatography (MRCP) can be used as a noninvasive alternative for direct imaging of the pancreatic duct. Secretin-stimulated MRCP provides dynamic information of leakage from the main pancreatic duct. In addition, MRCP may demonstrate the pancreatic parenchymal injury, as well as pathologic fluid collections and their ductal connections.

The most reliable method to assess the patency of the main pancreatic duct is to perform endoscopic retrograde cholangiopancreatography (ERCP), although it is usually not available outside office hours. ERCP is invasive and has potential complications but also includes a therapeutic option with the possibility to place a stent to control leak from a partially injured pancreatic duct.

4.8 Imaging Findings in Duodenal Injuries

CT findings of duodenal injuries range from contusion or intramural hematoma to complete perforation or devascularization. Distinction between duodenal wall hematoma and perforation is critical. On imaging, typical direct sign of duodenal hematoma or contusion is a focal asymmetric wall thickening (>4 mm) from edema or hyperdense intramural hematoma (Fig. 4.1). Gastric outlet obstruction is a common complication.

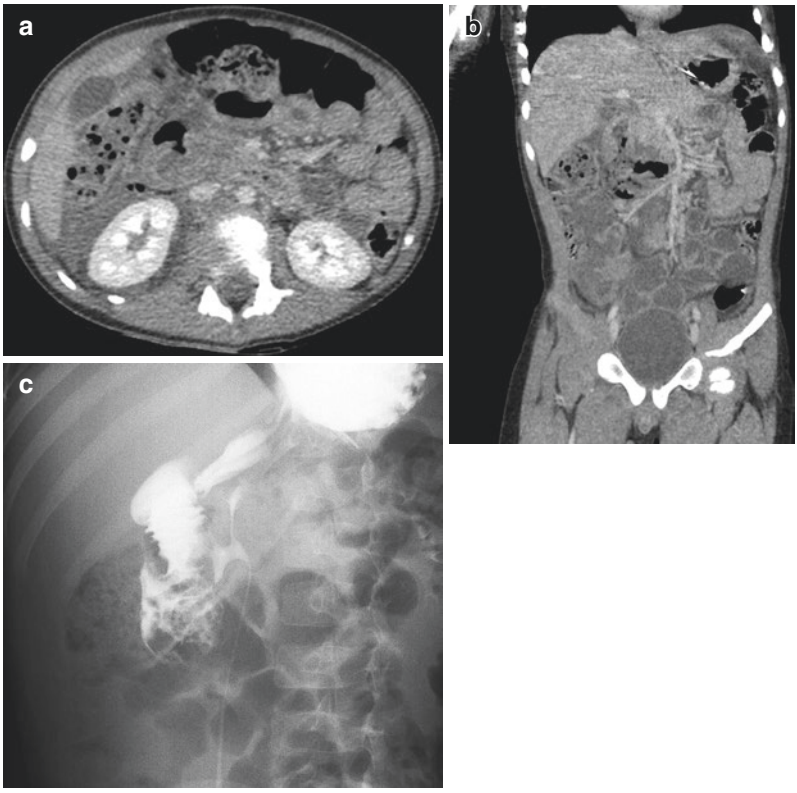

Fig. 4.10 (**a**–**c**) A 5-year-old boy with history of fall with a heavy object over the abdomen. (**a**) Axial and (**b**) coronal CT images show signs of duodenal perforation including discontinuity of the wall in descending part of the duodenum, extraluminal gas bubbles adjacent to the duodenum, and fluid in intra- and retroperitoneal space. (**c**) Fluoroscopy examination demonstrates leakage of contrast material outside the duodenum. At operation, the laceration involved 250° of the circumference of the descending part of the duodenum

Imaging findings in duodenal perforation include discontinuity and nonenhancement of the duodenal wall, extraluminal gas adjacent to the duodenum, and extravasation of positive contrast material (if administered) into the retroperitoneum (Figs. 4.9, 4.10, 4.11, and 4.12). Secondary signs are periduodenal fluid or hemorrhage and fat stranding, which can be associated with both intramural hematomas and perforations.

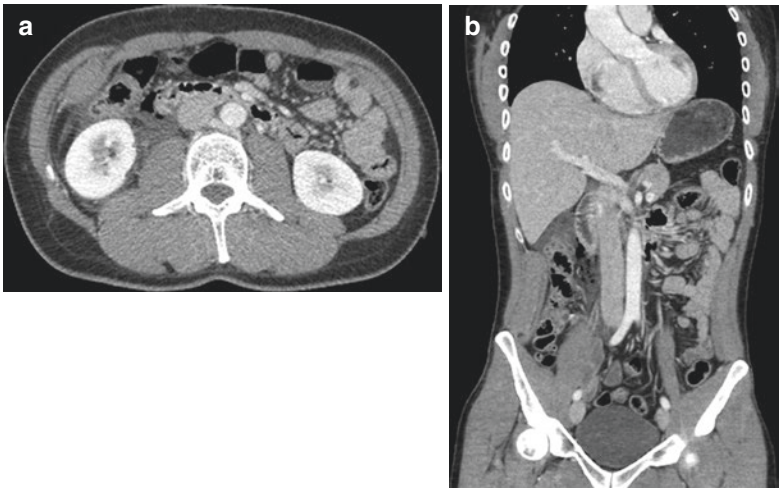

Fig. 4.11 (**a**, **b**) Duodenal perforation after accidental fall. Extraluminal gas bubbles adjacent to the duodenum in (**a**) axial and (**b**) coronal CT images. Free fluid is seen as a secondary sign of perforation

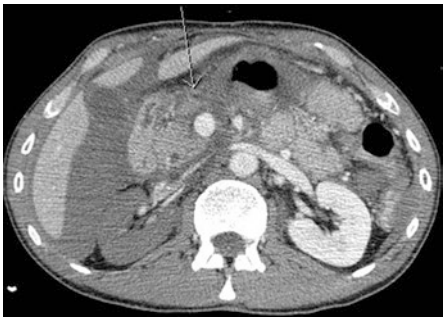

Fig. 4.12 Nonenhancement and discontinuity of the wall at the duodenal bulb after blunt abdominal trauma. There is also traumatic dissection in the right renal artery and nonenhancing right kidney

Bibliography

1. Asensio JA, Petrone P, Roldan G, Pak-art R, Salim A. Pancreatic and duodenal injuries. Complex and lethal. Scand J Surg. 2002;91:81–6.
2. Debi U, Kaur R, Prasad KK, Sinha KK, Sinha A, Singh K. Pancreatic trauma: a concise review. World J Gastroenterol. 2013;19(47):9003–11.
3. Gupta A, Stuhlfaut JW, Fleming KW, Lucey BC, Soto JA. Blunt trauma of the pancreas and biliary tract: a multimodality imaging approach to diagnosis. Radiographics. 2008;24:1381–95.
4. Leppäniemi A, Haapiainen R, Kiviluoto T, Lempinen M. Pancreatic trauma: acute and late manifestations. Br J Surg. 1988;75:165–7.
5. Melamud K, LeBedis CA, Soto JA. Imaging of pancreatic and duodenal trauma. Radiol Clin N Am. 2015;53:757–71.

CT Scan in Blunt Gastrointestinal Trauma

5

Gustavo Pereira Fraga and Rao Ivatury

5.1 Introduction

Abdominal injury as a result of penetrating or blunt trauma may represent a life-threatening condition requiring rapid diagnosis and treatment. The Eastern Association for the Surgery of Trauma Multi-institutional Hollow Viscus Injury (HVI) study, the largest retrospective hollow viscus injury to date, found the incidence of blunt small bowel injury (BSBI) of 1.1%, blunt colonic injury as 0.3% (30.2% of patients diagnosed with HVI had a colon injury), and the incidence of blunt gastric injury to be much lower (only 4.3% of a total of 2632 patients identified with HVI) [1, 2].

Direct bowel or mesenteric injury occurs in approximately 1–5% of all blunt abdominal traumas, and its incidence has increased with the growing number of automobile crashes [3–6]. The small bowel is the most frequently injured viscus in penetrating abdominal trauma and currently the third most common injury following blunt trauma. The frequency of isolated BSBI in abdominal trauma reported in the literature ranges from 31.4 to 59% [1, 3, 5]. The frequency of BSBI in children appears lower than the incidence rates reported for adult populations [7].

The diagnosis of significant intra-abdominal injury is a challenge in blunt trauma. The association between mechanism of trauma and a careful physical examination remains the most important method to determine the need for exploratory laparotomy. The sudden deceleration caused by the kinematics of automobile crashes, associated with the compression caused by the seat belt, stretching and pulling the

G.P. Fraga, M.D., Ph.D., F.A.C.S. (✉)
Division of Trauma Surgery, Department of Surgery, School of Medical Sciences, University of Campinas, Campinas, São Paulo, Brazil
e-mail: fragagp2008@gmail.com

R. Ivatury, M.D., F.A.C.S., F.C.C.M.
Virginia Commonwealth University, Richmond, VA, USA

F. Catena et al. (eds.), *CT Scan in Abdominal Emergency Surgery*, Hot Topics in Acute Care Surgery and Trauma, https://doi.org/10.1007/978-3-319-48347-4_5

bowel's attachment points, accounts for most injuries found. The diagnosis is notoriously difficult, as nearly half the patients may have no complaints or external signs of abdominal injury on admission to the hospital. Diagnosis of BSBI is sometimes delayed, especially in patients with multiple injuries, head trauma, or intoxicated [4, 5, 8–10]. A bruise across the abdomen inflicted by a seat belt ("seat belt sign") and ongoing abdominal pain are known associated risk factors of BSBI. Fakhry et al. [4] observed that 67.7% of 198 patients with BSBI initially presented with signs or symptoms highly suggestive of this injury. In the EAST study, the seat belt sign was associated with a 4.7-fold increase in relative risk of BSBI in patients following motor vehicle crashes [1].

The introduction and refinement of diagnostic procedures and imaging studies, such as computed tomographic (CT) scan and focused abdominal sonography for trauma (FAST), have contributed significantly in the new trends of abdominal injury management. CT scan is now considered as a rapid means of assessment for the early detection of intraperitoneal injury. In patients with multiple traumas, the "panscan" (CT of the head, neck, chest, abdomen, and pelvis) has become the necessary step to identify and define the severity of the injuries. With the increasing frequency of nonoperative management of blunt abdominal trauma, the diagnosis of BSBI is now more frequently made on the basis of clinical signs or an abnormal CT scan rather than as an associated injury at a trauma laparotomy. With the advancement of technology and the use of multislice CT scanners, capable of performing thinner sections more quickly, with fewer motion artifacts, and allowing multiplanar reformations, CT scan has a high sensitivity to diagnose BSBI, ranging from 64 to 95% and an accuracy of 80–90%, providing useful anatomic details such as contrast extravasation and extraluminal air. The longer the time interval between the trauma and the CT scan, the higher the chances of the CT scan diagnosing BSBI [11–15].

5.2 CT Technique

The advent of multidetector CT (MDCT) has increased image resolution with thinner collimation and fewer artifacts and has decreased scanning times. MDCT also allows high-quality two- or three-dimensional multiplanar reformatted images to be obtained, aiding in the diagnosis of injuries in the trauma patient. MDCT scanners offer the possibility to acquire images at multiple phases of intravenous contrast enhancement [16, 17]. The radiation dose delivered should be the minimum necessary.

The MDCT protocol includes arterial phase images to facilitate detection of trauma to the mesentery and portal veins or delayed phase images of the abdomen and pelvis, acquired 60–80 s after the beginning of intravenous contrast material administration [16, 17].

Besides requiring expertise in the interpretation of images, the sensitivity of the method depends on the technological generation of the device. Even using an advanced imaging technique MDCT, the diagnosis of BSBI can be missed or delayed [18–20].

5.3 CT Findings

BSBI can be classified as a partial- or full-thickness injury. Partial-thickness BSBI results in contusion of the bowel wall and can be seen on MDCT as a focal region of bowel wall thickening, usually greater than 3–4 mm in thickness. BSBI with full-thickness bowel injury includes CT findings considered to be specific: luminal or oral contrast content extravasation (rarely identified when no oral contrast is routinely given to trauma patients) and discontinuity of hollow viscus wall. CT findings considered suggestive of BSBI are pneumoperitoneum (sensitivity of 30–60% since extraintestinal barotraumas/mechanical ventilation may also cause it), gas bubbles close to the injured hollow viscus, thickened (>4–5 mm) bowel wall, bowel wall hematoma, and intraperitoneal fluid of unknown source.

The latter findings include the presence of free fluid in the cavity without solid organ injury, striking or focal densification of the mesenteric fat, dilated bowel loops, pneumoperitoneum, thickening of the intestinal wall, extravasation of contrast, and discontinuity of the intestinal wall (rarely identified). Most of these findings suggest but do not establish the diagnosis of BSBI [18–24]. Patients with a Chance-type vertebral fracture and large abdominal wall hematoma have a higher risk of injury to the bowel or mesentery.

The largest review of the literature, involving 518 patients subjected to abdominal trauma CT imaging, 13% of all BSBI (both small bowel and/or mesenteric injuries), had normal abdominal CT scans [22]. In the study by Ekeh et al. [18] analyzing 57 patients with BSBI who underwent CT, in 19.2% of examinations, findings were not identified to be consistent with bowel injury. In the reports by Matsushima et al. [19], 19% of the exam results were considered normal. The experience from University of Campinas with 26 patients with BSBI and CT exam considering "pre-MDCT" (period 1994–2005) and "post-MDCT" (2005–2012), according to the time of implementation of a 64-slice MDCT, there were 13% CT scans considered normal in the first period, and in the last period, after a detailed examination by an experienced radiologist, all had findings consistent with injury to hollow viscera [20]. Kemmeter et al. [23] reviewed 69 patients with blunt SBI and found that 13 of the cases (38%) had enteric injuries that were missed by the initial CT scan. Fang et al. [24] reported a 10.2% (5 out of 49 scans) false-negative rate in patients that had SBI with perforation.

The more specific signs are not highly sensitive, and the more sensitive signs are not highly specific (Table 5.1) [17].

Free fluid in the cavity is the most common CT finding noted in 50–90% of the patients with BSBI (Fig. 5.1) [18–22].

Pneumoperitoneum is a highly suggestive, but not pathognomonic, sign of bowel perforation (Figs. 5.2 and 5.3). It is important to review carefully all phases acquired because air outside the intestinal lumen may appear only on delayed images. Extraluminal air is usually a sign of intestinal perforation but can also be the consequence of intraperitoneal rupture of the urinary bladder and pulmonary trauma (pneumothorax or pneumomediastinum) or can be a "pseudopneumoperitoneum" that corresponds to air confined between the abdominal wall and the parietal peritoneum [13, 16, 18–22].

Table 5.1 Sensitivity and specificity of various CT signs of bowel injury

Sign	Sensitivity (%)	Specificity (%)
Free peritoneal fluid	90–100	15–25
Mesenteric fat striking or focal densification	70–77	40–90
Abnormal bowel wall enhancement	10–15	90
Focal bowel wall thickening	55–75	90
Extraluminal air	30–60	95
Extraluminal oral contrast material	8–15	100
Bowel wall discontinuity	5–10	100

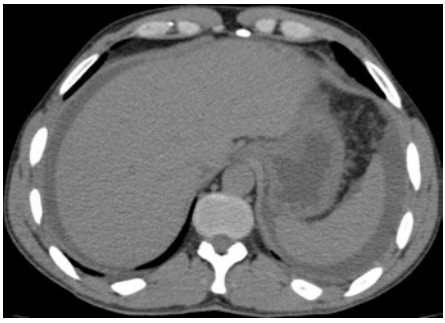

Fig. 5.1 Axial contrast-enhanced CT image in a BSBI patient with moderate amount of hyperattenuation of perihepatic and perisplenic free fluid, without injury to the solid viscera

Fig. 5.2 Axial contrast CT image showing pneumoperitoneum

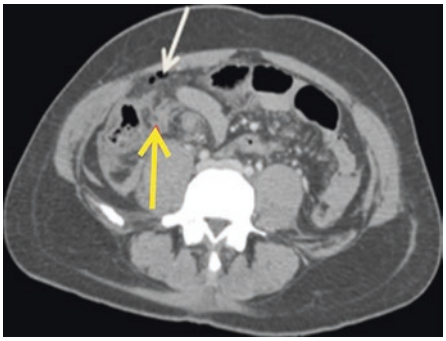

Fig. 5.3 Blunt abdominal trauma with injury to the distal ileum. CT of the abdomen after the intravenous administration of iodinated contrast shows evidence of small bubbles of pneumoperitoneum (*white arrow*), as well as densification of mesenteric fat, representing edema and hematoma (*yellow arrow*) adjacent to the lacerated segment of the small bowel

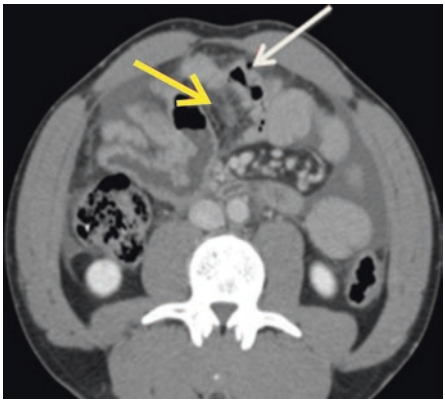

Fig. 5.4 Blunt abdominal trauma with injury to the jejunum-ileum transition. CT of the abdomen after the intravenous administration of iodinated contrast shows evidence of a small bubble of pneumoperitoneum (*white arrow*), as well as densification of mesenteric fat (*yellow arrow*) adjacent to the injured segment of the small bowel, which has thickened walls

Localized thickening or abnormal enhancement of a bowel loop or segment is highly suggestive of a BSBI, such as a contusion, hematoma, ischemia secondary to mesenteric vascular trauma, or perforation. CT findings of mesenteric hematoma or densification of mesenteric fat (Figs. 5.4 and 5.5) are associated with a high likelihood of BSBI. Peritoneal active extravasation of contrast-enhanced blood (blush), mesenteric rent with internal hernia, beading or abrupt termination of the mesenteric vessels, and mesenteric hematoma are signs of mesenteric injuries on CT images [6, 13, 16, 18–22]. The combination of these findings increases the risk of a clinically important injury.

Extravasation of enteral contrast material is the most specific sign of bowel injury, but this finding is not common in BSBI.

Ruptures of the small bowel can be fatal, due to peritonitis. In some cases, especially when there is a delay in diagnosis, they can lead to sepsis from bacterial contamination, as well as cause blood loss with secondary intraperitoneal hemorrhage, significantly increasing the morbidity and mortality. A delay of more than

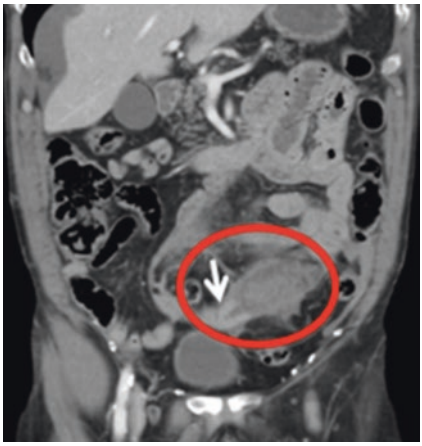

Fig. 5.5 Blunt abdominal trauma with injury to the ileal segment. CT of the abdomen after the intravenous administration of iodinated contrast, with coronal reformation, shows evidence of a large hematoma in the mesenteric fat adjacent to the injured segment of the small bowel, which has thickened walls (*white arrow*)

24 h is associated with approximately 30% of mortality [4, 5, 18, 22]. The role of CT in diagnosing hollow viscus injury after blunt abdominal trauma remains controversial, but the MDCT alone or in concert with physical examination is a valuable tool in the timely diagnosis and treatment of bowel and mesenteric injury caused by blunt trauma.

References

1. Watts DD, Fakhry SM. EAST multi-institutional hollow viscus injury research group. Incidence of hollow viscus injury in blunt trauma: an analysis from 275,557 trauma admissions from the East multi-institutional trial. J Trauma. 2003;54(2):289–94.
2. Williams MD, Watts D, Fakhry S. Colon Injury after blunt abdominal trauma: results of the EAST multi-institutional hollow viscus injury study. J Trauma. 2003;55(5):906–12.
3. Burney RE, Mueller GL, Coon WW, Thomas EJ, Mackenzie JR. Diagnosis of isolated small bowel injury following blunt abdominal trauma. Ann Emerg Med. 1983;12(2):71–4.
4. Fakhry SM, Brownstein M, Watts DD, Baker CC, Oller D. Relatively short diagnostic delays (<8 hours) produce morbidity and mortality in blunt small bowel injury: an analysis of time to operative intervention in 198 patients from a multicenter experience. J Trauma. 2000;48(3):408–15.
5. Fraga GP, Souza e Silva FHB, Almeida NA, Curi JCM, Mantovani M. Blunt abdominal trauma with small bowel injury: are isolated lesions riskier than associated lesions? Acta Cir Bras. 2008;23(2):196–201.
6. Yu J, Fulcher AS, Turner MA, Cockrell C, Halvorsen RA. Blunt bowel and mesenteric injury: MDCT diagnosis. Abdom Imaging. 2011;36(1):50–61.
7. Thompson SR, Holland AJA. Perforating small bowel injuries in children: influence of time to operative operation on outcome. Injury. 2005;36:1029–33.
8. Robbs JV, Moore SW, Pillay SP. Blunt abdominal trauma with jejunal injury: a review. J Trauma. 1980;20(4):308–11.
9. Schenk WG 3rd, Lonchyna V, Moylan JA. Perforation of the jejunum from blunt abdominal trauma. J Trauma. 1983;23(1):54–6.
10. Shapiro MB, Nance ML, Schiller HJ, Hoff WS, Kauder DR, Schwab CW. Nonoperative management of solid abdominal organ injuries from blunt trauma: impact of neurologic impairment. Am Surg. 2001;67:793–6.

11. Scaglione M, de Lutio di Castelguidone E, Scialpi M, Merola S, Diettrich AI, Lombardo P, et al. Blunt trauma to the gastrointestinal tract and mesentery: is there a role for helical CT in the decision-making process? Eur J Radiol. 2004;50(1):67–73.
12. Saku M, Yoshimitsu K, Murakami J, Nakamura Y, Oguri S, Noguchi T, et al. Small bowel perforation resulting from blunt abdominal trauma: interval change of radiological characteristics. Radiat Med. 2006;24(5):358–64.
13. Zissin R, Osadchy A, Gayer G. Abdominal CT findings in small bowel perforation. Br J Radiol. 2009;82(974):162–71.
14. Lawson CM, Daley BJ, Ormsby CB, Enderson B. Missed injuries in the era of the trauma scan. J Trauma. 2011;70(2):452–8.
15. Jha NK, Yadav SK, Sharma R, Sinha DK, Kumar S, Kerketta MD, et al. Characteristics of hollow viscus injury following blunt abdominal trauma; a single Centre experience from eastern India. Bull Emerg Trauma. 2014;2(4):156–60.
16. Miller LA, Shanmuganathan K. Multidetector CT evaluation of abdominal trauma. Radiol Clin North Am. 2005;43(6):1079–95.
17. Soto JA, Anderson SW. Multidetector CT of blunt abdominal trauma. Radiology. 2012;265(3):678–93.
18. Ekeh AP, Saxe J, Walusimbi M, Tchorz KM, Woods RJ, Anderson HL 3rd, et al. Diagnosis of blunt intestinal and mesenteric injury in the era of multidetector CT technology—are results better? J Trauma. 2008;65(2):354–9.
19. Matsushima K, Mangel PS, Schaefer EW, Frankel HL. Blunt hollow viscus and mesenteric injury: still underrecognized. World J Surg. 2013;37(4):759–65.
20. de Araújo RO, de Matos MP, Penachim TJ, Pereira BM, Mantovani ME, Rizoli S, et al. Jejunum and ileum blunt trauma: what has changed with the implementation of multislice computed tomography? Rev Col Bras Cir. 2014;41(4):278–84.
21. Brody JM, Leighton DB, Murphy BL, Abbott GF, Vaccaro JP, Jagminas L, et al. CT of blunt trauma bowel and mesenteric injury: typical findings and pitfalls in diagnosis. Radiographics. 2000;20(6):1525–37.
22. Fakhry SM, Watts DD, Luchette FA. Current diagnostic approaches lack sensitivity in the diagnosis of perforated blunt small bowel injury: analysis from 275,557 trauma admissions from the EAST multi-institutional HVI trial. J Trauma. 2003;54:295–306.
23. Kemmeter PR, Senagore AJ, Smith D, Oostendorp L. Dilemmas in the diagnosis of blunt enteric trauma. Am Surg. 1998;64:750–4.
24. Fang JF, Chen RJ, Lin BC, Hsu YB, Kao JL, Kao YC, et al. Small bowel perforation: is urgent surgery necessary? J Trauma. 1999;47(3):515–20.

6 Computed Tomography (CT Scan) in the Management of Genitourinary Trauma

Rodrigo Donalisio da Silva and Fernando J. Kim

6.1 Introduction

Trauma is a serious public health problem with significant social and economic costs. Worldwide, trauma accounts for 10% of all mortalities with approximately five million deaths each year. Trauma results in an exorbitant number of disabilities [1]. About half of the deaths due to trauma occur in people during their productive age, and it is the leading cause of death for people between 15 and 45 years old [2].

Genitourinary injury occurs in 2–5% of all trauma patients and in at least 10% of patients with abdominal trauma. Genitourinary trauma needs to be managed with close collaboration between the general and urologic trauma surgeons to improve outcomes.

6.2 Injury Grading and Scoring Systems for Genitourinary Injuries

The American Association for the Surgery of Trauma (AAST) Injury Scaling Committee devised a staging system for urologic injuries in 1989 [3, 4]. The system classifies organ-specific injuries which can help in decision-making regarding treatment options. The classifications of genitourinary injuries allow researchers to evaluate clinical significance, decision-making, complication rates, and outcomes [5–10].

R. Donalisio da Silva, M.D. • F.J. Kim, M.D., M.B.A., F.A.C.S. (✉)
Department of Urology, Denver Health Medical Center in Denver, Denver, CO, USA

Division of Urology, University of Colorado in Denver, Denver, CO, USA
e-mail: Fernando.Kim@dhha.org

F. Catena et al. (eds.), *CT Scan in Abdominal Emergency Surgery*, Hot Topics in Acute Care Surgery and Trauma, https://doi.org/10.1007/978-3-319-48347-4_6

6.3 Renal Trauma

Overall renal trauma is diagnosed in approximately 1–5% of all trauma patients and up to 10% of patients with abdominal trauma [11]. Blunt versus penetrating injuries vary according to the region analyzed and the population served, with penetrating injuries as high as 20% in urban centers [12–15]. Renal penetrating injuries caused by gunshot wounds are associated with other intra-abdominal organ injuries in nearly all patients and are close to 60% for patients with renal stab wounds. Other intra-abdominal organ injuries (non-urologic) are found in approximately 20–33% of patients with blunt renal trauma and 77–100% in penetrating renal injuries [6, 7, 11].

6.3.1 Indications for Image Studies in Patients with Suspected Renal Trauma

Deciding when to proceed with image workup for patient with suspected renal injuries should be based on clinical findings (vital signs, rib fracture, hematuria, flank ecchymosis, and others) and trauma mechanisms (rapid deceleration, significant trauma to the flank, rib fracture, flank ecchymosis, penetrating injuries of the abdomen or lower chest). Surgeons should not hesitate to order imaging studies in patients with known congenital conditions (i.e., UPJ obstruction) and/or anatomic abnormalities (renal cysts, horseshoe kidneys, etc.) because they are known to predispose patients to renal injury, even in lower energy accidents (Fig. 6.1). Recently, authors are attempting to identify which patients' image studies could be spared in an attempt to reduce radiation exposure, possible allergic reaction to contrast, and costs.

Indications for radiographic evaluation of patients with suspected renal trauma are gross hematuria, microscopic hematuria with hypotension, and the presence of associated injuries [11, 12]. Patients with penetrating trauma to the torso also benefit from image studies since they have a high incidence of renal injury. Children can be imaged using the same criteria as adults; however, indications such as hypotension are not as frequent as in adults.

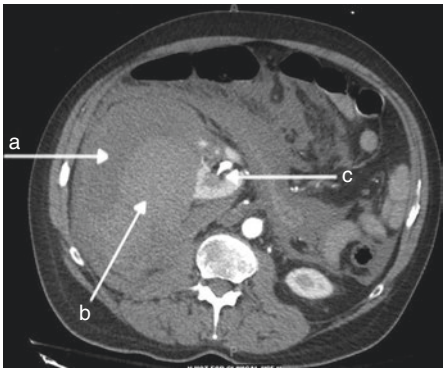

Fig. 6.1 Patient with known previous history of large renal cyst on the right kidney; (**a**) hematoma, (**b**) cyst, (**c**) kidney

CT scan is the image study that presents the higher sensitivity and specificity to diagnose and grade renal traumas compared to ultrasound (US), intravenous pyelogram (IVP), and angiography. CT scan can precisely identify the location of the injury and associated hematomas and evaluate other abdominal organs (Fig. 6.2).

CT scan of the abdomen and pelvis using IV contrast with immediate and delayed phases (10–15 min after IV contrast) should be done, unless there is a formal contraindication for the use of IV contrast. The immediate phase will be able to elucidate the location of the renal lacerations (Fig. 6.3); lack of contrast enhancement of the injured kidney may indicate a pedicle injury (Fig. 6.4). Delayed images will be

Fig. 6.2 Grade I renal laceration on the left kidney with small perirenal hematoma

Fig. 6.3 Contrast extravasation around the left kidney

Fig. 6.4 Lack of contrast in the right kidney

able to delineate the collecting system and ureters, demonstrating contrast extravasation if there is any injury involving the collecting system.

Spiral CT scan can be performed faster, generating fewer artifacts in patients with altered mental status who cannot cooperate adequately [11]. In some cases, three-dimensional reconstructions can improve the demonstration of complex lacerations of the parenchyma.

6.4 Ureteral Trauma

Ureteral trauma has a low incidence and accounts for approximately 1–2.5% of urinary tract trauma [10]. Most ureteral injuries are caused by penetrating trauma, particularly gunshot wounds (Fig. 6.5). Blunt trauma can damage the ureter in about 30% of patients [10]. The rates of missed ureteral injuries are reported to be 11% [13].

Patients with deceleration trauma mechanism and all penetrating injuries to the abdomen should raise suspicion for ureteral injuries. The upper ureter is more commonly injured in blunt trauma caused by decelerating mechanism, causing the renal pelvis to tear. In penetrating injuries, the lesions to the ureter are distributed along its length, but the upper ureter is also commonly injured [1, 10, 12].

Clinically, it is difficult to diagnose ureteral trauma. An isolated injury to the ureter is not common, and it is usually associated with severe injuries to the abdomen, pelvic bone, and spine [10]. The presence of hematuria is not a reliable indicator of the presence of ureteral injuries as it can be present in 50–70% of patients with ureteral injuries and is also associated with other more common urological traumas such as in the kidney, bladder, and urethra.

Iatrogenic injury may be noticed during the primary procedure (gynecologic, colorectal, and urologic procedures) when intravenous indigo carmine can be injected IV during cystoscopy to rule out ureteral injury. It may also be discovered later in the postoperative course by evidence of upper urinary tract obstruction, urinary fistula, sepsis, and/or flank pain. Early recognition is important because it facilitates the repair and reduces associated morbidity (renal damage, infection, and hypertension). Imaging studies are important to classify ureteral trauma because approach may vary depending on severity and trauma mechanism.

Fig. 6.5 Contrast extravasation on the left ureter

Fig. 6.6 Contrast extravasation on the left ureter

6.4.1 Radiological Evaluation of Patients with Suspected Ureteral Trauma

The radiological evaluation of ureteral trauma is a contrast-enhanced abdominal/pelvic CT with delayed imaging (CT-IVP) for stable trauma patients with suspected ureteral injuries [1, 12, 13]. The extravasation of contrast material of the ureter is the hallmark sign of ureteral injury (Fig. 6.6). Other signs that may be suggestive of ureteral injury are the presence of hydronephrosis, urinoma, or free liquid in the abdomen. In cases where the CT-IVP was not able to confirm the diagnoses, retrograde pyelogram is the gold standard to confirm the ureteral injury.

6.5 Bladder Trauma

The most common cause of traumatic bladder injury (excluding iatrogenic causes) is motor vehicle collisions, followed by falls, industrial trauma, and blows to the lower abdomen [14]. Pelvic fracture is found in 60–90% of patients with blunt bladder trauma, and 44% of the patients with bladder injuries have at least one intra-abdominal organ-associated injury [15]. The majority of bladder ruptures are extraperitoneal. A combination of bladder and urethral trauma can be found in 4.1–15% of the cases [15, 16]. Classification of traumatic bladder injuries can be done using the AAST injury scale or more commonly by classifying blunt vs. penetrating bladder injuries and extraperitoneal vs. intraperitoneal bladder injuries [4].

Extraperitoneal ruptures are almost always associated with pelvic fracture. The bladder can be injured on the same side as the fracture by the traction of its ligaments caused by the distortion of the pelvic anatomy. A countrecoup mechanism is the mechanism of injury when the bladder injury is found on the opposite side of the pelvic fracture. The bladder wall can be perforated by bone fragments [16].

The bladder dome is the weakest point of the bladder. A sudden rise in intravesical pressure can cause bladder rupture at the bladder dome, leading to intraperitoneal bladder rupture and urinary leakage inside the peritoneal cavity. A full bladder at the time of the trauma is a risk factor for intraperitoneal bladder rupture [16].

Bladder traumas can be graded according to AAST classification, but usually surgeons classify the bladder injuries according to mechanism of trauma (blunt vs. penetrating) and anatomical location (intraperitoneal, extraperitoneal, or combined intra- and extraperitoneal) [4].

6.5.1 Radiological Evaluation of Traumatic Bladder Injuries

Gross hematuria is the most common sign of bladder injury, while pelvic fracture is the most common associated injury with bladder rupture. In patients with gross hematuria and pelvic fracture, bladder injury can be found in 29% of patients. An absolute indication to proceed with CT cystography is the combination of gross hematuria and pelvic fracture [1, 12].

Classically, cystography is the diagnostic modality for suspected bladder rupture [1, 12]. Cystography can be performed by filling the bladder with at least 350 mL of contrast. Sensitivity (90–95%) and specificity (100%) of plain or CT cystography are similar [15]. The decision to perform a plain or CT cystography should be based on potential benefits of the CT scan in diagnosing associated injuries, time to perform the exam, availability of resources, and costs.

Surgeons must be aware that clamping the Foley catheter during the excretory phase of CT or IVP is not recommended to diagnose bladder injury because this procedure lacks the sensitivity to exclude bladder injuries [15].

The presence of contrast material within bowel loops and/or outlining abdominal viscera is diagnostic for intraperitoneal bladder rupture. Extraperitoneal bladder ruptures are associated with extravasation of the contrast in the perivesical soft tissue (Fig. 6.7).

Fig. 6.7 Extraperitoneal bladder rupture

6.6 Urethral Trauma

Trauma to the anterior urethra may be a result of sudden compression at the level of the mid-urethra to bulbar urethra against the pubic bones. The posterior urethral injuries can be found in 4–10% of patients. AAST grading scale can be used to grade urethral injuries; however, urologists usually classify these lesions in partial urethral disruption or complete urethral disruption [4].

Blood at the urethral meatus, urinary retention, perineal hematoma, and inability to palpate the prostate on a rectal exam should raise suspicion of urethral injuries.

6.6.1 Radiological Evaluation of Urethral Injuries

Although CT scan of the pelvis and urethra can demonstrate urethral injury, the retrograde urethrogram (RUG) is the image modality more frequently performed to evaluate urethral injuries. In patients with suspected urethral injuries, iodinated contrast is injected via a catheter within the urethral meatus followed by plain radiograph (Fig. 6.8). In the normal RUG, contrast can delineate normal anatomy of the urethra and bladder. In incomplete urethral transection, contrast extravasation will be seen in the urethra, and the contrast should still reach the bladder. In complete urethral transection, the contrast extravasation will be present in the location of the urethral injury, and no contrast will be present in the bladder (Fig. 6.9). Physicians must obtain plain and oblique films to better evaluate the urethra.

CT scan has a limited role in the acute phase of urethral disruption despite the good sensitivity in identifying associated injuries (pelvic fracture, pelvic hematomas, and rectal injuries) and the possibility to be used to guide the placement of suprapubic tubes (the bladder can be displaced by pelvic hematoma). CT scans can be less useful than other imaging modalities because in order to obtain good image quality, patients need to be fully cooperative and must have the ability to void.

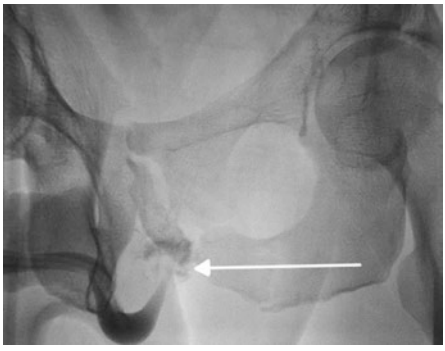

Fig. 6.8 Complete urethral disruption; contrast media not reaching the bladder

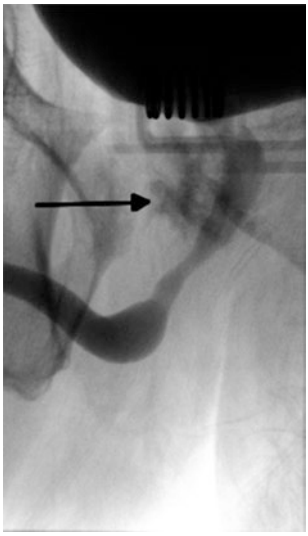

Fig. 6.9 Urethral injury with extravasation

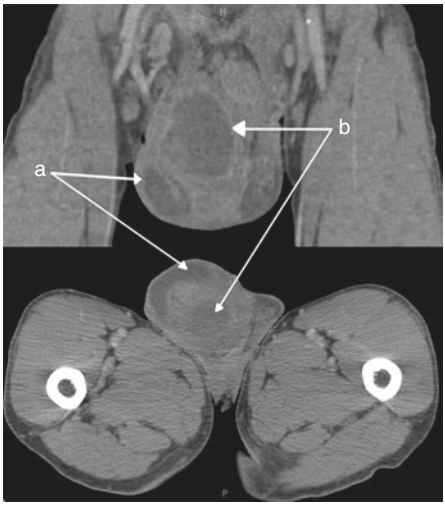

Fig. 6.10 Testicular trauma; (**a**) scrotal hematoma, (**b**) intratesticular hematoma

6.7 Testicular Trauma

Blunt scrotal trauma can cause testicular rupture in approximately 50% of cases. Testicular rupture is associated with pain, nausea, and vomiting. Ultrasonography is usually the first image study performed and can determine if the hematoma is intra- and/or extra-testicular with associated testicular contusion or rupture (Fig. 6.10).

Traumatic dislocation of the testis is reported in the literature associated with motor vehicle accidents and pelvic trauma. CT scan can easily diagnose and identify testicle dislocation in patients with pelvic trauma when the testicle cannot be identified in the physical exam.

Explosive device-related injuries can compromise the genitals in approximately 9% of patients. Most common CT scan findings related to testicular injury are loss of definition of the tunica albuginea and intratesticular contrast blushing. In patients with pelvic trauma that had a CT scan to evaluate the pelvis, CT findings related to the testis can contribute to the decision of additional US imaging with or without scrotal exploration.

References

1. Serafetinides E, Kitrey ND, Djakovic N, Kuehhas FE, Lumen N, Sharma DM, et al. Review of the current management of upper urinary tract injuries by the EAU Trauma Guidelines Panel. Eur Urol. 2015;67(5):930–6.
2. Søreide K. Epidemiology of major trauma. Br J Surg. 2009;96(7):697–8.
3. Moore EE, Moore FA. American Association for the Surgery of Trauma Organ Injury Scaling: 50th anniversary review article of the Journal of Trauma. J Trauma. 2010;69(6):1600–1.
4. Injury Scoring Scale A Resource for Trauma Care Professionals The American Association for the Surgery of Trauma. http://www.aast.org/Library/TraumaTools/InjuryScoringScales.aspx.
5. Tasian GE, Aaronson DS, McAninch JW. Evaluation of renal function after major renal injury: correlation with the American Association for the Surgery of Trauma Injury Scale. J Urol. 2010;183(1):196–200.
6. Shariat SF, Trinh QD, Morey AF, Stage KH, Roehrborn CG, Valiquette L, et al. Development of a highly accurate nomogram for prediction of the need for exploration in patients with renal trauma. J Trauma. 2008;64(6):1451–8.
7. Shariat SF, Roehrborn CG, Karakiewicz PI, Dhami G, Stage KH. Evidence-based validation of the predictive value of the American Association for the Surgery of Trauma Kidney Injury Scale. J Trauma. 2007;62(4):933–9.
8. Reis LO, Kim FJ, Moore EE, Hirano ES, Fraga GP, Nascimento B, et al. Update in the classification and treatment of complex renal injuries. Rev Col Bras Cir. 2013;40(4):347–50.
9. Kim FJ, Pompeo A, Sehrt D, Molina WR, Mariano da Costa RM, Juliano C, et al. Early effectiveness of endoscopic posterior urethra primary alignment. J Trauma Acute Care Surg. 2013;75(2):189–94.
10. Kim FJ, Chammas MF, Gewehr EV, Campagna A, Moore EE. Laparoscopic management of intraperitoneal bladder rupture secondary to blunt abdominal trauma using intracorporeal single layer suturing technique. J Trauma. 2008;65(1):234–6.
11. Lynch TH, Martínez-Piñeiro L, Plas E, Serafetinides E, Türkeri L, Santucci RA, et al. EAU guidelines on urological trauma. Eur Urol. 2005;47(1):1–15.
12. Morey AF, Brandes S, Dugi DD, Armstrong JH, Breyer BN, Broghammer JA, et al. Urotrauma: AUA guideline. J Urol. 2014;192(2):327–35.
13. Shariat SF, Jenkins A, Roehrborn CG, Karam JA, Stage KH, Karakiewicz PI. Features and outcomes of patients with grade IV renal injury. BJU Int 2008;102(6):728–733; discussion 33.
14. Bjurlin MA, Fantus RJ, Mellett MM, Goble SM. Genitourinary injuries in pelvic fracture morbidity and mortality using the National Trauma Data Bank. J Trauma. 2009;67(5):1033–9.
15. Deibert CM, Spencer BA. The association between operative repair of bladder injury and improved survival: results from the National Trauma Data Bank. J Urol. 2011;186(1):151–5.
16. Gomez RG, Ceballos L, Coburn M, Corriere JN, Dixon CM, Lobel B, et al. Consensus statement on bladder injuries. BJU Int. 2004;94(1):27–32.

Acute Cholecystitis

7

Giulia Montori, Anna Pecorelli, Sandro Sironi, Paola Fugazzola, Federico Coccolini, Cecilia Merli, Michele Pisano, and Luca Ansaloni

7.1 Introduction

Acute cholecystitis (AC) is considered the inflammation of the gallbladder, and it is caused in most cases by the presence of gallstones. It can be associated to local or general signs of inflammation and the diagnosis is given from a combination of detailed clinical history and clinical examination, laboratory tests and images as reported by the recent World Society of Emergency Surgery (WSES) guidelines [1]. AC can affect 10–20% of patients with gallstones, and in up to 39% of cases, a gangrenous AC was found [2, 3].

Another clinical entity that mimics the lithiasic AC is the acute acalculous cholecystitis (AAC) [4] that represents 2–15% of all AC. However, AAC is related with a high mortality (10% up to 90% comparing to 1% of AC) because patients with AAC are often critically ill patients with hypovolemic shock, heart failure, diabetes mellitus, dehydration, sepsis, and vasculitis.

Abdominal ultrasound (US) is considered the first and preferred initial imaging technique to detect the presence of gallstones and to evaluate the inflammatory changes in the gallbladder [1]. US is also valuable because it is free from ionizing radiation and is easily available and not invasive with a good diagnostic accuracy [1].

G. Montori • P. Fugazzola • M. Pisano
Unit of General and Emergency Surgery, Papa Giovanni XXIII Hospital, P.zza OMS 1, Bergamo 24128, Italy

A. Pecorelli • S. Sironi
Department of Radiology, Papa Giovanni XXIII Hospital, Milano-Bicocca University, Bergamo, Italy

F. Coccolini • L. Ansaloni, M.D. (✉)
General, Emergency and Trauma Surgery Department, Bufalini Hospital, Cesena, Italy
e-mail: lansaloni@asst-pg23.it

C. Merli
Unit of Emergency Medicine, Papa Giovanni XXIII Hospital, Bergamo, Italy

F. Catena et al. (eds.), *CT Scan in Abdominal Emergency Surgery*, Hot Topics in Acute Care Surgery and Trauma, https://doi.org/10.1007/978-3-319-48347-4_7

However computed tomography (CT), even if it is related to ionizing radiation, seems to be more useful when US is not diagnostic and in patients with confusing clinical condition or to evaluate eventual AC complications [1].

7.2 Value of Computed Tomography

As mentioned above, the role of CT in AC is not clearly defined. In the literature comparing with US, CT shows sensitivity from 85 to 94% (95% CI, 66–95 and 95% CI, 73, 99%, respectively) and specificity from 59 up to 81% (95% CI 42, 74 and 95% CI 69–90%, respectively), while for US they are, respectively, 81 and 83% [15].

A recent meta-analysis that summarized the role of the different diagnostic techniques in AC shows that cholescintigraphy has the highest diagnostic accuracy and the accuracy of US leaves a substantial margin of error, comparable to that of MR imaging, while CT is still under evaluation [5].

The use of US remains crucial in AC (Figs. 7.1 and 7.2), however there is an increased number of patients undergoing CT especially in suspected complicated AC (Table 7.1) [3, 6].

In patients where AC is suspected, in watching the CT images, the attention should be focused on the gallbladder wall (thickness, enhancement, continuity, irregularity, and the presence or absence of gas), the gallbladder lumen (presence or absence of gallstones, gas, high-density fluid, sloughed mucosa), the pericholecystic space (fat stranding, fluid, abscess), and the characteristics of pericholecystic organs (the liver, peritoneal collection, small bowel obstruction) [3, 6].

Gallbladder perforation is rare, without specific clinical signs at presentation, and often requires an urgent surgical intervention to reduce morbidity and mortality rates. For this reason, some authors like Niemeier proposed a classification for perforated gallbladder dividing it in type I (acute free perforation into the peritoneal cavity without protective adhesions), type II (subacute perforation surrounded by a pericholecystic abscess walled off by adhesions), and type III (chronic perforation with a fistula between the gallbladder and viscus) [7]. It has been pointed out that CT scan scores better than US in detecting gallbladder perforations, establishing a

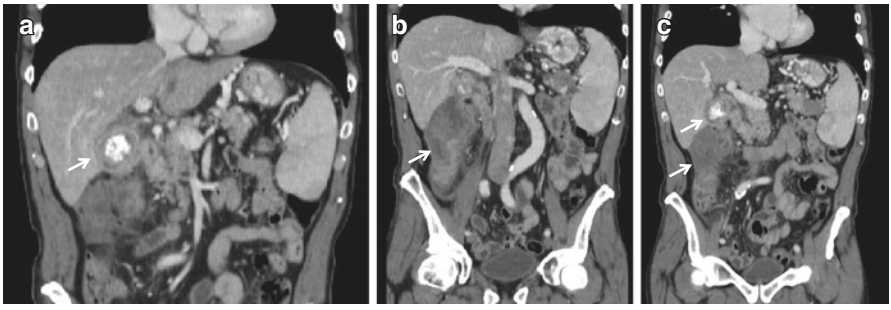

Fig. 7.1 Coronal reconstruction CT scan with use of intravenous contrast. (**a**, **c** *white arrow*) shows enhancing thickness wall of gallbladder with gallstone inside in acute cholecystitis. (**b**, **c** *white arrow*) shows pericholecystic fluid

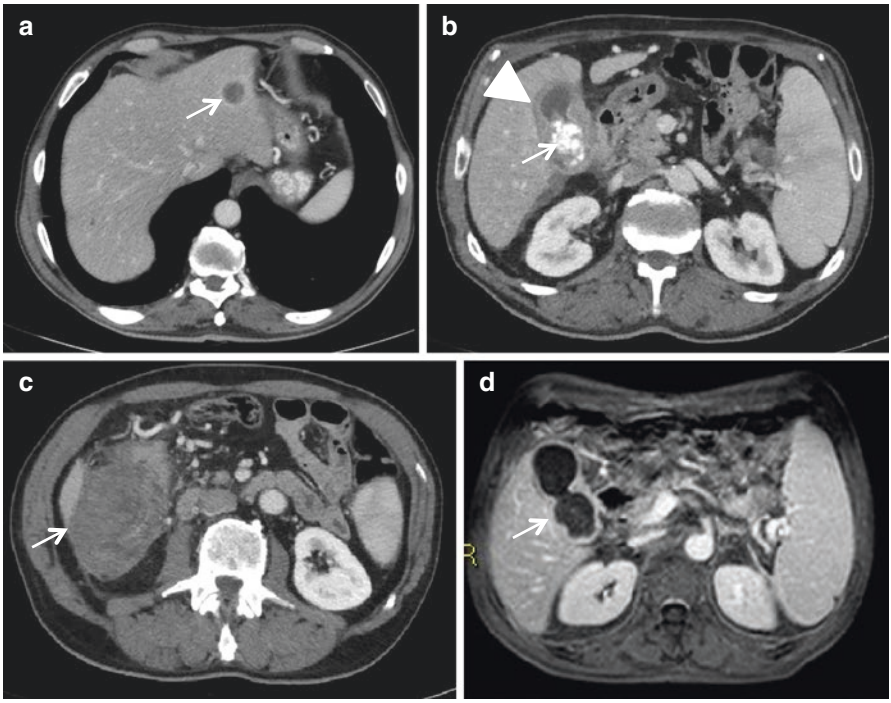

Fig. 7.2 Axial reconstruction of a CT scan with intravenous contrast shows gallbladder fundus with enhancing thickness wall (**a**, *white arrow*); enhancing thickness wall of gallbladder (**b**, *head-arrow*) with gallstone inside in acute cholecystitis (**b**, *white arrow*); pericholecystic fluid (**c**, *white arrow*); Magnetic Resonance Image shows acute cholecystits (**d**, *white arrow*)

Table 7.1 Clinical condition related to CT findings

Clinical condition	CT findings
Acute cholecystitis	Detecting (or not) gallstones in the gallbladder, thickened (more than 3 mm) and enhancing wall, stranding pericholecystic fat with or without pericholecystic fluid
Gangrenous cholecystitis	Detecting (or not) gallstones, non-enhancing wall or irregular enhancing wall with defect, sloughed membranes, pericholecystic fat with fluid
Perforated cholecystitis	Detecting (or not) gallstones, focal defect of gallbladder wall, pericholecystic fluid with or without pericholecystic or hepatic abscess
Emphysematous cholecystitis	Detecting (or not) gallstones in the gallbladder, presence of intramural gas and enhancing wall, stranding pericholecystic fat with or without pericholecystic fluid

prompt definitive diagnosis of gallbladder perforation and hence decreasing morbidity and mortality [7].

Some authors suggest that a dual-phase (unenhanced and contrast-enhanced images) abdominal CT can be important to predict the rate of conversion from laparoscopic to laparotomic cholecystectomy [8]. The most factors that seem to

be associated with conversion were the absence of gallbladder wall enhancement (58% vs. 40% in non-conversion group, $p = 0.02$) and the presence of infundibular gallstones (78% vs. 22% in non-conversion group, $p = 0.04$) [8]. These data could suggest that contrast-enhanced CT can give a better selection of patients and can minimize time of conversion.

7.3 CT Findings in AC

The detection of the following findings at the CT scan is reported as highest sensitivity and specificity criteria of AC: a gallbladder distention (in 41% of cases), pericholecystic fat density and collection (respectively, in 52 and 31% of cases), gallbladder wall thickness of more than 7 mm (in 59% of cases), subserosal edema (in 31% of cases), local or widespread absence of gallbladder wall enhancement, and high gallbladder bile attenuation (in 24% of cases) (Figs. 7.3, 7.4, and 7.5) [3, 8, 9]. In case of pericholecystic abscess, it is possible to find focal mural defects or mural abscess with a focal intramural bulge [3]. These signs have specificity for complicated or perforated AC close to 90% [3].

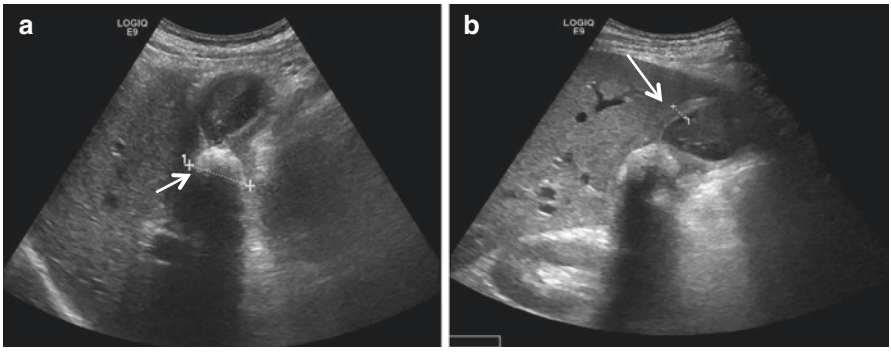

Fig. 7.3 Abdominal US shows acute cholecystits with gallstone inside and posterior shadow cone (**a**, *white arrow*); enhancing thickness wall of gallbladder (**b**, *white arrow*)

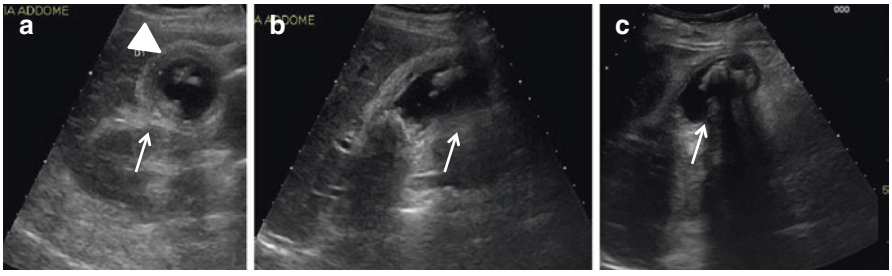

Fig. 7.4 Abdominal US shows acute cholecystits with enhancing wall with very thickness wall of gallbladder (**a**, *white arrow*); gallstone inside and posterior shadow cone (**b**, *white arrow*)

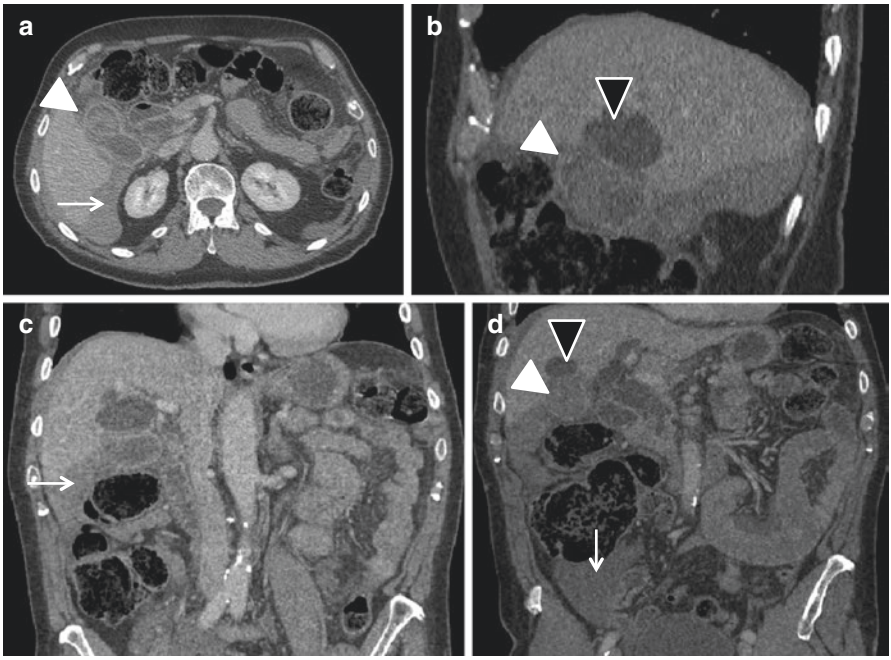

Fig. 7.5 Axial reconstruction of a CT scan with intravenous contrast shows gallbladder fundus with enhancing thickness wall (**a**, *headarrow*) and pericholecystic fluid (**a**, *white arrow*); sagittal reconstruction of CT scan with use of intravenous contrast shows irregular enhancing wall with defect (**b**, *white headarrow*) and intrahepatic abscess (**b**, *black headarrow*); coronal reconstruction of CT scan with use of intravenous contrast shows periheaptic fluid (**c**, *white arrow*); coronal reconstruction of CT scan with use of intravenous contrast shows periheaptic fluid (**d**, *white arrow*) with irregular enhancing wall with defect (**d**, *white headarrow*) and intrahepatic abscess (**d**, *black headarrow*)

However, it has to be pointed out that CT has a lower sensitivity in detecting gallstones compared to US [3].

Gangrenous AC (GAC) shows an increase in transient focal enhancement of the liver adjacent to the gallbladder during the arterial phase of dynamic CT and an attenuation ratio of the arterial phase ≥1.46 [10]. These characteristics seem to be predictive for GAC helping for a rapid diagnosis to reduce complication rates [10].

A particular entity is the xanthogranulomatous cholecystitis that is a rare inflammatory disease of the gallbladder due to an acute and chronic inflammatory cell infiltration and macrophages containing lipids forming such as foamy histiocytes [11]. Clinical manifestations are similar to AC, and the CT images show in most of patients a diffuse thickening of the gallbladder wall with an aggressive presentation and extent into adjacent structures, which mimic a gallbladder carcinoma, with intramural hypo-attenuated nodules that are suggestive for (but also similar to) adenomyomatosis [11].

A particular CT finding is the emphysematous AC secondary to infections by gas-forming organisms such as *Clostridium welchii*, especially in diabetic patients [3].

Other rare cases are the Mirizzi syndrome (impacted gallstone in the gallbladder neck or cystic duct that causes an extrinsic compression of the common hepatic duct, dilatation of intrahepatic bile ducts) and the cholecystocholedochal fistula from recurrent gallbladder inflammation around the impacted gallstones [3].

Conclusions

Although according to the literature and WSES guidelines the first radiologic technique for diagnosis of AC remains US, CT scan may play an important role in complicated AC or in patients where no clear symptoms are present. Furthermore, some CT scan findings may help to stratify patients with probable high or low difficulties in the execution of surgery, either laparoscopic or laparotomic.

References

1. Ansaloni L, Pisano M, Coccolini F, Peitzmann AB, Fingerhut A, Catena F, Agresta F, Allegri A, Bailey I, Balogh ZJ, Bendinelli C, Biffl W, Bonavina L, Borzellino G, Brunetti F, Burlew CC, Camapanelli G, Campanile FC, Ceresoli M, Chiara O, Civil I, Coimbra R, De Moya M, Di Saverio S, Fraga GP, Gupta S, Kashuk J, Kelly MD, Koka V, Jeekel H, Latifi R, Leppaniemi A, Maier RV, Marzi I, Moore F, Piazzalunga D, Sakakushev B, Sartelli M, Scalea T, Stahel PF, Taviloglu K, Tugnoli G, Uraneus S, Velmahos GC, Wani I, Weber DG, Viale P, Sugrue M, Ivatury R, Kluger Y, Gurusamy KS, Moore EE. 2016 WSES guidelines on acute calculous cholecystitis. World J Emerg Surg. 2016;11:25.
2. Strasberg SM. Acute calcolous cholecystitis. N Engl J Med. 2008;358:2804–11.
3. Chawla A, Bosco JI, Lim TC, Srinivasan S, Teh HS, Shenoy JN. Imaging of acute cholecystitis and cholecystitis-associated complications in the emergency setting. Singap Med J. 2015;56(8):438–43; quiz 444.
4. Tana M, Tana C, Cocco G. Acute acalculous cholecystitis and cardiovascular disease: a land of confusion. J Ultrasound. 2015;18:317–20.
5. Kiewiet JJ, Leeuwenburgh MM, Bipat S, Bossuyt PM, Stoker J, Boermeester MA. A systematic review and meta-analysis of diagnostic performance of imaging in acute cholecystitis. Radiology. 2012;264:708–20.
6. Soyer P, Hoeffel C, Dohan A, Gayat E, Eveno C, Malgras B, Pautrat K, Boudiaf M. Acute cholecystitis: quantitative and qualitative evaluation with 64-section helical CT. Acta Radiol. 2013;54(5):477–86.
7. Boruah DK, Sanyal S, Sharma BK, Boruah DR. Comparative evaluation of ultrasonography and cross-sectional imaging in determining gall bladder perforation in accordance to Niemeier's classification. J Clin Diagn Res. 2016;10(8):TC15–8.
8. Fuks D, Mouly C, Robert B, Hajji H, Yzet T, Regimbeau JM. Acute cholecystitis: preoperative CT can help the surgeon consider conversion from laparoscopic to open cholecystectomy. Radiology. 2012;263(1):128–38.
9. Fidler J, Paulson EK, Layfield L. CT evaluation of acute cholecystitis: findings and usefulness in diagnosis. AJR. 1996;166:1085–8.
10. Maehira H, Itoh A, Kawasaki M, Ogawa M, Imagawa A, Mizumura N, Okumura S, Kameyama M. Use of dynamic CT attenuation value for diagnosis of acute gangrenous cholecystitis. Am J Emerg Med. 2016;34(12):2306–9.
11. Zhao F, Lu PX, Yan SX, Wang GF, Yuan J, Zhang SZ, Wang YX. CT and MR features of xanthogranulomatous cholecystitis: an analysis of consecutive 49 cases. Eur J Radiol. 2013;82(9):1391–7.

CT Evaluation of Appendicitis

8

F. Monetti, A. Bhangu, S. Di Saverio, M. Stellino, P.E. Orlandi, and M. Imbriani

8.1 Background

Appendicitis is the most common acute abdominal emergency in the United States, with approximately 250,000 cases occurring annually. The lifetime risk of developing it is 7%, and it occurs more frequently in young white males (median age of 22 years) [1]. Acute appendicitis has traditionally been a clinical diagnosis, with early surgery thought to be mandatory to remove the appendix before it perforates, although more recent evidence suggests short delays of 12–24 h before surgery is safe [2]. Severity and natural history of acute appendicitis can be variable; differential diagnosis between uncomplicated and complicated/perforated appendicitis is of paramount importance since the former can be successfully treated by non-operative management and antibiotics alone [3] whereas the latter requires surgery and laparoscopy can aid both differential diagnosis and allow minimally invasive management [4].

The vermiform appendix arises 3–4 cm below the ileocecal valve from the cecum, and it has a high variability in location: paracolic, retrocolic, retrocecal (Fig. 8.1), and pericecal. Pathophysiology is often secondary to an obstruction (90%) of the lumen by fecalith, lymphoid hyperplasia, or cancer, which causes venous engorgement, arterial compromise, transmural inflammation, and finally ischemia with infarction of the wall leading to perforation. Ten percent of appendicitis have a nonobstructive etiology.

F. Monetti • P.E. Orlandi • M. Imbriani
Department of Radiology, Maggiore Hospital, Bologna Local Health District, Bologna, Italy

A. Bhangu
Academic Department of Surgery, University of Birmingham, Birmingham, UK

S. Di Saverio (✉)
Cambridge Colorectal Unit, Cambridge University Hospitals NHS Foundation Trust, Addenbrooke's Hospital, Cambridge, UK
e-mail: salomone.disaverio@gmail.com

M. Stellino
Department of Neuroradiology, Bellaria Hospital, Bologna Local Health District, Bologna, Italy

F. Catena et al. (eds.), *CT Scan in Abdominal Emergency Surgery*, Hot Topics in Acute Care Surgery and Trauma, https://doi.org/10.1007/978-3-319-48347-4_8

Fig. 8.1 Retrocecal-inflamed appendix

8.2 Radiological Diagnosis

The radiological diagnosis of appendicitis makes use of three methods: ultrasound (US), computed tomography (CT), and magnetic resonance (MR). US is the first-line investigation in suspected appendicitis, especially in young patients, women of childbearing age, and known pregnancy. The use of CT is highly variable around the world, although many reserve it for cases with atypical presentation and suspicion of cancer (e.g., elderly). For atypical presentation, it means the absence of at least one of the classic signs of appendicitis (fever, migrant pain, pain on palpation of the McBurney point, elevation of inflammatory laboratory tests) and usually occurs in the very young or very old. MRI is indicated in pregnant women or very young patients in the event of dubious or negative US with ongoing symptoms.

With recent reports on the high accuracy of CT examination in diagnosing appendicitis, CT has become the gold standard for the diagnosis of acute appendicitis in the United States. In Europe, the use of CT is more cautious, due to the risk associated with exposure to ionizing radiation. Recently, several low-dose protocols to overcome this problem are suggested. CT shows a sensitivity of 90–100%, a specificity of 91–99%, diagnostic accuracy of 94–95%, positive predictive value of 92–98%, and 95–100% of the negative predictive value. CT is strongly indicated in particular cases of atypical presentation, in suspected cases of perforation, and when the US is questionable or negative in the presence of clinical suspicion.

8.3 Computed Tomography

CT technique is still a controversial issue; in particular the subject of discussion is the utility or less of intravenous contrast medium and of water-soluble contrast medium orally or rectally and the use of low-dose protocols. CT scan can rule out the possibility of appendicitis when you see a normal appearance appendix or when the appendix is not displayed, in the absence of secondary signs in particular edema of pericecal adipose tissue.

Recent studies demonstrated that the oral contrast provides no benefits in the diagnosis of appendicitis. It is not associated with a significant increase of the sensitivity and the specificity and for the time required for the opacification of the lumen of the intestine, especially in the case of oral administration.

8.4 Computed Tomography Protocols

Low-dose protocols are obtained with intensity current reduction (mAs), reduction of the voltage (kV), automated systems of dose modulation, and implementation of reconstruction iterative systems. Many studies have demonstrated a high sensitivity and specificity of low-dose CT without intravenous (IV) contrast, compared to standard contrast-enhanced CT in the diagnosis of acute appendicitis.

The most common CT protocol covers the entire abdomen using IV-iodinated contrast without any oral or rectal contrast. It is mandatory to use thin section protocol (at least 2.5 mm) to obtain good multiplanar (coronal and sagittal) reconstruction images that are very helpful to find the appendix in uncommon position.

Diagnostic accuracy for the detection of appendicitis on CT scan with or without IV contrast is similar, but IV contrast can demonstrate the appendiceal wall enhancement and help to resolve complicated cases such as perforated appendicitis, abscess (Fig. 8.2), or atypical appendiceal location (Fig. 8.3).

8.5 Computed Tomography Signs

CT signs of acute appendicitis include a distended appendix measuring greater than 6 mm in diameter, an appendicolith (30% of cases) (Fig. 8.4), appendiceal wall enhancement or thickening, adjacent or periappendiceal fat stranding (Figs. 8.5, 8.6 and 8.7), fluid collections, phlegmon or abscess formation, extraluminal air, adenopathy, adjacent bowel wall thickening, and focal cecal-apical thickening (Table 8.1).

The arrowhead sign or the "cecal bar" sign is specific but rare signs, and they can be visualized only in the presence of positive contrast medium in the cecum. A sign that can be observed is the "target" or the spotlight ("bull's eye sign") due to edema of the submucosa that appears hypodense (Fig. 8.8).

The threshold of 6 mm is not absolute because it can be present in about 40% of healthy adults, so many authors suggest to consider an appendix from 6 to 10 mm indeterminate and to correlate this data with secondary signs. It is important to look

Fig. 8.2 Appendicitis complicated by perforation and wall enhancing abscess

Fig. 8.3 Ectopic pelvic-inflamed appendix with the apex in the left pelvis

for signs of inflammation of the periappendicular structures and especially the "fat stranding." Fat stranding and the clouding aspect and thickening of the periappendicular adipose tissue have an excellent sensitivity (100%) and good specificity (80%) in the diagnosis of acute appendicitis. CT findings of extraluminal

Fig. 8.4 Appendicolith at the base of the appendix with fat stranding around the cecum

Fig. 8.5 Thickening of the appendiceal wall with low-attenuation edema of the submucosal layer of the appendix

Fig. 8.6 Enlarged appendix with wall thickening, periappendicular fat stranding, and appendicolith. Features of acute appendicitis

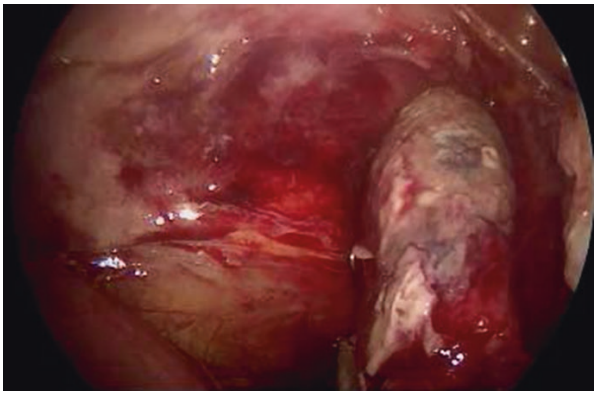

Fig. 8.7 Surgical appearance of the acute appendicitis in CT features. Intraoperative Picture courtesy of Dr. Salomone Di Saverio MD FACS FRCS

Table 8.1 CT signs of appendicitis

• Diameter of appendix ≥6 mm
• Wall thickness ≥3 mm
• Periappendiceal inflammatory changes:
Fat stranding
Fluid collections
Phlegmon
Abscess formation
Extraluminal air
Adjacent adenopathy
Adjacent bowel wall thickening
Focal cecal wall thickening

Fig. 8.8 Target sign: homogeneously enhancing thickened wall with mural stratification

appendicolith, extraluminal air, and presence of abscess, phlegmon, and defects in wall impregnation after IV contrast have an excellent accuracy for the diagnosis of perforated appendicitis.

The specificity is limited by the fact that the "stranding" can also be seen in the cecal diverticulitis. The sensitivity can be limited by the fact that sometimes the CT scan is requested and executed too soon, before the "stranding" is visible.

Air in the appendix lumen does not rule out appendicitis. Air is present in the lumen of the appendix in over 15% of cases of appendicitis imaged on CT.

CT is more sensitive than the US in the diagnosis of complications such as perforation and abscess. The perforation is associated with increased morbidity and mortality, and it is present in 30% of cases of acute appendicitis. The perforation rate is more common in very young patients (40–57%) and very elderly people (55–70%) in whom diagnosis of appendicitis can be misdiagnosed or delayed. In case of perforation, the transverse diameter of the appendix is greater than that of appendicitis inflamed but not perforated (15 mm vs. 11 mm), but in the absence of free air or abscesses in the periappendicular space, CT cannot make a diagnosis of perforation; the amount of extraluminal air is minimal or absent in case of perforation, usually not more than 1–2 mL, and a frank pneumoperitoneum is rare.

CT also allows distinguishing of complications such as appendiceal phlegmon, fluid collections delimitated by the wall with contrast enhancement, and adherences between the appendix and viscera such as inflamed bowel loops, greater omentum, or bladder.

8.6 Risks and Benefits of Computed Tomography

CT has a high sensitivity and specificity (respectively, 91% and 90%), has short acquisition times than US, allows diagnosis of complications, and has an important role in establishing differential diagnoses. The limits are represented by exposure to ionizing radiation and the risks associated with the possible IV administration of the contrast agent. In CT, false negatives are observed in very thin patients with little abdominal adipose tissue outlining the appendix, which can be confused with a loop bowel. False positives, however, are due to wrong identification of an appendix as another structure (loop of the intestine, in particular the last ileal loop, a dilated ureter, or gonadal veins). The terminal ileum does not originate from the base of the cecum, has peristaltic activity, and is not a dead end, and the cross section has an oval shape.

8.7 Differential Diagnosis

There are many diseases that can mimic appendicitis (Table 8.2). Acute appendicitis then enters in differential diagnosis with many diseases that cause abdominal pain in the right iliac fossa (enterocolitis, mesenteric lymphadenitis, diverticulitis,

Table 8.2 Most common differential diagnosis of appendicitis

Enterocolitis
Mesenteric lymphadenitis
Diverticulitis
Crohn's disease
Ulcerative colitis
Cancer of the cecum
Meckel's diverticulitis
Epiploic appendagitis
Omental infarction
Adnexitis
Tubo-ovarian abscesses
Ectopic pregnancy
Ovarian cyst pedicle torsion
Pelvic inflammatory disease, PID
Urolithiasis
Cystitis
Pyelonephritis

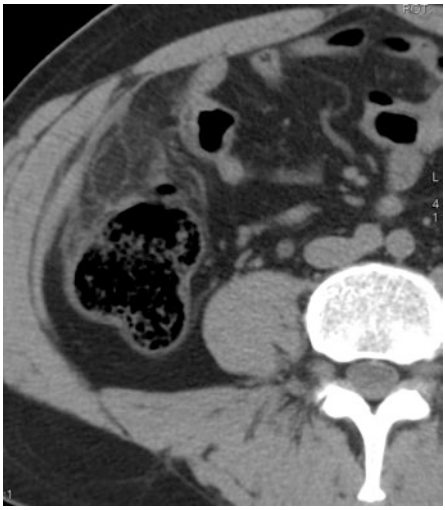

Fig. 8.9 Hypodense pericolonic oval mass with adjacent fat stranding: epiploic appendagitis

Crohn's disease, ulcerative colitis, cancer of the cecum, Meckel's diverticulitis, epiploic appendagitis (Fig. 8.9) omental infarction), as well as gynecological (adnexitis, tubo-ovarian abscesses, ectopic pregnancy, ovarian cyst pedicle torsion, pelvic inflammatory disease), urological (urolithiasis, cystitis, pyelonephritis), and primary neoplastic disease (e.g., carcinoid tumors, adenocarcinoma, mucocele and pseudomyxoma peritonei, lymphoma) and metastases (from leiomyosarcoma, ganglioneuroma, Kaposi's sarcoma, and granular cell tumors).

8.8 Appendiceal Tumors

Appendix tumors should be suspected when its transverse diameter exceeds 15 mm. Appendiceal neoplasms are still rare and found in 0.9–1.4% of all appendectomies. Carcinoid tumor is the most common and is characterized by nodular thickening of

the distal third of the appendiceal wall visible on CT, unlike adenocarcinoma that is most rare and is characterized by a diffuse thickening of the proximal third of the appendiceal wall.

Carcinoid tumor is detected in 0.3–0.9% of surgical findings. Therefore, the histological examination of the surgical specimen is mandatory. For small carcinoid tumors (<2 cm diameter), appendectomy is curative; if larger, or in the case of adenocarcinoma, right hemicolectomy is indicated.

Appendicitis associated with tumors of the cecum should be suspected in case of anemia, loss of weight, and a palpable mass associated with common symptoms of appendicitis in elderly patients. Carcinoma of the cecum in the elderly can long remain asymptomatic and occur because of over-infection and bleeding. CT shows a circumferential and asymmetrical thickening of the cecum, marked inflammation of the adipose pericecal tissue, and enlarged lymph nodes.

8.9 Other Differential Diagnoses

Stump appendicitis is rare but can occur months to years after a laparoscopic appendectomy or laparotomy.

Diverticulitis of a sigmoid loop present in the right iliac fossa may mimic appendicitis, as diverticulitis of the cecum.

In diverticulitis of the right colon, it is often observed that only one diverticulum with thickened wall is present, often containing one coprolith (hard feces lump, akin to appendicolith). CT can easily demonstrate the position of the coproliths inside the diverticulum that could be confused with appendicoliths.

The Meckel diverticulum, unlike the acquired diverticula of the ileum, is located on the anti-mesenteric side of the ileum at approximately 100 cm from the ileocecal valve. CT demonstrates a dead-end structure related to gastrointestinal tract with thickened wall, enhancement after contrast medium, and peridiverticular inflammation of the adipose tissue.

References

1. Bhangu A, Søreide K, Di Saverio S, Assarsson JH, Drake FT. Acute appendicitis: modern understanding of pathogenesis, diagnosis, and management. Lancet. 2015;386(10000):1278–87. doi:10.1016/S0140-6736(15)00275-5.
2. Di Saverio S, Birindelli A, Kelly MD, Catena F, Weber DG, Sartelli M, Sugrue M, De Moya M, Gomes CA, Bhangu A, Agresta F, Moore EE, Soreide K, Griffiths E, De Castro S, Kashuk J, Kluger Y, Leppaniemi A, Ansaloni L, Andersson M, Coccolini F, Coimbra R, Gurusamy KS, Campanile FC, Biffl W, Chiara O, Moore F, Peitzman AB, Fraga GP, Costa D, Maier RV, Rizoli S, Balogh ZJ, Bendinelli C, Cirocchi R, Tonini V, Piccinini A, Tugnoli G, Jovine E, Persiani R, Biondi A, Scalea T, Stahel P, Ivatury R, Velmahos G, Andersson R. WSES Jerusalem guidelines for diagnosis and treatment of acute appendicitis. World J Emerg Surg. 2016;11:34. doi:10.1186/s13017-016-0090-5.
3. Di Saverio S, Sibilio A, Giorgini E, Biscardi A, Villani S, Coccolini F, Smerieri N, Pisano M, Ansaloni L, Sartelli M, Catena F, Tugnoli G. The NOTA Study (Non Operative Treatment for Acute Appendicitis): prospective study on the efficacy and safety of antibiotics (amoxicillin and clavulanic acid) for treating patients with right lower quadrant abdominal pain and long-term

follow-up of conservatively treated suspected appendicitis. Ann Surg. 2014;260(1):109–17. doi:10.1097/SLA.0000000000000560.
4. Di Saverio S, Mandrioli M, Sibilio A, Smerieri N, Lombardi R, Catena F, Ansaloni L, Tugnoli G, Masetti M, Jovine E. A cost-effective technique for laparoscopic appendectomy: outcomes and costs of a case-control prospective single-operator study of 112 unselected consecutive cases of complicated acute appendicitis. J Am Coll Surg. 2014;218(3):e51–65. doi:10.1016/j.jamcollsurg.2013.12.003. Epub 2013 Dec 19.

Bibliography

5. Whitley S, et al. The appendix on CT. Clin Radiol. 2009;64(2):190–9.
6. Karul M, Berliner C, Keller S, Yamamura J, Tsui TY. Imaging of appendicitis in adults. Rofo. 2014;186(6):551–8.
7. Crownover BK, Bepko JL. Appropriate and safe use of diagnostic imaging. Am Fam Physician. 2013;87(7):494–501. PMID: 23547591.
8. Sartelli M, Viale P, Catena F, Ansaloni L, Moore E, Malangoni M, Moore FA, Velmahos G, Coimbra R, Ivatury R, Peitzman A, Koike K, Leppaniemi A, Biffl W, Burlew CC, Balogh ZJ, Boffard K, Bendinelli C, Gupta S, Kluger Y, Agresta F, Di Saverio S, Wani I, Escalona A, Ordonez C, Fraga GP, Junior GA, Bala M, Cui Y, Marwah S, Sakakushev B, Kong V, Naidoo N, Ahmed A, Abbas A, Guercioni G, Vettoretto N, Díaz-Nieto R, Gerych I, Tranà C, Faro MP, Yuan KC, Kok KY, Mefire AC, Lee JG, Hong SK, Ghnnam W, Siribumrungwong B, Sato N, Murata K, Irahara T, Coccolini F, Segovia Lohse HA, Verni A, Shoko T. WSES guidelines for management of intra-abdominal infections. World J Emerg Surg. 2013;8(1):3. doi:10.1186/1749–7922–8-3. PMID: 23294512; PMCID: PMC3545734.
9. Furukawa A, et al. Gastrointestinal tract perforation: CT diagnosis of presence, site, and cause. Abdom Imaging. 2005;30(5):524–34.
10. Liang MK, Lo HG, Marks JL. Stump appendicitis: a comprehensive review of literature. Am Surg. 2006;72(2):162–6.
11. Brown MA. Imaging acute appendicitis. Semin Ultrasound CT MR. 2008;29(5):293–307.
12. Millet I, et al. Infection of the right iliac fossa. Diagn Interv Imaging. 2012;93(6):441–52.
13. Birnbaum BA, Wilson SR. Appendicitis at the millennium 1. Radiology. 2000;215(2):337–48.
14. Wong KKY, Cheung TWY, Tam PKH. Diagnosing acute appendicitis: are we overusing radiologic investigations? J Pediatr Surg. 2008;43(12):2239–41.
15. Bhatt CJ, et al. Multidetector computed tomography in large bowel lesions—a study of 100 cases. Indian J Surg. 2011;73(5):352–8.
16. Atema JJ, et al. Comparison of imaging strategies with conditional versus immediate contrast-enhanced computed tomography in patients with clinical suspicion of acute appendicitis. Eur Radiol. 2015;25(8):2445–52.
17. Park G, et al. Stratified computed tomography findings improve diagnostic accuracy for appendicitis. World J Gastroenterol. 2014;20(38):13942–9.
18. Drake FT, Flum DR. Improvement in the diagnosis of appendicitis. Adv Surg. 2013;47:299.
19. Doria AS. Optimizing the role of imaging in appendicitis. Pediatr Radiol. 2009;39(2):144–8.
20. Petroianu A. Diagnosis of acute appendicitis. Int J Surg. 2012;10(3):115–9.
21. Rhea JT, et al. The status of appendiceal CT in an urban medical center 5 years after its introduction: experience with 753 patients. Am J Roentgenol. 2005;184(6):1802–8.
22. Moteki T, Horikoshi H. New CT criterion for acute appendicitis: maximum depth of intraluminal appendiceal fluid. Am J Roentgenol. 2007;188(5):1313–9.
23. Smith MP, et al. ACR appropriateness criteria® right lower quadrant pain—suspected appendicitis. Ultrasound Q. 2015;31(2):85–91.
24. Birchard KR, Brown MA, Hyslop WB, Firat Z, Semelka RC. MRI of acute abdominal and pelvic pain in pregnant patients. Am J Roentgenol. 2005;184:452–8.

25. Cobben LP, Groot I, Haans L, Blickman JG, Puylaert J. MRI for clinically suspected appendicitis during pregnancy. Am J Roentgenol. 2004;183:671–5.
26. Kessler N, Cyteval C, Gallix B, Lesnik A, Blayac PM, Pujol J, Bruel JM, Taourel P. Appendicitis: evaluation of sensitivity, specificity, and predictive values of US, Doppler US, and laboratory findings. Radiology. 2004;230:472–8.
27. Moteki T, Horikoshi H. New CT criterion for acute appendicitis: maximum depth of intraluminal appendiceal fluid. Am J Roentgenol. 2007;188:1313–9.
28. Nitta N, Takahashi M, Furukawa A, Murata K, Mori M, Fukushima M. MR imaging of the normal appendix and acute appendicitis. J Magn Reson Imaging. 2005;21:156–65.
29. Yu J, Fulcher AS, Turner MA, Halvorsen RA. Helical CT evaluation of acute right lower quadrant pain: part II, uncommon mimics of appendicitis. Am J Roentgenol. 2005;184:1143–9.
30. Weyant MF, Sr E, Maluccio MA, Barie PS. Is imaging necessary for the diagnosis of acute appendicitis? Adv Surg. 2003;37:327–45.
31. Otero HJ, Ondategui-Parra S, Erturk SM, Ochoa RE, Gonzalez-Beicos A, Ros PR. Imaging utilization in the management of appendicitis and its impact on hospital charges. Emerg Radiol. 2007;15:23–8.
32. Pedrosa I, Levine D, Eyvazzadeh AD, Siewert B, Ngo L, Rofsky NM. MR imaging evaluation of acute appendicitis in pregnancy. Radiology. 2006;238:891–9.
33. Tamburrini S, Brunetti A, Brown M, Sirlin CB, Casola G. CT appearance of the normal appendix in adults. Eur Radiol. 2005;15:2096–103.
34. Terasawa T, Blackmore CC, Bent S, Kohlwes RJ. Systematic review: computed tomography and ultrasonography to detect acute appenditicitis in adults and adolescents. Ann Intern Med. 2004;141:537–46.
35. Moteki T, Horikoshi H. New CT criterion for acute appendicitis: maximum depth of intraluminal appendiceal fluid. Am J Roentgenol. 2007;188(5):1313–9.
36. Megibow AJ, et al. Evaluation of bowel distention and bowel wall appearance by using neutral oral contrast agent for multi–detector row CT. Radiology. 2006;238(1):87–95.
37. Morrow SE, Newman KD. Current management of appendicitis. Semin Pediatr Surg. 2007;16:34–40.

Acute Diverticulitis

9

Massimo Sartelli, Fausto Catena, Salomone Di Saverio, Federico Coccolini, and Luca Ansaloni

9.1 Introduction

Diverticular disease is very common in western countries, even if the prevalence of colonic diverticulosis is increasing throughout the world, because of changes in lifestyle [1].

Acute diverticulitis is a usual complication of diverticulosis. It affects 15–25% of patients with diverticulosis [2].

Acute diverticulitis encompasses a variety of conditions, ranging from uncomplicated diverticular inflammation to fecal peritonitis.

Computed tomography (CT) imaging is now the gold standard in the diagnosis and staging of patients with acute diverticulitis. CT imaging with intravenous contrast has sensitivity and specificity, reported as high as 98 and 99% [3, 4].

The utility of CT imaging in studying acute diverticulitis goes beyond accurate diagnosis of diverticulitis; CT imaging can show the grade of severity and drive treatment planning of patients with acute diverticulitis.

M. Sartelli (✉)
Department of Surgery, Macerata Hospital, Macerata, Italy
e-mail: massimosartelli@gmail.com

F. Catena
Emergency and Trauma Surgery
Ospedale Maggiore di Parma Emergency and Trauma Surgery,
Parma, Parma, Italy

S. Di Saverio
Cambridge Colorectal Unit, Cambridge University Hospitals NHS Foundation Trust,
Addenbrooke's Hospital, Cambridge, UK

F. Coccolini • L. Ansaloni
General, Emergency and Trauma Surgery Department,
Bufalini Hospital,
Cesena, Italy

F. Catena et al. (eds.), *CT Scan in Abdominal Emergency Surgery*, Hot Topics in Acute Care Surgery and Trauma, https://doi.org/10.1007/978-3-319-48347-4_9

In the last years, detailed information provided by CT scans led to several modifications of the Hinchey classification. For example, in 1989, Neff et al. [5] presented a new classification based on CT findings. It consisted of five stages, ranging from radiological diagnosis of uncomplicated AD (Stage 0) to pneumoperitoneum with abundant free liquid (Stage 4):

Stage 0
Uncomplicated diverticulitis;
Diverticula, thickening of the wall, increased density of the pericolic fat
Stage 1 Locally complicated with local abscess
Stage 2 Complicated with pelvic abscess
Stage 3 Complicated with distant abscess
Stage 4 Complicated with other distant complications

In 1997, Sher et al. [6] introduced a modification of Hinchey classification. This classification divided abscesses into pericolic abscesses (Stage 1), distant abscesses amendable for percutaneous drainage (Stage 2A), and complex abscesses associated with a possible fistula (Stage 2B). This classification implied the use of new treatment strategies, such as CT-guided percutaneous drainage of abscesses.

In 2002, Ambrosetti et al. [7] classified diverticulitis into severe or moderate disease. In this classification, the CT scan determined the grade of severity guiding the physician in the treatment of acute complications. Moderate diverticulitis was defined by wall thickening of ≥5 mm and signs of inflammation of pericolic fat. Severe diverticulitis was defined by wall thickening accompanied by abscess formation, extraluminal air, or extraluminal contrast leak:

Moderate diverticulitis
Localized sigmoid wall thickening
Pericolic fat stranding
Severe diverticulitis
Abscess
Extraluminal air
Extraluminal contrast

In 2005, Kaiser et al. [8] modified Hinchey classification according to specific CT findings:

Stage 0 Mild clinical diverticulitis
Stage 1A Confined pericolic inflammation
Stage 1B Confined pericolic abscess
Stage 2 Pelvic or distant intra-abdominal abscess
Stage 3 Generalized purulent peritonitis
Stage 4 Fecal peritonitis at presentation

In 2015 a World Society of Emergency Surgery (WSES) working group published a new simple classification system based on CT scan results. The new classification divided acute diverticulitis into two groups: uncomplicated and complicated [9].

In the event of an uncomplicated case of acute diverticulitis, the infection only involves the colon and does not extend to the peritoneum.

In the event of complicated IAI, the infectious process proceeds beyond the colon. Complicated acute diverticulitis was divided into four stages, based on the extension of the infectious process.

Uncomplicated

Stage 0: Diverticula, thickening of the colonic wall or increased density of the pericolic fat

Complicated

Stage 1A: Pericolic air bubbles or little pericolic fluid without abscess (within 5 cm from inflamed bowel segment)
Stage 1B: Abscess ≤4 cm
Stage 2A: Abscess >4 cm
Stage 2B: Distant air (>5 cm from inflamed bowel segment)
Stage 3: Diffuse fluid without distant free air (no hole in colon)
Stage 4: Diffuse fluid with distant free air (persistent hole in colon)

9.2 WSES Classification

Stage 0 (Uncomplicated Diverticulitis).

Uncomplicated diverticulitis is a confined inflammatory process (Fig. 9.1). CT findings include diverticula, thickening of the wall, and increased density of the pericolic fat.

The current consensus in recent international literature is that uncomplicated diverticulitis may be a self-limiting condition in which local host defenses can manage the bacterial inflammation without antibiotics in immunocompetent patients. In this context, antibiotics may, therefore, not be necessary in the treatment of uncomplicated disease. In these patients, outpatient management is suggested for patients with uncomplicated acute diverticulitis, with no comorbidities [10].

Fig. 9.1 Slightly thickened sigmoid diverticular disease, without abscess or perforation

9.2.1 Stage 1A

Stage 1A diverticulitis is a confined inflammatory process that may include a microperforation but excludes an abscess and/or peritonitis (Fig. 9.2). CT findings include pericolic air in the form of air bubbles or little pericolic fluid without abscess. Patients with pericolic air or small fluid collection should be managed by antimicrobial therapy [10].

9.2.2 Stage 2A–1B

The therapeutic strategies for patients with diverticular abscesses are still debated (Fig. 9.3).

The size of 4–5 cm may be a reasonable limit between antibiotic treatment alone vs. percutaneous drainage combined with antibiotic treatment in the management of diverticular abscesses [10]. However, based on the clinical conditions, also patients with large abscesses can be initially treated by antibiotic therapy alone. However, careful clinical monitoring is mandatory. A CT scan should be repeated if the patient fails to show clinical and laboratory improvement [10].

Fig. 9.2 Diverticular disease, colonic wall thickening, fat stranding and pericolic fluid and air bubbles

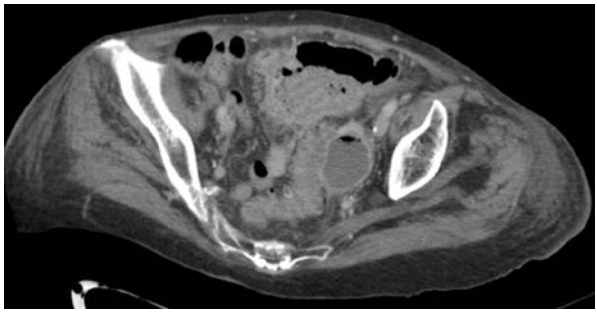

Fig. 9.3 Sigmoid diverticulitis with associated abscess formation

9.2.3 Stage 2B

A critical issue may be the CT presence of distant free air without diffuse fluid (Fig. 9.4).

Patients with distant air (>5 cm from inflamed bowel segment) may be treated by conservative treatment in selected cases [10].

However, it is associated with failure and may necessitate surgical operation. Careful clinical monitoring is mandatory [10].

9.2.4 Stage 3

Stage 3 includes diffuse fluid without CT findings of perforation. In this stage, CT does not reveal any evidence of distant free air [10]. Fluid should be visualized in at least two distant abdominal quadrants.

Although laparoscopic lavage and drainage have been debated in recent years, on the basis of SCANDIV, Ladies, and DILALA trials [11–13], it should not be considered the treatment of choice in patients with generalized peritonitis.

Hartmann resection is still advised for managing diffuse peritonitis in critically ill patients and in patients with multiple comorbidities. However, in clinically stable patients with no comorbidities, primary resection with anastomosis with or without a diverting stoma may be performed.

9.2.5 Stage 4

Stage 4 includes diffuse fluid with CT findings of perforation (Fig. 9.5). It may be still treated by the classic Hartmann procedure even if several reports indicated that primary resection and anastomosis with or without diversion have been reported as potential operative choices. Laparoscopic lavage and drainage are not suggested.

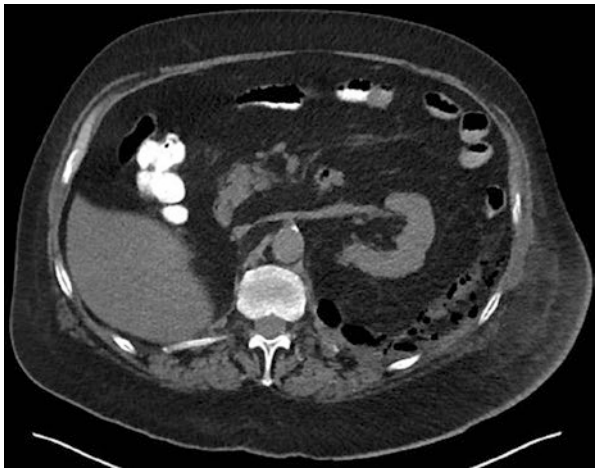

Fig. 9.4 Distant retroperitoneal free gas by perforated diverticular disease

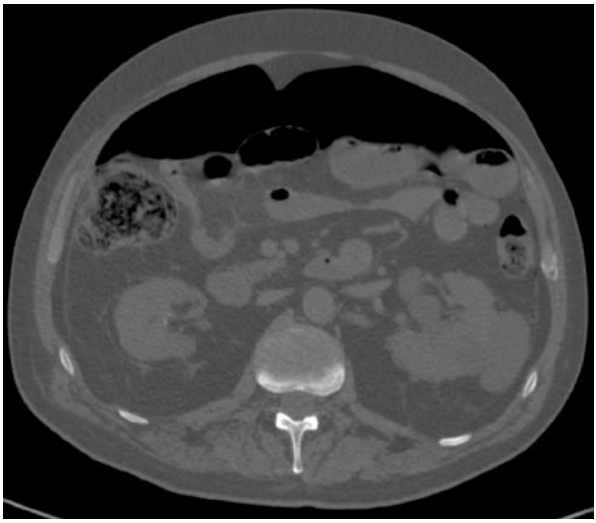

Fig. 9.5 Distant retroperitoneal free gas by perforated diverticular disease

Conclusions

Although the management strategy depends on more factors such as peritonitis diffusion, clinical conditions, and physiological reserve of the patient, the WSES classification system based on CT scan results may drive decision-making in nonoperative and operative management of acute diverticulitis and can help in making critical decisions in patients having acute diverticulitis.

References

1. Weizman AV, Nguyen GC. Diverticular disease: epidemiology and management. Can J Gastroenterol. 2011;25:385–9.
2. Laméris W, Van Randen A, Van Gulik TM, Bush OR, Winkelhagen J, Bossuyt PM, et al. A clinical decision rule to establish the diagnosis of acute diverticulitis at the emergency department. Dis Colon Rectum. 2010;53:896–904.
3. Laméris W, Van Randen A, Bossuyt PMM, Bipat S, Bossuyt PM, Boermeester MA, et al. Graded compression ultrasonography and computed tomography in acute colonic diverticulitis: meta-analysis of test accuracy. Eur Radiol. 2008;18:2498–511.
4. Ambrosetti P, Jenny A, Becker C, Terrier TF, Morel P. Acute left colonic diverticulitis–compared performance of computed tomography and water-soluble contrast enema: prospective evaluation of 420 patients. Dis Colon Rectum. 2000;43:1363–7.
5. Neff CC, van Sonnenberg E. CT of diverticulitis. Diagnosis and treatment. Radiol Clin N Am. 1989;27:743–52.
6. Sher ME, Agachan F, Bortul M, Nogueras JJ, Weiss EG, Wexner SD. Laparoscopic surgery for diverticulitis. Surg Endosc. 1997;11:264–7.
7. Ambrosetti P, Becker C, Terrier F. Colonic diverticulitis: impact of imaging on surgical management—a prospective study of 542 patients. Eur Radiol. 2002;12:1145–9.
8. Kaiser AM, Jiang JK, Lake JP, Ault G, Artinyan A, Gonzalez-Ruiz C, et al. The management of complicated diverticulitis and the role of computed tomography. Am J Gastroenterol. 2005;100:910–7.

9. Sartelli M, Moore FA, Ansaloni L, Di Saverio S, Coccolini F, Griffiths EA, et al. A proposal for a CT driven classification of left colon acute diverticulitis. World J Emerg Surg. 2015;10:3. doi:10.1186/1749-7922-10-3.
10. Sartelli M, Catena F, Ansaloni L, Coccolini F, Griffiths EA, Abu-Zidan FM, Di Saverio S, Ulrych J, Kluger Y, Ben-Ishay O, Moore FA, Ivatury RR, Coimbra R, Peitzman AB, Leppaniemi A, Fraga GP, Maier RV, Chiara O, Kashuk J, Sakakushev B, Weber DG, Latifi R, Biffl W, Bala M, Karamarkovic A, Inaba K, Ordonez CA, Hecker A, Augustin G, Demetrashvili Z, Melo RB, Marwah S, Zachariah SK, Shelat VG, McFarlane M, Rems M, Gomes CA, Faro MP, Júnior GA, Negoi I, Cui Y, Sato N, Vereczkei A, Bellanova G, Birindelli A, Di Carlo I, Kok KY, Gachabayov M, Gkiokas G, Bouliaris K, Çolak E, Isik A, Rios-Cruz D, Soto R, Moore EE. WSES Guidelines for the management of acute left sided colonic diverticulitis in the emergency setting. World J Emerg Surg. 2016;11:37.
11. Angenete E, Thornell A, Burcharth J, Pommergaard HC, Skullman S, Bisgaard T, et al. Laparoscopic lavage is feasible and safe for the treatment of perforated diverticulitis with purulent peritonitis: the first results from the randomized controlled trial DILALA. Ann Surg. 2016;263:117–22.
12. Schultz JK, Yaqub S, Wallon C, Blecic L, Forsmo HM, Folkesson J, et al. Laparoscopic lavage vs primary resection for acute perforated diverticulitis: the SCANDIV randomized clinical trial. JAMA. 2015;314:1364–75.
13. Vennix S, Musters GD, Mulder IM, Swank HA, Consten EC, Belgers EH, et al. Laparoscopic peritoneal lavage or sigmoidectomy for perforated diverticulitis with purulent peritonitis: a multicentre, parallel-group, randomised, open-label trial. Lancet. 2015;386(10000):1269–77.

Complicated Peptic Ulcer Findings on Abdominal CT Scan

10

Bruno M. Pereira, Thiago J. Penachim, and Gustavo P. Fraga

10.1 Introduction

Before focusing on complicated peptic ulcer computed tomography (CT) scan findings, a brief review on peptic ulcer disease (PUD) is necessary. PUD refers to a number of clinical signs and symptoms on the esophagus, stomach, or duodenum, united by the presence of mucosal ulceration usually secondary to the effects of gastric acid. Since the recognition of *Helicobacter pylori* as a common causative agent and the development of powerful antiacid medications such as the proton-pump inhibitors (PPI), PUD has become comparatively rare in western populations [1, 2].

Gastric and duodenal ulcers usually cannot be differentiated based on history alone, although some findings may be suggestive. Epigastric pain is the most common symptom of both gastric and duodenal ulcers. It is characterized by a gnawing or burning sensation and occurs more commonly after meals. In uncomplicated PUD, the clinical findings are few and nonspecific. Severity and signs of complications that warrant prompt investigation include excruciating abdominal epigastric pain, bleeding, acute anemia, unexplained weight loss, progressive dysphagia or odynophagia, recurrent vomiting, and family history of gastrointestinal (GI) cancer. Patients with perforated PUD usually present with a sudden onset of severe, sharp abdominal pain [1–5].

B.M. Pereira, MD, MHSc, PhD, FACS (✉)
Chief of the Division of Trauma Surgery, Department of Surgery, University of Campinas, Campinas, São Paulo, Brazil
e-mail: drbrunompereira@gmail.com

T.J. Penachim, MD
Division of Abdominal Radiology and Intervention, Department of Diagnostic Imaging, University of Campinas, Campinas, São Paulo, Brazil

G.P. Fraga, MD, PhD, FACS
Department of Surgery, University of Campinas, Campinas, São Paulo, Brazil

F. Catena et al. (eds.), *CT Scan in Abdominal Emergency Surgery*, Hot Topics in Acute Care Surgery and Trauma, https://doi.org/10.1007/978-3-319-48347-4_10

In most patients, documentation of PUD depends on endoscopic and/or radiographic confirmation. Upper GI endoscopy is the preferred diagnostic test in the evaluation of patients with suspected non-perforated PUD. Endoscopy provides an opportunity to visualize the ulcer, to determine the presence and degree of active bleeding (Forrest classification), and to attempt hemostasis by direct measures, if required. In the acute setting, CT scan is the modality of choice for assessing a patient with acute abdominal pain and suspicion of perforation and in some settings may be able to identify the site of bleeding prior to endoscopy [2–4].

CT is certainly not the diagnostic evaluation of choice for most patients with suspected peptic ulcer disease, but many patients with peptic ulcer disease will nonetheless present to the emergency department with unexplained abdominal pain and undergo CT evaluation as the initial diagnostic test. Besides that, although the overall prevalence of peptic ulcer disease and related hospitalizations are decreasing, the initial presentation of complicated peptic ulcer disease on CT remains common, with perforated peptic ulcer disease accounting for up to 48% of nontraumatic pneumoperitoneum [6].

Current emergency management includes the early use of high-dose intravenous PPIs, treatment to eradicate *Helicobacter pylori*, improved endoscopic methods for control of hemorrhage, and changes in surgical indications and procedures. Notwithstanding this fact, evolution of a nontreated or refractory PUD can happen, and complications include localized inflammation, perforation, ulcer penetration, hemorrhage, and obstruction. Perforation results in free communication between the GI tract lumen and adjacent peritoneal space. This generally occurs with ulcers of the anterior wall of the stomach and duodenum and curvatures of the stomach. Ulcer penetration refers to ulcers that have entered beyond the serosa of the stomach or duodenum wall with penetration into the adjacent soft tissue. These generally occur with posteriorly located ulcers with the exception of the posterior gastric wall in which free perforation can occur into the lesser sac [1–3].

In the United States, bleeding is the most common complication of PUD (73%), followed by perforation (9%) and obstruction (3%). The mortality rate from complications of PUD is more than ten times that of acute appendicitis or acute cholecystitis. Perforation has the highest mortality rate, followed by obstruction and hemorrhage. By contrast, a 13-year review of all surgical procedures for peptic ulcer complications at a Nigerian hospital found that obstruction was the most common complication (56%), followed by perforation (30%) and bleeding (10%). Some regional factors that may account for these differences include the rates of NSAID use, the prevalence of *H. pylori* infection, and the distribution and extent of gastritis [7, 8].

10.2 Complicated Peptic Ulcer CT Scan Findings

Recent advances in CT technology, including the introduction of multi-slice CT and the development of real-time three-dimensional (3D) imaging systems, have blossomed renewed interest in using CT to evaluate the GI tract. The same

technology that is applied to CT colonography and the generation of 3D and endoluminal images of the colon can be used to perform a detailed CT examination of the stomach.

For detailed imaging of the stomach, adequate distention is essential. If the entire stomach is not well distended, disease may be overlooked or, conversely, the collapsed gastric walls may mimic disease. Traditionally, high-attenuation contrast agents have been administered to enhance and distend the stomach and gastrointestinal tract. These agents can be categorized as positive contrast agents because they have a greater CT attenuation than that of water. Although these agents are safe, well tolerated, and result in good gastric distention, they may not be optimal when evaluating the gastrointestinal tract and stomach. Occasionally, positive oral contrast material may not mix uniformly with gastric contents, and pseudotumors can be created, on both axial and endoluminal images [9]. Because the wall of the gastrointestinal tract can enhance up to 120 HU after the intravenous administration of contrast material, the high-attenuation intraluminal contrast material may mask subtle disease. Also, the use of positive contrast agents can complicate 3D imaging and CT angiography: the contrast agent may obscure enhanced vessels, thereby necessitating extensive editing [9–18].

Recently, there has been interest in using alternative oral contrast agents for CT of the GI tract. There is an advantage to using low-attenuation agents with attenuation values similar to those of water. These agents allow better evaluation of the enhancing gastric wall and may allow better detection of subtle disease [15–18]. In addition, low-attenuation agents do not interfere with 3D imaging and CT angiography. Oil-based oral contrast agents have been tested and allow adequate depiction of the stomach wall but are not very palatable and result in significant steatorrhea, although newer preparations may be better [15–17]. Whole milk has been proposed as a possible CT oral contrast agent and is routinely used for CT angiography by some groups. Milk is emptied from the stomach relatively slowly and has a slower small bowel transit time than water. However, many adults are lactose intolerant and may experience cramping and diarrhea.

Water can be used as an oral contrast agent when patients clinical conditions allows. Water is often well tolerated and results in good gastric distention, which is necessary for a dedicated gastric imaging as well as excellent visualization of the enhancing gastric wall. Volume rendering of CT data coupled with interactive 3D and stereoscopic display can then be used to more clearly depict gastric disease. Water is inexpensive (usually free) and well tolerated. It distends the stomach well, allows good visualization of the enhancing wall, and does not interfere with the manipulation of the 3D data sets. When CT is performed specifically to evaluate the stomach, the patient is given 750 mL of water approximately 15 min before scanning. An additional 250 mL is given immediately prior to the study (Fig. 10.1). Some authors have suggested combining prone and supine imaging for optimal distention of all parts of the stomach. In addition, in certain cases, decubitus imaging may help distend the gastric antrum and pyloric region [15–18].

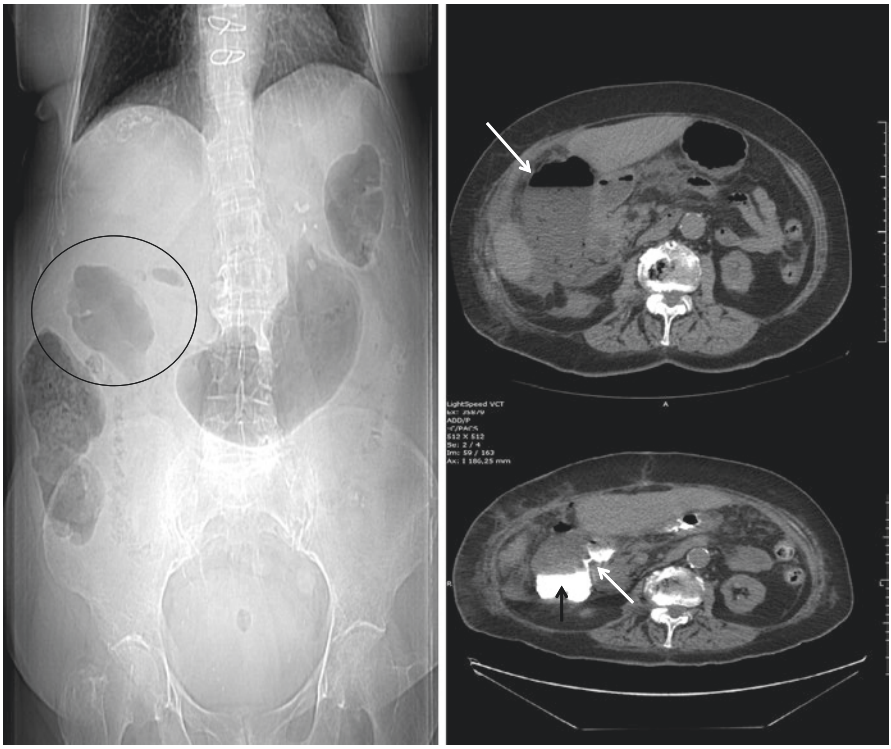

Fig. 10.1 Patient with epigastric pain and fever. X-ray shows air collection in the right upper quadrant projection (*black circle*). Computed tomography after oral administration of water shows subhepatic collection containing gas and fluid adjacent to the second duodenal portion. The diagnostic of perforated ulcer was considered, and positive oral contrast was administrated that clearly showed the perforated ulcer in the second duodenal portion, with extravasation (*white arrow*) of iodinated contrast into the collection (*black arrow*)

One disadvantage of using water as an oral contrast agent is that it results in suboptimal distention of the distal small bowel. Some authors have advocated administering positive contrast material initially, followed by water. The positive contrast material will fill the distal small bowel loops, and the water will distend the stomach and proximal small bowel [16, 17].

In addition to an oral contrast agent, which allows good gastric distention, intravenous contrast material is essential for complete evaluation of neoplastic and inflammatory diseases of the stomach. Some authors recommend administration of 120 mL of nonionic contrast material at a rate of 3 mL/s [15–17].

The diagnosis of complicated peptic ulcer in CT scan depends on close attention and active search in recognizing multiple signs. Recognition of complications of peptic ulcer disease on CT is vital for directing appropriate patient management in these acutely ill patients (Table 10.1).

Table 10.1 CT protocol used in our service

Preparation	Three glasses of water (750 mL) orally immediately before the image acquisition
Positioning	Dorsal decubitus
Contrast	Nonionic iodinated intravenous contrast
Phases	Pre-contrast and post-contrast 60 s delay

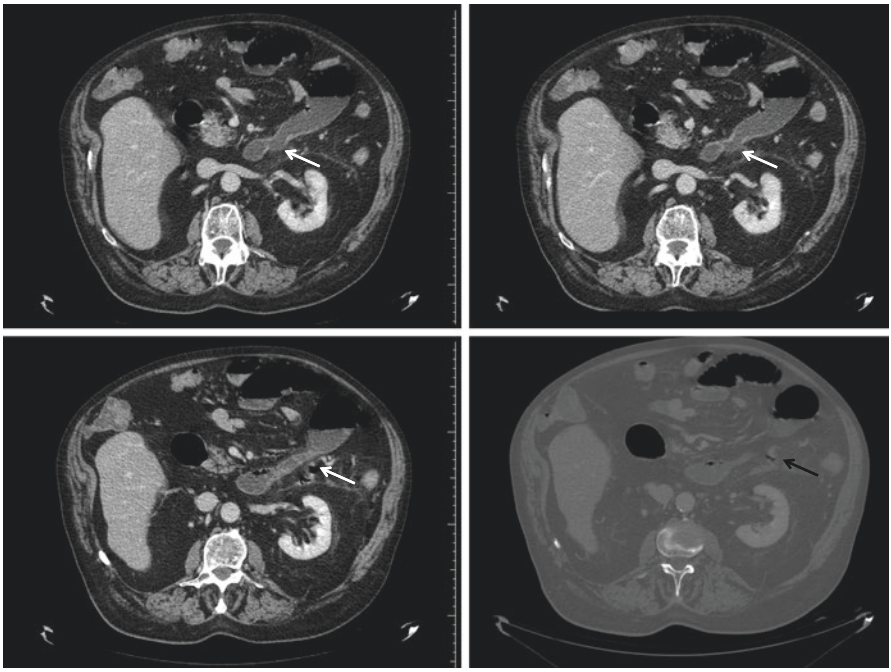

Fig. 10.2 Post-contrast abdominal computed tomography demonstrates disruption of mucosal enhancement in the transition of the third and fourth portion of the duodenum, representing an ulcer (*white arrow*). It is also possible to recognize minimum amount of retroperitoneal gas compatible with perforation (*black arrow*)

Signs of gastroduodenal PUD can be very difficult to recognize on CT, but close attention to discrete findings may serve as an important clue to the underlying diagnosis. These signs are:

– Disruption of mucosal enhancement: Represents erosion through the muscularis mucosa and has been shown to be a useful finding for identifying the site of GI perforation (Fig. 10.2)
– Focal luminal outpouching: Represents the ulcer crater and is one of the earliest described CT signs of PUD (Fig. 10.3)
– Low-attenuation wall thickening: Represents submucosal edema, a marker of underlying bowel inflammation

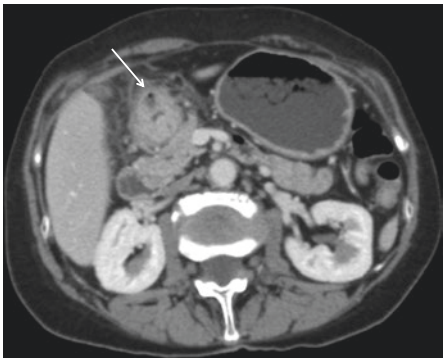

Fig. 10.3 Focal luminal outpouching in the first portion of the duodenum (*white arrow*), representing the ulcer crater, associated with fat stranding surrounding the stomach and duodenum (*white circle*), compatible with perigastric/periduodenal inflammation

– Mucosal hyperenhancement: Represents mucosal hyperemia related to the underlying gastritis or duodenitis
– Perigastric/periduodenal inflammation: Fat stranding surrounding the stomach and duodenum, secondary to inflammatory changes (Fig. 10.3)

10.3 Images Related to Complicated PUD

- *Hemorrhage*: Bleeding due to gastric ulcers often presents with hematemesis, while duodenal bleeds may present with tarry stools or even occasionally hematochezia, depending on the rate of bleeding. The most common vessels affected are the left gastric artery in cases of gastric ulcers along the lesser curvature and the gastroduodenal artery by duodenal ulcers. Hemorrhage can be challenging to identify and requires a multiphase scan without positive oral contrast (typically non-contrast, arterial, and delayed phase scans are obtained) and the presence of active bleeding. Extravasation and accumulation of intravenous contrast into the lumen of the bowel may be seen. CT scan can also identify bleeding through recognition of amorphous high-attenuation (more than + 40 UH) content (hematoma/clot), which can be intraluminal or extraluminal—situation when the source of bleeding cannot be seen through endoscopy (Fig. 10.4).
- *Perforation*: Perforation from a penetrating ulcer is a life-threatening condition, usually requiring emergency surgery. It is usually a straightforward diagnosis, often with abundant pneumoperitoneum visible (Fig. 10.5). The site of perforation is sometimes visible as a region of discontinuity in the stomach or duodenal wall. Extraluminal fluid can also indicate perforation; however,

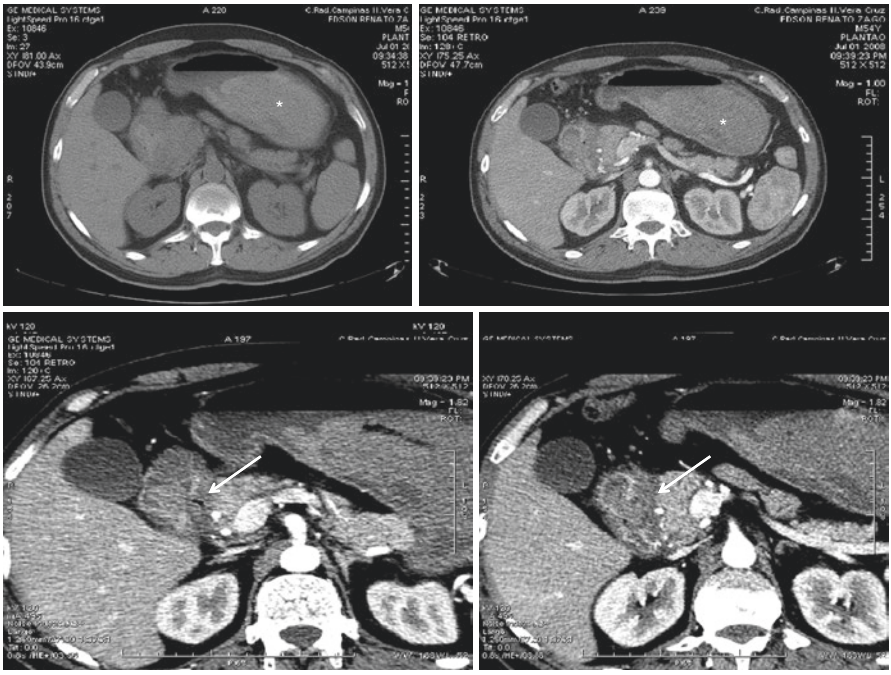

Fig. 10.4 Focal luminal outpouching in the second portion of the duodenum (*white arrow*), representing a perforated gastric ulcer with high-attenuating amorphous content in gastric lumen, compatible with blood (*asterisk*)

extraluminal oral contrast is seen in less than 50% of patients with perforation, as many perforated ulcers seal off rapidly (Fig. 10.1). While gastric perforation typically extends into the peritoneal space, duodenal ulcers can result in either intraperitoneal or retroperitoneal perforations, depending on ulcer location (Fig. 10.2). Primary CT findings of acute bowel perforation include pneumoperitoneum, bowel wall thickening and inflammatory changes in soft tissues and organs adjacent to the ulcer site, extravasation of ingested contrast media, and visualization of discontinuity of the bowel wall (demonstration of an ulcer crater). Secondary findings include collection of gas in a loculated space or unusual location. Therefore, extraluminal gas and fluid in the peritoneum or retroperitoneum are frequently seen in such cases. Perforation can also be contained resulting in collections that communicate to the gastric/bowel lumen (Fig. 10.5).

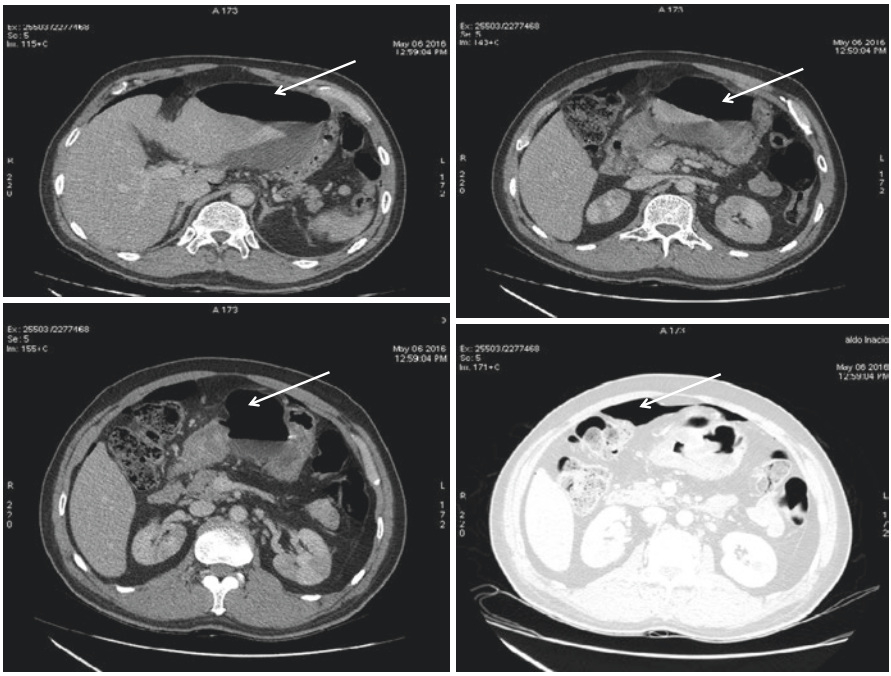

Fig. 10.5 Extraluminal gas and fluid in the peritoneum (*white arrow*), compatible with intraperitoneal perforation of a gastric ulcer

References

1. Lau JY, Sung J, Hill C, et al. Systematic review of the epidemiology of complicated peptic ulcer disease: incidence, recurrence, risk factors and mortality. Digestion. 2011;84:102.
2. Sung JJ, Tsoi KK, Ma TK, et al. Causes of mortality in patients with peptic ulcer bleeding: a prospective cohort study of 10,428 cases. Am J Gastroenterol. 2010;105:84.
3. Møller MH, Adamsen S, Thomsen RW, Møller AM. Preoperative prognostic factors for mortality in peptic ulcer perforation: a systematic review. Scand J Gastroenterol. 2010;45:785.
4. Noguiera C, Silva AS, Santos JN, et al. Perforated peptic ulcer: main factors of morbidity and mortality. World J Surg. 2003;27:782.
5. Sharma SS, Mamtani MR, Sharma MS, Kulkarni H. A prospective cohort study of postoperative complications in the management of perforated peptic ulcer. BMC Surg. 2006;6:8.
6. Ghekiere O, Lesnik A, Hoa D, et al. Value of computed tomography in the diagnosis of the cause of nontraumatic gastro- intestinal tract perforation. J Comput Assist Tomogr. 2007;31(2):169–76.
7. Bashinskaya B, Nahed BV, Redjal N, et al. Trends in peptic ulcer disease and the identification of Helicobacter Pylori as a causative organism: population-based estimates from the US Nationwide Inpatient Sample. J Glob Infect Dis. 2011;3:366.
8. Leontiadis GI, Sreedharan A, Dorward S, et al. Systematic reviews of the clinical effectiveness and cost-effectiveness of proton pump inhibitors in acute upper gastrointestinal bleeding. Health Technol Assess. 2007;11:iii–v.
9. Jacobs JM, Hill MC, Steinberg WM. Peptic ulcer disease: CT evaluation. Radiology. 1991;178(3):745–8.

10. Behrman SW. Management of complicated peptic ulcer disease. Arch Surg. 2005;140(2):201–8.
11. Madrazo BL, Halpert RD, Sandler MA, Pearlberg JL. Computed tomographic findings in penetrating peptic ulcer. Radiology. 1984;153(3):751–4.
12. Ongolo-Zogo P, Borson O, Garcia P, Gruner L, Valette PJ. Acute gastroduodenal peptic ulcer perforation: contrast-enhanced and thin-section spiral CT findings in 10 patients. Abdom Imaging. 1999;24(4):329–32.
13. Furukawa A, Sakoda M, Yamasaki M, et al. Gastrointestinal tract perforation: CT diagnosis of presence, site, and cause. Abdom Imaging. 2005;30(5):524–34.
14. Pun E, Firkin A. Computed tomography and complicated peptic ulcer disease. Australas Radiol. 2004;48(4):516–9.
15. Ramsay DW, Markham DH, Morgan B, Rodgers PM, Liddicoat AJ. The use of dilute Calogen as a fat density oral contrast medium in upper abdominal computed tomography, compared with the use of water and positive oral contrast media. Clin Radiol. 2001;56:670–3.
16. Thompson SE, Raptopoulos V, Sheiman RL, McNicholas MM, Prassopoulos P. Abdominal helical CT: milk as a low-attenuation oral contrast agent. Radiology. 1999;211:870–5.
17. Matsuoka Y, Masumoto T, Koga H, et al. Positive and negative oral contrast agents for combined abdominal and pelvic helical CT: first iodinated agent and second water. Radiat Med. 2000;18:213–6.
18. Lee DH. Two-dimensional and three-dimensional imaging of gastric tumors using spiral CT. Abdom Imaging. 2000;25:1–6.

Computed Tomography Evaluation of Small Bowel Ischemia

11

Gavin Sugrue and Michael Sugrue

"Occlusion of the mesenteric vessels is apt to be regarded as one of those conditions of which the diagnosis is impossible, the prognosis hopeless, and the treatment almost useless."
Cokkinis, 1930 [1]

11.1 Introduction

Mesenteric ischemia is a life-threatening condition characterized by insufficient blood supply to the bowel [2]. It is subclassified as acute mesenteric ischemia (AMI) and chronic mesenteric ischemia (CMI), the latter accounting for only 5% of mesenteric ischemia [3]. Mesenteric ischemia is associated with a high mortality rate of 50–90% [4, 5] despite advances in diagnostic tools and treatment options. Failure to recognize AMI can result in mesenteric infarction, intestinal necrosis, and ultimately death. Due to the nonspecific symptoms and lack of clinical signs of intestinal ischemia, a high index of suspicion is required for a prompt and accurate diagnosis.

G. Sugrue, M.B., B.C.H., B.A.O., M.R.C.P (✉)
Department of Radiology, Mater Misericordiae University Hospital, Dublin 7, Ireland
e-mail: g_sugrue@hotmail.com

M. Sugrue, MB, BCh, BAO, MD, FRCSI, FRACS
Department of Surgery, Letterkenny University Hospital, Donegal Clinical Research Academy, Donegal, Ireland

F. Catena et al. (eds.), *CT Scan in Abdominal Emergency Surgery*, Hot Topics in Acute Care Surgery and Trauma, https://doi.org/10.1007/978-3-319-48347-4_11

11.1.1 Tips

- A provisional working diagnosis of mesenteric ischemia should be made within <30 min of presentation.
- Formal diagnosis of mesenteric ischemia should be made <2 h after presentation.
- Surgery should be performed <4 h after diagnosis.
- Surgery +− interventional radiology is required in select cases (if available <90 min).

Advances in CT technology has established MDCT as the first-line imaging modality in suspected mesenteric ischemia [6–9]. It is a sensitive and noninvasive imaging tool that allows for rapid assessment of the patency of mesenteric vessels, bowel wall, mesenteric abnormalities and identifies a possible differential diagnosis. In this chapter, we provide an overview of the etiology and clinical features of small bowel intestinal ischemia, with a focus on optimal CT imaging techniques and characteristic imaging features of AMI.

11.2 Etiology

Four etiological forms of AMI are described (Table 11.1) and include arterial embolism (EAMI), arterial thrombosis (TAMI), venous thrombosis (VAMI), and nonocclusive mesenteric ischemia (NOMI) [10]. Mesenteric ischemia can be further subclassified into acute and chronic, which are characterized by the timing of symptom onset and degree of reduction in blood flow.

11.2.1 Tip

Sudden onset of severe epigastric pain in elderly patients with minimal clinical signs, often not relived by opioid analgesia, should lead to an immediate potential working diagnosis of AMI.

Firstly, EAMI is the most frequent cause of mesenteric ischemia contributing up to 45% of cases of AMI [4, 11]. Emboli typically arise from the left atrium/atrial appendage or cardiac valves in the setting of myocardial ischemia or arrhythmia [12] and occlude the proximal superior mesenteric artery (SMA). The classic finding of vomiting and/or diarrhea, with acute severe abdominal pain out of proportion clinical examination findings, is well described in EAMI in 40–80% of patients [13].

Secondly, TAMI accounts for approximately 25% of cases of AMI [4, 11] and may be acute or acute on chronic. It arises within an atherosclerotic plaque, often at the ostium of the SMA, which serves as a nidus for thrombosis. Thus, patients typically present with similar symptoms as EAMI due to the acute mesenteric vessel

Table 11.1 Risk factors and symptoms for acute and chronic mesenteric ischemia

		Incidence 95%	Risk factors	Symptoms	Acuity
AMI	EAMI	45%	Systemic emboli (arising from left atrium or cardiac valve), arrhythmia, myocardial infarct, aortic dissection, vasculitis	Acute severe abdominal pain, vomiting, and diarrhea	Acute
	TAMI	25%	Atherosclerosis, dyslipidemia, hypertension, aortic dissection, vasculitis	Similar to EAMI with antecedent progressive mesenteric angina	Acute
	VAMI	5–10%	Strangulated small bowel obstruction (e.g., closed loop bowel, internal hernia, intussusception), intra-abdominal malignancy or infection, cirrhosis, portal hypertension, hypercoagulable states (e.g., factor V Leiden deficiency), prior DVT or PE	Nonspecific abdominal pain	Subacute
	NOMI	10–20%	Hypotension, hypovolemia, trauma, recent surgery, low cardiac output, medications (vasopressin, cocaine, digitalis, beta-blockers)	Nonspecific abdominal pain, nausea, ileus	Acute or subacute
CMI		5%	Atherosclerosis (>90%), fibromuscular dysplasia, vasculitis, median arcuate ligament syndrome, tumors invading the mesenteric vessels	Postprandial pain, sitophobia, weight loss	Chronic

occlusion but often describe antecedent progressive mesenteric angina [12]. Major risk factors include atherosclerotic disease, hypertension, dyslipidemia, an aortic dissection or aneurysm, vasculitis, and dehydration.

Thirdly, VAMI accounts for 10% of AMI cases. It can be caused by both the mechanical obstructions of mesenteric vessels or mesenteric vein thrombus. VAMI usually occurs in patients aged >40 years, contrasting to EAMI, and TAMI is seen predominately in patients aged >60 years [14, 15]. Patients often present with acute or subacute abdominal pain. A focused history will identify risk factors for venous thrombosis including pregnancy, protein C and S or antithrombin deficiencies, intra-abdominal malignancy or acute infection, portal hypertension, or trauma [16]. In fact, up to 50% of patients with VAMI will have had a prior pulmonary embolus or deep venous thrombus [17]. The most commonly associated hypercoagulability state is Factor V Leiden mutation, seen in 20–40% of VAMI cases [18].

Finally, NOMI accounts for 20% of cases of mesenteric ischemia. NOMI is due to mesenteric hypoperfusion secondary to systemic hypotension or vasoconstrictive medication (e.g., vasopressin, digitalis, amphetamine, and cocaine) [19]. Unlike

EAMI, TAMI, or VAMI, there is no arterial or venous mesenteric vessel occlusion. It is most commonly seen in postoperative patients with severe systemic illnesses and with a poor cardiac output. While symptoms of NOMI are nonspecific and difficult to elicit in the critical care setting, they include acute abdominal pain, distension, and occult blood in the stools [17, 20].

CMI is a rare condition and only accounts for 5% of all cases of mesenteric ischemia [21]. In contrast to AMI, CMI is associated with atherosclerotic stenosis of the mesenteric vessels in 90% of cases [22, 23]. CMI presents with insidious nonspecific symptoms and may include postprandial pain, fear of eating (sitophobia), or weight loss [24]. Less commonly, non-atherosclerotic causes of CMI include fibromuscular dysplasia, vasculitis, median arcuate ligament syndrome, and tumors invading mesenteric vessels [25]. Symptoms typically arise when two of the three major mesenteric vessels (i.e the celiac, SMA, and IMA), often the SMA and celiac artery, demonstrate severe atherosclerotic stenosis.

11.3 CT Techniques for the Evaluation of Acute Mesenteric Ischemia

MDCT and CT angiography (CTA) has established itself as the first-line imaging tool in the acute evaluation of AMI [26] (Table 11.2). MDCT and CTA are rapidly acquired, noninvasive, and highly sensitive in the diagnosis of AMI. Recent meta-analysis demonstrates the diagnostic sensitivity for CT ranges from 89 to 100% [27, 28]. However, this is often not the case in clinical practice and must be interpreted with caution. CT demonstrates a reduced sensitivity of 67–85% [29, 30] in the diagnosis of AMI if possible diagnosis of AMI is provided in the clinical information prior to CT. Conventional angiography, once the gold standard diagnostic tool, is not routinely employed first-line, as it is invasive, more time-consuming, and not as readily accessible as CT.

Table 11.2 CT imaging protocol for suspected mesenteric ischemia

Multiphase imaging	Unenhanced, arterial (30 s post-IV contrast), portovenous (60 s post-IV contrast)
Oral contrast	Not routinely used for suspected AMI. If oral contrast is given, 500–600 mls of a neutral oral contrast (water). Positive oral contrast is not indicated
Rectal contrast	Not indicated
Intravenous contrast	120 mls of iodinated contrast (350 mg iodine/mL) administered at 5 mL/s
Detector collimation	128 × 0.6 mm
Reconstruction slice	1.0 mm and 5.0 mm
Reconstruction images	Axial, coronal, and sagittal reformats. 3D maximum intensity projection (MIP) and volume-rendered images
Scan field of view	From xiphoid process to pubic symphysis

11.4 Oral Contrast Agents

"Positive" and "neutral" oral contrast agents are routinely used in abdominal CT imaging. Contrast agents which are >50 Hounsfield units (HU) are "positive" agents (e.g., iodinated compounds or barium sulfate). Agents with HU near water (−20 to +20 HU) are considered "neutral" agents (e.g., water or sorbitol solutions with 0.1% barium sulfate). Positive oral contrast may be of detriment in the evaluation of AMI. The presence of hyperdense oral contrast within the bowel lumen limits assessment of bowel wall enhancement, intramural hematoma, and the mesenteric vessels [31, 32]. Conversely, "neutral" oral contrast agents distend the bowel lumen with low-attenuating material which may be of value in assessing bowel wall enhancement patterns [33, 34]. Unfortunately, the transit time for oral contrast through the small bowel is often poor in the setting of AMI due to vomiting, abdominal pain, or an adynamic ileus [32, 35]. Thus, the decision to administer oral contrast poses a risk of aspiration and may delay prompt diagnosis of AMI. Delays in diagnosis of AMI can be fatal, with microscopic changes of bowel ischemia detected within minutes [36] of arterial mesenteric vessel occlusion.

There are no consensus guidelines on the CT protocol recommended for AMI. In routine clinical practice, AMI is evaluated with a biphasic CTA, using arterial and portal venous phases [37]. Incorporating an initial non-contrast computed tomography (NECT) phase, termed triphasic CTA, remains controversial. An initial NECT provides an assessment of the extent of calcified atherosclerotic plaque, bowel wall enhancement, and the presence of intramural hematoma. Current opinion is that although triphasic imaging may mildly improve the specificity and sensitivity in detection of AMI, it comes at the expense of a one-third increase in radiation dose [6, 31, 38, 39]. Further, assessment for bowel wall hypoenhancement on biphasic CT can be performed by comparing the suspected region of AMI to a loop of normally enhancing bowel which acts as the internal control [6]. The arterial phase of the CTA delineates the mesenteric arterial supply to allow for precise evaluation of the mesenteric vessels and bowel wall enhancement. The venous phase provides a further assessment of bowel wall enhancement and thickness, visualization of the mesentery, and venous drainage, crucial in suspected VAMI.

Prior to IV contrast administration, a non-contrast CT can be performed. This is not essential, and within our institution, we do not routinely perform a non-contrast CT. To acquire the arterial phase, we administer 120 mL of nonionic iodinated contrast (350 mg iodine/mL) injected at 5 mL/s. A region of interest is placed over the proximal abdominal aorta, triggering image acquisition when a 150 HU threshold is reached [6], with images acquired 30 s post-IV contrast administration. A portal venous phase is acquired at 60 s after IV contrast administration. Images are reformatted into 2.5 mm axial, 2.5 mm sagittal, and 3 mm coronal images. Certain radiological features, like small mesenteric vessel branch vessels or air bubbles in pneumatosis intestinalis, are 1–2 mm in size and require high spatial resolution to be visualized [32, 40]. Recent advances in CT technology and post-processing techniques, such as dual-energy CT, have shown promise in sensitivity and diagnostic confidence of bowel wall hypoenhancement [41, 42]; however, they are not currently routinely employed in our clinical practice.

11.5 CT Imaging Features of AMI

There is no single CT finding that is both sensitive and specific for the diagnosis of mesenteric ischemia (Table 11.3). In particular, bowel wall changes, as outlined below, may be subtle or focal in nature, and thus, high index of clinical and radiological suspicious is required.

Table 11.3 Spectrum of CT findings of AMI and CMI

	Arterial ischemia (EAMI and TAMI)	Venous ischemia (VAMI)	Nonocclusive ischemia (NOMI)	CMI
Vasculature	Mesenteric artery filling defect, atherosclerosis, dissection flap. SMA > SMV caliber	Venous filling defect, engorged mesenteric veins. SMV > SMA caliber	Patent mesenteric vessels, mesenteric artery vasospasm	Atherosclerosis
Bowel dilation	Variable	↑↑	Variable	Variable
	Dilation associated with transmural ischemia or infarction	Mild-moderate dilation. If present often associated with transmural ischemia or infarction	If present often associated with transmural ischemia or infarction	If present often associated with transmural ischemia or infarction
Bowel wall thickness	↑ or ↓	↑↑↑	↑	↑ or ↓
	Thin ("paper thin") in acute ischemia or thickened with reperfusion	Thick and edematous due to mural edema and hemorrhage	Diffuse thickening	Thin in acute ischemia or thickened with reperfusion
Bowel wall attenuation	↑ or ↓	↑ or ↓	↑ or ↓	↑ or ↓
	Hypodense (edema seen post-reperfusion) or hyperdense (hemorrhage)	Hypodense (edema) or hyperdense (hemorrhage)	Hypodense (edema) or hyperdense (hemorrhage)	Hypodense (edema) or hyperdense (hemorrhage)
Bowel wall enhancement	↑ or ↓	↑ or ↓	↑ or ↓	↑ or ↓
	Reduced, normal, or increased (with reperfusion). Target sign	Reduced, normal, or increased. Target sign	Reduced, normal, or increased. Diffuse non-focal segments of bowel involved. Target sign	Reduced, normal, or increased
Mesentery inflammation	— or ↑	↑↑↑	— or ↑	Not specific
	If present, associated with bowel ischemia or superimposed infection	Associated with mesenteric fat stranding, fluid, and ascites	If present, associated with bowel ischemia or superimposed infection	If present, associated with bowel ischemia or superimposed infection
Pneumatosis	Nonspecific in absence of other bowel wall abnormalities	Nonspecific in absence of other bowel wall abnormalities	Nonspecific in absence of other bowel wall abnormalities	Nonspecific in absence of other bowel wall abnormalities

AMI acute mesenteric ischemic, *CMI* chronic mesenteric ischemia, *EAMI* arterial embolus mesenteric ischemia, *TAMI* arterial thrombosis mesenteric ischemia, *VAMI* venous thrombosis mesenteric ischemia, *NOMI* nonocclusive mesenteric ischemia, *DVT* deep venous thrombus, *PE* pulmonary embolus

↑ mild increase, ↑↑ moderate increase, ↑↑↑ moderate-severe increase, ↓ mild decrease, — no change

11.6 Mesenteric Arteries

EAMI accounts for 60% of cases of mesenteric ischemia, most often secondary to an embolus occluding the proximal SMA (Figs. 11.1, 11.2 and 11.3) [32]. Emboli have a predilection for the SMA due to its large caliber, narrow angulation with the aorta, and high flow rates [43] compared to the celiac and IMA. An embolus

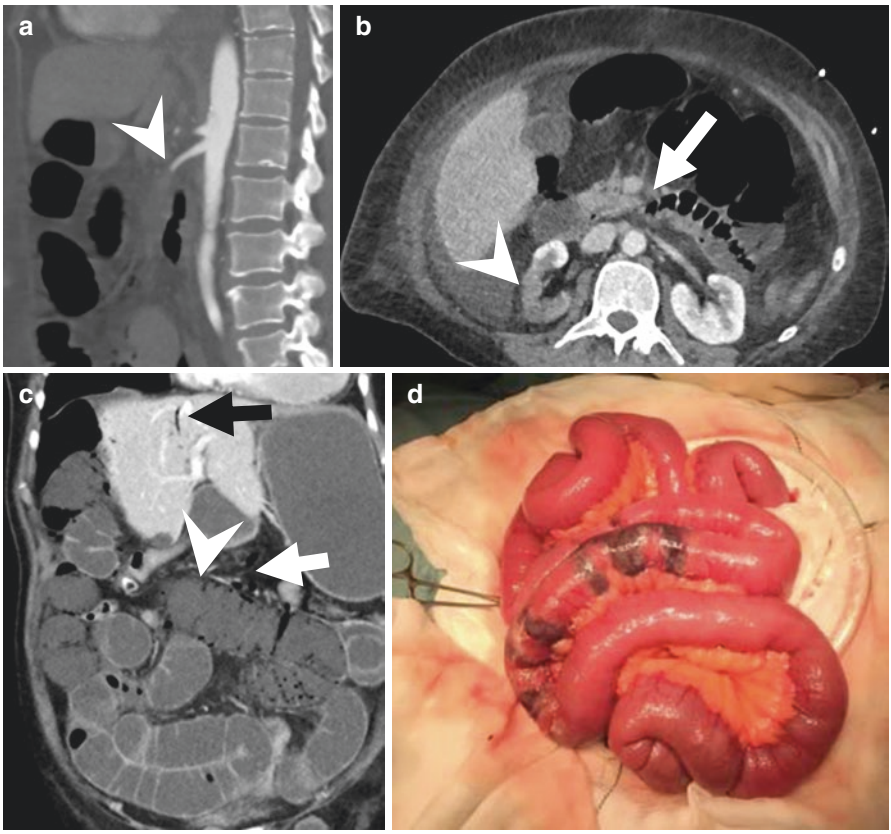

Fig. 11.1 A 77-year-old female with atrial fibrillation presented with acute abdominal pain. (**a**) Sagittal CT shows abrupt occlusion of the SMA 2 cm from its origin (*arrowhead*). (**b**) Axial CT identifies total occlusion of the proximal SMA (*arrow*) and infarction of the right kidney (*arrowhead*). (**c**) Coronal CT demonstrates diffuse small bowel dilation. There is evidence of thinning of the small bowel wall, hypoenhancement and pneumatosis (*arrowhead*), portomesenteric gas (*white arrow*), and intrahepatic portal venous gas (*black arrow*) consistent with ischemia. (**d**) Intraoperative image demonstrating multifocal regions of ischemia of the jejunum correlating to the region of pneumatosis identified on preoperative CT

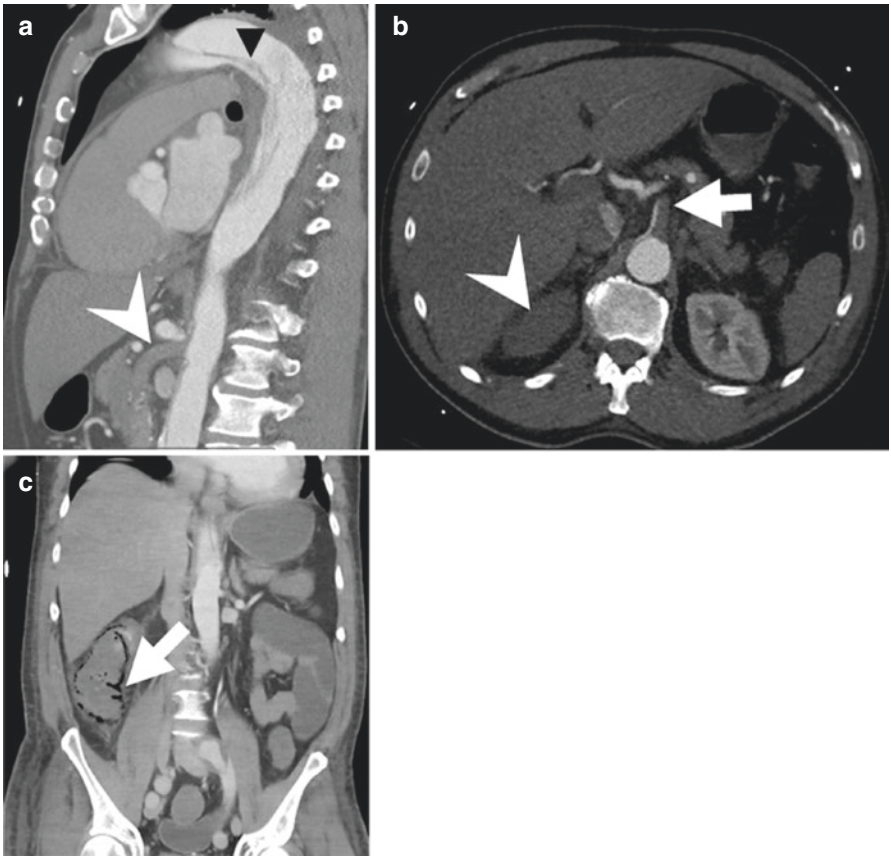

Fig. 11.2 A 42-year-old male with Ehlers-Danlos presented with an acute aortic dissection. (**a**) Sagittal CT demonstrates a type B aortic dissection (*black arrowhead*) extending to involve the SMA ostium with secondary SMA thrombosis (*white arrowhead*). (**b**) Axial CT shows near-occlusive thrombus at the origin of the SMA (*arrow*) and infarction of the right upper pole of the kidney (*arrowhead*). Dilated loop of jejunum within the right flank suggestive of ischemia or infarction

can be identified on CT as centrally located hypodense filling defect within a mesenteric vessel, usually the SMA, best visualized on arterial phase imaging. The presence of infarction of other organs (e.g., the spleen and kidney) raises the suspicion of embolic etiology. TAMI has a predilection for the ostium of mesenteric vessels. In contrast to an embolus, the thrombus is usually eccentric, located within the first 2 cm of the origin of the SMA, occurring on the background of calcified atherosclerosis plaque [32]. An aortic dissection [44] or malignant tumor encasement of mesenteric vessels is a less common cause of AMI.

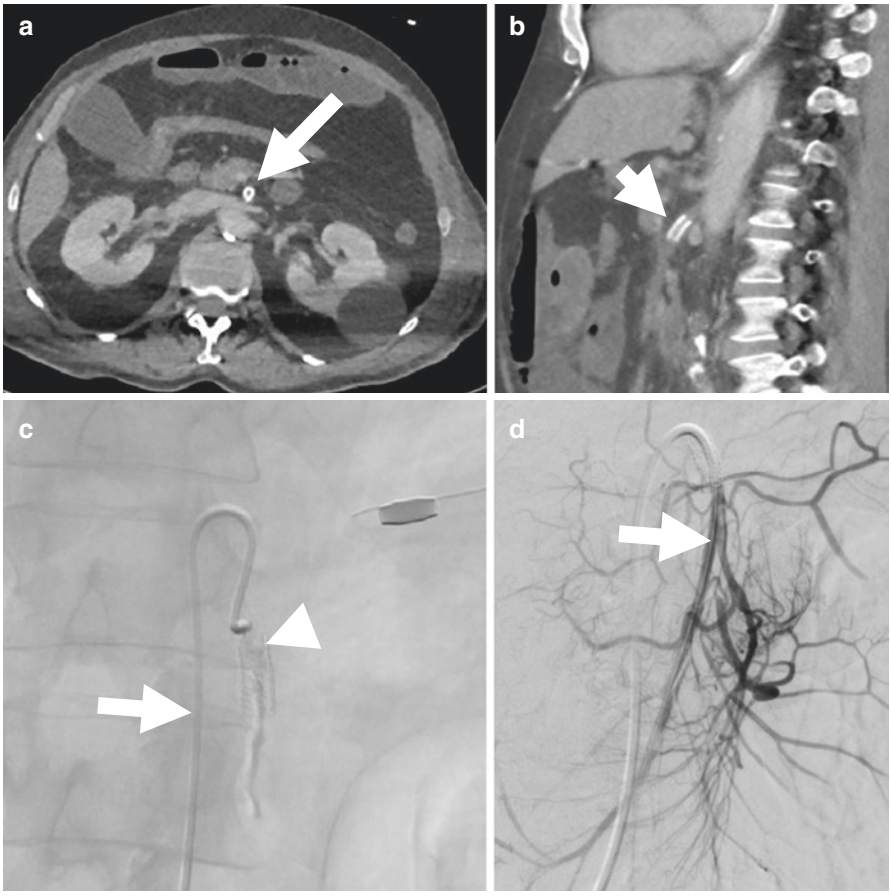

Fig. 11.3 A 56-year-old male, with prior SMA stenting, presents with acute abdominal pain. (**a** and **b**) Axial and sagittal CT demonstrates total occlusion of the SMA stent with thrombus. (**c**) SMA angiography via catheter (*arrow*) shows absence of flow in the stent and SMA (*arrowhead*). (**d**) Catheter-delivered tissue plasminogen activator (tPA) and repetitive aspiration thrombectomy successfully removed thrombus with significant improved flow within the SMA (*arrow*)

11.7 Mesenteric Veins

VAMI accounts for 10% of AMI (Figs. 11.4 and 11.5). It may arise in secondary to venous thrombosis from a local inflammatory process (e.g., pancreatitis, diverticulitis, intra-abdominal abscess, neoplasm) or hypercoagulable states. VAMI can also arise in the setting of mechanical bowel obstruction, such as a volvulus, intussusception, or closed-loop bowel obstruction. A venous thrombus is identified as a low-attenuation filling defect on portovenous phase and is seen in up to 90% of

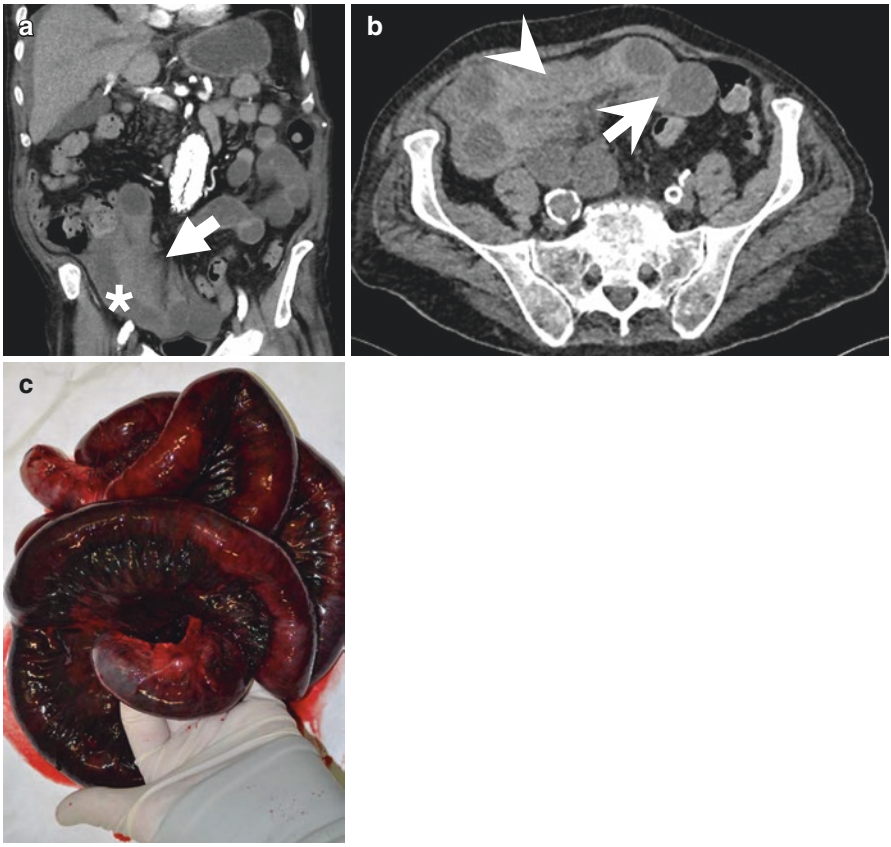

Fig. 11.4 A 55-year-old male with acute abdominal pain and bilious vomiting. (**a**) Coronal CT shows a strangulated small bowel internal hernia. Focally dilated loops of small bowel (*asterisk*) in the right flank are consistent with a closed loop bowel obstruction. Bowel wall thickening and adjacent mesenteric edema is noted (*arrow*). (**b**) Non-contrast axial CT demonstrates increased density of the bowel wall (*arrow*) and mesentery (*arrowhead*) suspicious for hemorrhagic infarction. (**c**) Intraoperative image of the resected small bowel, demonstrating diffuse small bowel ischemia

cases of venous bowel ischemia [45]. Venous thrombosis causes venous congestion manifested by mesenteric veins [46].

11.8 Bowel Dilation

Focal dilation of the bowel in the setting of AMI (Fig. 11.1) demonstrates a moderate sensitivity and specificity of 65% and 78%, respectively [47]. Interruption of normal peristalsis in AMI is a reflex to mesenteric ischemia, with resultant focal

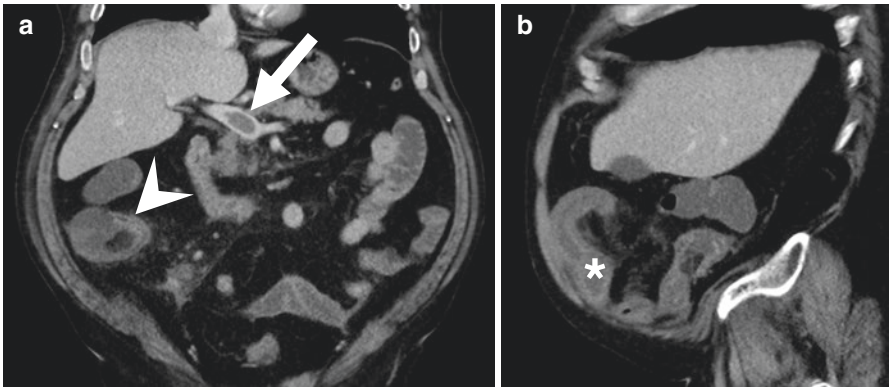

Fig. 11.5 A 52-year-old male with subacute abdominal pain and diarrhea. (**a**) Coronal CT shows a nonocclusive thrombus within the distal portal and proximal superior mesenteric veins (*arrow*). There is secondary focal bowel wall thickening, hyperenhancement, and dilation of a loop of ileum (*arrowhead*). (**b**) Sagittal CT shows further focal small bowel wall thickening, mucosal hyperenhancment (*asterisk*) with adjacent mesenteric fat stranding (*arrowhead*)

distention of bowel from the pooling of intraluminal secretions from aperistaltic segments of bowel [34]. The presence of bowel dilation is associated with transmural ischemia or infarction [48].

11.9 Bowel Wall Thickness

In AMI, the bowel wall can be thickened, thinned, or normal in caliber. While bowel wall thickening is not specific for AMI, it is the most frequently observed CT finding in non-arterial AMI due to mural edema and/or hemorrhagic of the ischemic bowel wall [34]. Normal bowel wall thickness is 3–5 mm. A thickened bowel wall is typically 6–8 mm but can measure up to 1.5 cm in the setting of VAMI [32]. In contrast, thinning of the bowel wall is observed in EAMI and TAMI. It is classically described as a "paper-thin" bowel wall secondary to a reduction or absence of arterial inflow. The distribution of bowel wall thickening or thinning provide clues to the arterial or venous distribution that is involved. For example, in acute SMA or SMV occlusion, the small bowel, right colon, and proximal transverse colon may be thinned or thickened, respectively [25]. In NOMI, due to diffuse vessel hypoperfusion, bowel wall thickening may be diffuse involving multiple vascular territories. Cautious interpretation of bowel wall thickening is required, as firstly it is not a consistent CT finding in mesenteric ischemia. Secondly, the degree of thickening does not correlate with severity [25] and must be interpreted relative to the degree of bowel distention [49, 50].

11.10 Bowel Wall Attenuation

Increased bowel wall attenuation on unenhanced CT images is a specific sign for bowel ischemia as a result of submucosal hemorrhage [6, 51]. In cases of intramural hemorrhage, misinterpretation of the high density of the bowel wall as the physiological enhancement on contrast-enhanced CT can be avoided by comparing the degree of bowel wall enhancement on the initial non-contrast study. If only biphasic imaging is acquired, comparing a suspected region of AMI to a loop of normally enhancing bowel can act as the internal control [6]. In contrast, decreased bowel wall attenuation is secondary to bowel wall edema, often identified in mesenteric arterial occlusion after reperfusion, VAMI, and cases of bowel strangulation. The stratified enhancement pattern of the bowel wall is known as the "target sign" and is described in AMI subtypes: inner mucosal and outer serosal hyperdense layers interposed by a layer of submucosal hypodensity (Fig. 11.6). The hyperdense inner and outer layers correlate with hyperemia or hyperperfusion and the hypodense middle submucosal layer reflects submucosal edema.

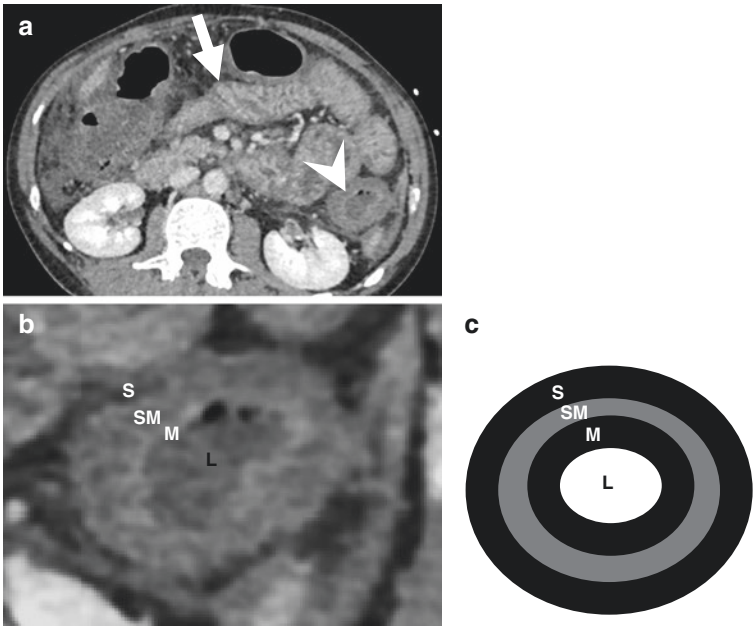

Fig. 11.6 A 50-year-old male with prolonged severe hypotension and abdominal pain. (**a**) Axial CT shows a stratified enhancement pattern of the jejunum (*arrowhead*) consistent with the "target sign." Jejunal mucosal hyperenhancment and bowel wall thickening (*arrow*) consistent with hyperemia. (**b** and **c**) Axial CT shows the "target sign": enhancing inner mucosal (M) and enhancing outer serosal (S) layers due to hyperemia. A middle layer of submucosal (SM) hypodensity is secondary to edema and/or inflammation (L: lumen)

11.11 Bowel Wall Enhancement

In AMI, bowel wall enhancement may be absent, decreased, or increased. Focal wall hypoenhancement (Fig. 11.1) pooled from two studies [37, 40] demonstrates a high specificity of 97% and poor specificity of 42% on biphasic imaging [47]. Nonetheless, bowel wall enhancement should be interpreted with caution, especially in cases of AMI with reperfusion [46] where increased mural enhancement, paradoxically, can be seen in hyperperfusion (e.g., reperfusion post-EAMI, TAMI, or NOMI) or hyperemia in VAMI [6]. Restoration of mesenteric arterial blood flow (via surgical or embolectomy or spontaneous means) results in bowel wall thickening, a hyperdense inner mucosal and outer serosal layer known as the "target sign" (Fig. 11.6) [6]. This bowel wall enhancement pattern confers good prognostic value, felt to represent bowel wall viability [6, 52].

11.12 Mesentery

Ascites or mesenteric stranding is an uncommon finding in EAMI or TAMI. When present, it is often associated with severe disease [53] with bowel ischemia or infarction frequently observed [6]. In contrast, mesenteric inflammation and ascites are present in the majority of patients with VAMI and thus not a sensitive indicator of disease severity [48]. Mesenteric inflammatory fat stranding and edema seen in VAMI are due to engorgement of the draining mesenteric veins. This causes an elevation in the bowel wall hydrostatic pressure with resultant leakage of extravascular fluid into the bowel wall, mesentery, and peritoneal cavity [45] (Fig. 11.4). This impaired venous drainage may result in arterial sufficiency from increased intravascular/interstitial pressure in the bowel wall ultimately leading to bowel ischemia [48, 54].

11.13 Pneumatosis Intestinalis and Portomesenteric Gas

Pneumatosis intestinalis (PI) and portomesenteric gas are the presence of air dissecting between the layers of the bowel wall and air within the portovenous system, respectively (Figs. 11.7 and 11.8). The presence of PI or portomesenteric gas is up to 100% specific for bowel ischemia, particularly when associated with key imaging findings such as abnormal bowel wall enhancement [47]. In AMI, PI develops at a late stage [55, 56] when the friable layers of the bowel wall can be dissected by air particles. PI is suspicious for transmural infarction, particularly when associated with portomesenteric gas [25]. The presence of PI and portomesenteric gas, in the absence of other concomitant bowel findings such as abnormal bowel wall thickening or enhancement, should be interpreted in the correct clinical context. A broad spectrum of nonischemic and benign causes of PI have been well described [57] including inflammatory bowel disease, iatrogenic abdominal distention, asthma, chronic obstructive pulmonary disease, and connective tissue disorders.

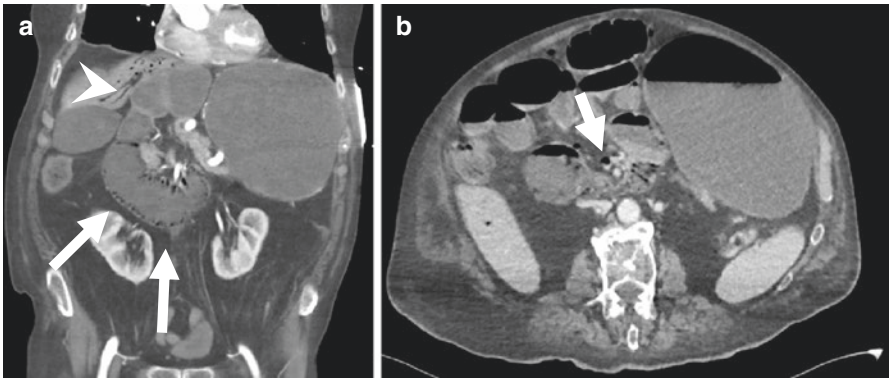

Fig. 11.7 A 65-year-old female with acute severe abdominal pain. (**a**) Coronal CT shows focal dilation of the duodenum with marked hypoenhancement and pneumatosis (*arrows*) and intrahepatic portovenous gas (*arrowhead*) consistent with a closed looped small bowel obstruction. (**b**) Axial CT shows portomeseteric gas in the SMA (*arrow*)

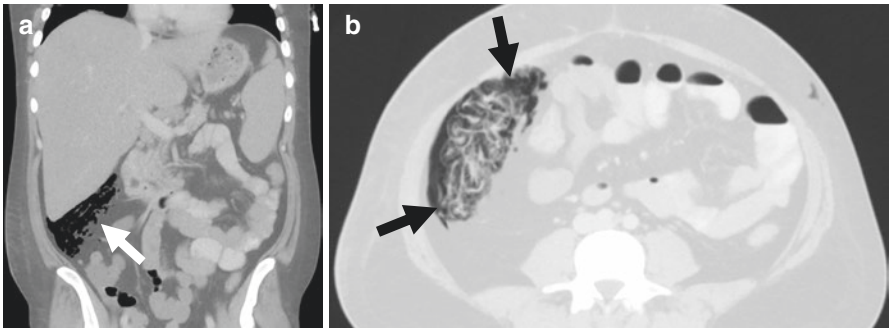

Fig. 11.8 Outpatient staging CT abdomen in a 42-year-old male, currently on biological therapy for leukemia. No abdominal pain. (**a** and **b**) Axial and coronal CT shows focal pneumatosis (*white and black arrows*) within the large bowel at the hepatic flexure. This bowel segment demonstrates normal wall thickness and enhancement. No portovenous gas or mesenteric vessel abnormality, findings consistent with benign pneumatosis

Conclusion

Prompt and accurate diagnosis of mesenteric ischemia is required to optimize survival. The broad spectrum of clinical symptoms and radiological findings can make the early diagnosis of mesenteric ischemia challenging. An understanding of multiphase imaging protocols, characteristic radiological findings, and potential limitations of CT plays a pivotal role in establishing the diagnosis and early initiation of appropriate management.

References

1. Cokkinis AJ. Observations on the mesenteric circulation. J Anat. 1930;64:200.
2. Ozden N, Gurses B. Mesenteric ischemia in the elderly. Clin Geriatr Med. 2007;23:871–87.
3. Costa A, Chidambaram V, Lee J, et al. Multidetector computed tomography of mesenteric ischaemia. Insights Imaging. 2014;5:657–66.
4. Oldenburg W, Lau L, Rodenberg T, et al. Acute mesenteric ischemia. Arch Intern Med. 2004;164:1054.
5. Segatto E, Mortelé K, Ji H, et al. Acute small bowel ischemia: CT imaging findings. Semin Ultrasound CT MR. 2003;24:364–76.
6. Schieda N, Fasih N, Shabana W. Triphasic CT in the diagnosis of acute mesenteric ischaemia. Eur Radiol. 2013;23:1891–900.
7. McLeod R, Lindsay T, O'Malley M. For members of the evidence based reviews in surgery group. Canadian Association of General Surgeons and American College of surgeons evidence based reviews in surgery. 15: biphasic computed tomography with mesenteric evaluation of acute mesenteric ischemia. Can J Surg. 2005;48:491–3.
8. Barmase M, Kang M, Wig J, et al. Role of multidetector CT angiography in the evaluation of suspected mesenteric ischemia. Eur J Radiol. 2011;80:e582–7.
9. Yikilmaz A, Karahan O, Senol S, et al. Value of multislice computed tomography in the diagnosis of acute mesenteric ischemia. Eur J Radiol. 2011;80:297–302.
10. Stamatakos M, Stefanaki C, Mastrokalos D, et al. Mesenteric ischemia: still a deadly puzzle for the medical community. Tohoku J Exp Med. 2008;216:197–204.
11. Acosta SBjörck M. Modern treatment of acute mesenteric ischaemia. Br J Surg. 2013;101:e100–8.
12. Berland T, Oldenburg W. Acute mesenteric ischemia. Curr Gastroenterol Rep. 2008;10:341–6.
13. Block T. Acute occlusion of the superior mesenteric artery. 1st ed. Uppsala: Acta Universitatis Upsaliensis; 2010.
14. Vokurka J, Olejnik J, Jedlicka V, et al. Acute mesenteric ischemia. Hepato-Gastroenterology. 2007;55:1349–52.
15. Alvi AR, Khan S, Niazi SK, et al. Acute mesenteric venous thrombosis: improved outcome with early diagnosis and prompt anticoagulation therapy. Int J Surg. 2009;7:210–3.
16. Golino A, Crawford EM, Gathe JC, et al. Recurrent small bowel infarction associated with antithrombin deficiency. Am J Gastroenterol. 1997;92:323–5.
17. Cangemi JR, Picco MF. Intestinal ischemia in the elderly. Gastroenterol Clin N Am. 2009;38:527–40.
18. Dewitte A, Biais M, Coquin J, et al. Diagnosis and management of acute mesenteric ischemia. Ann Fr Anesth Reanim. 2011;30:410–20.
19. Trompeter M, Brazda T, Remy C, et al. Non-occlusive mesenteric ischemia: etiology, diagnosis, and interventional therapy. Eur Radiol. 2001;12:1179–87.
20. Dorudi S, Lamont PM. Intestinal ischaemia in the unconscious intensive care unit patient. Ann R Coll Surg Engl. 1992;74:356–9.
21. Bockel JV, Geelkerken RH, Wasser MN. Chronic splanchnic ischaemia. Best Pract Res Clin Gastroenterol. 2001;15:99–119.
22. Cognet FCA, Salem DB, Dranssart M, et al. Chronic mesenteric ischemia: imaging and percutaneous treatment. Radiographics. 2002;22:863–879.7.
23. Feldman M, Friedman L, Sleisenger M. Sleisenger & Fordtran's gastrointestinal and liver disease. 1st ed. Philadelphia: Saunders; 2002. p. 2321–40.
24. Sreenarasimhaiah J. Chronic mesenteric ischemia. Best Pract Res Clin Gastroenterol. 2005;19:283–95.
25. Levy AD. Mesenteric Ischemia. Radiol Clin N Am. 2007;45:593–9.

26. Oliva IB, Davarpanah AH, Rybicki FJ, et al. ACR appropriateness criteria® imaging of mesenteric ischemia. Abdom Imaging. 2013;38:714–9.
27. Menke J. Diagnostic accuracy of multidetector CT in acute mesenteric ischemia: systematic review and meta-analysis. Radiology. 2010;256:93–101.
28. Cudnik MT, Darbha S, Jones J, et al. The diagnosis of acute mesenteric ischemia: a systematic review and meta-analysis. Acad Emerg Med. 2013;20:1087–100.
29. Lehtimäki TT, Kärkkäinen JM, Saari P, et al. Detecting acute mesenteric ischemia in CT of the acute abdomen is dependent on clinical suspicion: review of 95 consecutive patients. Eur J Radiol. 2015;84:2444–53.
30. Wadman M, Block T, Ekberg O, et al. Impact of MDCT with intravenous contrast on the survival in patients with acute superior mesenteric artery occlusion. Emerg Radiol. 2009;17:171–8.
31. Geffroy Y, Boulay-Coletta I, Jullès M-C, et al. Increased unenhanced bowel-wall attenuation at multidetector CT is highly specific of ischemia complicating small-bowel obstruction. Radiology. 2014;270:159–67.
32. Horton KM, Fishman EK. Multidetector CT angiography in the diagnosis of mesenteric ischemia. Radiol Clin N Am. 2007;45:275–88.
33. Furukawa A, Kanasaki S, Kono N, et al. CT diagnosis of acute mesenteric ischemia from various causes. Am J Roentgenol. 2009;192:408–16.
34. Wasnik A, Kaza RK, Al-Hawary MM, et al. Multidetector CT imaging in mesenteric ischemia—pearls and pitfalls. Emerg Radiol. 2010;18:145–56.
35. Lee SS, Park SH. Computed tomography evaluation of gastrointestinal bleeding and acute mesenteric ischemia. Radiol Clin N Am. 2013;51:29–43.
36. Robinson JW, Mirkovitch V, Winistorfer B, Saegesser F. Response of the intestinal mucosa to ischaemia. Gut. 1981;22:512–27.
37. Aschoff A, Stuber G, Becker B, et al. Evaluation of acute mesenteric ischemia: accuracy of biphasic mesenteric multi-detector CT angiography. Abdom Imaging. 2008;34:345–57.
38. Jang KM, Min K, Kim MJ, et al. Diagnostic performance of CT in the detection of intestinal ischemia associated with small-bowel obstruction using maximal attenuation of region of interest. Am J Roentgenol. 2010;194:957–63.
39. Chuong AM, Corno L, Beaussier H, et al. Assessment of bowel wall enhancement for the diagnosis of intestinal ischemia in patients with small bowel obstruction: value of adding unenhanced CT to contrast-enhanced CT. Radiology. 2016;280:98–107.
40. Kirkpatrick IDC, Kroeker MA, Greenberg HM. Biphasic CT with mesenteric CT angiography in the evaluation of acute mesenteric ischemia: initial experience. Radiology. 2003;229:91–8.
41. Darras KE, Mclaughlin PD, Kang H, et al. Virtual monoenergetic reconstruction of contrast-enhanced dual energy CT at 70keV maximizes mural enhancement in acute small bowel obstruction. Eur J Radiol. 2016;85:950–6.
42. Potretzke TA, Brace CL, Lubner MG, et al. Early small-bowel ischemia: dual-energy CT improves conspicuity compared with conventional CT in a swine model. Radiology. 2015;275:119–26.
43. Gore R, Thakrar K, Mehta U, et al. Imaging in intestinal ischemic disorders. Clin Gastroenterol Hepatol. 2008;6:849–58.
44. Jung SC, Lee W, Park E-A, et al. Spontaneous dissection of the splanchnic arteries: CT findings, treatment, and outcome. Am J Roentgenol. 2013;200:219–25.
45. Bradbury M, Kavanagh P, Bechtold R, et al. Mesenteric venous thrombosis: diagnosis and noninvasive imaging. Radiographics. 2002;22:527–41.
46. Duran R, Denys AL, Letovanec I, et al. Multidetector CT features of mesenteric vein thrombosis. Radiographics. 2012;32:1503–22.
47. Wallace AB, Raptis CA, Mellnick VM. Imaging of bowel ischemia. Curr Radiol Rep. 2016;4:29.
48. Lee SS, Ha HK, Park SH, et al. Usefulness of computed tomography in differentiating transmural infarction from nontransmural ischemia of the small intestine in patients with acute mesenteric venous thrombosis. J Comput Assist Tomogr. 2008;32:730–7.

49. Macari M, Megibow AJ, Balthazar EJ. A pattern approach to the abnormal small bowel: observations at MDCT and CT enterography. Am J Roentgenol. 2007;188:1344–55.
50. Wittenberg J, Harisinghani MG, Jhaveri K, et al. Algorithmic approach to CT diagnosis of the abnormal bowel wall. Radiographics. 2002;22:1093–107.
51. Tseng C-Y, Chiu Y-H, Chuang J-L, et al. How to differentiate spontaneous intramural intestinal hemorrhage from acute mesenteric ischemia. Am J Emerg Med. 2013;31:1586–90.
52. Taourel PG, Deneuville M, Pradel JA, et al. Acute mesenteric ischemia: diagnosis with contrast-enhanced CT. Radiology. 1996;199:632–6.
53. Chou CK. CT manifestations of bowel ischemia. Am J Roentgenol. 2002;178:87–91.
54. Patel A, Kaleya RN, Sammartano RJ. Pathophysiology of mesenteric ischemia. Surg Clin N Am. 1992;72:31–41.
55. Ho LM, Paulson EK, Thompson WM. Pneumatosis intestinalis in the adult: benign to life-threatening causes. Am J Roentgenol. 2007;188:1604–13.
56. Morris MS, Gee AC, Cho SD, et al. Management and outcome of pneumatosis intestinalis. Am J Surg. 2008;195:679–83.
57. Peter SDS. The spectrum of pneumatosis intestinalis. Arch Surg. 2003;138:68.

The Role of Computed Tomography in the Acute Presentation of Colorectal Cancer

12

Laura Lomaglio, Giulia Montori, Anna Pecorelli, Sandro Sironi, Massimo Sartelli, Luca Ansaloni, and Federico Coccolini

12.1 Introduction

Colorectal cancer (CRC) is the third most common malignancy in both men and women and also the third cause of cancer death among both male and female oncologic patients (8% of all cancer-related deaths in both categories) [1].

The symptoms and signs of CRC depend on the location of tumor and whether it has progressed or metastasized elsewhere in the body. Screening programs are not being systematically conducted yet, and this is surely one of the causes that can explain the number of emergency presentations of CRC [2]. Over 15% of patients will present at the emergency department (ED) with acute colonic perforation or obstruction as primary signs of the disease. Colonic hemorrhage causing hemorrhagic shock is a less frequent presentation for CRC. If one of these presentations occurs, prognosis is poorer as compared to the patients presenting under elective admissions, with a postoperative mortality rate of 8.2% after an emergency operation [3]. This could be explained by the fact that these patients have more advanced tumors, are older, and have more comorbidities. Right-sided lesions are seen more often in elder patients than in younger ones. Finally, rectal tumors present rarely as surgical emergencies [3].

L. Lomaglio • G. Montori
Unit of General and Emergency Surgery, Papa Giovanni XXIII Hospital, P.zza OMS 1, Bergamo 24128, Italy

A. Pecorelli • S. Sironi
Department of Radiology, Papa Giovanni XXIII Hospital, Milano-Bicocca University, Bergamo, Italy

M. Sartelli
Department of Surgery, Macerata Hospital, Macerata, Italy

F. Coccolini, M.D. (✉) • L. Ansaloni
General, Emergency and Trauma Surgery Department, Bufalini Hospital, Cesena, Italy
e-mail: federico.coccolini@gmail.com

F. Catena et al. (eds.), *CT Scan in Abdominal Emergency Surgery*, Hot Topics in Acute Care Surgery and Trauma, https://doi.org/10.1007/978-3-319-48347-4_12

12.2 Value of Computed Tomography

Abdominopelvic contrast CT provides the most accurate information especially in the diagnostic setting. Modern multidetector CT (MDCT) provides superb anatomic details of the bowel, detecting both primary and secondary signs of acute presentation of CRC. This is the reason why CT scan should be performed promptly to avoid any delay in the management of these complex patients [3–6].

It demonstrates the tumor as thickening of the colonic wall, evidence of locoregional extension into adjacent organs (Fig. 12.1) and/or regional lymph nodes (e.g., involvement of mesentery and small bowel, with concomitant small bowel obstruction), and distant spread to the liver and peritoneum, allowing the staging of the tumor according to TNM system (Figs. 12.2 and 12.3).

Ideally, CT should be performed with intravenous contrast medium (ICM) injection to optimize the imaging of the intestinal wall, the mesenteries, lymph nodes, liver, and peritoneum. However, the incremental benefit of ICM injection must be

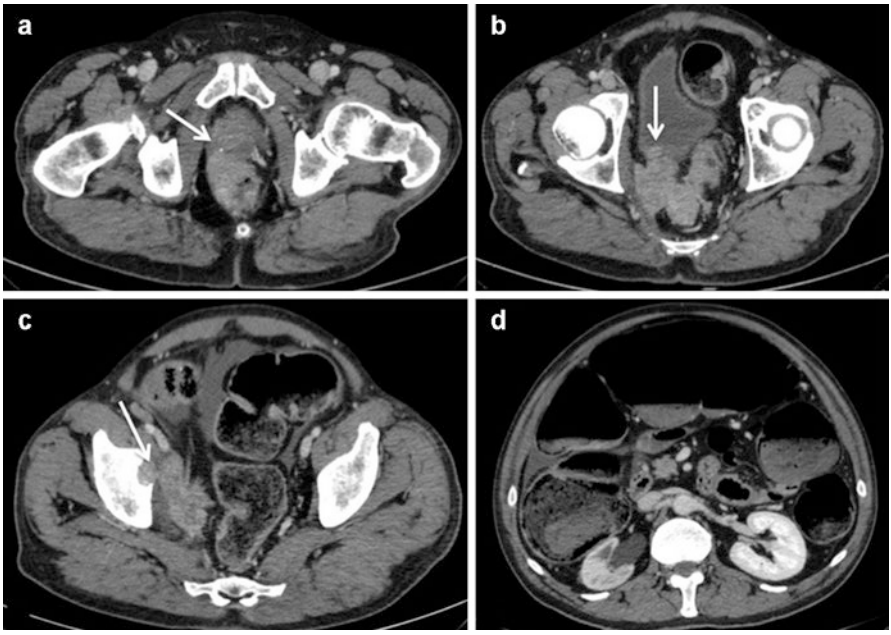

Fig. 12.1 Advanced rectal cancer: infiltration of the serosa and mesorectum (**a**), of the posterior wall of the bladder (**b**), of both the obturator right muscles and the medial wall of the cotyloid fossa (**c**). Massive dilatation of colon is present, with classical air-fluid levels (**d**). Contrast enhancement of the neoplastic mass allows the determination of its limits

Fig. 12.2 Multiplanar reconstruction of a CT scan with the use of intravenous contrast shows multiple hepatic lesions which causes compression of the vena (*white arrow*). The compression determined intravenous thrombus

weighed against an increased risk of renal failure related to renal function and obstruction-related dehydration [6, 7]. CT also shows the consequences of obstruction, including the diameter of cecal distention and pneumatosis of the colonic wall, which may be signs of impending perforation (Fig. 12.4).

In the last decade, the progression of technology has brought to the development of more sophisticated CT devices, with the implementation of multidetector modality. Multidetector CT (MDCT) is replacing conventional radiology as first-line diagnostic modality in many cases. Volume data of the abdomen are acquired with a helical technique during a single breath hold, usually with a collimation of 5 mm [5]. MDCT scanners enable better spatial resolution through thinner collimation. The use of both water-soluble oral or rectal contrast (as leakage of barium causes peritonitis) and ICM added important value to the exam, unless contraindications exist (Fig. 12.5) [5]. Even if oral contrast is not used, however, the diagnosis of colon perforation can still nearly always be made in the presence of specific CT features [5]. Modern software also enables multiplanar reconstructions (MPR): axial, sagittal, coronal, and curved multiplanar reformatted images are created at a workstation from the acquired volume data. MPR may help identify the site, level, and cause of obstruction when axial findings are indeterminate [8, 9]. Multiplanar images are also useful for staging the tumor and providing information about local or distant metastases.

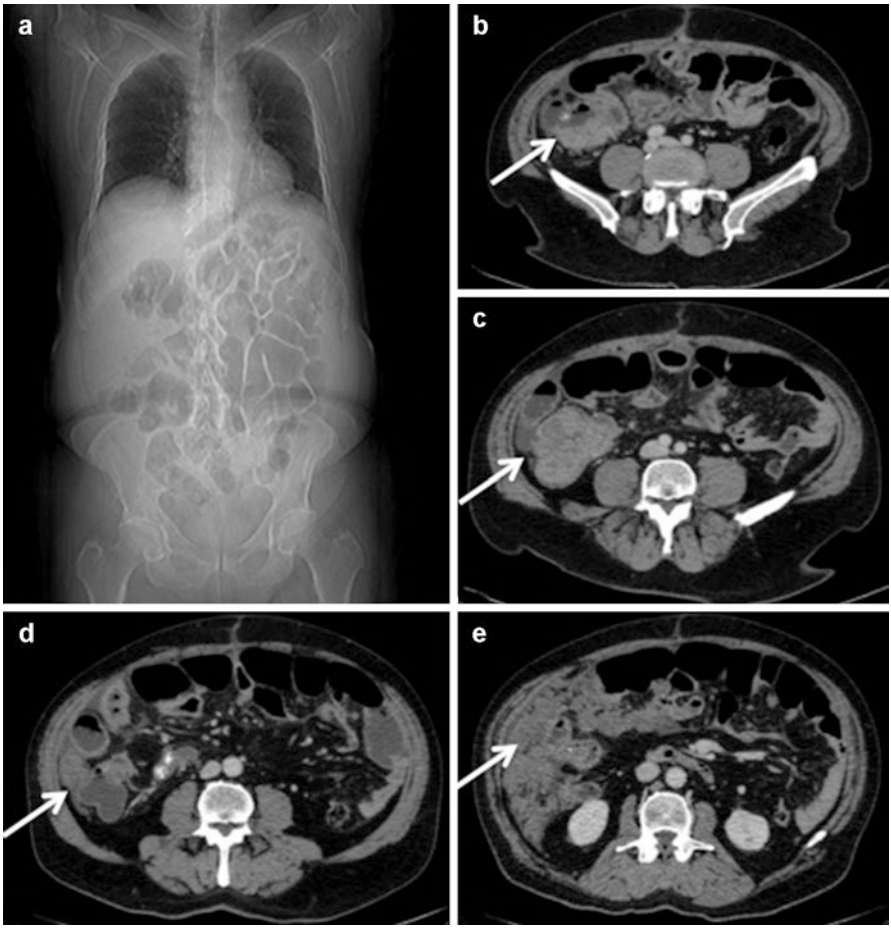

Fig. 12.3 CT scout with diffuse ileal occlusion in peritoneal carcinomatosis (**a**). Advanced right colic cancer (**b**, **c**: *white arrows*). Peritoneal carcinomatosis from right colic cancer (**d**, **e**: *white arrow*)

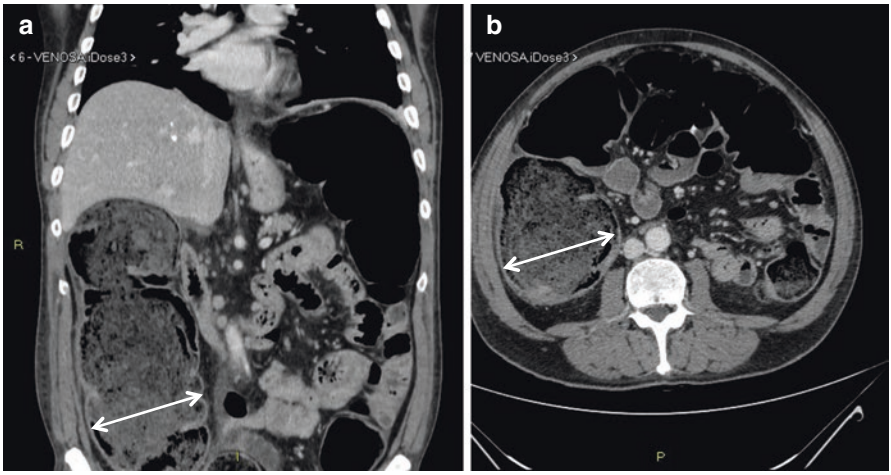

Fig. 12.4 Stenosing adenocarcinoma of the rectum: the distension of cecum was showed by the *white arrows* (**a**, **b**)

CT scans showed high diagnostic accuracy with values of sensitivity and specificity above 90% in some studies, being particularly useful not only in detecting the site and the cause of obstruction but also in the evaluation of the severity of the obstruction and its complications. Moreover, in acute conditions, CT can easily image obese patients with gaseous distension of the intestine. CT remains the standard for the diagnosis of peritoneal carcinomatosis (PC); however, its sensitivity is moderate (23–76%) (Fig. 12.3) [10]. ICM with multiplanar reconstructions (especially in the coronal plan) are fundamental to distinguish PC from small bowel loops [10].

One potential limitation of MDCT could be the differential diagnosis between acute diverticulitis and colorectal cancer, particularly when the parietal thickening is not circumferential [9]. In other studies, detection of the perforation site by MDCT is generally possible in 80–85% of cases when MPR is applied to improve the image definition, but diagnosis relies more on indirect radiologic signs (regional parietal thickening with some contiguous fluid collection and air bubbles in the perivisceral adipose tissue) rather than direct visualization of the intestinal wall break [11, 12].

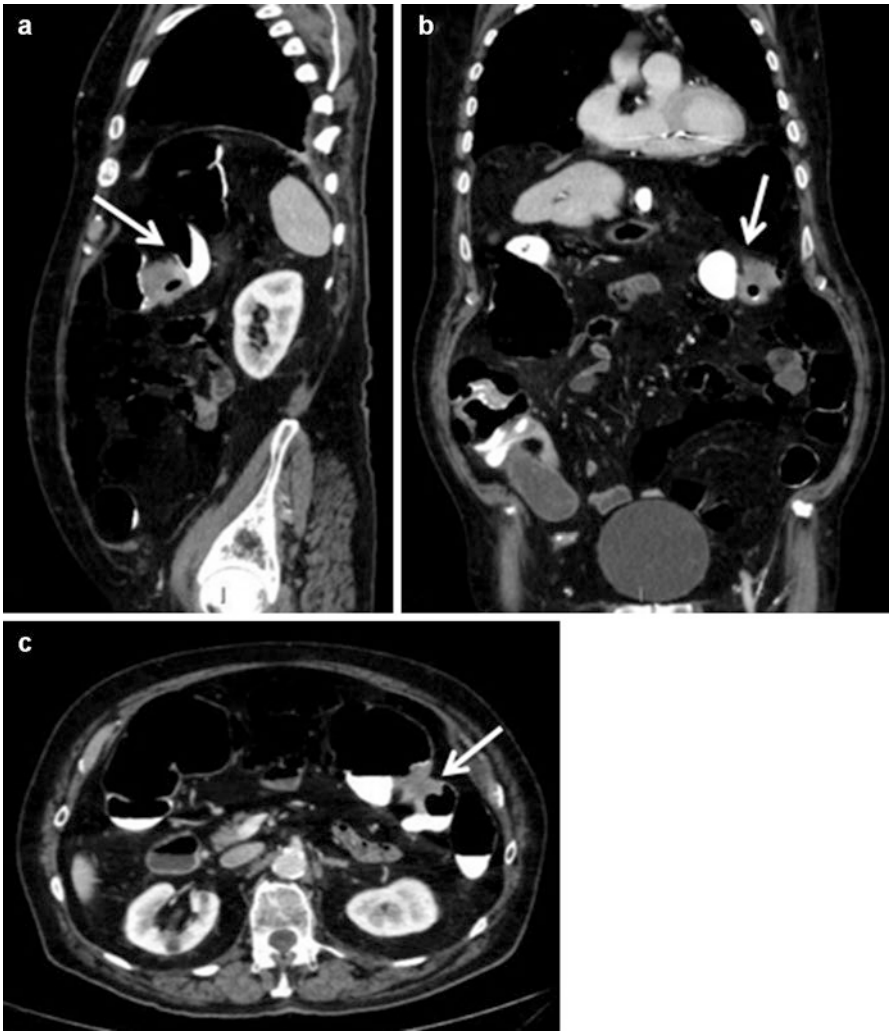

Fig. 12.5 CT scan after administration of enteroclysis contrast: the neoplastic wall thickening determines the stop of the contrast immediately proximal to the stenosis localized at the splenic flessure (*white arrows*, **a**–**c**)

12.3 CT Findings in Colonic Obstruction from CRC

CRC causes approximately 50% of symptoms of large bowel obstruction. Colonic distention is more likely in the setting of a closed loop or in patients with a competent ileocecal valve (Fig. 12.6) [4]. In contrast, an incompetent ileocecal valve allows for colonic decompression into the small bowel (Fig. 12.7). Intestinal obstruction of the

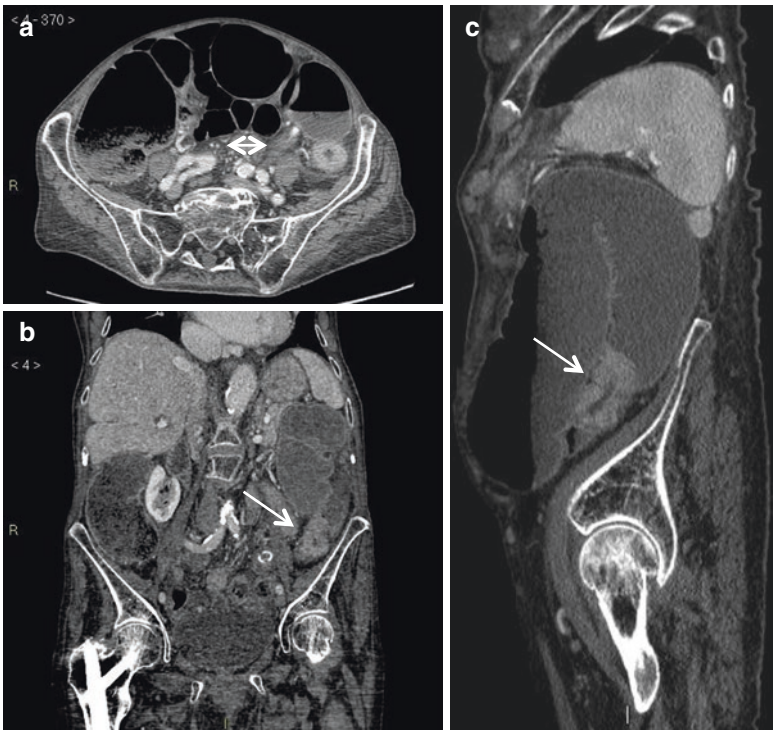

Fig. 12.6 Multiplanar reconstructions of a CT scan with the use of intravenous medium contrast showing a sigmoid colorectal cancer: substantial colonic distention (**a**: the *white arrow* indicates the small bowel lumen), caused by a stenosing lesion (**b**, **c**: *white arrow*), in the setting of competent ileocecal valve. Wall thickening with contrast enhancement at cancer site is evident in all planes

Fig. 12.7 Massive occlusion with bowel dilatation caused by rectal cancer **a–c** (**a** and **b**: the *white arrow* indicates the small bowel lumen). In the coronal reconstruction, at the lower margin of the right hepatic lobe, a metastasis is clearly detectable (**c**)

colon represents an emergency condition when at the late stage of disease (Fig. 12.8). The main problem of the diagnostic imaging method in evaluating intestinal occlusions is to determine the degree of colonic/cecum distention, its viability, and perfusion. These are all crucial information in order to choose a more indicated timing of the surgical intervention [4]. In patients with large intestine obstruction due to CRC, it is important to pay attention to the imaging findings. As an example, cecal pneumatosis does not always indicate transmural infarction, given it may be related to a viable bowel if not associated to other findings of ischemia [13]. In the setting of an incomplete or partial obstruction, a CT enteroclysis is particularly helpful to evaluate the grade and the severity of the obstruction (Fig. 12.4) [8]. However, some authors suggest that it is contraindicated in patients with acute and complete or high-grade bowel obstruction, in patients with strangulation or suspected perforation and in patients with markedly reduction of the intestinal peristalsis [8].

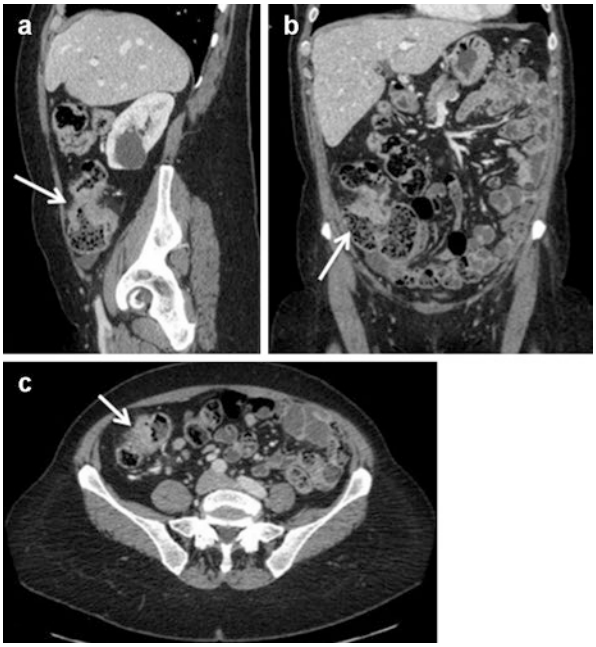

Fig. 12.8 Stenosing adenocarcinoma of the proximal right colon (**a**–**c**: *white arrows*): the distension of cecum and the wall contrast enhancement at the lesion site, along with MPR, allow exact localization of the tumor

12.4 CT Findings in Colonic Perforation from CRC

Perforated CRC is a rare condition estimated in the literature from 1.2 to 9% [5]. The site of perforation may be at the primary site of pathology (i.e., stricture at tumor site) or at the cecum, which becomes distended secondary to distal obstruction. On contrast CT scans, both the perforation and the colonic tumor can be observed. Extraluminal air or bubbles and/or enteric contrast (in case of CT with water-soluble contrast) are, indeed, considered specific signs of gastrointestinal perforation in an intact abdomen (Fig. 12.9). CT is the most reliable modality for detecting even a small amount of free air (sensitivity near to 100% in gastrointestinal perforation), seen more clearly at a lung window setting [5, 11, 14, 15]. The location of the pneumoperitoneum can help to localize the site of the perforation: frequently, a significant amount of free air in the upper abdomen and the pelvis can be related with both low and upper gastrointestinal perforations, while extraluminal gas bubbles seen only at the pelvis are most often related to colonic perforation [5, 11, 14]. In a study conducted by Yeung et al. [16], the CT-falciform ligament sign, scattered pockets of air, bowel wall thickening, and fat stranding are the statistically significant CT features for differentiating the proximal and distal gastrointestinal (GI) perforation ($P < 0.05$).

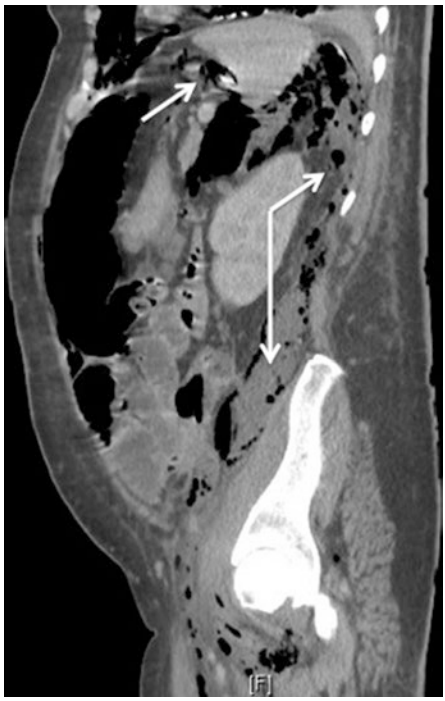

Fig. 12.9 Left colonic perforation: extended pneumo peritoneum (*single white arrow*) and retropneumoperitoneum (*double white arrows*)

Additional CT signs that may indicate the site of the perforation include interruption or lack of bowel wall enhancement on an enhanced scan and focal thickening of the bowel wall (>5 mm) adjacent to extraluminal gas bubbles, with localized mesenteric fatty infiltration [5, 11, 14].

12.5 CT Findings in Colonic Hemorrhage from CRC

Intestinal hemorrhage is another diagnostic problem in emergency evaluation of the colon for acute disease, although rare. A history of bright red blood per rectum vs. melanotic stools can aid in differentiating a left-sided source of bleeding from a right-sided one. Colonic hemorrhage when presenting as a colonic emergency from CRC, may require investigation with nuclear scanning or angiography to detect the source of bleeding after resuscitation. CT scan with intravenous medium contrast (IMC) is considered a safe, convenient, and accurate diagnostic tool for rapid localization of the source of lower GI bleeding. Positive CT may allow directed therapeutic angiography in addition to allow the staging of the tumor [17].

12.6 Computed Tomographic Colonography

Computed tomographic colonography (CTC) is considered as the radiological examination of choice for the diagnosis of CRC in elective settings (Fig. 12.10). It is particularly useful in the diagnostic process when colonoscopy is incomplete, contraindicated, or not possible (e.g., CRC that presents with an occlusive mass preventing colonoscopic examination beyond the level of the occlusion) and represents an acceptable and equally sensitive alternative for patients with symptoms suggestive of CRC [18, 19]. Allowing endoluminal three-dimensional views, CTC can also be used to assess strictures before planning interventions, both surgical and endoscopic.

Complete preoperative evaluation of the entire colon is important because identification of synchronous cancers, which are present in 1–7% of CRC patients [20, 21], may determine the extent of surgical resection. CTC is known to be a safe procedure, particularly when it is performed using the low-pressure carbon dioxide insufflation, with reported rates of overall procedure-related colonic perforations ranging between 0.009 and 0.06% [22–24]. However, data are largely taken from screening CTC practices or from patients who did not have colonic obstruction. There is no conclusive evidence about the risk of CTC-related colonic perforation for patients with an emergent occlusive cancer, since this condition is generally regarded as one risk factors for colonic perforation following CTC [24–26]. Other acute abdominal conditions (e.g., diverticulitis or active inflammatory bowel disease) are absolute contraindications to CTC.

A further advantage of CTC is that it can serve as a "one-stop-shop" examination for the proximal colonic evaluation, as well as for overall pretreatment cancer staging of the abdomen and pelvis when performed with ICM enhancement [19, 27]. Contrast-enhanced CTC is essentially the same imaging method as the routine contrast-enhanced abdominopelvic CT, except for the use of gaseous colonic distention in the former. Therefore, the two methods are expected to be similarly effective and accurate for tumor staging, although published data on the accuracy of contrast-enhanced CTC for general TNM staging of colorectal cancers are limited. According to several published studies, the accuracy of contrast-enhanced CTC for tumor staging is 83–95% for T-staging, 80–85% for N-staging, and 100% for M-staging [28, 29].

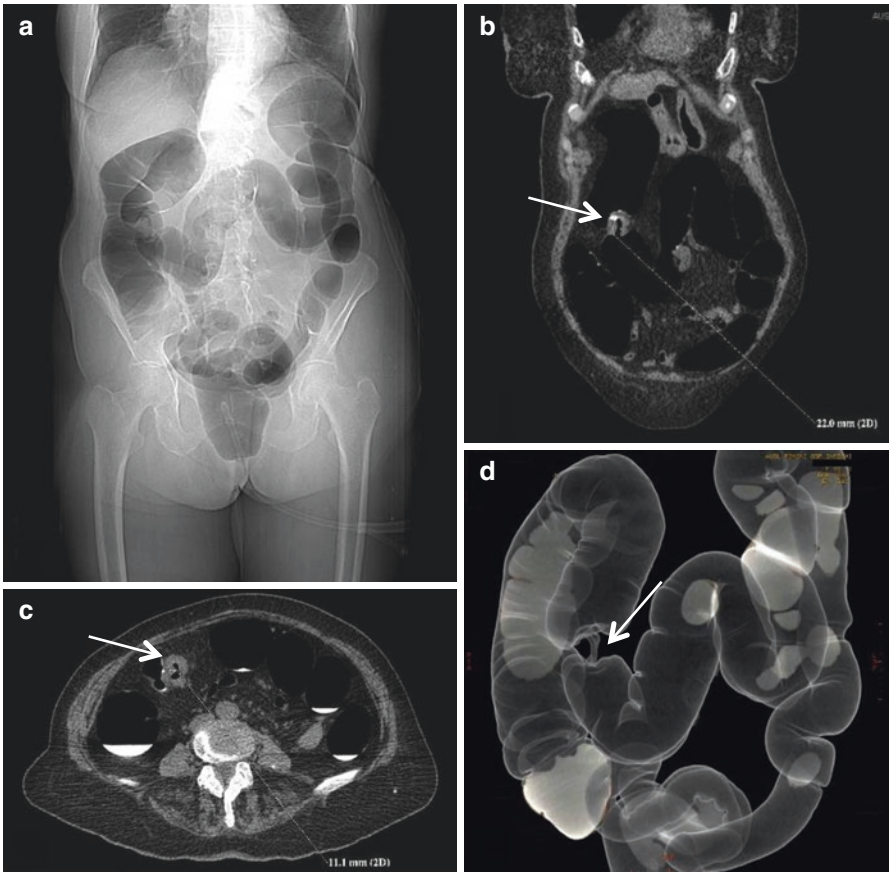

Fig. 12.10 Computed tomographic colonography (CTC): gaseous colonic distention permits the detection of marked stenosis already at the scout scan (**a**). The tumor is located in the proximal transverse colon, as well demonstrated from coronal and axial reconstructions (**b**, **c**: *white arrow*) that permit the exact measurement of the wall thickening. The 3D reconstruction shows the stricture and permits to exclude other tumor localizations in the colon (**d**, *white arrow*)

Conclusions

Patients affected by CRC can present acutely in a setting of occlusion, perforation, and lower gastrointestinal hemorrhage, which can all be life-threatening conditions. Traditional radiology (e.g., ultrasonography, X-ray radiographies) is not sufficient for a complete clinical assessment, causing an unnecessary delay in the diagnostic process. MDCT is the most accurate diagnostic tool in the evaluation of patients with acute presentation of CRC. It allows identification of the tumor site and of potential local and distant complications, in addition to its TNM staging. In order to optimize the imaging of the intestinal wall, the mesenteries, lymph nodes, liver, and peritoneum, CT should be performed with ICM injection, if no absolute contraindications are present. CTC can be a valid diagnostic tool when patients are stable and perforation is not suspected and should be performed cautiously in the case of occlusion, since it increases the risk of perforation.

References

1. American Cancer Society. Cancer facts & figures 2016. Atlanta: American Cancer Society; 2016.
2. Aakif M, Balfe P, Elfaedy O, Awan FN, Pretorius F, Silvio L, Castinera C, Mustafa H. Study on colorectal cancer presentation, treatment and follow-up. Int J Color Dis. 2016;31:1361–3.
3. Cuffy M, Abir F, Audisio RA, Longo WE. Colorectal cancer presenting as surgical emergencies. Surg Oncol. 2004;13:149–57.
4. Romano S, Lombardo P, Cinque T, Tortora G, Romano L. Acute colonic disease: how to image in emergency. Eur J Radiol. 2007;61:424–32.
5. Zissin R, Hertz M, Osadchy A, Even-Sapir E, Gayer G. Abdominal CT findings in nontraumatic colorectal perforation. Eur J Radiol. 2008;65:125–32.
6. Gainant A. Emergency management of acute colonic cancer obstruction. J Visc Surg. 2012;149:e3–e10.
7. Sinha R, Verma R. Multidetector row computed tomography in bowel obstruction. Part 2. Large bowel obstruction. Clin Radiol. 2005;60:1068–75.
8. Matrawy KA, El-Shazly M. Intestinal obstruction: role of multi-slice CT in emergency department. Alexandria J Med. 2014;50:171–8.
9. Priola AM, Priola SM, Volpicelli G, Giraudo MT, Martino V, Fava C, Veltri A. Accuracy of 64-row multidetector CT in the diagnosis of surgically treated acute abdomen. Clin Imaging. 2013;37:902–7.
10. Bhatt A, Goere D. Cytoreductive surgery plus HIPEC for peritoneal metastases from colrectal cancer. Indian J Surg Oncol. 2016;7(2):177–87.
11. Hainaux B, Agneessens E, Bertinotti R, De Maertelaer V, Rubesova E, Capelluto E, Moschopoulos C. Accuracy of MDCT in predicting site of gastrointestinal tract perforation. AJR Am J Roentgenol. 2006;187:1179–83.
12. Ghekiere O, Lesnik A, Millet I, Hoa D, Guillon F, Taourel P. Direct visualization of perforation sites in patients with a non-traumatic free pneumoperitoneum: added diagnostic value of thin transverse slices and coronal and sagittal reformations for multi-detector CT. Eur Radiol. 2007;17:2302–9.
13. Taourel P, Garibaldi F, Arrigoni J, Le Guen V, Lesnik A, Bruel JM. Cecal pneumatosis in patients with obstructive colon cancer: correlation of CT findings with bowel viability. AJR Am J Roentgenol. 2004;183:1667–71.
14. Miki T, Ogata S, Uto M, Nakazono T, Urata M, Ishibe R, Shinyama S, Nakajo M. Multidetector-row CT findings of colonic perforation: direct visualization of ruptured colonic wall. Abdom Imaging. 2004;29:658–62.
15. Cho HS, Yoon SE, Park SH, Kim H, Lee YH, Yoon KH. Distinction between upper and lower gastrointestinal perforation: usefulness of the periportal free air sign on computed tomography. Eur J Radiol. 2009;69(1):108–13.
16. Yeung K-W, Chang M-S, Hsiao C-P, Huang J-F. CT evaluation of gastrointestinal tract perforation. Clin Imaging. 2004;28:329–33.
17. Sabharwal R, Vladica P, Chou R, Law WP. Helical CT in the diagnosis of acute lower gastrointestinal haemorrhage. Eur J Radiol. 2006;58:273–9.
18. Spada C, Stoker J, Alarcon O, Barbaro F, Bellini D, Bretthauer M, De Haan MC, Dumonceau J-M, Ferlitsch M, Halligan S, Helbren E, Hellstrom M, et al. Clinical indications for computed tomographic colonography: European Society of Gastrointestinal Endoscopy (ESGE) and European Society of Gastrointestinal and Abdominal Radiology (ESGAR) guideline. Eur Radiol. 2015;25:331–45.
19. Hong N, Park SH. CT colonography in the diagnosis and management of colorectal cancer: emphasis on pre- and post-surgical evaluation. World J Gastroenterol. 2014;20:2014–22.
20. Mulder SA, Kranse R, Damhuis RA, de WJHW, Ouwendijk RJT, Kuipers EJ, van LME. Prevalence and prognosis of synchronous colorectal cancer: a Dutch population-based study. Cancer Epidemiol. 2011;35:442–7.
21. Adloff M, Arnaud JP, Bergamaschi R, Schloegel M. Synchronous carcinoma of the colon and rectum: prognostic and therapeutic implications. Am J Surg. 1989;157:299–302.

22. Pickhardt PJ. Incidence of colonic perforation at CT colonography: review of existing data and implications for screening of asymptomatic adults. Radiology. 2006;239:313–6.
23. Burling D, Halligan S, Slater A, Noakes MJ, Taylor SA. Potentially serious adverse events at CT Colonography in symptomatic patients: National Survey of the United Kingdom. Radiology. 2006;239:464–71.
24. Sosna J, Blachar A, Amitai M, Barmeir E, Peled N, Goldberg SN, Bar-Ziv J. Colonic perforation at CT colonography: assessment of risk in a multicenter large cohort. Radiology. 2006;239:457–63.
25. Atalla MA, Rozen WM, Niewiadomski OD, Croxford MA, Cheung W, Ho Y-H. Risk factors for colonic perforation after screening computed tomographic colonography: a multicentre analysis and review of the literature. J Med Screen. 2010;17:99–102.
26. Berrington de Gonzalez A, Kim KP, Yee J. CT colonography: perforation rates and potential radiation risks. Gastrointest Endosc Clin N Am. 2010;20:279–91.
27. Sali L, Falchini M, Taddei A, Mascalchi M. Role of preoperative CT colonography in patients with colorectal cancer. World J Gastroenterol. 2014;20:3795–803.
28. Chung DJ, Chung DJ, Huh KC, Choi WJ, Kim JK. CT colonography using 16-MDCT in the evaluation of colorectal cancer. AJR Am J Roentgenol. 2005;184:98–103.
29. Utano K, Endo K, Togashi K, Sasaki J, Kawamura HJ, Horie H, Nakamura Y, Konishi F, Sugimoto H. Preoperative T staging of colorectal cancer by CT colonography. Dis Colon Rectum. 2008;51:875–81.

13 Adhesive Small Bowel Obstruction (ASBO): Role of CT Scan in Guiding Choice and Timing for Treatment Options

Hariscine Keng Abongwa, Paolo Bresciani, Antonio Tarasconi, Gennaro Perrone, and Fausto Catena

13.1 Introduction

Bowel obstruction also called "ileus" (of Greek origin meaning to tighten or twist) is defined as the arrest or the prevention of progression of intestinal contents in both the small and large intestines. Mechanical bowel obstruction comprises about 15% of all emergency admissions for abdominal pain. The most important risk factor for ASBO is the type of surgery and extent of peritoneal damage. Open surgery and major abdominal surgery entailing extensive dissections have a higher risk for ASBO. The lower incidence of adhesions expected after laparoscopic surgery likely translates into long-term benefits in terms of reduced ASBO. Abdominal adhesions, which can begin forming within a few hours after an operation, represent the most common cause of intestinal obstruction being responsible for 70–80% of small bowel obstruction (SBO) and typically occur in patients with a history of abdominal surgery or inflammatory bowel disease.

H.K. Abongwa • G. Perrone
Department of Emergency and Trauma Surgery, Parma University Hospital, Parma, Italy

P. Bresciani
Section of Radiological Sciences, Department of Surgical Sciences, Parma University Hospital, Parma, Italy

A. Tarasconi
Department of Clinical and Experimental Sciences, Surgical Clinic, University of Brescia, Brescia, Italy

F. Catena (✉)
Emergency and Trauma Surgery,
Ospedale Maggiore di Parma Emergency and Trauma Surgery,
Parma, Parma, Italy
e-mail: faustocatena@gmail.com

F. Catena et al. (eds.), *CT Scan in Abdominal Emergency Surgery*, Hot Topics in Acute Care Surgery and Trauma, https://doi.org/10.1007/978-3-319-48347-4_13

13.2 Classifications

There are various classifications aimed at reaching a precise etiological definition, clinical stratification, and treatment options of bowel obstruction (Table 13.1). Depending on the anatomical location of the bowel obstruction, it is divided into small bowel obstruction (SBO) when the halt in transit involves the small bowel and large bowel obstruction (LBO) when the arrest of transit involves the large intestine. When the obstacle to progression is physical, it is termed *mechanical* bowel obstruction, also called mechanical ileus, while when it is due to the paralysis of the intestinal smooth muscle or to neural or humoral or metabolic causes that block peristalsis, it is termed *functional* bowel obstruction, also known as functional or dynamic or paralytic or adynamic ileus. There can also be cases with a joint mechanical and functional obstacles accounting for the bowel obstruction.

Close to 70% of mechanical bowel obstructions involve the small intestine. The mechanisms responsible for bowel obstruction include (1) obstruction, (2) stenosis, (3) angulation, (4) Ab-extrinsic compression, and (5) strangulation. It should be noted that the obstruction mechanisms of adhesion-related SBO can give rise to a clinical presentation varying from simple (angulation) to strangulated (volvulus, strangulation) obstruction. The most frequent causes of mechanical SBO in the order of incidence are represented by bowel obstructions due to postoperative adhesions (65%), external hernias (17%), tumors (8%), and bowel obstruction secondary to outcomes (adhesions, edema) of inflammatory processes (6%) like Crohn's disease, diverticulitis, pelvic inflammatory disease, and appendicitis. ASBO can therefore be classified according to its etiology in adhesional vs. non-adhesional.

Table 13.1 Classification of ASBO

Etiogenesis	– Post-abdominopelvic **surgery** (85–90%) – Post-**inflammatory** or infectious (10–15%) – Post-abdominopelvic **radiation** therapy (10–5%) – **Congenital** (rare)
Etiology	– Intramural – Extrinsic
Time to onset from surgery	– Early (<30 days after surgery) – Late (>30 days after surgery)
Speed of onset	– Acute – Subacute – Chronic
Location or level	– Proximal – Distal
Degree or grade of obstruction	– Partial (low grade) – Complete (high grade)
Loop vascularization	– Simple – Strangulated
Progression or number of adhesive bands	– Open loop – Closed loop

The most frequent cause of ASBO in order of frequency are post-abdominopelvic **surgery** (extramural origin) in 85–90% of cases, with the highest risk of the disease associated with operations on the large bowel and gynecological procedures, and followed by those originating from the outcomes of **inflammatory** or infectious bowel processes (intramural origin) in 10–15% of cases, those secondary to post **radiation** therapy (circa 5%) and those of the **congenital** origin (rare). The causes of mechanical SBO are divided into *extramural* when the occlusion is due to a pathology that determines angulation or extrinsic compression (e.g., postoperative adhesions), *intramural* when it is due to a disease of the intestinal wall (e.g., Adhesions secondary to IBD), and *intraluminal* when it is due to obstruction of lumen. ASBO is therefore a mechanical obstruction of the small bowel of extramural and intramural origin. ASBO is also classified according to the time of onset from surgery in *Early* vs. *Late* (for onset < or >30 days after surgery, respectively) and according to the speed of onset in *acute* vs *subacute* vs *chronic*. In function of the grade or completeness of obstruction, we talk of *complete* (or high-grade) bowel obstruction when there is a complete and sustained halt in the transit and *partial* (or low-grade) bowel obstruction in case of partial and/or periodic obstruction of the intestine that occurs with subacute and/or recurrent occlusive episodes.

A further classification of ileum, especially mechanical ileum like ASBO, considers *simple* bowel obstruction when the obstruction involves only the intestinal wall and *strangulated* or ischemic bowel obstruction when obstruction involves both the bowel wall and the mesenteric blood vessels with impaired vascularization of the obstructed bowel loop.

Topographically ASBO, like the SBO, is divided into *proximal* and *distal* ASBO with respect to Treitz ligament and in function of the incontinency or continency of the obstructed loop, into *open-loop* and *closed-loop* ASBO, respectively, when the bowel is obstructed at one or two adjacent locations. It should be worth noting that LBO is divided into proximal and distal occlusion of the colon with respect to the splenic flexure and into open-loop and closed-loop LBO, respectively, in relation to the incontinency or continency of the ileocecal valve.

13.3 Pathophysiology

Bowel obstruction causes distention of the gut through the accumulation of both gas and fluid. The gas that accumulates proximal to the obstruction is primarily swallowed air (reflected by its high nitrogen content of 70–80%), and the contribution of bacterial gas is thought to be small. The fluid and gas cause increased intraluminal pressure and distention of the bowel that also affect the motility of the intestine: initially causing increased peristalsis and then leading to decreased peristalsis and relaxation. This decrease in motility and stasis caused by the obstruction itself promote bacterial overgrowth, markedly increasing the normally low levels of both gram-negative enteric and anaerobic organisms found in the small intestine. Obstruction leads to increased permeability of the intestinal mucosal barrier, hence

an increase in the translocation of bacteria and endotoxins to both mesenteric lymph nodes and possibly the systemic circulation, which may be responsible for some of the systemic septic consequences of bowel obstruction. With continued bowel obstruction, if the intraluminal pressure continues to rise, perfusion of the bowel wall may be impaired, which promotes the development of ischemia, necrosis, and perforation. This most commonly occurs in closed-loop obstruction in which both the afferent and efferent limbs of an obstructed segment of bowel are occluded. The intraluminal pressure rises rapidly, impairing first the venous drainage and then the arterial supply to the bowel wall. Ischemia and gangrene of the bowel permit the escape of enteric organisms and their toxins into the portal and systemic circulation, adding to the clinical picture of sepsis. Dissection of air into the wall results in pneumatosis, which may precede frank perforation. Ischemia and bacterial overgrowth also play a role in GI tract perforation and the systemic effects seen with strangulating obstruction. A simple obstruction implies that the lumen is partially or completely occluded but that blood flow is preserved. A simple obstruction can therefore be complete (i.e., no fluid or gas passes beyond the site of obstruction) or incomplete (i.e., some fluid and gas does pass beyond the site of obstruction). Strangulation or strangulated obstruction means that blood flow is compromised, leading to bowel wall edema, intestinal ischemia, and, if left untreated, necrosis, and perforation. In open loop obstruction, intestinal flow is blocked distally, but the proximal loops are open and can be decompressed by vomiting or nasogastric intubation. In closed-loop obstruction, both flow into and flow out of the closed-loop are blocked, resulting in progressive accumulation of fluid and gas within the isolated loop, placing it at risk for ischemia, volvulus, and perforation.

13.4 Diagnosis

The clinical diagnosis of bowel obstruction can be challenging because results of physical examination, clinical presentation, and laboratory values are often nonspecific and nondiagnostic.

The role of the radiologist is to answer several key questions: Is obstruction present? What is the level of the obstruction? What is the cause of the obstruction? What is the severity of the obstruction? Is the obstruction simple or closed loop? Is strangulation, ischemia, or perforation present?

13.4.1 Patient History

Previous abdominopelvic surgery and inflammatory bowel disease in the patient's medical history are fundamental to guide diagnosis. Tumors with a predilection for peritoneal spread such as ovarian carcinoma should be excluded as their CT findings are similar to those of ASBO. Patients with fever upon admission should generate suspects of inflammatory etiology or the presence of peritonitis.

13.4.2 Symptoms and Signs

The symptoms depend on the speed of onset, degree, level, cause, and severity of the obstruction, evolution or not to shock, and the general conditions of the patient. The symptoms can be classified into:

Abdominal symptoms

1. Constipation: It is the pathognomonic symptom. In complete occlusion of the small bowel, constipation without passing feces and especially gas is total. In incomplete obstruction, bowel function can be opened with semisolid stools and intervals of constipation. In the initial phase of the mechanical obstruction of the small bowel, the gut can be open to feces and gas due to the normal progression of residual stool in the gastrointestinal tract distal to the obstruction site.
2. Abdominal pain: The pain frequently originates in a point of the abdomen and ends at a different venue, since it follows the peristaltic movement and gets extinguished at the occlusion site. The interval between the painful periods is characterized by a dull epi-mesogastric pain. In the early stage, the pain is hyperperistaltic (cramps), is intermittent, and is usually poorly localized and of a variable intensity (more attenuated in LBO than that in SBO). LBO at a more distal level has a longer period of quiescence of pain. In proximal obstruction of the small intestine (pylorus, duodenum), the pain is intermittent and located in the epigastric region. In cases of a distal SBO, the pain is initially intermittent and crampy, and then it becomes severe and frequent (poussè) with crises every 1–3 min and then fade and eventually disappear (free interval of about 10 min) or remain constant and widespread. In case of strangulated ASBO, the pain will be intense, persistent, non-morphine responsive, and localized with abdominal tenderness. These later findings (non-morphine responsiveness and abdominal tenderness) should orientate physicians to suspect ischemia.
3. Meteoric abdominal distension: The distension may be diffused or circumscribed. It is a more obvious symptom colonic obstruction, with the possibility of breathing impairment. Usually it is more prominent in the distal SBO, and it is absent or not significant in proximal SBO.
4. Vomiting: Initially vomiting results from the neurovegetative reflex of pain, and then later on, it becomes secondary to antiperistaltic reflux caused by the intraluminal sequestration and stasis of fluid and intestinal contents in the loop proximal to the obstruction site. Vomiting in cases of proximal obstruction is precocious, irrepressible, constant, continuous, biliary, and abundant. In the distal SBO, it will be late, less frequent with progressive change of the characteristics in alimentary, biliary, intestinal, and fecaloid vomiting.

Systemic symptoms

1. Systemic symptoms are related to dehydration (tachycardia, hypotension, oliguria), SBO complicated by ischemia (fever, tachycardia, suffering facies), or the evolution to sepsis (cloudy sensorium). Fever in SBO patients may be suggestive for inflammatory etiology of simple SBO or suggest the onset of strangulation.

13.4.3 Physical Examination

Physical examination of patient with SBO should include:

1. Inspection: It should be aimed at finding scars of previous surgery scars, signs of abdominal distension in the initial stage of the bowel obstruction (iliac, umbilical or epigastric bulges) or in the late stage (Schlange's sign) and signs of dehydration (especially for proximal SBO).
2. Palpation: It is very important as it allows you to exclude vascular suffering that characterizes the strangulated SBO. The presence of a marked tenderness on deep and/or superficial palpation and/or positivity of the Blumberg sign is indicative of peritoneal suffering, and so it may be suggestive of intestinal obstruction with strangulation or perforation.
3. Percussion: Percussion detects a tympanic sound in meteoric districts and a dull sound in areas of liquid distention. Areas of air-fluid levels will determine a tympanic sound with high metallic tones.
4. Auscultation: In the early stages of mechanical obstruction of the small bowel, auscultation reveals hyperistalsis with ticks/metallic timbres and occasional borborygmi synchronous with peristaltic waves that evoke abdominal pain. In the late phase (after 48 h) or in case of peritonitis, auscultation detects a hypoperistaltic due to the inhibition of motory activity resulting from the bowel distention. Also, the peristaltic sound is heard at increasing intervals, alternating with periods of silence. The absence of peristaltic sound even after compression or stimulation of the abdominal wall with the finger may express a change in the vascularization status leading to strangulation.
5. Digital rectal examination: In patients with suspected SBO, digital rectal examination can reveal the presence of blood in feces in patients with strangulated ASBO.

13.4.4 Laboratory Findings

Laboratory findings in ASBO patients (WBC, PCR, lactate, PCT, electrolytes, BUN/creatinine, hyperamylasemia) should be aimed at excluding inflammatory processes with peritonitis (leukocytosis, increased PCR level), signs of ischemia (leukocytosis, hyperlactatemia, hyperamylasemia), and/or signs of sepsis and shock (increased PCT level).

13.4.5 Imaging in ASBO Patients

The upright *plain abdominal radiograph* is traditionally the first radiology study in the workup of acute abdominal pain and suspected bowel obstruction. After an accurate patient history, evaluation of clinical signs and symptoms, physical examination, and the evaluation of laboratory findings (WBC, PCR, lactate, electrolytes,

BUN/creatinine), the first step of the diagnostic workup for ASBO is supine and erect plain abdominal X-ray. Surgical guidelines recommend plain radiographs as part of this initial assessment, as these can confirm the diagnosis of ASBO and identify some complications such as perforation.

Because adhesive bands are typically not visible on *computerized tomography* (CT) scan, the diagnosis of adhesions is often one of the exclusions. *The presence on CT scan of kinking or tethering of the bowel at the transition zone (bird beak sign) without any other identifiable cause of small bowel obstruction or without a history of a tumor with a predilection for peritoneal spread such as ovarian carcinoma, particularly in a patient with a history of surgery or with a known history of inflammatory bowel disease, is highly suggestive of an adhesion.* Appropriate treatment of patients with ASBO depends on prompt diagnosis of the obstruction and accurate identification of those patients who require surgical management. Initial assessment focuses on identifying those patients with signs and symptoms consistent with peritonitis or ischemic bowel. Delays in surgery can result in increased morbidity and mortality. An appropriate use of abdominal CT can aid timely triage to surgical management. CT is therefore particularly useful in those patients who do not demonstrate clear symptoms of peritonitis or ischemia at presentation, especially if they have equivocal or negative findings on plain radiographs.

13.4.6 Radiological Signs of ASBO

The main imaging findings in ASBO patients include upright plain abdominal radiograph and computed tomography. Plain abdominal radiographs have only a moderate sensitivity of between 48% and 80% of diagnosing SBO and are poor at suggesting the diagnosis of open versus closed-loop, ischemic, or strangulated obstruction.

CT can accurately predict the etiology of obstruction in 70–90% of patients and can always suggest superimposed ischemia or perforation. CT is most valuable when there are systemic signs suggesting infection, bowel infarction, or an associated palpable mass. **CT signs of SBO** (small bowel obstruction) include:

1. Dilated/distended air-filled or fluid-filled small bowel greater than 2.5–3 cm seen proximal to collapsed loops (Fig. 13.1).
2. Air-fliud levels greater than 2.5 cm or at disparate levels within the same loop that transverse the entire lumen of the obstructed bowel loops (Fig. 13.2) or trapped air bubbles between folds at the top of a fluid-filled bowel loop known as the string of pearls sign (Fig. 13.3). Care should be made to differentiate LBO with an incompetent ileocecal valve as this type of obstruction can simulate a SBO (Fig. 13.4).
3. Gastric distention (Fig. 13.5).
4. Small bowel dilated out of proportion to colon (Fig. 13.6a, b).
5. Paucity of colorectal gas (Fig. 13.6c, d).

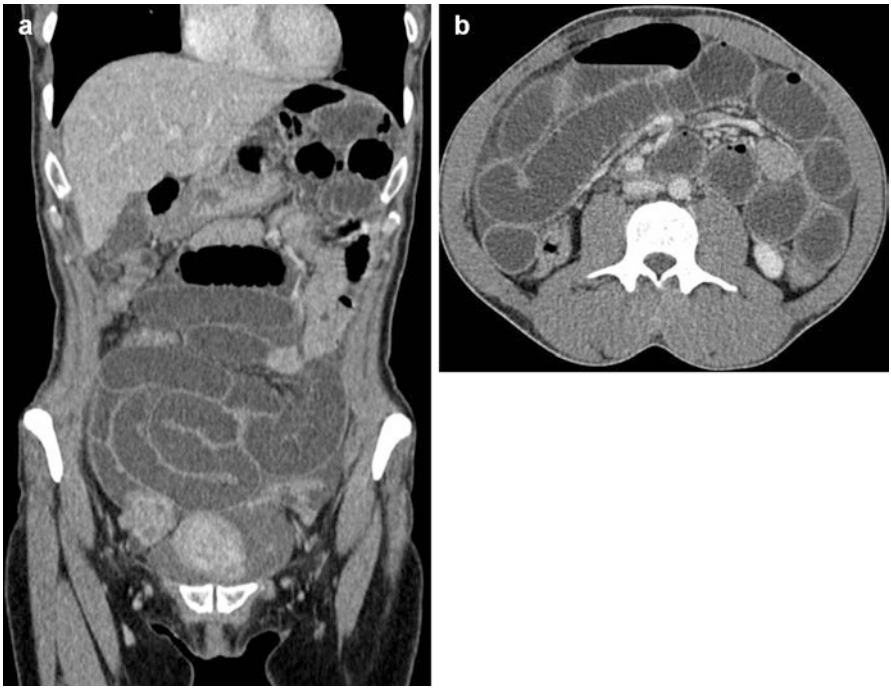

Fig. 13.1 Dilated air-filled (*arrow*) or fluid-filled (*double arrow*) small bowel

Fig. 13.2 Air-fluid levels (*arrow*)

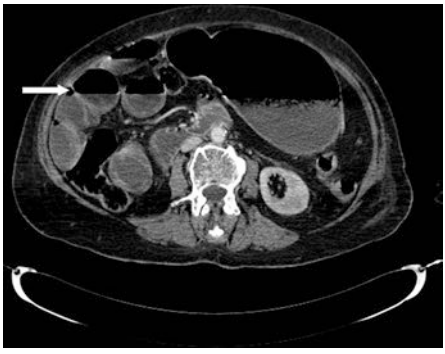

Fig. 13.3 String of pearls sign (*rectangle*)

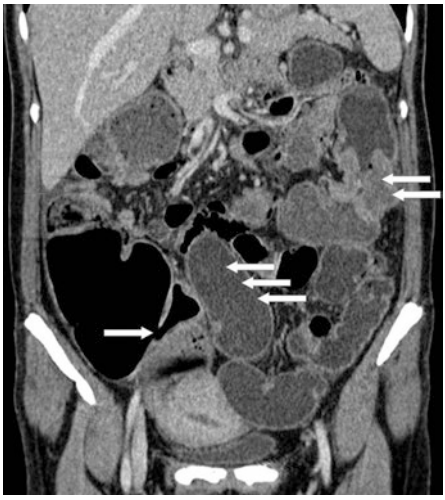

Fig. 13.4 Fluid-filled dilated small bowel (*triple arrow*) simulating SBO in a case of LBO (*double arrow*) with an incompetent ileocecal valve (*single arrow*)

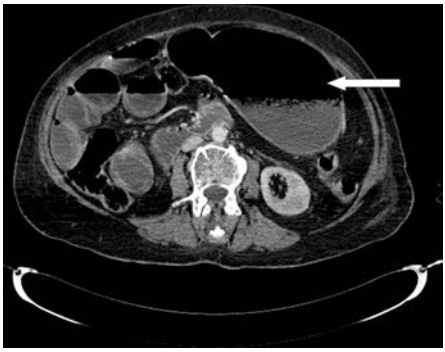

Fig. 13.5 Significant gastric distension (*arrow*)

The CT diagnosis of adhesions is accurate in 70–95% of patients. CT findings in ASBO patients can be divided in signs of simple and signs of strangulated or complicated ASBO. CT findings could also permit a further classification of strangulated ASBO in those with signs of reversible or signs of irreversible ischemia. This later classification is of primary importance in determining the timing for surgery.

13.4.6.1 CT Signs of Simple ASBO

1. Bird beak sign: This is the most important radiographic sign/finding in the diagnosis of ASBO. Because adhesions are not usually seen on CT, the CT diagnosis of adhesions is a diagnosis of exclusion, by identifying where there is an abrupt transition from dilated to non-dilated small bowel (the obstruction site) and associating this finding to the exclusion of any apparent cause of SBO. The bird beak sign is the fusiform tapering of the transition site marking the abrupt transition from dilated to non-dilated small bowel at the obstruction site without any apparent cause of SBO (Fig. 13.7).

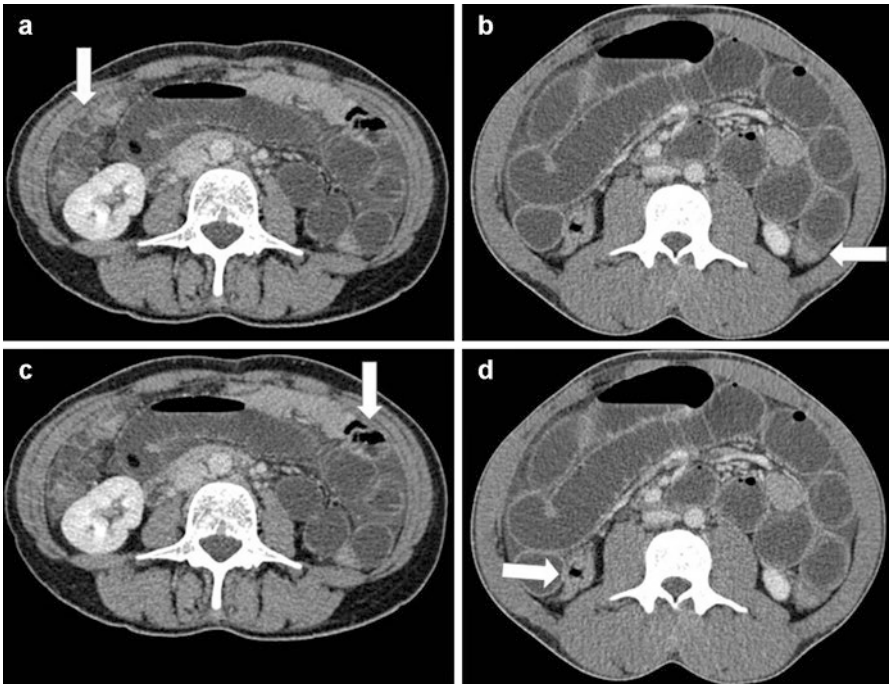

Fig. 13.6 (**a** and **b**) Small bowel dilated out of proportion to colon (the *arrows* indicate the collapsed colonic lumen). (**c** and **d**) Paucity of colorectal gas (the *arrows* point out the lack or scarcity of gas inside the colonic lumen)

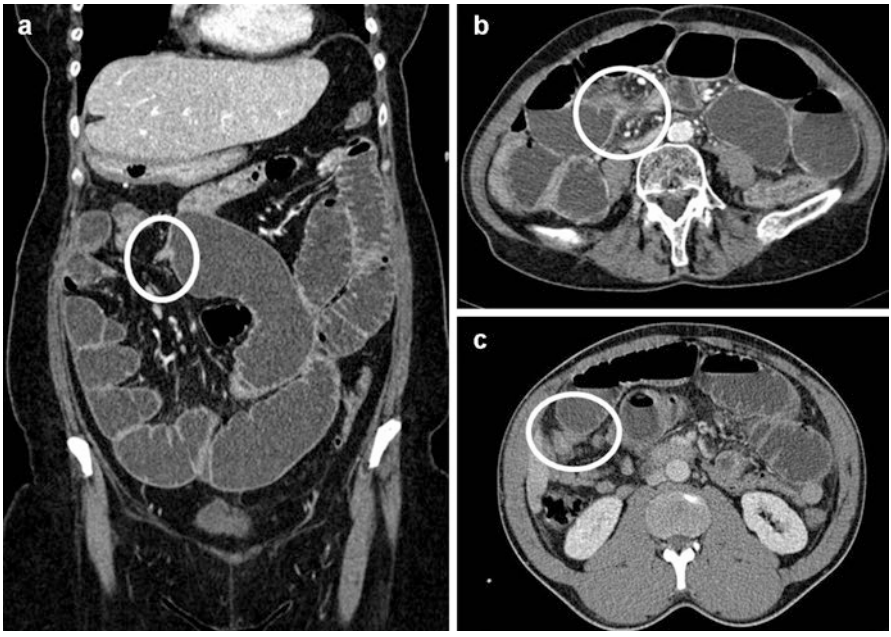

Fig. 13.7 The bird beak sign—abrupt transition from dilated to non-dilated small bowel at the obstruction site (*circles*) without apparent cause

2. Small bowel feces sign: A finding often in close proximity to the point of obstruction or the transition zone is the small bowel feces sign. This sign refers to the presence of particulate material admixed with air in the small bowel. This situation reflects the stasis of contents in the small bowel, resulting in increased resorption of fluid in bowel contents as well as possible gases released from bacterial overgrowth. Although the small bowel feces sign can be seen in patients without SBO, this finding is highly specific for obstruction when seen in combination with dilated bowel and distal decompressed loops (Fig. 13.8).
3. Smooth-thick transverse valvulae conniventes: The presence of smooth-thick transverse valvulae conniventes (also known as Kerckring folds or plicae circulares or circular folds) implies edema with possible ischemia (Fig. 13.9).

13.4.6.2 CT Signs of Strangulated ASBO

1. Gasless abdomen (CT scout) or fluid-filled abdomen: This can be seen in the setting of high-grade bowel obstruction and ischemia in which the gut is completely filled with fluid (Fig. 13.10). Fluid-filled loops may not be visible, leading to a false-negative diagnosis.
2. Circumferential mural thickening >3 mm (Fig. 13.11).

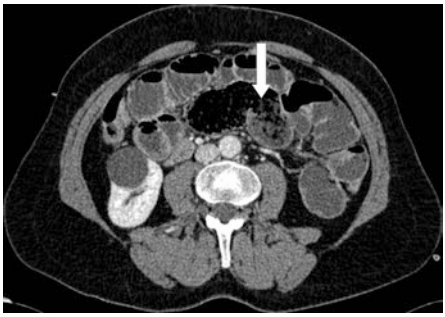

Fig. 13.8 Small bowel feces sign (*arrow*)

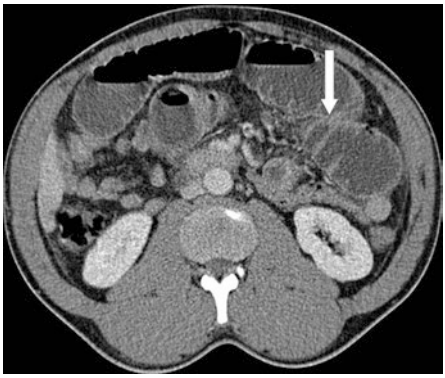

Fig. 13.9 Smooth-thick transverse valvulae conniventes (also known as Kerckring folds or plicae circulares) (*arrow*)

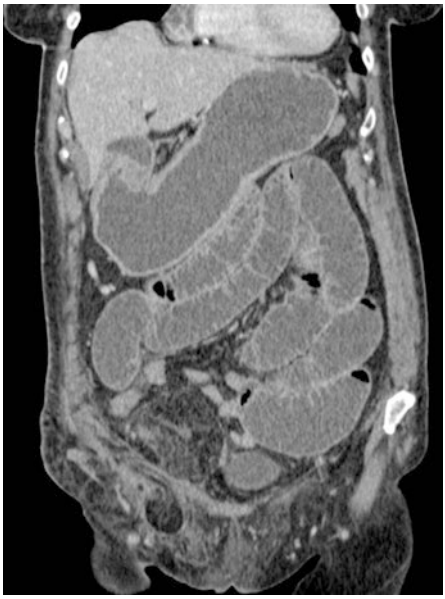

Fig. 13.10 Gasless abdomen or fluid-filled abdomen

Fig. 13.11 Circumferential mural thickening (*arrow*)

3. Target or halo sign: This sign indicates the presence of submucosal edema (Fig. 13.12).
4. Mural pneumatosis: It indicates breakdown in the mucosal integrity of the mural wall and is strongly suggestive of ischemia (Fig. 13.13). However, CT findings of pneumatosis do not always predict irreversible ischemia at surgery.
5. Portomesenteric gas: If present together with mural pneumatosis, it has a much greater likelihood of predicting irreversible transmural necrosis (Fig. 13.14).
6. Free intraperitoneal gas or extraluminal perivisceral air bubbles: It has a much greater likelihood of predicting both irreversible transmural necrosis and perforation (Fig. 13.15).
7. Hyperenhanced wall (indicates initial ischemia), decreased or focal loss of mural enhancement marking impaired arterial flow (highly specific for ischemia), delayed or prolonged or persistent mural enhancement as sign of impaired venous outflow (indicates ischemia but is not specific for ischemia) (Fig. 13.16).
8. Mesenteric fluid, mesenteric congestion, and free fluid: The presence of two or more signs, on unenhanced CT scan, is highly specific (>94%) for ischemia (Fig. 13.17).

Fig. 13.12 Target or halo sign (submucosal edema) (*arrow*)

Fig. 13.13 Mural pneumatosis (*rectangle*)

Fig. 13.14 Portomesenteric gas (*circle*)

Fig. 13.15 Free intraperitoneal gas (*arrow*)

Fig. 13.16 Hyperenhanced walls (*arrow*)

Fig. 13.17 Mesenteric fluid (*square*), mesenteric congestion (*circle*), and free fluid (*arrow*)

Fig. 13.18 Mural hemorrhage or haziness on non-contrast CT scan (*arrow*)

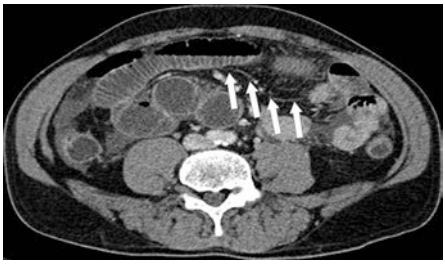

Fig. 13.19 The *arrows* highlight the progressive torsion of the mesenteric blood vessels, which constitute the whirl sign

9. Mural hemorrhage or haziness on unenhanced CT scan (Fig. 13.18).
10. Whirl sign: The rotation of the bowel, vessels, and mesenteric fat at the site of obstruction in a closed-loop obstruction is known as the whirl sign (Fig. 13.19).

13.4.7 Clinical Presentations at Risk of Transmural Necrosis at Surgery: Closed-Loop ASBO

Closed-loop obstructions with (strangulated) or without (simple) ischemia are at high risk of transmural necrosis. Ischemia can arise from torsion of the vascular pedicle as is the case of closed-loop ASBO associated with volvulus or form compression of a single tight adhesive band. CT findings of closed-loop ASBO include:

1. C-shaped (Fig. 13.20), U-shaped (Fig. 13.21), or coffee bean (Fig. 13.22) configuration of the bowel loop with converging toward the site of torsion
2. Beak (Fig. 13.7) or whirl (Fig. 13.19) sign at the site of obstruction
3. Radial configuration of bowel loops when vertically oriented (Fig. 13.23)
4. Convergence of mesenteric vessels to a single point (Fig. 13.24)
5. Close proximity of afferent and efferent limbs, often at the site of mesenteric convergence (Fig. 13.22)

13.4.7.1 Simple Closed-Loop ASBO

A closed-loop obstruction is present when the bowel is obstructed at two adjacent locations, which can be the case with hernias and adhesions. Because of the two adjacent foci of obstruction, the patient is at risk of torsion at the narrow pedicle. The finding of a closed-loop obstruction, even without other evidence of ischemia, is associated with a **high risk of transmural necrosis at surgery**. In a closed-loop obstruction associated with volvulus, the rotation of the bowel, vessels, and mesenteric fat at the site of obstruction is known as the whirl sign (Fig. 13.19). The whirl sign has not been shown to be sensitive or specific for SBO. In patients with clinical and radiologic findings consistent with an ASBO, however, the presence of a whirl sign is associated with a markedly increased need for surgical intervention. In addition, the identification of the combination of multiple transition points, the whirl sign, and a relatively posterior site of obstruction in patients with an ASBO has a

Fig. 13.20 C-shaped configuration of bowel loop (*arrow*) indicating closed-loop obstruction

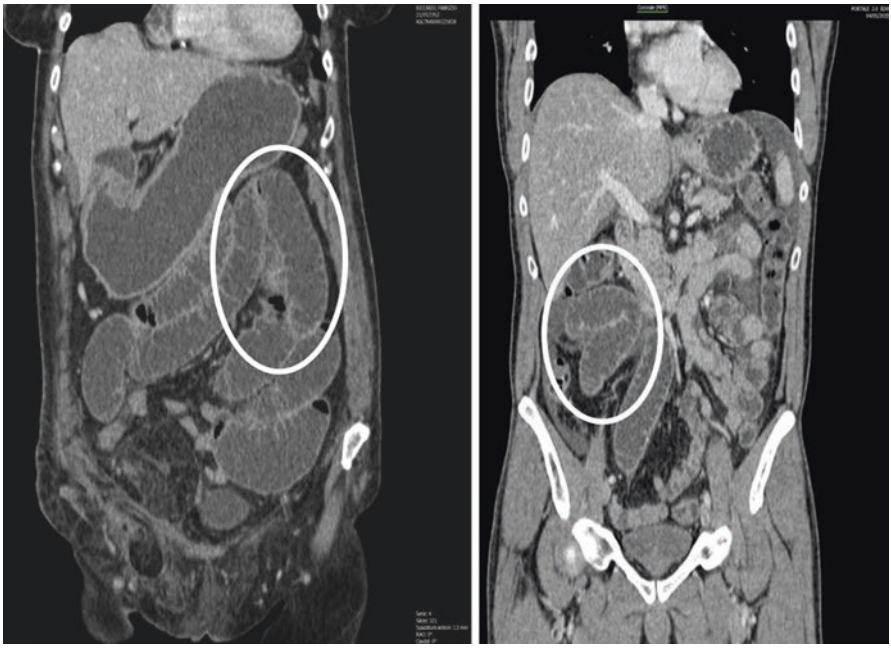

Fig. 13.21 Inverted U-shaped configuration of bowel loop (*circle*) indicating a closed-loop obstruction

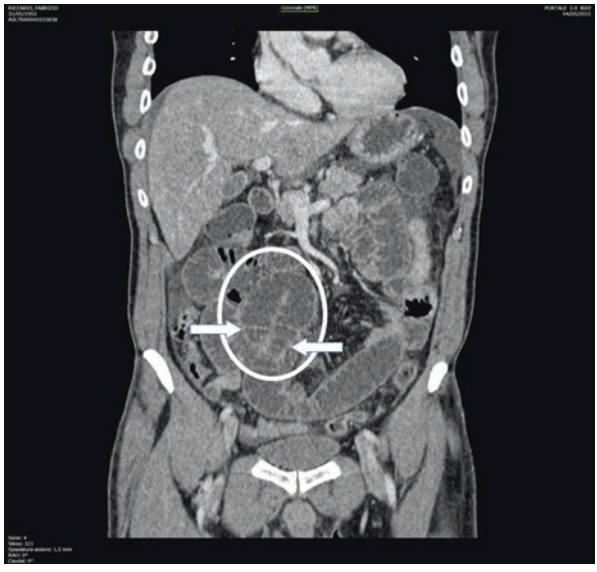

Fig. 13.22 Coffee bean configuration of bowel loop (*circle*) and proximity of afferent and efferent limbs (*arrows*)

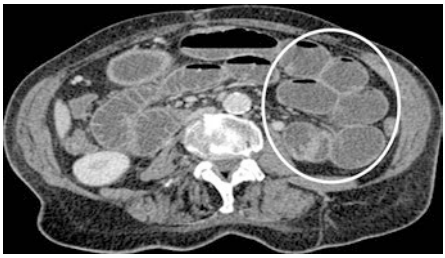

Fig. 13.23 Radial configuration of bowel loop (*circle*) when vertically oriented, indicating a closed-loop obstruction

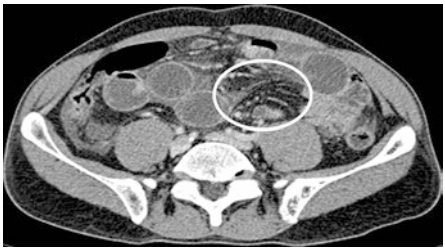

Fig. 13.24 Convergence of mesenteric vessels to a single point (*circle*), indicating a closed-loop obstruction

specificity of 100% for small bowel volvulus. Simple closed-loop ASBO is caused by single adhesive bands. The trapped loop or loops become progressively dilated and fluid-filled. The vessels feeding the trapped intestine may be compressed by the band resulting in strangulation. Both dilatation and the risk of strangulation of the trapped loops depend on the stage and degree of compression.

13.4.7.2 Strangulated Closed-Loop ASBO

Ischemia in SBO can arise from two mechanisms. The first is increasing intraluminal fluid resulting in increased pressure within the bowel wall or tight adhesive bands. CT signs of ischemia warrant **immediate surgical intervention**. In early ischemia, the bowel wall will often hyperenhance, an indication of vasodilation in an attempt to preserve perfusion. As the vascular supply becomes further compromised, the bowel wall will exhibit decreased or absent enhancement, which is a highly specific sign of ischemia. Delayed or prolonged enhancement of the bowel can also indicate ischemia. Although wall thickening can indicate ischemia, this finding can be present because of edema from impaired venous outflow caused by the obstruction and is not specific for ischemia in isolation. In addition, wall thickening may not be present when ischemia has progressed to transmural infarction, as infarcted bowel loses its tone and the wall can become extremely thin. Pneumatosis can be an important indicator of bowel ischemia and can suggest an increased risk of transmural infarction when present in combination with portal venous gas.

Although mesenteric fluid and free fluid are present in higher frequencies in SBOs complicated by ischemia than in uncomplicated obstructions, overall, the presence of any one of these findings is not specific for the diagnosis of ischemia.

Although one study found that the specificity of mesenteric fluid, mesenteric congestion, and free fluid for ischemia was 90, 79, and 76%, respectively, the specificity for ischemia increased to 94% when two or more of these findings were present. With a strangulated obstruction, there is a continuum from bowel wall edema, to mild, to moderate ischemia, to transmural infarction, and, finally, to perforation. CT has a sensitivity of approximately 80–90% in the diagnosis of strangulation in patients with closed-loop obstruction. CT may reveal circumferential bowel wall thickening of low, normal, or high attenuation. Following intravenous contrast material administration, the obstructed segment of bowel may be normal or have increased thickness and may show normal enhancement, delayed enhancement, diminished enhancement, or no enhancement. On unenhanced CT scans, high-attenuation bowel wall thickening implies hemorrhage with ischemia (Fig. 13.18). Diminished or lack of contrast enhancement is very suspicious for vascular compromise. A mural stratification pattern with low attenuation of the submucosa, reflecting submucosal edema (Fig. 13.12), may indicate a spectrum of pathology ranging from bowel wall edema to full thickness infarction. Pneumatosis (Fig. 13.13) in the wall of the closed loop indicates a rent in the mucosa and strangulation. Sloughed mucosa or debris in lumen may have the appearance of feces. If the closed loop is twisted, its mesentery also will appear twisted or whirled (Fig. 13.19). Fluid in the leaves of the small bowel mesentery is suggestive but not specific for ischemia, because intraperitoneal fluid can occur in simple SBOs. However, strangulation is implied by haziness of the mesenteric fat and large mesenteric vessels, findings reflecting mesenteric edema, and venous engorgement, respectively, related to compression or twisting of mesenteric vessels. Volvulus is implied by twisting of the folds at the point of obstruction. Smooth, thick valvulae conniventes in a partially closed loop imply edema with possible ischemia (Fig. 13.9).

13.5 Treatment

The management of ASBO is controversial because surgery can induce new adhesions, whereas conservative treatment does not remove the cause of the obstruction. Delay in surgical treatment may cause a substantial increase of morbidity and mortality. However repeated laparotomy and adhesiolysis may worsen the process of adhesion formation and their severity. Furthermore, the introduction and widespread of laparoscopy has raised the question of selection of appropriate patients with ASBO good candidate for laparoscopic approach. On the other hand, several adjuncts for improving the success rate of nonoperative management (NOM) and clarifying indications and timing for surgery are currently available, such as hyperosmolar water-soluble contrast medium. The 2013 revised and updated guideline of the WSES Working Group on diagnosis and management of ASBO puts to light evidence-based algorithms and focuses on indications and safety of conservative treatment, timing of surgery, and indications for laparoscopy.

13.6 Conservative Management (NOM)

13.6.1 Indications for NOM

Patients without signs of strangulation or signs of peritonitis or history of persistent vomiting or combination of CT scan signs (free fluid, mesenteric edema, lack of feces signs, devascularized bowel) and those with partial ASBO can be managed safely with NOM (nonoperative management). Conservative treatment involves nasogastric intubation, intravenous fluid administration, and clinical observation. These patients are good candidates for water-soluble contrast medium (WSCM) with both diagnostic and therapeutic purposes. In these patients, the radiologic appearance of WSCM in the colon within 24 h from administration predicts resolution. WSCM such as gastrografin may be administered on the dosage of 50–150 mL either orally or via NGT (nasogastric tube) both immediately at admission upon confirmation of a low output of the NGT or after failed conservative treatment for 48 h. The use of WSCM is safe and reduces need for surgery, time to resolution, and hospital stay. Tachycardia, fever, focal tenderness, increased white blood cell counts, and elevated lactate levels can indicate intestinal ischemia, but these indicators are not very specific. When intestinal ischemia is unlikely, a conservative approach can be followed for 24–48 h. NOM, in the absence of signs of strangulation or peritonitis, can be prolonged up to 72 h. After 72 h of NOM without resolution, surgery is recommended. Patients treated nonoperatively have shorter hospital stay, but higher recurrence rate and shorter time to re-admission, although the risk of new surgically treated episodes of ASBO is unchanged. Risk factors for recurrences are age < 40 years and matted adhesions. It should be noted that WSCM does not decrease recurrence rates or recurrences needing surgery.

13.7 Surgical Management

According to the WSES evidence-based guidelines on diagnosis and management of ASBO, patients who had surgery within the 6 weeks before the episode of small bowel obstruction and patients with signs of strangulation or peritonitis (fever, tachycardia and leukocytosis, metabolic acidosis, and continuous pain or pain not responsive to morphine-like drugs) are not candidate for conservative treatment +/− WSCM administration (Level of Evidence 1a GoR A).

Open surgery is often used for ASBO patients with signs of strangulation or peritonitis as well as after failed conservative management for 72 h. In highly selected group of patients, the laparoscopic approach can be attempted using an open access technique. Access in left upper quadrant or left flank is the safest, and only completely obstructing adhesions should be identified and lysed with cold scissors. Laparoscopic lysis of adhesions should be attempted preferably in case of first episode of ASBO and/or anticipated single band adhesion (e.g., SBO after

appendectomy or hysterectomy). A low threshold for open conversion should be maintained if extensive adhesions are found.

a) Indications for Emergent Surgery: ***Strangulated ASBO.***

Strangulation of the bowel requires *immediate* surgery, but intestinal ischemia can be difficult to determine clinically. Free intraperitoneal fluid, mesenteric edema, lack of the "small bowel feces sign" at CT, and history of persistent vomiting, severe abdominal pain (VAS > 4), abdominal guarding, raised WBC, and devascularized bowel at CT predict the need for emergent laparotomy at the time of admission.

b) Indications for Early (Urgent) Surgery: ***Non-strangulated ASBO with High Risk of Failing NOM.***

Early surgery should be indicated in non-strangulated ASBO patients with a high risk of failing NOM. The ability to identify patients who will fail conservative management despite the absence of an acute abdomen at presentation may result in better outcomes for these patients. To this end, multivariate predictive models combining imaging findings, laboratory results, and clinical findings have been developed to identify those patients requiring surgery earlier in their presentation. In consideration of the high accuracy of CT in diagnosing ASBO, CT findings can guide clinical decision-making for treatment choice. Mortality associated with ischemic SBO is approximately 8% if surgery is performed within **36 h** of presentation. If surgery is delayed more than 36 h, however, mortality increases to 25%. However, in those patients who ultimately require surgery after failing decompression, there is increased mortality and prolonged hospital stay in comparison with those undergoing more prompt surgical intervention, and CT may help to more appropriately risk stratify these patients. Small bowel feces have been found to be inversely related to ischemia and failure of conservative management. Because this sign indicates ongoing fluid resorption, the presence of small bowel feces likely reflects preserved function and perfusion of the small bowel. This relationship is further supported by findings that patients with longer segments of bowel with small bowel feces (>10 cm) are less likely to fail conservative management than are patients with shorter segments of small bowel feces. In a study by Schwenter and colleagues, the clinical factors of pain, guarding, leukocytosis, and elevated C-reactive protein were combined with reduced wall enhancement and greater than 500 mL of free fluid on CT into a scoring system. The presence of three factors yielded specificity of 91% and sensitivity of 68% for surgical resection of ischemic bowel within 24 h in comparison with successful conservative management. With four factors present, the specificity was 100%. Zielinski and colleagues found that patients with SBO who presented with lack of flatus for at least 24 h, mesenteric edema, and lack of small bowel feces had an 86% chance of undergoing surgical exploration during their admission. There is a growing body of literature investigating the ability of CT to accurately identify those patients without clear indications for urgent surgery who will likely fail conservative management and may benefit from earlier intervention. In one study of adhesion-related SBO, an anterior parietal adhesion, the presence of a small bowel feces sign, and the lack of a bird beak sign were associated with successful nonsurgical treatment, whereas two bird beak signs or more, a whirl sign, a

C-shaped or U-shaped appearance of the bowel loop, and a high degree of obstruction were associated with nonsurgical treatment failure.

Some of the findings under investigation include small bowel feces, mesenteric edema, mesenteric fluid, and free fluid. Models that incorporate both clinical and imaging findings may allow for further risk stratification of patients without signs of ischemia who will ultimately fail conservative management. The ability to identify these patients earlier in their course shows promise in significantly decreasing the morbidity and mortality associated with acute ASBO. According to the WSES evidence-based guidelines on diagnosis and management of ASBO, complete ASBO (no evidence of air within the large bowel) and increased serum creatine phosphokinase predict NOM failure (Level of vidence 2b GoR C).

c) Indications for Delayed Surgery: ***Non-strangulated and Non-peritonitic ASBO Without Risk of Failing NOM, with Draining Volume of NGT on Day 3 > 500 ml.***

Usually NOM, in the absence of signs of strangulation or peritonitis, can be prolonged up to **72 h** of ASBO. In conservatively treated patients with ASBO, the drainage volume through the long tube on day 3 (cutoff value, 500 mL) is the indicator for surgery. After 3 days without resolution, WSCA study (for NGT output in 24 h <500 ml) or surgery (for NGT output in 24 h >500 mL) is recommended. If ileus persists more than 3 days and the drainage volume on day 3 is >500 mL, surgery for ASBO is recommended. If the drainage volume on day 3 is <500 mL in the absence of signs suggestive of complications, close monitoring with an observation period even longer than 10 days before proceeding to surgical intervention appears to be safe. However at any time, if onset of fever and leukocytosis greater than 15,000/mm^3 (predictors of intestinal complications) are observed, then NOM should be discontinued and surgery is recommended. The patient nonresponders to the long tube and conservative treatment within 72 h have a considerable risk of recurrent ASBO. Risk factors for recurrences are age <40 years, matted adhesion (Level of Evidence 1b GoR A), and postoperative surgical complications. Gastrografin use does not affect the recurrence rates or recurrences needing surgery when compared to traditionally conservatively treated patients.

13.8 Prevention of Adhesion After Adhesiolysis

There is no unanimous consensus to guide the need or not to prevent peritoneal adhesions after adhesiolysis. Hyaluronic acid-carboxycellulose (HA) membrane and icodextrin are known to decrease the incidence of adhesions. Icodextrin may reduce the risk of re-obstruction, while HA cannot reduce the need of surgery. Adhesions quantification and scoring may be useful for achieving standardized assessment of adhesions severity and for further research in diagnosis and treatment of ASBO. Among the different adhesions scoring systems which have been proposed mainly by gynecologists, the more complete and easy to use one is the PAI score proposed by Coccolini et al. (Fig. 13.25). This classification is based on the macroscopic appearance of adhesions and their extent to the different regions of the

Peritoneal Adhesion Index:

Regions:	Adhesion grade:
A Right upper	____
B Epigastrium	____
C Left upper	____
D Left flank	____
E Left lower	____
F Pelvis	____
G Right lower	____
H Right flank	____
I Central	____
L Bowel to bowel	____
PAI	☐

Adhesion grade score:

0 No adhesions

1 Filmy adhesions, blunt dissection

2 Strong adhesions, sharp dissection

3 Very strong vascularized adhesions, sharp dissection, damage hardly preventable

Fig. 13.25 Peritoneal adhesion index. By ascribing to each abdomen area an adhesion-related score as indicated, the sum of the scores will result in the PAI

abdomen. Using specific scoring criteria, clinicians can assign a peritoneal adhesion index (PAI) ranging from 0 to 30, thereby giving a precise description of the intra-abdominal condition. In fact, specific attention should be paid to uniformity of measurement. A regimented classification system for adhesions should be used in an effort to standardize their definition and subsequent analysis. In this way, different surgeons in different treatment centers can more effectively evaluate patients and compare their conditions to past evaluations using a universal classification system. Adhesion quantification scores like the intraoperative PAI score proposed by Coccolini et al. could represent a useful tool in guiding decision-making as to the use or not of adhesion prevention agents after adhesiolysis.

Bibliography

1. Tabibian N, Swehli E, Boyd A, Umbreen A, Tabibian JH. Abdominal adhesions: a practical review of an often overlooked entity. Ann Med Surg (Lond). 2017;15:9–13.
2. Morawski B, Nawrot I, Klonowski W, Mądrecki M, Tarnowski W. Peritoneal adhesions as a cause of mechanical small bowel obstruction based on own experience. Pol Przegl Chir. 2015;86(11):523–31.

3. Stacey R, Green JT. Radiation-induced small bowel disease: latest developments and clinical guidance. Ther Adv Chronic Dis. 2014;5(1):15–29.
4. Ha GW, Lee MR, Kim JH. Adhesive small bowel obstruction after laparoscopic and open colorectal surgery: a systematic review and meta-analysis. Am J Surg. 2016;212(3):527–36.
5. Qalbani A, Paushter D, Dachman AH. Multidetector row CT of small bowel obstruction. Radiol Clin N Am. 2007;45(3):499–512, viii.
6. Gore RM, Silvers RI, Thakrar KH, Wenzke DR, Mehta UK, Newmark GM, Berlin JW. Bowel obstruction. Radiol Clin N Am. 2015;53(6):1225–40.
7. Santillan CS. Computed tomography of small bowel obstruction. Radiol Clin N Am. 2013; 51(1):17–27.
8. Rami Reddy SR, Cappell MS. A systematic review of the clinical presentation, diagnosis, and treatment of small bowel obstruction. Curr Gastroenterol Rep. 2017;19(6):28.
9. Di Saverio S, Coccolini F, Galati M, Smerieri N, Biffl WL, Ansaloni L, Tugnoli G, Velmahos GC, Sartelli M, Bendinelli C, Fraga GP, Kelly MD, Moore FA, Mandalà V, Mandalà S, Masetti M, Jovine E, Pinna AD, Peitzman AB, Leppaniemi A, Sugarbaker PH, Goor HV, Moore EE, Jeekel J, Catena F. Bologna guidelines for diagnosis and management of adhesive small bowel obstruction (ASBO): 2013 update of the evidence-based guidelines from the world society of emergency surgery ASBO working group. World J Emerg Surg. 2013;8(1):42.
10. Coccolini F, Ansaloni L, Manfredi R, Campanati L, Poiasina E, Bertoli P, Capponi MG, Sartelli M, Di Saverio S, Cucchi M, Lazzareschi D, Pisano M, Catena F. Peritoneal adhesion index (PAI): proposal of a score for the "ignored iceberg" of medicine and surgery. World J Emerg Surg. 2013;8(1):6.

Colonic Volvulus

14

Julia Miladore Ng, Haley Chang, and Oreste M. Romeo

14.1 History

This condition with its acute and recurring presentations has been described for thousands of years, as have the rudimentary therapies used. The first recording of volvulus dates to ancient Egypt, where it was noted on the *Ebers Papyrus* (ca. 1550 BC) the description of its natural course to be either spontaneous reduction or "rotting" of the intestines. In addition, some rudimentary techniques were described for the manipulation of the abdomen to stimulate its resolution. Hippocrates (about 400 BC) later noted in his "diseases" and "affections" that certain bowel obstructions, possibly caused by sigmoid volvulus, could be resolved and decompressed with the use of a long suppository ten digits long or ~22 cm, injecting a large quantity of air into the intestines via the anus. To date, the modern proctoscopic decompression requires similar instrument length. It was later in the nineteenth century that this intervention was reexplored as a potential technique in clinical use.

It was in this period that the first report appeared in the Western literature by von Rokitansky who described it as one possible etiology of intestinal strangulation (2). It wasn't until Gay's publication of transanal volvulus reduction on the cadaver of a patient with sigmoid volvulus that therapeutic options started being reviewed more in detail (1). In 1883, Atherton described surgical laparotomy with lysis of adhesions for treatment of volvulus. Eventually, three main surgical approaches came to be employed in the treatment of volvulus: (1) detorsion and plication of the mesentery, (2) colonic resection and primary anastomosis, and later (3) the Hartmann

J.M. Ng, M.D. • H. Chang, M.D. • O.M. Romeo, M.D., F.A.C.S. (✉)
Bronson Methodist Hospital, Western Michigan University,
601 John Street, Box 67, Kalamazoo, MI 49007, USA
e-mail: ROMEOO@bronsonhg.org

F. Catena et al. (eds.), *CT Scan in Abdominal Emergency Surgery*, Hot Topics in Acute Care Surgery and Trauma, https://doi.org/10.1007/978-3-319-48347-4_14

procedure. Surgical management came to eventually become the main therapeutic option into the mid-twentieth century.

The use of laparotomy as the only modality available in the face of volvulus was challenged by Brusgaard in 1947. He described sigmoidoscopy as a mean to decompression and placement of a rectal tube for patients without peritonitis. Successful decompression with a rigid proctoscope in 91 patients with sigmoid volvulus was reported by this author, with a mortality rate of only 14%. Recurrence however remained a common event. After successful nonoperative decompression, high propensity for recurrence is well recognized, remaining in some series as high as 90%, with an attendant mortality of up to 40%.

In time, a more frequent use of this approach found favor for early reduction of sigmoid volvulus, especially when considering the extensive comorbidities most of these patients have at presentation along with baseline frailty and consequently poor tolerance of anesthesia. With better technologies, detorsion with a rigid proctoscope and eventually with flexible sigmoidoscopy continues to gain favor as early modalities in decompression. Many authors have reported success in conservative early approaches to decompress volvulus not only in the sigmoid colon but also in other anatomic locations advocating its use in patients unable to tolerate laparotomy. Because of high rates of recurrence, endoscopic decompression is most often considered as a temporizing measure.

14.2 Introduction

The term colonic volvulus comes from the Latin term “volvere” meaning “to twist,” which occurs when the colon twists axially on its mesentery. Worldwide colonic volvulus is the third leading cause of large bowel obstruction. Populations most affected reside in the “volvulus belt” of Africa, the Middle East, India, and Russia. In these regions, the average age is younger than Western countries, ranging from 40 to 50 years and in patient populations generally in better health. In the United States, colonic volvulus accounts for 10–15% of all colon obstructions. It accounts for 1–3% of all bowel obstruction presentations, ranking behind cancer and diverticulitis. It occurs when a mobile portion of the colon twists around a fixed base, causing obstruction of a segment of colon at the point of maximal torsion. In effect, it results in a closed-loop obstruction. In a study of 546 cases of colonic volvulus, it is most often found in the sigmoid (60.9%), followed by the cecum (34.5%), the transverse colon (3.6%), and splenic flexure (1%). It is most often seen in the elderly, in patients with neuropsychiatric disorders, and those in nursing care facilities. Predisposing factors include previous episodes of volvulus, previous abdominal operations, institutionalization, megacolon, and chronic constipation with sigmoid volvulus as the leading cause of acute colonic obstruction. Colonic volvulus can resolve spontaneously, but more commonly, it can cause obstruction that can progress to strangulation, ischemia, and perforation.

14.3 Overview

Sigmoid volvulus represents 50–90% of colonic volvulus cases. Predisposition to sigmoid volvulus occurs secondary to redundant colon on a narrow mesenteric attachment. A high-fiber diet and chronic constipation can also contribute to an overloaded sigmoid colon resulting in counterclockwise torsion of the colon. Elderly institutionalized patients and those with underlying colonic motility issues also are at higher risk for developing sigmoid volvulus. Overall sigmoid volvulus has an equal sex distribution.

Cecal volvulus also occurs in debilitated patients although less prevalent than sigmoid volvulus occurring 15–40% of all cases of colonic volvulus. In order for cecal volvulus to occur, there must be a portion of cecum that is freely mobile and a fixed point to torse upon. The Jackson veil is an abnormal membrane that contains blood vessels from the renal and lumbar arteries that crosses over the right colon creating a fixed point at the inferior edge upon which the cecum can twist. The cecum can torse in an organo-axial fashion or mesenterico-axial fashion. Organo-axial torsion occurs when the terminal ileum and cecum twist clockwise. Mesenterico-axial torsion also known as cecal bascule occurs when a malfixed cecum flips anteriorly of the right colon. Vascular compromise occurs when the cecum becomes significantly distended. Ischemia does not occur initially as there is no twisting of the mesentery to immediately occlude blood supply. In as many as

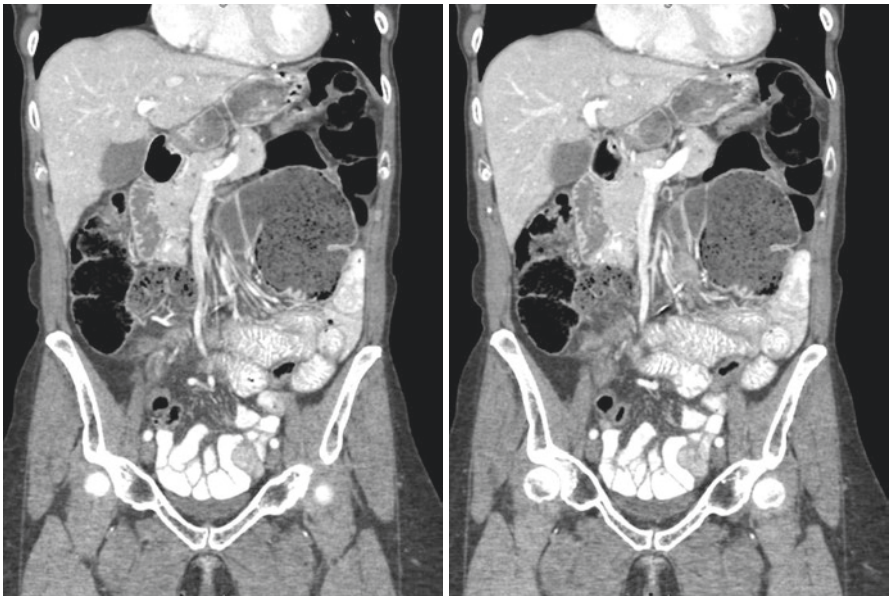

Fig. 14.1 CT image of colonic volvulus. The patient in the image went on to operative management. Courtesy Bronson Methodist Hospital, Kalamazoo, Michigan. Department of Radiology

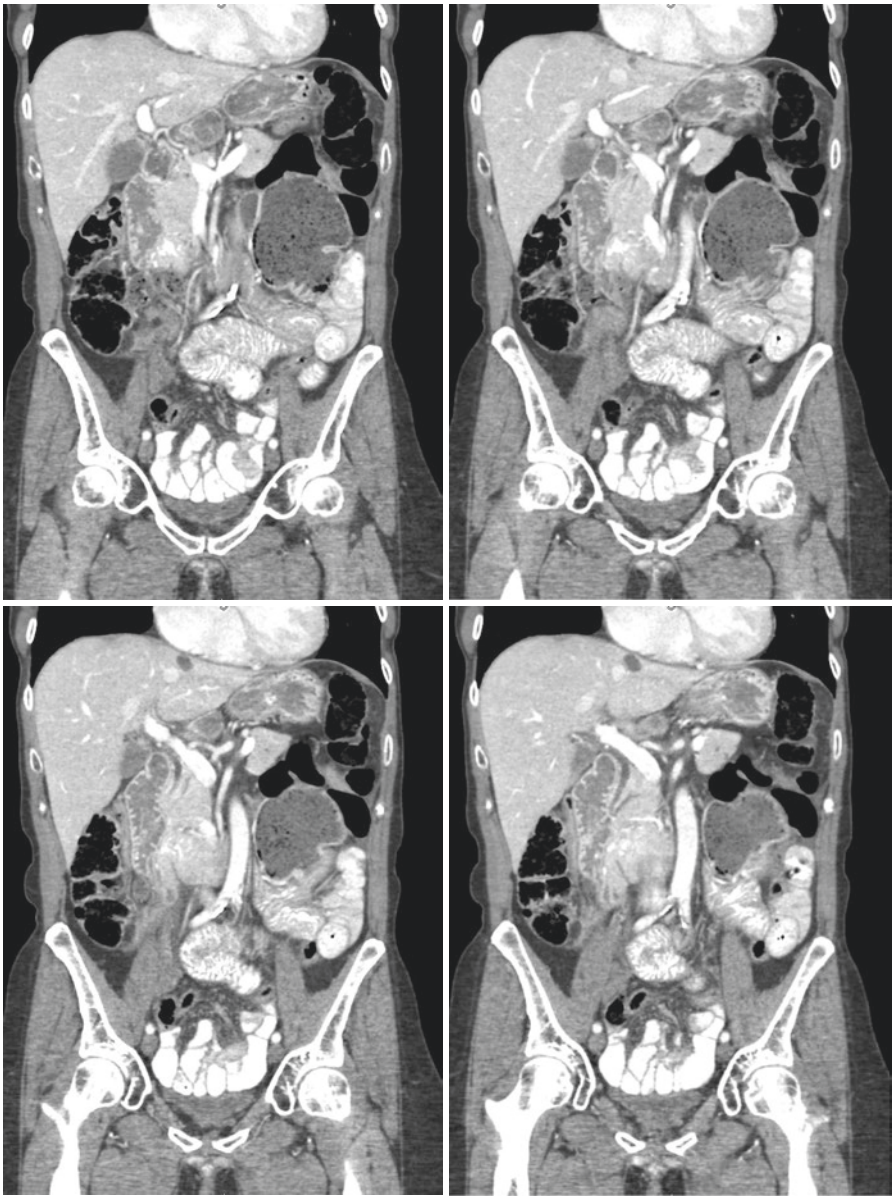

Fig. 14.1 (continued)

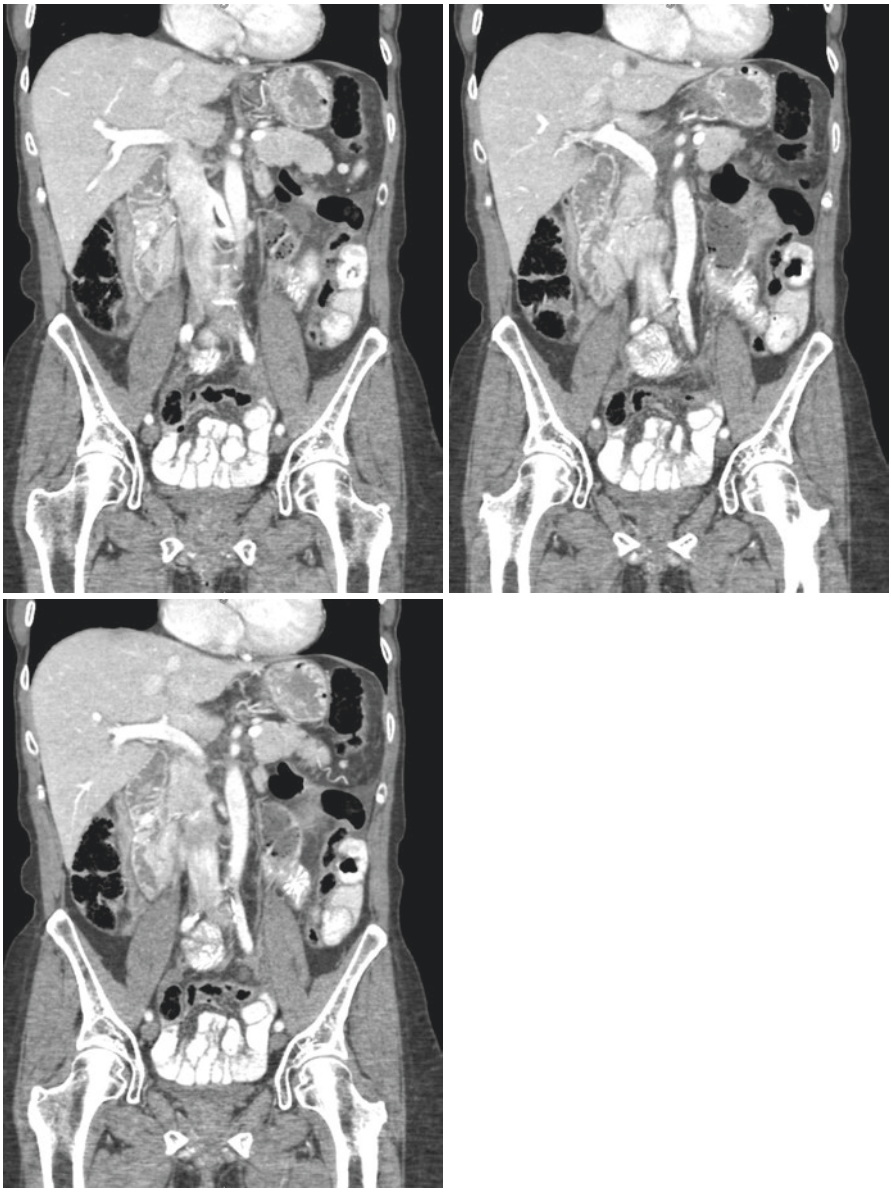

Fig. 14.1 (continued)

50% of patients, intermittent symptoms due to a floppy cecum prior to presentation will be elicited upon history review.

14.4 Presentation

The presentation of sigmoid and cecal volvulus can be very similar. Patients can present with abdominal pain, distention, nausea, vomiting, obstipation, or constipation. These symptoms may occur acutely or chronically. In more severe cases, patients can present with peritonitis or hemodynamic instability. In cecal bascule, patients may have a chronic history of intermittent pain or obstructive symptoms.

14.5 Diagnosis

The diagnosis of sigmoid volvulus can be made on abdominal x-ray. These films will demonstrate a "coffee bean" appearance with convexity to the patient's right. A gastrografin enema will demonstrate a "bird's beak" sign at the site of narrowing.

Diagnosis of cecal volvulus can also be made with abdominal plain films. A kidney bean-shaped air-filled structure in the LUQ will be seen. CT scan will demonstrate the "whirl" sign which is a spiraled loop of cecum with engorged mesenteric vessels (Fig. 14.1).

14.6 Treatment

If a patient is stable with no signs of peritonitis or hemodynamic instability, then sigmoid volvulus can initially be treated with decompression by a rigid proctoscope, flexible sigmoidoscope, or colonoscope. There is a 75% success rate of decompression with endoscopic means. A rectal tube is placed to maintain decompression. Although the success rate is high, the recurrence of the volvulus is also high with the recurrence rate being 60–75%. For this reason, endoscopic decompression should be followed by definitive surgery. Along the course of treatment, if there is any clinical evidence of peritonitis, then immediate surgery should be performed. There are two main surgical options in the treatment of sigmoid volvulus. The first is sigmoid resection with primary anastomosis. This is utilized when upon exploration the patient has viable bowel with no contamination regardless of successful endoscopic decompression. If endoscopic decompression is successful, then bowel prep prior to surgery is preferred. If there is any evidence of ischemia or contamination upon operation then sigmoidectomy with end colostomy or Hartmann's procedure should be performed. A Mikulicz operation has also been reported where the volvulus is exposed through a lateral oblique incision and a double barrel colostomy is created. This is mentioned for historical importance as it is not routinely used today.

Cecal volvulus is not amenable to endoscopic decompression, so surgical intervention is the treatment of choice. These patients usually undergo a right hemicolectomy with ileorectal anastomosis. If the patient is extremely debilitated, then cecostomy is performed. Cecostomy has a low recurrence rate of 1–3% but high wound infection rate. Cecopexy alone is not recommended as the recurrence rate is high as 15–20%.

14.7 Complications

The main complications after treatment of sigmoid and cecal volvulus are surgical wound infections; anastomotic complications with leak, fistula, or abscess; and recurrence.

14.8 Outcomes

In emergent surgery for sigmoid volvulus, the mortality rate ranges from 17 to 40%. If decompression is successful, the mortality rate drops to 0–6% with surgical intervention. The overall mortality rate is 9.4% but is 50% if there is colonic perforation. Overall, the incidence of sigmoid volvulus is small, so any outcome measures are based on small sample sizes. Since the recurrence rate of sigmoid volvulus is high and there is greater mortality associated with emergent surgery, the recommendation would be for decompression followed by semi-elective surgery. The long-term rates of constipation are higher in patients undergoing primary anastomosis versus Hartmann's procedure, but neither operations result in recurrence of the volvulus.

Cecal volvulus has an overall mortality of 6.7%. This mortality increases to 35% with ischemic bowel. The mortality for surgical intervention is 12%. Given the rarity of cecal volvulus, many long-term outcomes have not been studied or identified.

Transverse colon volvulus can also occur but is rare, less than 3% of all cases of colonic volvulus. It is due to abnormal fixation of the colon and presents with similar symptoms as sigmoid and cecal volvulus. Diagnosis is made on contrast enema where contrast travels more proximally than the sigmoid colon. This requires surgical exploration with segmental colectomy, extended right hemicolectomy, or ileostomy with mucus fistula.

Bibliography

1. Ballantyne GH. Review of sigmoid volvulus: history and results of treatment. Dis Colon Rectum. 1982;25(5):494–501.
2. Freiherr von Rokitansky C. Handbuch der Pathologischen Anatomie, vol 1. Wien: Braumüller u. Seidel, Anatomie; 1841.
3. Case by Dr. Atherton. Boston Med Surg J. 1883;CVIII(24):553.

4. Bruusgaard C. Volvulus of the sigmoid colon and its treatment. Surgery. 1947;22(3):466–78.
5. Grossmann EM, Longo WE, Stratton MD, Virgo KS, Johnson FE. Sigmoid volvulus in Department of Veterans Affairs Medical Centers. Dis Colon Rectum. 2000;43(3):414–8.
6. Hines JR, Geurkink RE, Bass RT. Recurrence and mortality rates in sigmoid volvulus. Surg Gynecol Obstet. 1967;124(3):567–70.
7. Gingold D, Murrell Z. Management of colonic volvulus. Clin Colon Rectal Surg. 2012;25(4):236–44.
8. Orchard JL, Mehta R, Khan AH. The use of colonoscopy in the treatment of colonic volvulus: three cases and review of the literature. Am J Gastroenterol. 1984;79(11):864–7.
9. Anderson MJ, Okike N, Spencer RJ. The colonoscope in cecal volvulus: report of three cases. Dis Colon Rectum. 1978;21(1):71–4.
10. Joergensen K, Kronborg O. The colonoscope in volvulus of the transverse colon. Dis Colon Rectum. 1980;23(5):357–8.
11. Brothers TE, Strodel WE, Eckhauser FE. Endoscopy in colonic volvulus. Ann Surg. 1987;206(1):1–4.
12. Ghazi A, Shinya H, Wolfe WI. Treatment of volvulus of the colon by colonoscopy. Ann Surg. 1976;183(3):263–5.
13. Halabi WJ, Jafari MD, Kang CY, Nguyen VQ, Carmichael JC, Mills S, Pigazzi A, Stamos MJ. Colonic volvulus in the United States: trends, outcomes, and predictors of mortality. Ann Surg. 2013;259:293–301.
14. Ballantyne GH, Brandner MD, Beart RW Jr, Ilstrup DM. Volvulus of the colon incidence and mortality. Ann Surg. 1985;202(1):83–92.
15. Isbister WH. Large bowel volvulus. Int J Colorectal Dis. 1996;11(2):96–8.
16. Hougaard HT, Qvist N. Elective surgery after successful endoscopic decompression of sigmoid volvulus may be considered. Dan Med J. 2013;60(7):A4660.
17. Tan KK, Chong CS, Sim R. Management of acute sigmoid volvulus: an institution's experience over 9 years. World J Surg. 2010;34(8):1943–8. doi:10.1007/s00268-010-0563-8.
18. Safioleas M, Chatziconstantinou C, Felekouras E, Stamatakos M, Papaconstantinou I, Smirnis A, Safioleas P, Kostakis A. Clinical considerations and therapeutic strategy for sigmoid volvulus in the elderly: a study of 33 cases. World J Gastroenterol. 2007;13(6):921–4.
19. Suleyman O, Kessaf AA, Ayhan KM. Sigmoid volvulus: long-term surgical outcomes and review of the literature. S Afr J Surg. 2012;50(1):9–15.
20. Oren D, Atamanalp SS, Aydinli B, Yildirgan MI, Başoğlu M, Polat KY, Onbaş O. An algorithm for the management of sigmoid colon volvulus and the safety of primary resection: experience with 827 cases. Dis Colon Rectum. 2007;50(4):489–97.
21. Consorti ET, Liu TH. Diagnosis and treatment of caecal volvulus. Postgrad Med J. 2005;81:772–6. doi:10.1136/pgmj.2005.035311.
22. Habre J. Caecal volvulus. Am J Surg. 2008;196(5):e48–9.

Computerized Tomography in the Diagnosis and Treatment of Acute Pancreatitis

15

Itamar Ashkenazi and Yoram Kluger

Acute pancreatitis is encountered commonly in the surgical emergency department [1]. Epidemiological studies from several countries indicate that the incidence of acute pancreatitis is rising [2, 3]. The most common etiologies of pancreatitis are gallstones and alcoholism [4, 5]. Other etiologies include hypertriglyceridemia, mumps virus, hypercalcemia, drugs, and post-endoscopic retrograde cholangiopancreatography (ERCP). Tumor of the pancreas should be ruled out in any patient older than 45–50 years suffering from a first bout of acute pancreatitis of obscure etiology [5]. Acute pancreatitis can be temporally subdivided into a clinical early phase (within 1 week of onset) and a clinical late phase (>1 week after onset) [6]. The topic of diagnosis corresponds to the clinical early phase, while the role of CT in the follow-up and in management of complications corresponds to the clinical late phase.

15.1 The Role of CT in the Diagnosis of Acute Pancreatitis

Following the revision of the Atlanta classification in 2012, the International Association of Pancreatology and the American Pancreatic Association updated their guidelines concerning management of acute pancreatitis (Scheme 15.1) [7, 8]. According to these guidelines, the definition of acute pancreatitis is based on the fulfillment of two out of three criteria: clinical (upper abdominal pain), laboratory (serum amylase or lipase over three times the upper limit of normal), and imaging (CT or magnetic resonance imaging or ultrasonography). As such, imaging studies,

I. Ashkenazi, M.D.
Hillel Yaffe Medical Center, Hadera, Israel

Y. Kluger, M.D., F.A.C.S. (✉)
Division of General Surgery, Rambam Health Care Center, Haifa, Israel
e-mail: y_kluger@rambam.health.gov.il

F. Catena et al. (eds.), *CT Scan in Abdominal Emergency Surgery*, Hot Topics in Acute Care Surgery and Trauma, https://doi.org/10.1007/978-3-319-48347-4_15

Scheme 15.1 Classification of collections according to the revised Atlanta Criteria

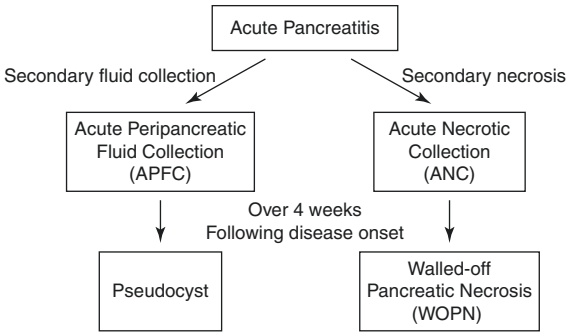

such as CT, are not required for the diagnosis of acute pancreatitis in patients in whom the first two criteria can be confirmed. These guidelines call into question the role of CT in the acute phase of the disease, as will be elaborated below.

Most patients who present with acute pancreatitis suffer from a relatively mild disease, manifested pathologically as acute interstitial edematous pancreatitis [7]. These patients recover without any major morbidity. For this group of patients, CT does not change or contribute much to management if the diagnosis is supported by clinical and laboratory criteria. Contrast-induced nephrotoxicity may impose a real risk in any patient who presents to the emergency department with a decrease in effective blood volume secondary to an acute inflammatory process. In such circumstance, ultrasound should be performed to establish the possibility of gallstone disease as a probable cause of acute pancreatitis.

Up to 40% of patients with pancreatitis present with a moderate to severe form of acute disease [7, 9]. Of them, about one quarter progress to severe necrotizing pancreatitis [6]. Necrosis develops in either the pancreatic tissue or the peripancreatic fat or in both pancreatic tissue and peripancreatic fat in 5%, 20%, and 75–80% of patients, respectively [10, 11]. Pancreatic and peripancreatic necrosis develops within hours of the onset of acute pancreatitis and becomes established after 72 h [6, 7, 10]. Therefore, current guidelines advocate performing contrast-enhanced CT only 72 h after the onset of pain, in order to better evaluate the extent of necrosis [7, 8, 12]. Length of hospitalization, development of complications, and mortality risk are directly related to the extent of the necrosis detected on CT [13].

The main concern in postponing CT for 72 h from the onset of the attack is delaying diagnosis of some pathologies that may mimic clinical presentation and initial laboratory of acute pancreatitis and are best treated early with surgery. Patients presenting at the emergency department with moderate or severe acute pancreatitis may present signs of established systemic inflammatory response syndrome (SIRS) and even organ failure [7]. Examination of the impact of blood urea nitrogen on survival in 1043 patients admitted for acute pancreatitis in three university hospitals revealed abnormal levels on presentation in 311 (29.8%) [14]. When clinical and laboratory criteria of acute pancreatitis are present, the physician must consider the differential diagnoses, especially in patients who present with hemodynamic instability or SIRS or with evidence of acute organ failure. Differential diagnoses

include intestinal perforation and mesenteric ischemia. Rare cases of ruptured ectopic pregnancy and incarcerated diaphragmatic hernia mimicking acute pancreatitis have been described [15, 16]. Contrast-enhanced CT may be necessary to differentiate these from acute pancreatitis [4, 8]. Occasionally, ascending cholangitis may be difficult to differentiate from acute pancreatitis. If the adequately resuscitated patient deteriorates during the first 24 h, CT may be necessary to differentiate between acute pancreatitis and nonresponsive ascending cholangitis in need of an urgent ERCP [17]. Data in the literature concerning the actual proportion of patients presenting to the emergency department for which contrast-enhanced CT can be avoided is not available. A retrospective case note audit of all patients admitted with a confirmed diagnosis of acute pancreatitis in Western Sydney revealed that 31% underwent CT earlier than 72 h with the purpose of confirming the diagnosis [18].

Since Ranson et al. introduced criteria for early identification of severe acute pancreatitis in 1974, severity scoring has become part of the diagnostic process in this disease [19]. Other scores have been developed. Most of these are based on clinical data [20–22]. In 1990, Balthazar et al. published criteria based on CT imaging findings (Tables 15.1 and 15.2) [13]. The severity of acute pancreatitis was recognized as related to the presence and degree of pancreatic necrosis. Accordingly, if contrast-enhanced CT demonstrates the absence of necrosis of the pancreatic gland, mortality and complication rates are 0% and 6%, respectively. However, in patients with pancreatic necrosis, mortality and complication rates reach 23% and 82%, respectively. In that publication, severity of pancreatic necrosis was categorized as involving up to 30% of the gland, over 30% and up to 50% of the gland, and greater than 50% of the gland. The presence and degree of pancreatic necrosis form the basis of the CT severity index score (CTSI) and the modified CTSI score (Tables 15.1 and 15.2) [23, 24].

Table 15.1 Computed tomography severity index (CTSI) is a classifying system used to define the severity of acute pancreatitis

Balthazar grade	Appearance on CT	CT grade points
Grade A	Normal CT	0
Grade B	Focal or diffuse enlargement of the pancreas	1
Grade C	Pancreatic gland abnormalities and peripancreatic inflammation	2
Grade D	Fluid collection in a single location	3
Grade E	Two or more fluid collections and/or gas bubbles in or adjacent to pancreas	4

CTSI has a maximum of ten points. It is the sum of the Balthazar grade points and pancreatic necrosis grade points

Table 15.2 Necrosis score

Necrosis percentage	Points
No necrosis	0
0–30	2
30–50	4
Over 50	6

Despite the recommendation by a number of guidelines to delay CT for 72 h from the onset of the attack [7, 8, 12], many patients with severe disease on presentation undergo contrast-enhanced CT soon after admission, in order to rule out the differential diagnoses, as detailed above. A second contrast-enhanced CT a few days later, with the sole purpose of evaluating the extent of necrosis, is better avoided. Of those who were not evaluated with contrast-enhanced CT upon admission, some improve with time and resuscitation. CT scan for these patients is unnecessary. This leaves a minority of patients who are candidates for contrast-enhanced CT once 72 h have passed from the onset of the disease. Even for these patients, it is uncertain if contrast-enhanced CT is needed. Current guidelines advocate assessing patients using the SIRS criteria upon admission and follow-up [8]. SIRS is defined by the presence of two or more of the following four criteria: hypothermia (<36 °C) or hyperthermia (>38 °C), increased heart rate (>90/min), tachypnea (>20/min), and leukopenia ($<4 \times 10^9$/L), leukocytosis ($>12 \times 10^9$/L), or 10% bands. Follow-up of these criteria is simple and has been shown to be a reliable marker of severe pancreatitis [25]. If SIRS persists beyond 48 h (i.e., persistent SIRS), patients are at increased risk for multiple organ failure and death from acute pancreatitis [26]. In practical terms, if acute pancreatitis is deemed severe by persistent SIRS, and the patient does not deteriorate, then contrast-enhanced CT is best postponed to evaluate possible complications, as described in the next section.

One last comment concerns the potential of contrast-enhanced CT to exacerbate the severity of acute pancreatitis. This negative potential of intravenous contrast medium on the severity of acute necrotizing pancreatitis was described mainly in animal models. Foitzik et al. described how intravenous contrast material decreases oxygen saturation of hemoglobin and decreases pancreatic microcirculation in a rat model of acute necrotizing pancreatitis [27]. These authors postulated that intravenous contrast material may convert borderline ischemia to irreversible necrosis, which explains the increased necrosis score and mortality seen in exposed rats [28]. Data from human subjects is observational. Some of the older studies supported the animal studies and showed mainly that the duration of disease in those undergoing contrast-enhanced CT is longer, regardless of the initial severity score [29]. Duration of illness was determined from the date of onset of pain to the date of resolution of pain and the resumption of oral nutrition. Nevertheless, a negative impact of CT images on clinical decision-making concerning resumption of oral nutrition cannot be ruled out. Other human studies do not support the negative impact of contrast on acute pancreatitis. Sharma et al. compared 114 patients who underwent early CT (within 5 days) to 79 patients who underwent late CT (6–14 days) [30]. No differences were found in the need for percutaneous drainage, need for surgery, persistent organ failure, and mortality. Uhl et al. compared 264 patients with moderate to severe pancreatitis who underwent contrast-enhanced CT within 96 h of onset of symptoms, to 38 patients with similar characteristics who did not undergo CT [31]. No differences were found in complication rate and length of hospital stay. If contrast-enhanced CT is deemed necessary, it should not be considered contraindicated in the evaluation of patients in whom the differential diagnosis includes acute severe pancreatitis.

To summarize this section, contrast-enhanced CT is valuable in differentiating acute pancreatitis from other diagnoses in patients for whom the diagnosis is uncertain. The best time to evaluate pancreatic necrosis is beyond 72 h from the onset of the attack. However, CT may not be beneficial or necessary in patients who show improvement or who are stable.

15.2 The Role of CT in the Treatment of Complications During the Acute Attack

In patients with severe or moderate acute pancreatitis, the main complications observed in the clinical early phase (within 1 week of onset) are single or multiple organ failures resulting from hypovolemia and excessive leukocyte activation and consequent inflammatory mediator release [32]. Exacerbation of pre-existing comorbidities, such as congestive heart failure, chronic liver disease, and chronic lung disease, has an additive effect [6]. Organ failure at this stage is treated by supportive care, most commonly, in an intensive care setting. Beyond its role in establishing the diagnosis, CT scan has no real role in the treatment at this stage.

Complications that become clinically manifested at the clinical late phase (>1 week after onset) result from necrosis and fluid collections (Fig. 15.1) [6]. Necrosis may be either sterile or secondarily infected (Fig. 15.2). The original

Fig. 15.1 Contrast-enhanced CT scan of the abdomen showing lack of tissue enhancement of the body and tail of the pancreas (**a**) with peripancreatic fluid collection (**b**)

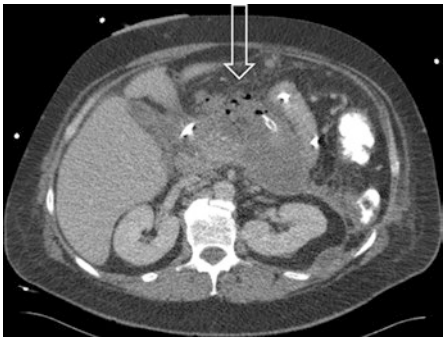

Fig. 15.2 CT scan showing air bubbles (*arrow*) in peripancreatic fluid collection with percutaneous drain in place

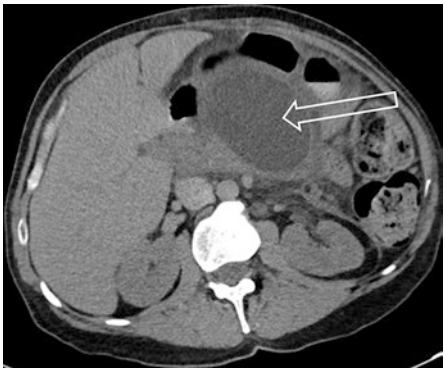

Fig. 15.3 CT scan showing a well-formed pseudocyst that evolved from necrotizing pancreatitis. The stomach is displaced anteriorly. The *arrow* points at the pseudocyst filled with thick liquid

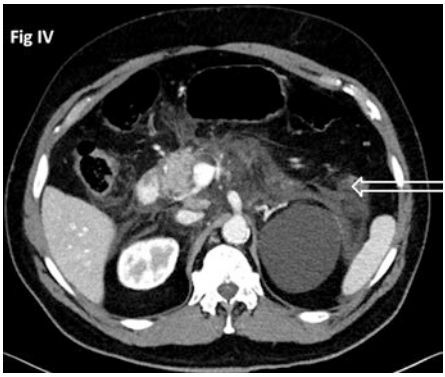

Fig. 15.4 Homogenous collection with fluid density that develops adjacent to the pancreas. It is confined by a normal peripancreatic fascial plane with no definable wall encapsulating the collection (*arrow*)

Atlanta Symposium classified pancreatic fluid collections as either acute (<4 weeks) or chronic (>4 weeks), with chronic collections further subdivided into pancreatic necrosis, whether sterile or infected, acute pseudocyst (Fig. 15.3), and pancreatic abscess [33, 34]. The revised Atlanta criteria further classify acute and chronic collections into those containing fluid alone versus those arising from necrosis and/or containing solid components [7, 35]. Acute collections are divided into acute peripancreatic fluid collections (APFC) and acute necrotic collections (ANC). APFC is described as a homogenous collection with fluid density that develops adjacent to the pancreas. It is confined by a normal peripancreatic fascial plane with no definable wall encapsulating the collection (Fig. 15.4). APFC that develops in patients with edematous pancreatitis commonly resolves spontaneously [36]. ANC is a collection containing variable amounts of both fluid and necrosis (Fig. 15.5). Since necrosis develops either in the pancreatic parenchyma or the peripancreatic fat, the collection is either intrapancreatic or extrapancreatic. The content of the collection is heterogenous. Again, no definable wall is identifiable. The chronic fluid collections are divided into pancreatic pseudocysts and walled-off pancreatic necrosis (WOPN). Pancreatic pseudocysts and WOPN evolve from their respective acute counterparts [37]. Pancreatic pseudocysts are chronic encapsulated collections of

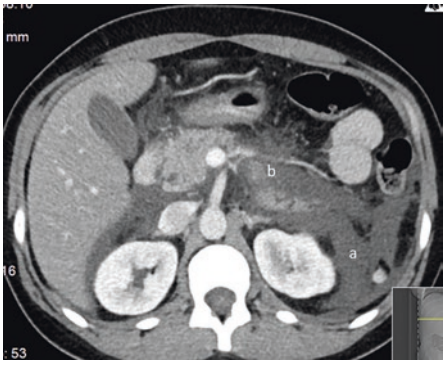

Fig. 15.5 Peripancreatic collection containing variable amounts of both fluid (**a**) and necrosis (**b**)

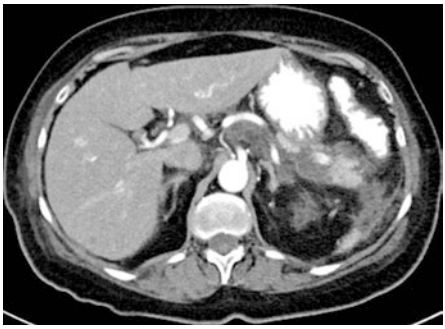

Fig. 15.6 The tail of the pancreas is hypodense. Peripancreatic fluid collection as well as thickening of the Gerota's fascia is consistent with CTSI of 5

fluid with well-defined inflammatory walls and are identified adjacent to the pancreas 4 or more weeks after the onset of acute pancreatitis. WOPN are chronic collections of variable amounts of necrotic tissue and fluid that are completely encapsulated with a well-defined wall. APFC are the most common fluid collection, compromising three fourths of the collections observed, followed by ANC, pancreatic pseudocysts, and WOPN [9].

With improved management of organ failure, secondary infection has become the most common cause of morbidity and mortality in patients suffering from acute pancreatitis [38–42]. Secondary infection develops in patients with evidence of necrosis and/or collections, typically 8–20 days following the onset of pancreatitis [43]. In patients with pancreatic necrosis, the extent of necrosis is predictive of the development of septic complications [40]. While only 22% of patients with <30% pancreatic necrosis were shown to develop infection, infection developed in 32% and 48% of patients with 30–50% and >50% pancreatic necrosis, respectively. Secondary infection of collections is more common in patients with ANC or WOPN [6].

Patients with infection commonly present with persistent SIRS [8, 26]. This occurs when there is no sign of clinical improvement following 1 week of intensive treatment. Fever, hyperglycemia, and leukocytosis are common [43]. CT is performed with the aim of identifying areas of necrosis and fluid collections

(Figs. 15.6, 15.7, 15.8, and 15.9). CT may also demonstrate the presence of gas within the collection, which suggests secondary infection. Nonetheless, the absence of gas does not rule out infection since only a minority of infected collections contains gas [6].

Under CT guidance, aspiration is performed [44]. The aspirate is submitted for both gram stain and culture. Infection is most commonly due to gram-negative rods (*E. coli*, *Klebsiella pneumoniae*, and *Pseudomonas Aeruginosa*) followed by *Enterococci*, *Streptococcus*, and *Bacteroides* [43, 45]. If the aspirate is sterile, the patient is best treated with intensive medical care [46, 47]. If the patient's situation

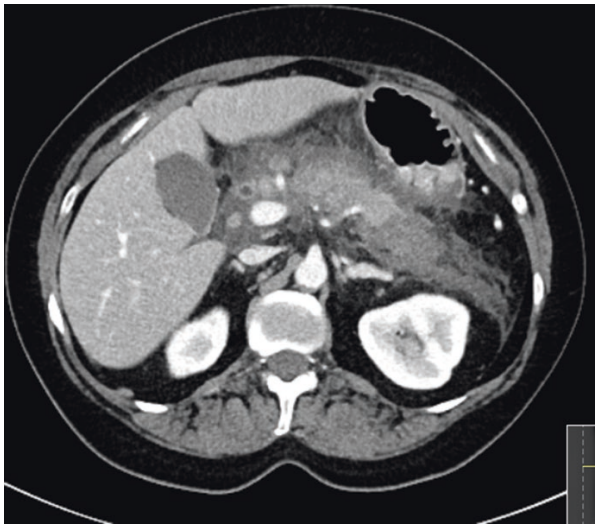

Fig. 15.7 Balthazar score *c* with 50% necrosis of the pancreas corresponding to CTSI of 6

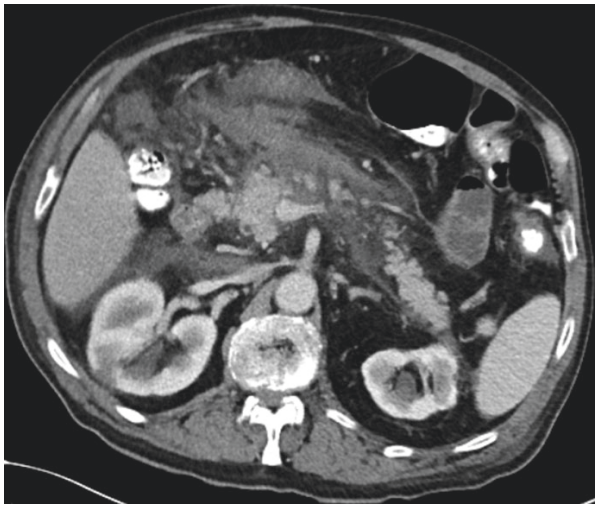

Fig. 15.8 Balthazar score *d* (localized fluid collection) with necrosis of the body of the pancreas (50%) corresponding to CTSI of 7

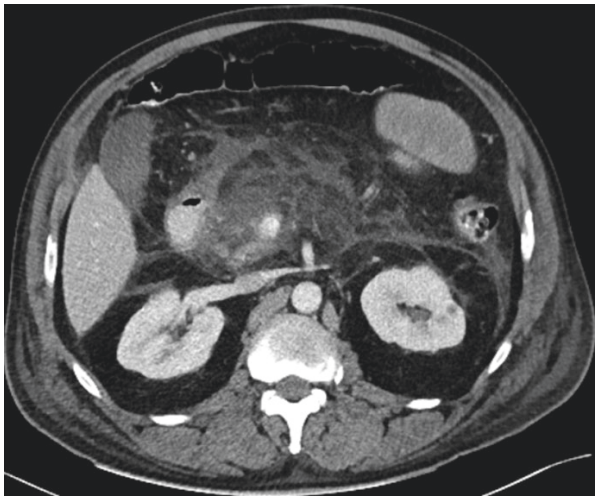

Fig. 15.9 Balthazar score *d* (localized fluid collection) with necrosis of the body of the pancreas (>50%) corresponding to CTSI of 10

does not improve, CT, and if needed, diagnostic aspiration, is repeated after 5–7 days. Some authors have claimed that aspiration may be diagnostic of infection in over 90%, but the actual figure may be much lower [48].

Aggressive surgical treatment of symptomatic or infected necrosis and/or collections has been largely replaced by a step-up approach [49]. This consists of percutaneous drainage followed, if necessary, by minimally invasive approaches to necrosectomy [49, 50]. Compared to surgical necrosectomy, this has been shown to reduce the need of surgery and to decrease morbidity, without increasing mortality.

The first stage in the step-up approach is percutaneous drainage of the infected necrosis and/or collection. This is most commonly performed, CT guided, through either the peritoneal or the retroperitoneal approach. CT is the preferred modality to insert the draining catheter, as it enables identification of nearby bowel or other critical structures throughout the procedure [6]. Additional catheters are inserted if needed, as indicated by repeated CT assessment. The main limitation of this approach is the difficulty in effectively draining infected collections that contain necrotic tissue through relatively small bore catheters. For this reason, the typical range of catheters that are currently used to drain is 12F–30F [6]. With this approach, CT-guided drainage is the only intervention needed in 35–84% of patients [35, 49]. The remaining patients need additional interventions such as endoscopic necrosectomy and/or surgical necrosectomy to control their symptoms [51].

15.3 The Role of CT in the Follow-Up of Patients Following an Attack of Acute Pancreatitis

In 54–57% of patients who undergo routine imaging following an attack of acute pancreatitis, the presence of pseudocysts is demonstrated [52]. Most of them are asymptomatic, and resolution is spontaneous without any adverse events. Persistent

pseudocysts may be manifested by continuous high levels of serum amylase. Common symptoms are abdominal pain, nausea, and weight loss. Observation is well accepted as the primary management strategy for all patients with pseudocysts, provided that the symptoms are mild, the pseudocysts do not enlarge, and there are no secondary complications.

The diagnosis of a pseudocyst is made with CT or US. CT scan is more useful in defining the precise location and relation of the pseudocyst to adjacent structures. This information is crucial for patients for whom endoscopic drainage is considered.

Many complications secondary to pseudocysts have been described; some of them are rare [52]. CT has a role in evaluating suspected complications. Infection is the most common of these, occurring in as many as 10% of patients with persistent pseudocysts. Such patients typically present with abdominal pain and fever. CT scan may demonstrate gas bubbles within the pseudocyst. Otherwise, CT-guided needle aspiration sent for gram stain and culture may confirm the infection. Infected pseudocysts must be drained immediately. Hemorrhage into the pseudocyst may result from erosion of blood vessels lining the cyst wall. Bleeding leads to rapid enlargement of the pseudocyst. Patients will generally complain of sudden pain and may present with signs of shock. In the case of intra-pseudocyst bleeding, CT shows a significant increase in the density of the pseudocyst (from 0–25 to 50–100 Hounsfield units) [52]. Angiography is essential to confirm the site of the bleeding and to attempt embolization.

Pancreatic pseudocysts are single and unilocular in nearly 90% of patients [52]. In such cases, drainage procedures enable resolution of the pseudocyst. Several drainage procedures have been described including CT-guided needle aspiration, CT-guided continuous catheter drainage, endoscopic drainage, and surgical drainage [35, 52–55]. Failure rates reported for CT-guided needle aspiration and CT-guided continuous catheter drainage are 54% and 16%, respectively [52]. Failure is considered if a pseudocyst cannot be completely evacuated, if recurrence cannot be managed successfully by repeat percutaneous techniques, and if a patient is eventually treated with surgery. Recurrence rates are 63% for CT-guided needle aspiration and 7% for CT-guided continuous catheter drainage [52]. While complications of CT-guided needle aspiration are minimal, 18% of patients who undergo CT-guided continuous catheter drainage develop a complication, most commonly a secondary infection of the non-infected pseudocyst [52]. Other serious complications include hemorrhage and the formation of enterocutaneous fistula. If the pancreatic duct is partially blocked or stenosed, there is a real possibility that following continuous drainage, a pancreaticocutaneous fistula will form [56]. Akshintala et al. compared 40 patients who underwent percutaneous drainage (either CT or US guided) with 41 who underwent endoscopic drainage; all had symptomatic pseudocysts [55]. Completion rates for the intended index procedures and the proportions of patients in need of a different technique because of pseudocyst persistence were similar in the two groups. Nevertheless, endoscopic drainage proved to be the preferred modality since patients who underwent this procedure needed fewer reinterventions, fewer follow-up abdominal imaging studies, and shorter length of hospital stay. Figure 15.10 depicts a patient in whom a pseudocyst

Fig. 15.10 Compound pseudocyst of the pancreas that required surgical drainage

evolved after acute pancreatitis. This was managed by repeated attempts at endoscopic gastro-cystostomy drainage but eventually because of retained pseudocyst underwent surgical drainage.

As stated in the introduction, tumors of the pancreas should be ruled out in patients who have a first attack of acute pancreatitis at age older than 45–50 years and for whom no risk factors for acute pancreatitis are found [5]. Both adenocarcinoma and neuroendocrine tumors have been reported in patients with acute pancreatitis [57–59]. Tumors are identifiable on CT done during the index hospitalization and on CT done during follow-up. Though uncommon, tumors of the pancreas should be considered as a possible cause of acute pancreatitis, especially in patients in whom other etiologies have been ruled out. Since most of these patients undergo endoscopic ultrasound as part of their evaluation, the need for mandatory follow-up CT in these patients should be further investigated.

References

1. Lowenfels AB, Maisonneuve P, Sullivan T. The changing character of acute pancreatitis: epidemiology, etiology, and prognosis. Curr Gastroenterol Rep. 2009;11(2):97–103.
2. Yadav D, Lowenfels AB. Trends in epidemiology of the first attack of acute pancreatitis: a systematic review. Pancreas. 2006;33(4):323–30.
3. O'Farrell A, Allwright S, Toomey D, Bedford D, Conlon K. Hospital admission for acute pancreatitis in Irish population, 1997–2004: could the increase be due to an increase in alcohol-related pancreatitis? J Public Health (Oxf). 2007;29(4):398–404.
4. Lankisch PG, Apte M, Banks PA. Acute Pancreatitis. Lancet. 2015;386(9988):85–96.
5. Bank S, Indaram A. Causes of acute and recurrent pancreatitis. Gastroenterol Clin N Am. 1999;28(3):571–89.
6. Shyu J, Sainani NI, Sahni VA, Chick JF, Chauhan NR, Conwell DL, Clancy TE, Banks PA, Silverman SG. Necrotizing pancreatitis: diagnosis, imaging and intervention. Radiographics. 2014;34:1218–39.
7. Banks PA, Bollen TL, Dervenis C, Gooszen HG, Johnson CD, Sarr MG, Tsiotos GG, Vege SS. Acute pancreatitis classification working group. Gut. 2013;62(1):102–11.
8. Working Group IAP/APA Acute Panreatitis Guidelines. IAP/APA evidence-based guidelines for the management of acute pancreatitis. Pancreatology. 2013;13:e1–15.
9. Xu XD, Wang ZY, Zhang LY, Ni R, Wei FX, Han W, Zhang HH, Zhang YW, Wei ZG, Guo XH, Guo LQ, Ma JZ, Zhang YC. Acute pancreatitis classifications: basis and key goals. Medicine (Baltimore). 2015;94(48):e2182.

10. Isenmann R, Buchler M, Uhl W, Malfertheiner P, Martini M, Beger HG. Pancreatic necrosis: an early finding in severe acute pancreatitis. Pancreas. 1993;8(3):358–61.
11. Sakorafas GH, Tsiotos CG, Sarr MG. Extrapancreatic necrotizing pancreatitis with viable pancreas: a previously under-appreciated entity. J Am Coll Surg. 1999;188(6):643–8.
12. The Italian Association for the Study of the Pancreas. Consensus guidelines on severe acute pancreatitis. Dig Liver Dis. 2015;47:532–43.
13. Balthazar EJ, Robinson DL, Megibow AJ, Ranson JHC. Acute pancreatitis: value of CT in establishing prognosis. Radiology. 1990;174(2):331–6.
14. BU W, Bakker OJ, Papachristou GI, Besselink MC, Repas K, van Santvoort HC, Muddan V, Singh VK, Whitcomb DC, Gooszen HG, Banks PA. Blood urea nitrogen in the early assessment of acute pancreatitis. Arch Intern Med. 2011;17(7):669–76.
15. Islah MA, Jiffre D. A rare case of incarcerated bochdalek diaphragmatic hernia in a pregnant lady. Med J Malaysia. 2010;65(1):75–6.
16. Mitura K, Romanczuk M. Ruptured ectopic pregnancy mimicking acute pancreatitis. Ginekol Pol. 2009;80(5):383–5.
17. Nitsche R, Folsch UR, Ludtke R, Hilgers RA, Creutzfeldt W. Urgent ERCP in all cases of acute biliary pancreatitis? A prospective randomized multicenter study. Eur J Med Res. 1995;1(3):127–31.
18. Nesvaderani M, Eslick GD, Faraj S, Vagg D, Cox MR. Study of the early management of acute pancreatitis. Anz J Surg. 2015. doi: 10.111/ans.13330. [Epub ahead of print].
19. Ranson JH, Rifkind KM, Roses DF, Fink SD, Eng K, Spencer FC. Prognostic signs and the role of operative management in acute pancreatitis. Surg Gynecol Obstet. 1974;139(1):69–81.
20. Gross V, Leser H, Heinisch A, Scholmerich J. Inflammatory mediators and cytokines—new aspects of the pathophysiology and assessment of severity of acute pancreatitis? Hepato-Gastroenterology. 1993;40(6):522–30.
21. Yeung YP, Lam B, Yip A. APACHE system is better than Ranson system in the prediction of severity of acute pancreatitis. Hepatobiliary Pancreat Dis Int. 2006;5(2):294–9.
22. Bu W, Johannes RS, Sun X, Tabak Y, Conwell DL, Banks PA. The early prediction of mortality in acute pancreatitis: a large population-based study. Gut. 2008;57(12):1698–703.
23. Balthazar EJ, Freeny PC, Vansonnenberg E. Imaging and intervention in acute pancreatitis. Radiology. 1994;193(2):297–306.
24. Mortele KJ, Wiesner W, Intriere L, Shankar S, Zhou KH, Kalantari BN, Perez A, van Sonnenberg E, Ross PR, Banks PA, Silverman SG. A modified CT severity index for evaluating acute pancreatitis: improved correlation with patient outcome. Am J Roentgenol. 2004;183(5):1261–5.
25. Singh VK, BU W, Bollen TL, Repas K, Maurer R, Mortele KJ, Banks PA. Early systemic inflammatory response syndrome is associated with severe acute pancreatitis. Clin Gastroenterol Hepatol. 2009;7(11):1247–51.
26. Mofidi R, Duff MD, Wigmore SJ, Madhavan KK, Garden OJ, Parks RW. Association between early systemic inflammatory response, severity of multiorgan dysfunction and death in acute pancreatitis. Br J Surg. 2006;93(6):738–44.
27. Foitzik T, Bassi DG, Fernandez-del Castillo C, Warshaw AL, Rattner DW. Arch Surg. 1994;129(1):706–11.
28. Foitzik T, Bassi DG, Schmidt J, Lewandrowski KB, Fernandez-del Castillo C, Rattner DW, Warshaw AL. Intravenous contrast medium accentuates the severity of acute necrotizing pancreatitis in the rat. Gastroenterology. 1994;106(1):207–14.
29. McMenamin DA, Gates LK Jr. A retrospective analysis of the effect of contrast-enhanced CT on the outcome of acute pancreatitis. Am J Gastroenterol. 1996;91(7):1384–7.
30. Sharma V, Rana SS, Sharma SK, Gupta R, Bhasin DK. Clinical outcomes and prognostic significance of early vs. late computed tomography in acute pancreatitis. Gastroenterol Rep (Oxf). 2015;3(2):144–7.
31. Uhl W, Roggo A, Kirschstein T, Anghelacopoulos SE, Gloor B, Muller CA, Malfertheiner P, Buchler MW. Influence of contrast-enhanced computed tomography on course and outcome in patients with acute pancreatitis. Pancreas. 2002;24(2):191–7.

32. Akinosoglou K, Gogos C. Immune-modulating therapy in acute pancreatitis: fact of fiction. Wold J Gastroenterol. 2014;20(41):15200–15.
33. Bradley EL III. A clinically based classification system for acute pancreatitis. Summary of the international symposium on acute pancreatitis, Atlanta, GA, September 11 through 13, 1992. Arch Surg. 1993;128(5):586–90.
34. Bollen TL, van Santvoort HC, Besselink MG, van Es WH, Gooszen HG, van Leeuwen MS. Update on acute pancreatitis: ultrasound, computed tomography, and magnetic resonance imaging features. Semin Ultrasound CT MR. 2007;35(2):107–13.
35. Tyberg A, Karia K, Gabr M, Desai A, Doshi R, Gaidhane M, Sharaiha RZ, Kahleh M. Management of pancreatic fluid collections: a comprehensive review of the literature. World J Gastroenterol. 2016;22(7):2256–70.
36. Sarathi Patra P, Das K, Bhattacharyya A, Ras S, Hembram J, Sanyal S, Dhali GK. Natural resolution or intervention for fluid collections in acute severe pancreatitis. Br J Surg. 2014;101(13):1721–8.
37. Turkvatan A, Erden A, Turkoglu MA, Secil M, Yuce G. Imaging of acute pancreatitis and its complications. Part 2: complications of acute pancreatitis. Diagn Intev Imaging. 2015;96(2):161–9.
38. Mann DV, Hershman MJ, Hittinger R, Glazer G. Multicentre audit of death from acute pancreatitis. Br J Surg. 1994;81(6):890–3.
39. Lumsden A, Bradley EL III. Secondary pancreatic infections. Surg Gynecol Obstet. 1990;170(5):459–67.
40. Schmid SW, Uhl W, Freiss H, Malfertheiner P, Buchler MW. The role of infection in acute pancreatitis. Gut. 1999;45(2):311–6.
41. Baron TH, Morgan ED. Acute necrotizing pancreatitis. N Engl J Med. 1999;340(18):1412–7.
42. Dellinger EP, Tellado JM, Soto NE, Ashley SW, Barie PS, Dugernier T, Imrie CW, Johnson CD, Knaebel HP, Laterre PF, Maravi-Poma E, Kissler JJ, Sanchez-Garcia M, Utzolino S. Early antibiotic treatment for severe acute necrotizing pancreatitis: a randomized, double-blind, placebo controlled study. Ann Surg. 2007;245(5):674–83.
43. Forsmark CE, Toskes PP. Acute pancreatitis: medical management. Crit Care Clin. 1995;11(2):295–309.
44. Gerzof SG, Banks PA, Robbins AH, Johnson WC, Spechler SJ, Wetzner SM, Snider JM, Langevin RE, Jay ME. Early diagnosis of pancreatic infection by computed tomography-guided aspiration. Gastroenterology. 1987;93(6):1315–20.
45. Barie PS. A critical review of antibiotic prophylaxis in severe acute pancreatitis. Am J Surg. 1996;172(Suppl 6A):38S–43S.
46. Rau B, Pralle U, Uhl W, Schoenberg MH, Beger HG. Management of sterile necrosis in instances of severe acute pancreatitis. J Am Coll Surg. 1995;181(4):279–88.
47. Bradley EL III. Operative vs. non-operative management in sterile necrotizing pancreatitis. HPB Surg. 1997;10(3):188–91.
48. Warshaw AL. To debride on not to debride—that is the question. Ann Surg. 2000;232(5):627–9.
49. Van Santvoort HC, Besslink MG, Bakker OJ, Hofker HS, Boermeester MA, Dejong CH, van Goor H, Schapherder AF, van Eijck CH, Bollen T, van Ramshorst B, Nieuwenhijs VB, Timmer R, Lameris JS, Kruyt PM, Manusama ER, van der Harst E, van der Schllng GP, Karsten T, Hesselink EJ, van Laarhoven CJ, Rosman C, Bosscha K, de Wit RJ, Houdijk AP, van Leeuwen MS, Buskens E, Gooszen HG. Dutch pancreatitis study group. A step-up approach or open necrosectomy for necrotizing pancreatitis. N Engl J Med. 2010;362(16):1491–502.
50. Loveday BP, Petrov MS, Connor S, Rossaak JI, Mittal A, Phillips AR, Winsdor JA. A comprehensive classification of invasive procedures for treating the local complications of acute pancreatitis based on visualization, route and purpose. Pancreatology. 2011;11(4):406–13.
51. Gardner TB, Coelho-Prabhu N, Gordon SR, Gelrud A, Maple JT, Papchristou GI, Freeman ML, Topazian MD, Attam R, Mackenzie TA, Baron TH. Direct endoscopic necrosectomy for the treatment of walled-off pancreatic necrosis: results from a multicenter U.S. series. Gastrointest Endosc. 2011;73(4):718–26.

52. Gumaste VV, Pitchumoni CS. Pancreatic pseudocyst. Gastroenterologist. 1996;4(1):33–43.
53. Heider R, Meyer AA, Galanko JA, Behrns KE. Percutaneous drainage of pancreatic pseudocysts is associated with higher failure rate than surgical treatment in unselected patients. Ann Surg. 1999;229(6):781–9.
54. Lawson JM, Baillie J. Endoscopic therapy for pancreatic pseudocysts. Gastrointest Endosc Clin N Am. 1995;5(1):181–93.
55. Akshintala VS, Saxena P, Zaheer A, Rana U, Hutfless SM, Lennon AM, Canto MI, Kalloo AN, Khashab MA, Singh VK. A comparative evaluation of outcomes of endoscopic versus percutaneous drainage for symptomatic pancreatic pseudocysts. Gastrointest Endosc. 2014;79(6):921–8.
56. van Baal MC, van Santvoort HC, Bollen TL, Bakker OJ, Besselink MG, Gooszen HG. Systematic review of percutaneous catheter drainage as primary treatment of necrotizing pancreatitis. Br J Surg. 2011;98(1):18–27.
57. Tejedor Bravo M, Justo LM, Lasala JP, Moreira Vicente VF, Ruiz AC, Scapa Mde L. Acute pancreatitis secondary to neuroendocrine pancreatic tumors: report of 3 cases and literature review. Pancreas. 2012;41(3):485–9.
58. Kimura Y, Kikuyama M, Kodama Y. Acute pancreatitis as a possible indicator of pancreatic cancer: the importance of mass detection. Intern Med. 2015;54(17):2109–14.
59. Cho JH, Choi JS, Hwang ET, Park JY, Jeon TJ, Kim HM, Cho JH. Usefulness of scheduled follow-up CT in discharged patients with acute pancreatitis. Pancreatology. 2015;15(6):642–6.

AAA and Visceral Aneurysms

16

Jaap Ottevanger, Stephen Merrilees, and Ian Civil

16.1 Introduction

An aneurysm is a section of artery which is dilated in comparison to its original vessel diameter. By definition this is generally accepted as dilatation by at least one and a half times the normal vessel diameter. Therefore aneurysms are defined by the artery affected rather than by absolute diameters. Aneurysms can be classified as either true or false. True aneurysms are those which are bound by all three layers of the artery (intima, media, and adventitia), whereas false aneurysms, also known as pseudoaneurysms, are bound only by adventitia. As an aneurysm enlarges, the risk of rupture increases, but for any given size, pseudoaneurysms have a relatively higher rupture risk when compared to true aneurysms of the same size.

Aneurysms occur in multiple locations in the abdomen including aorta, iliac, and visceral arteries; however, the infrarenal aorta is the most common location.

16.2 Abdominal Aortic Aneurysm

The abdominal aorta is the most common site of aneurysm development, and approximately 90% of aortic aneurysms are found below the renal arteries. The normal infrarenal aorta measures around 2 cm in diameter [1]. Therefore aneurysmal dilatation of the infrarenal aorta (AAA) is generally accepted once the maximum aortic diameter reaches 3 cm. Fusiform aneurysms are far more common (around 80%) than saccular aneurysms and develop in the setting of atherosclerosis.

J. Ottevanger
Interventional Radiology Fellow, Auckland City Hospital, Auckland, New Zealand

S. Merrilees
Interventional Radiologist, Auckland City Hospital, Auckland, New Zealand

I. Civil (✉)
Professor of Surgery, Vascular Surgeon, Auckland City Hospital, Auckland, New Zealand
e-mail: icivil@xtra.co.nz

F. Catena et al. (eds.), *CT Scan in Abdominal Emergency Surgery*, Hot Topics in Acute Care Surgery and Trauma, https://doi.org/10.1007/978-3-319-48347-4_16

They are therefore associated with the usual risk factors of smoking, male sex, increasing age, hypertension, and hypercholesterolemia all of which have been shown to be associated with an increased risk of developing an AAA [2, 3]. A positive family history also increases the risk of developing AAA in first-degree relatives. Saccular aneurysms are more likely to have an infectious or inflammatory cause but may develop in the setting of a penetrating ulcer.

16.2.1 AAA Rupture

We know from Laplace's law that wall tension is directly proportional to radius. Therefore, the risk of rupture of an AAA obviously increases with increasing aortic diameter. The generally accepted threshold to treat an AAA (endovascular or open surgery) is set at 5.5 cm [4]. This diameter is set from observational data relating to rupture risk at various aortic diameters. A report by the Joint Council of the American Association of Vascular Surgery and Society for Vascular Surgery reported the following yearly rupture rates for AAA [5].

AAA diameter (cm)	Rupture risk (%/year)
<4	0
4–5	0.5–5
5–6	3–15
6–7	10–20
7–8	20–40
>8	30–50

There is however substantial variation in reported rupture risk of untreated AAAs, with newer data suggesting much lower rates of rupture. A recent study reports a yearly incidence of rupture in patients with an AAA of <7 cm as <5%, with significantly increased rates for AAAs ≥7 cm at >35% [6].

As we know a positive family history for AAA increases the risk in other first-degree relatives, but it may also increase the rupture risk [7]. Serial preoperative screening in patients with a known AAA is needed to assess growth rate and plan appropriate treatment once the 5.5 cm threshold is achieved.

The larger an aneurysm, the faster the rate of growth (also explained by Laplace's law). An AAA of less than 4.0 cm will on average expand by only 1–4 mm each year, whereas an AAA measuring 4.0–6.0 cm will show an average annual expansion of 4–6 mm each year. Therefore larger aneurysms require more frequent screening. If an AAA demonstrates an expansion rate above these levels, then early treatment (before the 5.5 cm threshold) may be warranted [8].

A ruptured abdominal aortic aneurysm is one of the most lethal surgical emergencies with an overall mortality rate of up to 90% [9–11]. Thirty-day mortality rates for patients with a ruptured AAA who have undergone operative repair are between 40 and 50% [12, 13]. Introduction of endovascular repair for RAAA has shown to lower 30-day mortality rates [14]. Classic symptoms accompanying a ruptured AAA are abdominal and/or back pain, hypotension, and a palpable, pulsatile abdominal mass. However, only 50% of patients will present with this classic triad of symptoms.

Patients presenting to the hospital with abdominal and/or back pain, with a pulsatile abdominal mass, require urgent triaging to determine if they require emergency surgery or transfer to computed tomography (CT) for assessment of the aorta to confirm AAA and plan treatment.

16.2.2 AAA Treatment

Ruptured or symptomatic aortic aneurysms are treated with either endovascular or open surgical repair. An endovascular approach, via the common femoral arteries, is at present the preferred method of treatment but can only be used if the aneurysm meets certain morphological requirements. The stent graft needs adequate sealing to successfully exclude the aneurysm. These sealing zones are located at the infrarenal neck of the aneurysm and common iliac arteries. The majority of stent grafts used for AAA repair require an infrarenal neck diameter of ≤32 mm, a proximal neck length of ≥10 mm, and a proximal angulation between aorta and aneurysm of no more than 60°. The use of stent grafts outside of their instructions for the use

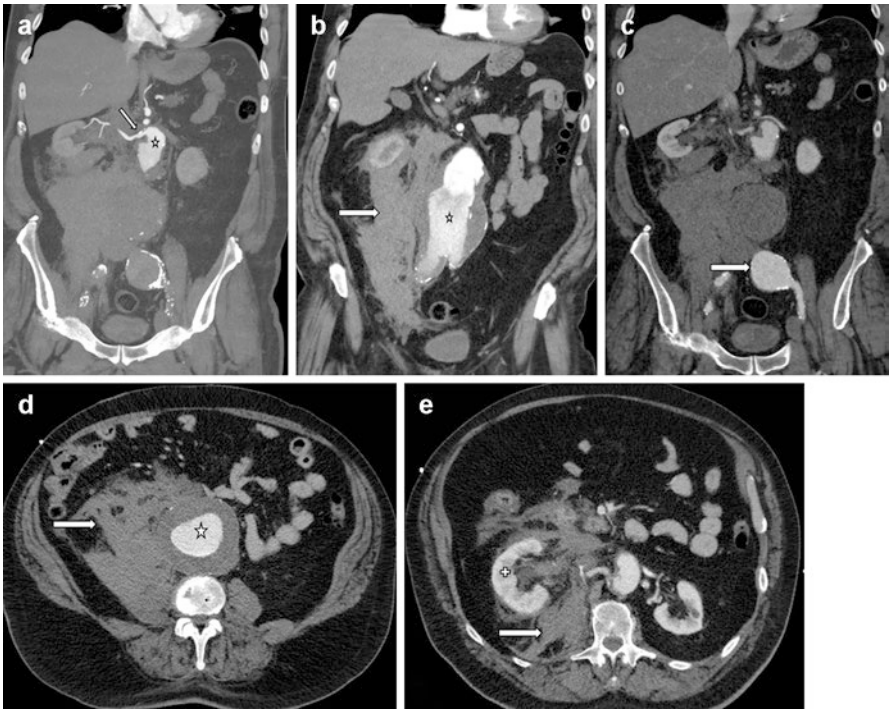

Fig. 16.1 Arterial phase coronal (**a**, **b**, and **c**) images of a ruptured aortic aneurysm. Image a depicts the aneurysmal dilatation of the aorta (*arrow*) starting directly below the right renal artery (*star*). Image (**b**, **d**, and **e**): Retroperitoneal hematoma (*arrow*) associated with the RAAA (*star*), with anterior displacement of the right kidney (*plus*). Image (**c**): The patient was also noted to have a left common iliac artery aneurysm (*arrow*), measuring 4–5 cm in diameter. The patient was successfully treated operatively, during which the left common iliac artery aneurysm was also surgically repaired

Fig. 16.2 Reformatted arterial phase coronal CT showing an aortic aneurysm with suitable morphology for endovascular repair: There is a long narrow proximal infrarenal neck, and the common iliac arteries are not dilated

increases the risk of complications. Patients who do not fit criteria for endovascular treatment will need to be treated surgically. Figure 16.1 demonstrates a patient with an RAAA unsuitable for endovascular repair as the dilatation of the aorta starts directly below the right renal artery. Figure 16.2 depicts an aortic aneurysm which is suitable for endovascular repair. An unstable patient with an RAAA may however benefit from urgent operative repair, as this procedure can be performed more quickly by experienced surgeons.

Successful surgical repair is facilitated by early recognition of the diagnosis, minimal fluid resuscitation, and rapid transfer to the operating room. The availability of an experienced team both in the operating room and in the ICU also increases the chances of a successful outcome. Simple clamp and suture techniques, designed to minimize operating times, are preferred, and non-ruptured components of aneurysm disease (such as iliac artery aneurysms) can be left for later endovascular treatment.

16.2.3 CT Imaging Technique in Acute Aortic Disease

Modern CT scanners, above 64 slice, are quick and readily available and produce images with high spatial and contrast resolution and rapid image availably for prompt interpretation. It is therefore the first-choice imaging modality used in identifying and assessing any stable patient suspected of having a RAAA or impending rupture of an aortic aneurysm. The CT scan gives an overview of the anatomy of the aorta and side branches in multiplanar views (axial, sagittal, and coronal) and the location of rupture/impending rupture and if positive allows planning for an acute endovascular repair if appropriate. In many cases it will also provide the reason for the patient's symptoms when these are not related to the aorta.

Using contrast with higher concentration of iodine (≥350 mg iodine / mL) has shown to produce better arterial enhancement of abdominal aorta branches; however, 300 mg iodine/mL is also acceptable [15]. Generally, between 80 and 140 mL of

contrast will be administered at an infusion rate of at least 4–5 mL/s. Differences in body size and cardiac output may require adjusting the protocol to suit each patient. Usually, contrast administration is followed by a 30 mL saline flush for better visualization of the arteries. Bolus triggering with a region of interest (ROI) placed in the descending thoracic aorta will generally be set at 100–150 Hounsfield units (HU) but will vary depending on the type of scanner. Oral contrast is not needed in cases of suspected acute aortic disease and can in fact detract from image quality in this setting.

In patients suspected of having acute aortic pathology, an unenhanced CT of the abdomen and pelvis should be performed first. This may, in addition to the arterial phase, help in diagnosing an intramural hematoma and will, in most cases, display sequelae of an RAAA (retroperitoneal hemorrhage, Fig. 16.1). The unenhanced CT can demonstrate anatomic features of the aorta which may allow for exclusion of an endovascular option or suggest possible inclusion in this treatment pathway. In cases in which an AAA can be excluded, the precontrast scan may also demonstrate an alternative diagnosis.

In the setting of an unstable patient with a ruptured AAA, in which use of an endovascular option can be ruled out on the unenhanced CT, no subsequent contrast-enhanced imaging will be needed. This saves precious time to commence operative repair and avoids unnecessary use of potentially harmful intravascular contrast.

The unenhanced phase is followed by an arterial phase, obtained around 35–40 s after contrast injection or 15–20 s after bolus tracking, which will in most cases demonstrate adequate enhancement of the aorta and side branches. A portal-venous phase is then often performed at around 75–80 s postinjection or 40–60 s post bolus tracking. Large, ruptured aneurysms may not show contrast extravasation (hemorrhage) on an early arterial phase. In these cases, and nearly all cases of RAAA, a late arterial and/or portal venous phase will demonstrate the hemorrhage.

There are a range of CT findings that point to either aortic rupture or impending rupture. If any of these are present, as discussed below, urgent treatment is required whether it be surgical or endovascular. If there are no CT features present, but the patient has a tender AAA, the patient should generally be treated as semi-acute on the next available elective list.

16.2.4 CT Signs in Aortic Rupture

The CT signs of frank rupture relate to changes resulting from loss of wall integrity and passage of blood into the surrounding soft tissues.

16.2.4.1 Retroperitoneal Hematoma

The aorta, along with other organs, is located in the retroperitoneal space. Abdominal aortic ruptures most often involve the posterolateral wall, and subsequently hemorrhage into the retroperitoneal space is very common. Retroperitoneal hematoma (Fig. 16.1) is the most frequently seen sign in RAAA and is essentially an extension of periaortic hematoma, the two differing only in volume and extent of hematoma [16]. Subsequently those patients with retroperitoneal hematoma tend to demonstrate more signs of hemodynamic instability.

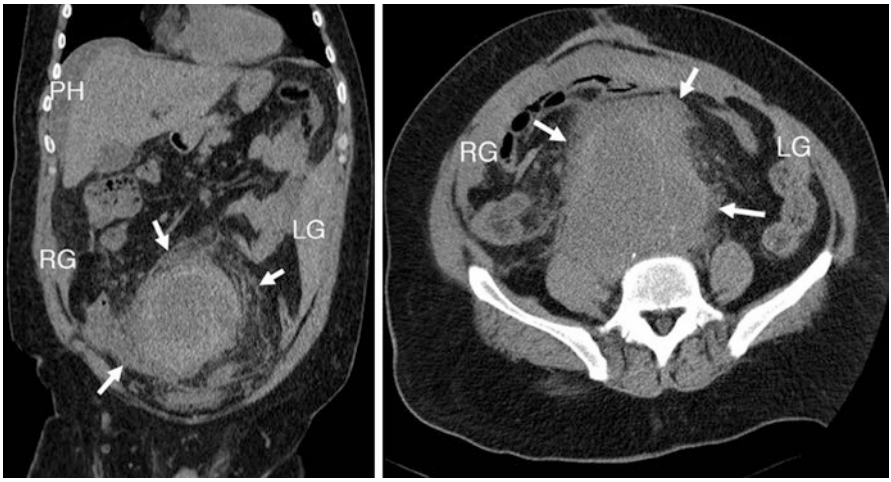

Fig. 16.3 Coronal and axial CT images depicting a ruptured abdominal aortic aneurysm (*arrows*). Blood is seen extending into the right and left paracolic gutters (RG, LG) and along the perihepatic space (PH) demonstrating intraperitoneal and retroperitoneal hemorrhage

16.2.4.2 Intraperitoneal Hematoma

Intraperitoneal hematoma (Fig. 16.3), mostly in anterior or anterolateral wall ruptures, is less common but does occur [17]. These patients often do not reach hospital, and if they do are generally very unstable due to the large potential space of the peritoneal cavity. They are often too unstable to allow for CT examination and diagnosis and proceed directly to the operating room based on clinical suspicion of the diagnosis.

16.2.4.3 Extravasation of IV Contrast

This is the most specific CT finding in aortic rupture, and when seen aortic rupture is unquestionably present. On CT, extravasation of contrast is shown as intraluminal contrast extending past the boundaries of the aortic wall into the periaortic areas of hemorrhage (Fig. 16.4). As stated above, sometimes this may only be seen on the delayed venous phases if the loss of integrity is small.

16.2.5 CT Signs Impending Aortic Rupture

In some cases patients present before frank rupture has occurred. These patients are generally more stable and most often proceed to CT where they may show one of the following signs.

16.2.5.1 Periaortic Stranding

Periaortic stranding (Fig. 16.5) refers to an area of edema or hematoma immediately adjacent to the aorta and is frequently seen in impending aortic aneurysm rupture. Periaortic hematoma is associated with a high risk of frank rupture [18].

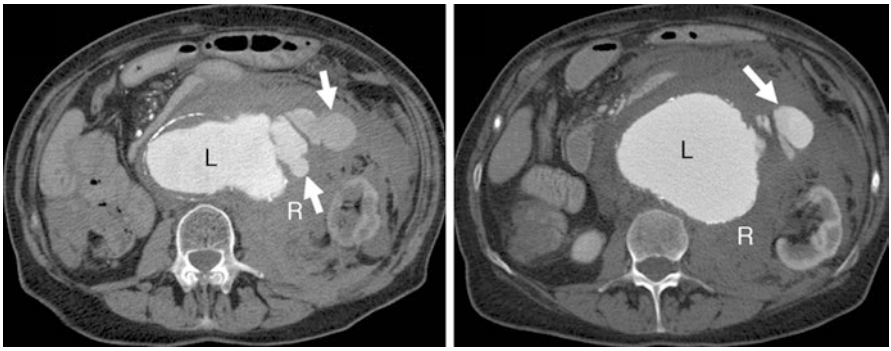

Fig. 16.4 Arterial phase axial CT images demonstrating active contrast extravasation (*arrows*) from the aneurysm lumen (*L*) extending into the retroperitoneal space (*R*)

Fig. 16.5 Axial enhanced image of a patient with abdominal pain shows periaortic stranding (*arrows*) before any retroperitoneal hemorrhage can be seen

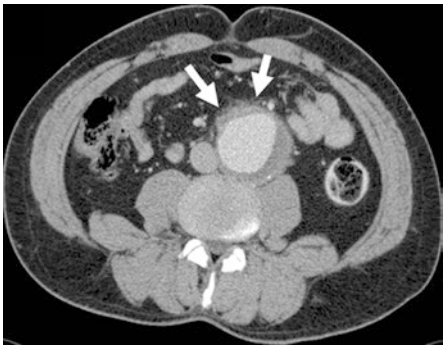

16.2.5.2 Hyperattenuating Crescent Sign

The hyperattenuating crescent sign (Fig. 16.6) is seen on an unenhanced CT as curvilinear-shaped area of high-density material representing fresh hemorrhage within mural thrombus or the aneurysm wall [19]. The infiltration of intraluminal blood into the mural thrombus or aortic wall weakens the wall of the aorta, causing instability, and represents an early sign of aortic rupture [19]. In the arterial and venous phase, contrast may be seen invaginating or fissuring mural thrombus.

16.2.5.3 Focal Discontinuity of Intimal Calcification or Focal Wall Bulge

Focal discontinuity of intimal calcification or aneurysm wall bulging (Fig. 16.7) is another sign of impending rupture and is more often seen in unstable or ruptured aneurysms [18]. This sign is often seen concomitant to the tangential calcium sign along with periaortic hematoma.

16.2.5.4 Tangential Calcium

This sign is largely comparable to focal intimal calcium discontinuity but has the additional feature of calcium pointing away from the aneurysm (Fig. 16.7). It is seen immediately adjacent to the point of focal wall integrity loss.

Fig. 16.6 Unenhanced axial CT image of a patient presenting with abdominal pain, demonstrating a crescent-shaped intramural hematoma (H). The crescent is of higher attenuation (*brighter*) than the aortic lumen (L)

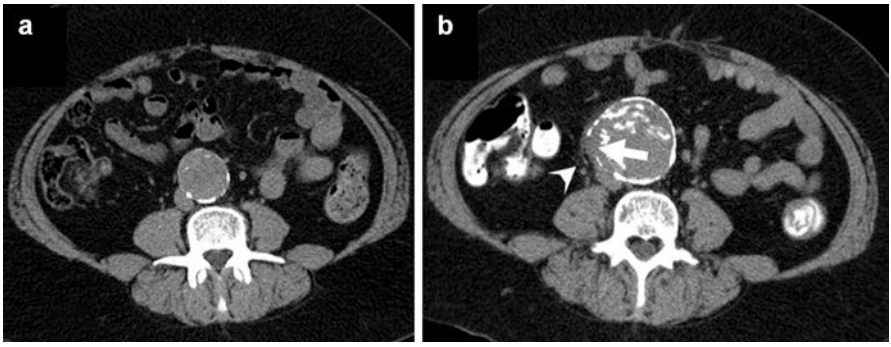

Fig. 16.7 Image (**a**): Unenhanced axial CT image showing an intact circumferential calcified wall of the aortic aneurysm in an asymptomatic patient. Image (**b**): Unenhanced axial CT image in the same patient presenting with back pain 4 years later, showing growth of the aortic aneurysm. There is a new focal gap in the calcified aneurysm wall (*arrow*) as well as periaortic infiltration near the rupture site (*arrowhead*)

16.2.5.5 Draped Aorta

Posterior bulging or outpouching of the aorta is a particular form of focal bulging. It follows the contour of the adjacent vertebral body and signals aortic wall insufficiency and contained rupture (Fig. 16.8) [20]. The normal convex shape of the aorta is thereby lost as is the normal fat plane between the aorta and vertebral body.

Comparison with previous CT images must always be done when available as significant interval changes may help in diagnosing acute aortic disease in symptomatic patients.

16.2.5.6 Thrombus Fissuration

Thrombus fissuration is seen on an enhanced CT as linear contrast (blood) infiltrations from aneurysm lumen into mural thrombus (Figs. 16.8 and 16.9). This may increase tension of the aneurysm wall and thus indicate impending rupture.

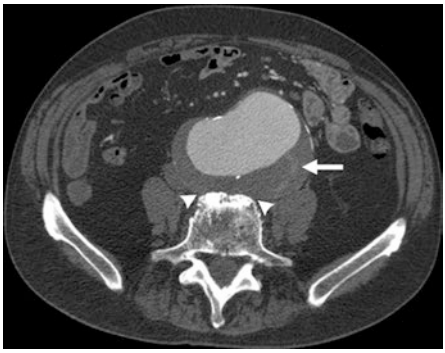

Fig. 16.8 Arterial phase CT image depicting loss of the normal convex shape of the aorta as well as loss of the normal fat plane between aneurysm and vertebral body (*arrow heads*). Thrombus fissuration is also seen (*arrow*)

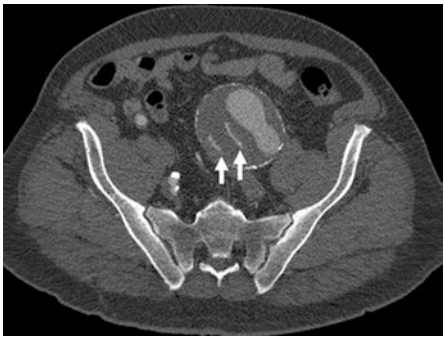

Fig. 16.9 Arterial phase CT image depicting blood dissecting into the mural thrombus from the aortic lumen (*arrows*). The patient underwent successful emergent AAA repair before complete rupture occurred

16.3 Visceral Artery Aneurysms

Aneurysms of visceral vessels are less common than the aorta, however are now more frequently detected with increased use of imaging. The incidence of visceral aneurysms has been estimated at 0.01–0.2% but is a highly significant finding due to a high mortality rate after rupture [21, 22]. As with the abdominal aorta, aneurysms can be either true or false. The underlying cause of true aneurysm formation is varied and can be congenital (e.g., Ehlers-Danlos syndrome), inflammatory (vasculitis), infectious, or atherosclerotic. Pseudoaneurysms tend to have either a traumatic or inflammatory/infectious etiology.

The general consensus is to treat asymptomatic true aneurysms that are ≥2 cm in diameter. This is in comparison to pseudoaneurysms and symptomatic true aneurysms which, regardless of size, require emergency treatment. Treatment options for visceral artery aneurysms are either open surgical repair or via an endovascular approach. Both options have the eventual goal of excluding the aneurysm from circulation and thus preventing further growth and eventual rupture. Surgical options often result in loss of the end organ or a substantial part of it. Endovascular options include the use of embolization material (e.g., Histoacryl or coils) and stent grafts with the goal of preserving the end-organ blood supply and its function.

Strict follow-up and early treatment are necessary to prevent potential life-threatening rupture.

16.3.1 CT Imaging Technique in Acute Visceral Artery Aneurysms

As previously mentioned, modern CT scanners are quick and readily available and produce images with high spatial and contrast resolution with rapid image availably for prompt interpretation which is essential in emergency settings. The CT imaging technique used is the same as for acute aortic disease.

In the paragraphs below, the most common locations of visceral artery aneurysms and pseudoaneurysms will be analyzed in order of decreasing frequency of occurrence.

16.3.2 Splenic Artery Aneurysms

With an estimated prevalence of around 0.1%, splenic artery aneurysms (SAA) are the most common abdominal visceral artery aneurysm [23]. SAA account for between 60 and 80% of all abdominal visceral artery aneurysms. Possible correlation between splenic aneurysm formation and pregnancy has been proposed, as women are affected four times as much as men, with a higher frequency seen in multiparous women [24]. This might suggest a relationship between hemodynamic and hormonal changes in pregnancy and SAA formation. Systemic hypertension, fibromuscular dysplasia, atherosclerosis, portal hypertension, and α-1 antitrypsin deficiency are other associated findings in SAA. Incidence of SAA rupture is reported to be between 3 and 10% [24]. Pseudoaneurysms, more often seen in men, are seen in trauma or infection and need urgent treatment regardless of size. A patient with a symptomatic SAA will generally present with pain in the left upper quadrant along with other signs and symptoms relating to rupture and hemoperitoneum. An example of a symptomatic splenic artery aneurysm, treated by stent-assisted coil embolization, is shown in Figs. 16.10 and 16.11.

16.3.3 Hepatic Artery Aneurysms

True hepatic artery aneurysms (HAA) are mostly located in the extrahepatic arteries and account for 12–20% of nontraumatic visceral artery aneurysms. They are predominantly seen in males [25, 26]. Hepatic artery pseudoaneurysms, traditionally seen in blunt or penetrating traumatic injury, have increased in incidence more recently, likely due to an increase in hepatic intervention due to procedures such as liver transplantation and transhepatic or laparoscopic hepatic procedures. Symptomatic patients may present with abdominal pain, hematemesis, hemobilia, or obstructive jaundice, although only a minority of patients will present with symptoms [26–28]. Again, strict follow-up is warranted as high mortality rate of 40% has been reported in ruptured HAA [26].

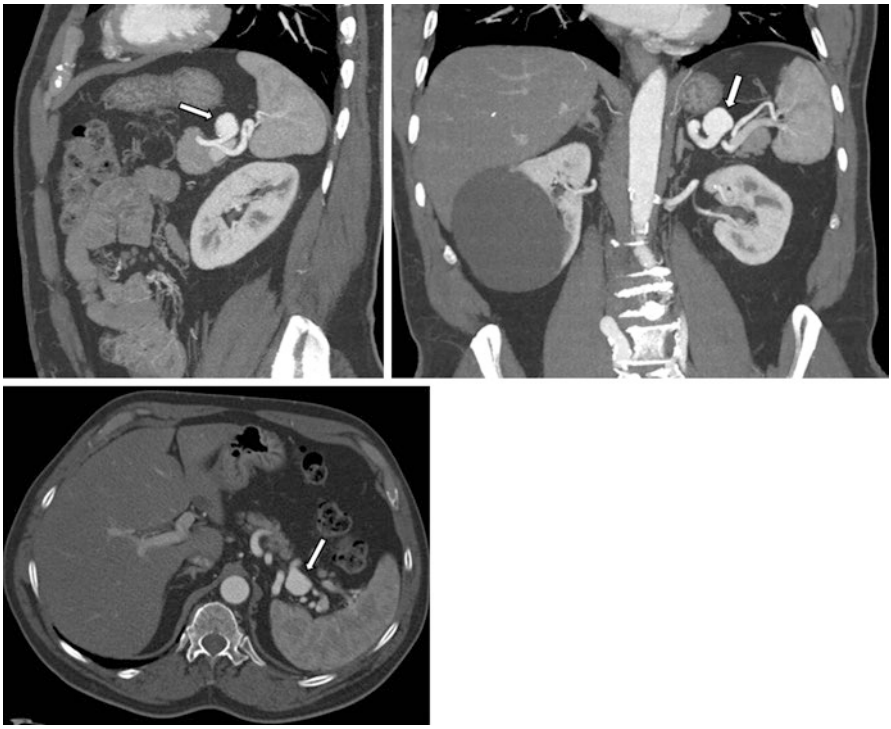

Fig. 16.10 Sagittal, coronal, and axial images of a splenic artery aneurysm (*arrows*)

16.3.4 Renal Artery Aneurysms

Renal artery aneurysms (RAA) are uncommon and found in around 0.09% of the population [29]. True renal artery aneurysms are most often saccular, right sided and asymptomatic and are therefore generally an incidental finding. They have reported associations with hypertension in 73–80%, fibromuscular dysplasia in 34%, and atherosclerosis in 25% [29, 30]. Renal artery pseudoaneurysms are most often seen in trauma or after renal intervention and as previously mentioned warrant treatment irrespective of size. Repair of a RAA has been shown to reduce hypertension and is also advised in women of childbearing age as pregnancy is thought to be associated with increased RAA rupture rate [29–31]. RAA complications include renal artery thrombosis and rupture. The true risk of rupture, which is life-threatening, is not known, but logically rupture requires acute treatment. Currently endovascular treatment is preferred, using stent grafts or embolization coils (Figs. 16.12 and 16.13).

16.3.5 Celiac Artery and Superior Mesenteric Artery Aneurysms

Celiac artery (CA) and superior mesenteric artery (SMA) aneurysms are far less common than hepatic and splenic artery aneurysms. Reported rupture mortality

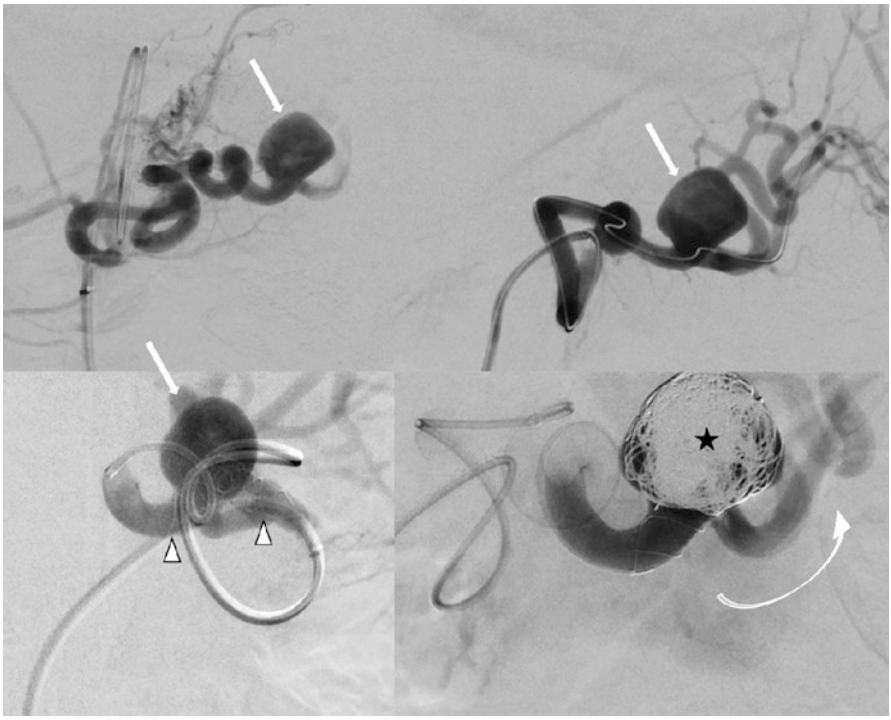

Fig. 16.11 Angiographic images showing the treatment of the splenic artery aneurysm. The symptomatic splenic artery aneurysm (*arrow*) as shown in Fig. 16.9 was treated using stent-assisted coil embolization. The stent is placed in the splenic artery, across the aneurysm (*arrow heads*), and coils (*star*) were placed into the aneurysm sac through the struts of the stent. The splenic artery remains patent after embolization (*curved arrow*)

rates vary greatly between 35 and 80% for CA aneurysms and 37.5% for SMA aneurysms [32, 33]. The majority of CA aneurysms are asymptomatic and seen in atherosclerosis. Not infrequent causes of CA aneurysms are primary celiac artery dissection, extension of an aortic dissection into the celiac artery and in median arcuate ligament compression [34, 35]. On the contrary, the majority of SMA aneurysms are symptomatic, presenting with abdominal pain. They are more often mycotic aneurysms but also seen in atherosclerosis or as a sequelae of dissection [36, 37]. SMA aneurysms are also associated with the potentially life-threatening complication of bowel ischemia due to thrombosis or thromboembolic phenomenon.

16.3.6 Pancreaticoduodenal Arcade and Gastroduodenal Artery Aneurysms

Pancreaticoduodenal arcade (PDA) and gastroduodenal artery (GDA) pseudoaneurysms are more common than true aneurysms, have a higher risk of rupture, and are often caused by inflammation associated with pancreatitis. PDA and GDA

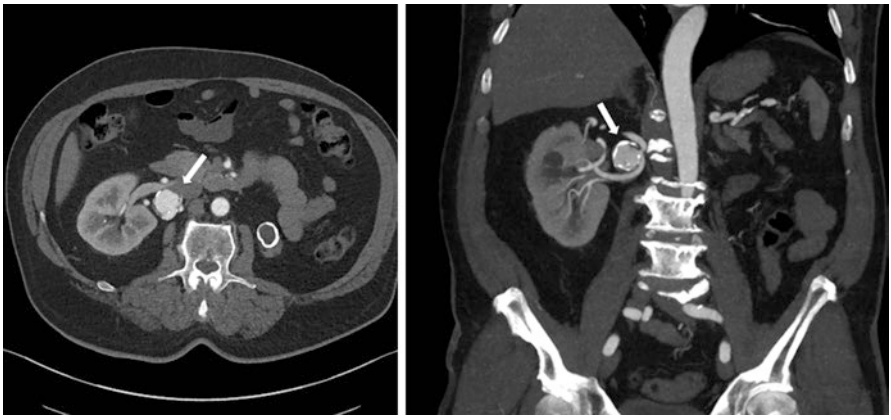

Fig. 16.12 Axial and coronal CT images of a renal artery aneurysm (*arrow*)

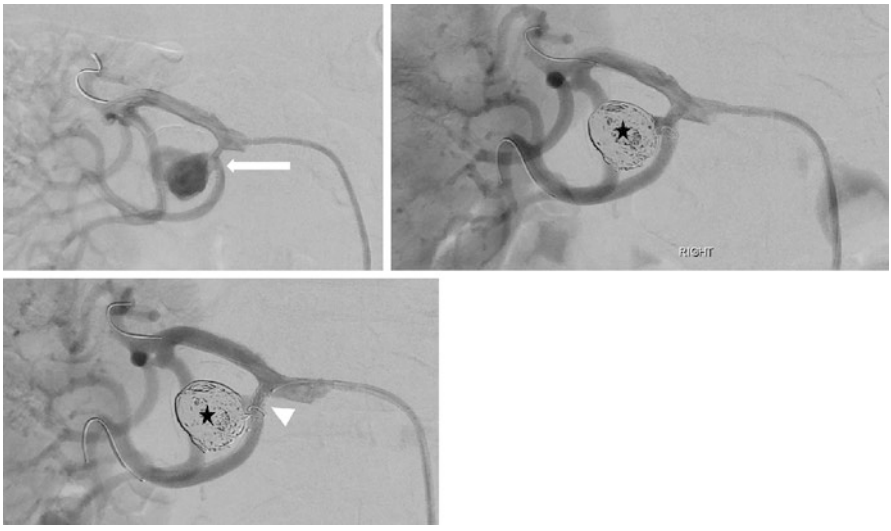

Fig. 16.13 Angiographic images showing the treatment of the renal artery aneurysm. The symptomatic patient with a renal artery aneurysm originating from the lower pole artery (*arrow*) was successfully treated by stent (*arrow head*)-assisted coil embolization (*star*)

aneurysms combined account for around 3.5% of all visceral aneurysms. A reported 35% of GDA aneurysms and 62% PDA aneurysms present with rupture, with a mortality rate of 21% [38]. Pain followed by gastrointestinal hemorrhage and hypotension is the most frequently encountered symptoms [38]. PDA aneurysms more often bleed into the retroperitoneum due to their deeper retroperitoneal location compared to GDA, making surgical repair, with possible partial pancreatic resection, challenging. PDA and GDA aneurysms are therefore preferentially treated by an endovascular approach [38]. Possible correlation with a celiac artery stenosis or occlusion has been reported and is an important finding as this may impede

endovascular treatment of the aneurysm or determine adjunctive treatment such that end-organ perfusion to the liver, spleen, and pancreas is not compromised.

16.4 Summary

Aortic and visceral artery aneurysms are an infrequent but potentially lethal cause of acute abdominal pain. Early recognition with a combination of clinical examination and radiological investigation allows the best treatment options to be chosen and employed in a timely manner. Hemostatic, limited volume fluid resuscitation and effective post intervention care play a large role in producing a successful outcome, but selection of an appropriate intervention for the underlying pathology is the key factor.

Acknowledgements *A special thanks to associate professor An Tang (University of Montreal) for allowing us to use his previously published illustrative images* (Figs. 16.3, 16.4, 16.5, 16.6, 16.7, and 16.8) [39].

References

1. Ouriel K, Green RM, Donayre C, et al. An evaluation of new methods of expressing aortic aneurysm size: relationship to rupture. J Vasc Surg. 1992;15:12–8.
2. Forsdahl SH, Singh K, Solberg S, Jacobsen BK. Risk factors for abdominal aortic aneurysms: a 7-year prospective study: the Tromsø Study, 1994–2001. Circulation. 2009;119:2202–8.
3. Landenhed M, Engström G, Gottsäter A, et al. Risk profiles for aortic dissection and ruptured or surgically treated aneurysms: a prospective cohort study. J Am Heart Assoc. 2015;4:e001513. doi:10.1161/JAHA.114.001513.
4. The UK Small Aneurysm Trial Participants. Mortality results for randomized controlled trial of early elective surgery or ultrasonographic surveillance for small abdominal aortic aneurysms. Lancet. 1998;352:1649–55.
5. Brewster DC, Cronenwett JL, Hallett JW Jr, et al. Guidelines for the treatment of abdominal aortic aneurysms. Report of a subcommittee of the Joint Council of the American Association for Vascular Surgery and Society for Vascular Surgery. J Vasc Surg. 2003;37:1106–17.
6. Scott SWM, Batchelder AJ, Kirkbride D, Naylor AR, Thompson JP. Late survival in non-operated patients with infrarenal abdominal aortic aneurysm. Eur J Vasc Endovasc Surg. 2016;52(4):444–9.
7. Darling RC III, Brewster DC, Darling RC, LaMuraglia GM, Moncure AC, Cambria RP, et al. Are familial abdominal aortic aneurysms different? J Vasc Surg. 1989;10:39–43.
8. ACC/AHA. 2005 Practice Guidelines for the management of patients with peripheral arterial disease (lower extremity, renal, mesenteric, and abdominal aortic): a collaborative report from the American Association for Vascular Surgery/Society for Vascular Surgery, Society for Cardiovascular Angiography and Interventions, Society for Vascular Medicine and Biology, Society of Interventional Radiology, and the ACC/AHA Task Force on Practice Guidelines (Writing Committee to Develop Guidelines for the Management of Patients With Peripheral Arterial Disease): endorsed by the American Association of Cardiovascular and Pulmonary Rehabilitation; National Heart, Lung, and Blood Institute; Society for Vascular Nursing; TransAtlantic Inter-Society Consensus; and Vascular Disease Foundation. Hirsch AT, Haskal ZJ, Hertzer NR, Bakal CW, Creager MA, Halperin JL, Hiratzka LF, Murphy WR, Olin JW, Puschett JB, Rosenfield KA, Sacks D, Stanley JC, Taylor LM Jr, White CJ, White J, White RA, Antman EM, Smith SC Jr,

Adams CD, Anderson JL, Faxon DP, Fuster V, Gibbons RJ, Hunt SA, Jacobs AK, Nishimura R, Ornato JP, Page RL, Riegel B, American Association for Vascular Surgery, Society for Vascular Surgery, Society for Cardiovascular Angiography and Interventions, Society for Vascular Medicine and Biology, Society of Interventional Radiology, ACC/AHA Task Force on Practice Guidelines Writing Committee to Develop Guidelines for the Management of Patients With Peripheral Arterial Disease, American Association of Cardiovascular and Pulmonary Rehabilitation, National Heart, Lung, and Blood Institute, Society for Vascular Nursing, TransAtlantic Inter-Society Consensus, Vascular Disease Foundation Circulation. 2006; 113(11):e463–654.

9. Mealy K, Salman A. The true incidence of ruptured abdominal aortic aneurysms. Eur J Vasc Surg. 1988;2:405–8.
10. Johansen K, Kohler TR, Nicholls SC, et al. Ruptured abdominal aortic aneurysm: the Harborview experience. J Vasc Surg. 1991;13:240–5. discussion 245–7
11. Heikkinen M, Salenius J, Zeitlin R, et al. The fate of AAA patients referred electively to vascular surgical unit. Scand J Surg. 2002;91:345–52.
12. Dueck AD, Kucey DS, Johnston KW, Alter D, Laupacis A. Survival after ruptured abdominal aortic aneurysm: effect of patient, surgeon, and hospital factors. J Vasc Surg. 2004;39:1253–60. [PubMed]
13. Heikkinen M, Salenius JP, Auvinen O. Ruptured abdominal aortic aneurysm in a well-defined geographic area. J Vasc Surg. 2002;36:291–6.
14. Starnes BW, Quiroga E, Hutter C, Tran NT, Hatsukami T, Meissner M, et al. Management of ruptured abdominal aortic aneurysm in the endovascular era. J Vasc Surg. 2010;51:9–17. discussion: 18
15. Johnson PT, Fishman EK. IV contrast selection for MDCT:current thoughts and practice. Am J Roentgenol. 2006;186(2):406–15.
16. Siegel CL, Cohan RH, Korobkin M, Alpern MB, Courneya DL, Leder RA. Abdominal aortic aneurysm morphology: CT features in patients with ruptured and nonruptured aneurysms. Am J Roentgenol. 1994;163:1123–9.
17. Schwartz SA, Taljanovic MS, Smyth S, O'Brien MJ, Rogers LF. CT findings of rupture, impending rupture, and contained rupture of abdominal aortic aneurysms. Am J Roentgenol. 2007;188:W57–62.
18. Wadgaonkar AD, Black JH, Weihe EK, Zimmerman SL, Fishman EK, Johnson PT. Abdominal aortic aneurysms revisited: MDCT with multiplanar reconstructions for identifying indicators of instability in the pre- and postoperative patient. Radiographics. 2015;35(1):254–68. doi:10.1148/rg.351130137.
19. Mehard W, Heiken J, Sicard G. High-attenuating crescent in abdominal aortic aneurysm wall at CT: a sign of acute or impending rupture. Radiology. 1994;192(2):359–62.
20. Halliday KE, Al-Kutoubi A. Draped aorta: CT sign of contained leak of aortic aneurysms. Radiology. 1996;199:41–3.
21. Huang YK, Hsieh HC, Tsai FC, et al. Visceral artery aneurysm: risk factor analysis and therapeutic opinion. Eur J Vasc Endovasc Surg. 2007;33:293–301.
22. Carr SC, Pearce WH, Vogelzang RL, McCarthy WJ, Nemcek AA Jr, Yao JST. Current management of visceral artery aneurysms. Surgery. 1996;120(4):627–34. doi:10.1016/s0039-6060(96)80009-2.
23. Berceli SA. Hepatic and splenic artery aneurysms. Semin Vasc Surg. 2005;18(4):196–201.
24. Abbas MA, Stone WM, Fowl RJ, et al. Splenic artery aneurysms: two decades experience at Mayo clinic. Ann Vasc Surg. 2002;16:442–9.
25. O'Arend P, Douillez V. Hepatic artery aneurysm: case report. Acta Chir Belg. 2007;107(4):409–11.
26. Abbas MA, Fowl RJ, Stone WM, Panneton JM, Oldenburg WA, Bower TC, et al. Hepatic artery aneurysm: factors that predict complications. J Vasc Surg. 2003;38:41–5.
27. Nathan DP, Wang GJ, Woo EY, Fairman RM, Jackson BM. Open and endovascular repair of hepatic artery aneurysm: two case reports and review of the literature. Vascular. 2011;19:42–6.
28. Vultaggio F, Morère P-H, Constantin C, Christodoulou M, Roulin D. Gastrointestinal bleeding and obstructive jaundice: Think of hepatic artery aneurysm. World J Gastrointest Surg. 2016;8(6):467–71.

29. Henke PK, Cardneua JD, Welling TH, et al. Renal artery aneurysms: a 35-year clinical experience with 252 aneurysms in 168 patients. Ann Surg. 2001;234:454–62. discussion 462–3
30. Reiher L, Grabitz K, Sandmann W. Reconstruction for renal artery aneurysm and its effect on hypertension. Eur J Vasc Endovasc Surg. 2000;20:454–6.
31. Cohen JR, Shamash FS. Ruptured renal artery aneurysms during pregnancy. J Vasc Surg. 1986;6:51–9.
32. Connell JM. Han DC Celiac artery aneurysms: a case report and review of the literature. Am Surg. 2006;72(8):746–9.
33. Stone WM, Abbas M, Cherry KJ, et al. Superior mesenteric artery aneurysms: Is presence an indication for intervention? J Vasc Surg. 2002;36:234–7.
34. Sun J, Li DL, Wu ZH, He YY, Zhu QQ, Zhang HK. Morphologic findings and management strategy of spontaneous isolated dissection of the celiac artery. J Vasc Surg. 2016;64(2):389–94.
35. Corey MR, Ergul EA, Cambria RP, English SJ, Patel VI, Lancaster RT, Kwolek CJ, Conrad MF. The natural history of splanchnic artery aneurysms and outcomes after operative intervention. J Vasc Surg. 2016;63(4):949–57.
36. Lorelli DR, Cambria RA, Seabrook GR, Towne JB. Diagnosis and management of aneurysms involving the superior mesenteric artery and its branches: a report of four cases. Vasc Endovasc Surg. 2003;37(1):59–66.
37. Kordzadeh A, Watson J, Panayiotopolous YP. Mycotic aneurysm of the superior and inferior mesenteric artery. J Vasc Surg. 2016;63(6):1638–46.
38. Moore E, Matthews MR, Minion DJ, et al. Surgical management of peripancreatic arterial aneurysms. J Vasc Surg. 2004;40(2):247–53.
39. Vu KN, Kaitoukov Y, Morin-Roy F, Kauffmann C, Giroux MF, Thérasse E, Soulez G, Tang A. Rupture signs on computed tomography, treatment, and outcome of abdominal aortic aneurysms. Insights Imaging. 2014;5(3):281–93.

Pelvic Inflammatory Disease

17

Goran Augustin and Maja Prutki

17.1 General Considerations

Pelvic inflammatory disease (PID) represents a clinical continuum of an infection of upper female genital tract not associated with surgery or pregnancy. Ascending infection from the endocervix causes endometritis, salpingitis, oophoritis, pyosalpinx, tubo-ovarian abscess, and pelvic abscesses. PID is one of the most serious complications of sexually transmitted diseases most commonly caused by *Neisseria gonorrhoeae* or *Chlamydia trachomatis*, although 30–40% are polymicrobial [1].

In 2001 more than 750,000 cases of PID occurred in the United States [2]. Over the past two decades, the rates and severity of pelvic inflammatory disease have declined in North America and Western Europe [3–5].

Risk factors include young age, multiple sex partners (without using condoms), douching, the use of an intrauterine device (especially during the first month after insertion), and prior episode of PID.

The most common presenting symptom is bilateral, lower abdominal pain that may be associated with fever, vaginal discharge, uterine bleeding, dyspareunia, dysuria, adnexal or cervical tenderness, nausea, vomiting, and other vague constitutional symptoms. PID frequently causes tubal damage, scarring, and occlusion, which can result in long-term complications. Patients who have had PID have increased risk of subsequent episodes of PID, ectopic pregnancy, and infertility due to Fallopian tube occlusion [1]. It is of great importance to diagnose PID and treat it properly due to the severity of these long-term sequelae. For uncomplicated cases,

G. Augustin (✉)
Department of Surgery, University Hospital Centre Zagreb and School of Medicine, University of Zagreb, Trg maršala Tita 14, 10000 Zagreb, Croatia
e-mail: augustin.goran@gmail.com

M. Prutki
Department of Radiology, University Hospital Centre Zagreb and School of Medicine, University of Zagreb, Trg maršala Tita 14, 10000 Zagreb, Croatia

F. Catena et al. (eds.), *CT Scan in Abdominal Emergency Surgery*, Hot Topics in Acute Care Surgery and Trauma, https://doi.org/10.1007/978-3-319-48347-4_17

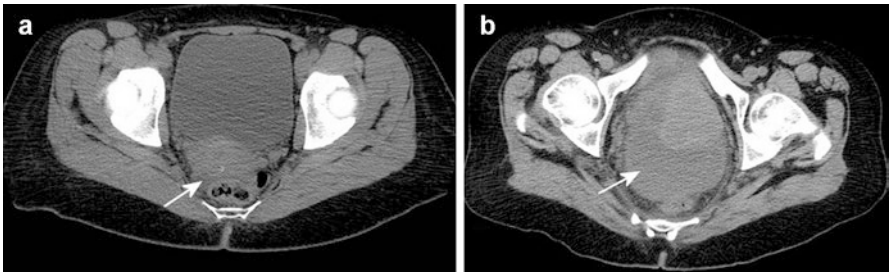

Fig. 17.1 Unenhanced CT scans showing small amounts of pelvic free fluid in cul-de-sac (*arrow*) representing normal finding (**a**) and larger amounts of pelvic free fluid (*arrow*) as an important finding of early PID in patient with right-sided acute oophoritis (**b**)

antibiotic therapy is sufficient, but in case of abscess, percutaneous or open drainage is required.

The role of imaging in PID is to estimate disease severity, to evaluate complications and help in potential treatment planning. Computed tomography (CT) is often the first imaging study because of (1) nonspecific symptoms of PID and (2) advantage over US in the detection of involvement of adjacent structures. CT allows complete visualization of the gastrointestinal and urinary tract, and it is not hampered by the presence of bowel gas [6].

In early or uncomplicated PID, CT findings may be normal. Subtle CT findings in early PID may be pelvic free fluid or mild pelvic edema. Small amounts of pelvic free fluid are a common finding throughout the menstrual cycle and are best seen in the cul-de-sac [7]. Only larger amounts of pelvic free fluid may be an important adjunct finding (Fig. 17.1) [8]. As the infection progresses, pyosalpinx develops, and in later stages, tubo-ovarian and pelvic abscess may evolve. In addition, other pelvic and abdominal structures may be involved.

17.2 CT Findings in Early PID

In early PID, the CT findings often are mild pelvic edema, mild salpingitis, mild oophoritis, and endometritis. Mild pelvic edema causes haziness of the pelvic fat, obscuration of the pelvic fascial planes, and thickening of the uterosacral ligaments. Pelvic fat haziness is identified as increased attenuation and stranding of the pelvic fat in comparison to the retroperitoneal fat (Fig. 17.2). Patients may also have a mild salpingitis with inflammatory thickening and contrast enhancement of the Fallopian tubes but without tubal dilatation (Fig. 17.3) [9]. Tubal thickening refers to a notable tubal structure with an axial diameter of more than 5 mm. Mild oophoritis is presented with enlarged (short axis diameter > 3 cm) and abnormal enhancing ovaries that may demonstrate a polycystic appearance (Fig. 17.4). Endometritis is defined as abnormal endometrial enhancement of more than the surrounding inner myometrium with fluid in cavity or free fluid in pelvis (Fig. 17.5).

Fig. 17.2 Early PID in 23-year-old girl. Contrast-enhanced CT scan demonstrates mild pelvic edema that results in haziness of the pelvic fat (*arrow*)

Fig. 17.3 Contrast-enhanced CT of 19-year-old women with early PID shows left-sided salpingitis with enhancing, thickened Fallopian tube (*arrow*) without significant dilatation of Fallopian tubes

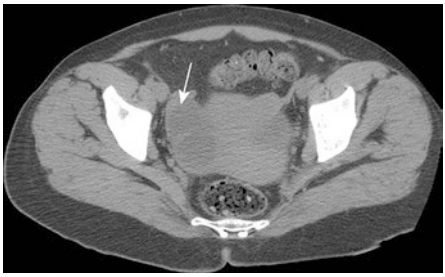

Fig. 17.4 Unenhanced CT scan of 35-year-old women with early PID demonstrates oophoritis with enlarged right ovary with a polycystic appearance (*arrow*)

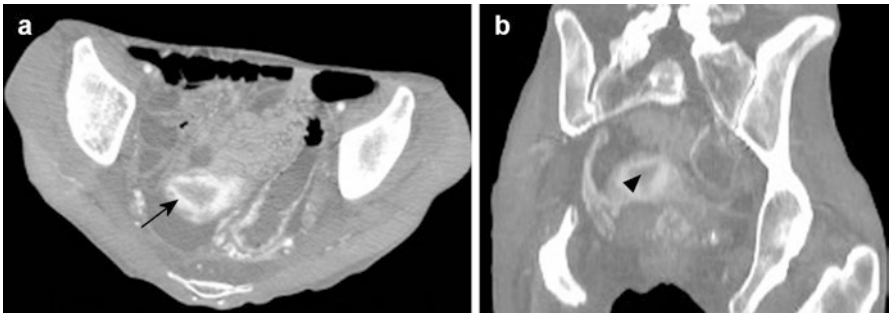

Fig. 17.5 Transverse (**a**) and sagittal reconstructed (**b**) contrast-enhanced CT scans of 34-year-old women with early PID showing abnormal endometrial enhancement (*arrow*) and simple fluid due to endometritis (*arrowhead*)

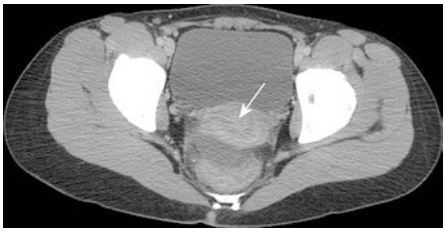

Fig. 17.6 43-year-old women with early PID. Contrast-enhanced CT shows enlarged cervix with abnormal internal enhancement findings consistent with cervicitis (*arrow*)

Similarly, cervicitis is shown as enlarged cervix with abnormally enhancing endocervical canal (Fig. 17.6) [6].

Any other gastrointestinal, genitourinary, or gynecological conditions in addition to PID could cause pelvic peritonitis and pelvic fat edema. Especially, the finding of the lowest specificity and accuracy for all of the CT findings for pelvic peritonitis was right pelvic fat stranding [10]. Periappendiceal inflammation can progress to the right pelvic fat. Therefore, it is suggested that a CT finding of mid or left pelvic fat stranding is an important finding of pelvic peritonitis from PID.

17.3 CT Findings in Advanced PID

Pyosalpinx, tubo-ovarian, and pelvic abscesses may occur throughout the progression of the infectious process. The rupture of such mass might result in severe peritonitis with potential risk for death [11]. Pyosalpinx is characteristically seen as greater degree of wall thickening and enhancement of Fallopian tubes that are filled with complex fluid (Fig. 17.7). To differentiate pyosalpinx from hydrosalpinx, intravenous contrast must be applied since in hydrosalpinx, contrast enhancement of tubal wall is absent. Tubo-ovarian and pelvic abscesses on CT examination are shown as thick-walled, complex fluid collection(s) that may contain internal septa, a fluid-debris level, or gas (Fig. 17.8) [12–14]. Although the presence of gas in PID is not frequently present, it represents a quite specific finding (Fig. 17.9) [11].

17.4 Involvement of Adjacent Structures in PID

Other pelvic and even abdominal organs may also be involved in addition to the female reproductive tract in PID, such as small (Fig. 17.10) or large bowels, ureters, and vessels. Adynamic ileus, as dilatation of pelvic small bowel loops seen on CT, is a result of adjacent inflammation. Mechanical obstruction may be caused by inflamed, enlarged, and tethered pelvic structures. In addition, megaureter and/or hydronephrosis may result from functional or mechanical obstruction. PID may also induce thrombophlebitis of pelvic vessels and may cause ovarian vein thrombosis [6]. Fitz-Hugh-Curtis syndrome is inflammation of the right upper abdominal quadrant. In this syndrome, inflammation of peritoneal surfaces and the right liver

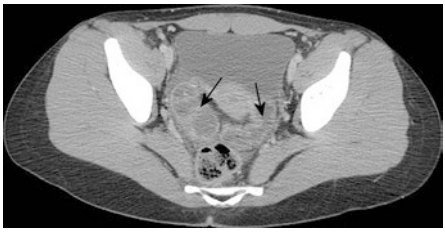

Fig. 17.7 Contrast-enhanced CT in 43-year-old women with advanced PID demonstrates pyosalpinx with dilated, thick-walled, enhancing Fallopian tubes containing fluid (*arrow*)

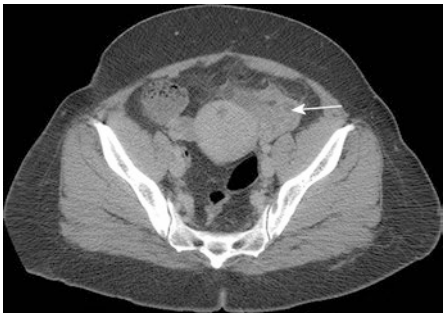

Fig. 17.8 Advanced PID in 49-year-old women with left-sided tubo-ovarian abscess. Contrast-enhanced CT scans demonstrate enlarged ovary with abnormal enhancement and periovarian pelvic edema (*arrow*)

Fig. 17.9 Advanced PID in 21-year-old women. Non-contrast CT shows tubo-ovarian abscess on the left side (*arrowhead*) and multiple areas of extraluminal air (*arrows*)

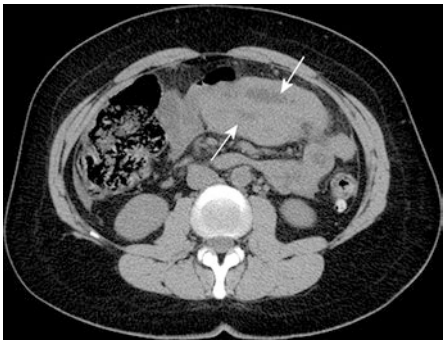

Fig. 17.10 Involvement of adjacent structures in advanced PID in the same patient as in Fig. 17.9. CT scan demonstrates small bowel wall thickening (*arrows*) due to PID in the patient with tubo-ovarian abscess

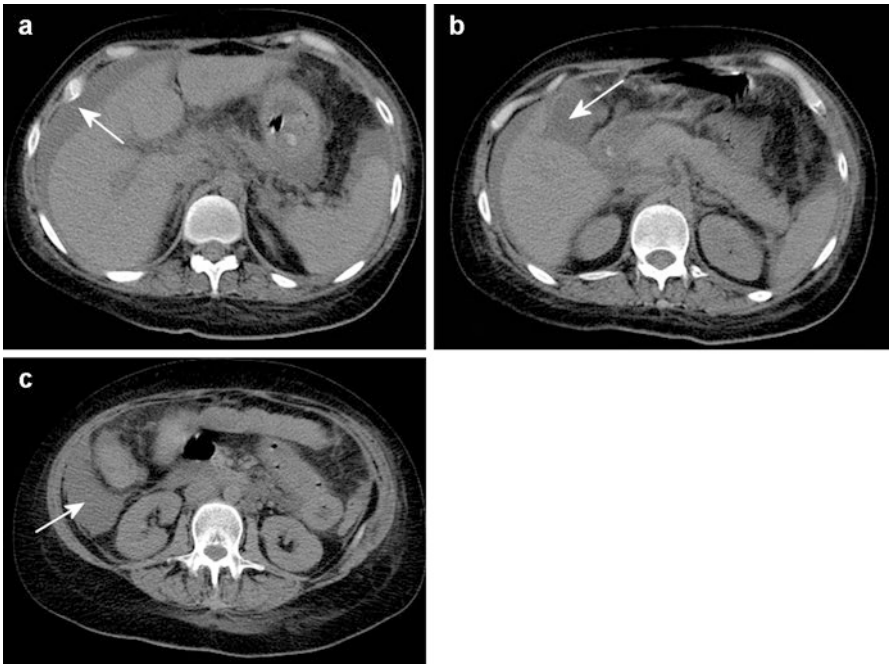

Fig. 17.11 Fitz-Hugh-Curtis syndrome in 21-year-old patient with advanced PID. (**a**) Non-contrast CT demonstrating inflammatory stranding and fluid in the perihepatic region (*arrow*); (**b**) pericholecystic inflammatory changes and gallbladder wall thickening (*arrow*); (**c**) fluid along the right paracolic gutter (*arrow*)

lobe is a consequence of direct spread of bacterial infection extending up right paracolic gutter or through the lymphatic system (Fig. 17.11). Hepatic capsular enhancement (late arterial phase) is found to be specific finding of PID. It represents perihepatitis with periportal and subcapsular perfusion abnormalities and gallbladder wall thickening [15].

17.5 Differential Diagnosis of PID

The differential diagnosis of PID includes appendicitis (Fig. 17.12), urinary tract infection, endometriosis, ovarian torsion (Fig. 17.13), Fallopian tube torsion (twisted and/or dilated with tapered ends, the so-called beak sign, and the walls of the Fallopian tube may be thickened and enhancing), interstitial cystitis, and, less commonly, adnexal tumors (Fig. 17.14).

Although free fluid in the cul-de-sac is also known as an important ancillary finding for PID, this finding was identified in 68.3% of the non-PID cases, such as acute appendicitis, ovarian cyst rupture, ileocolitis, gastroenteritis, endometriosis, ectopic pregnancy, and ovarian cyst torsion [10].

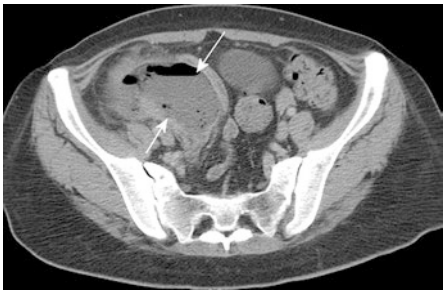

Fig. 17.12 Differential diagnosis of PID. Contrast-enhanced CT scan shows a gas-containing collection (*arrows*) on the right side consistent with large abscess due to acute appendicitis

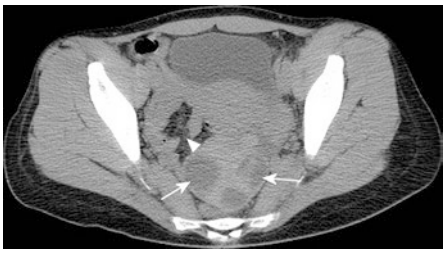

Fig. 17.13 Differential diagnosis of PID. Unenhanced CT scan in 18-year-old women demonstrates the right ovarian torsion with enlarged ovary, abnormally positioned posterior to uterus with polycystic appearance due to early oophoritis (*arrow*). Pelvic fat inflammation is also evident and obscures the normal pelvic fascial planes (*arrowhead*)

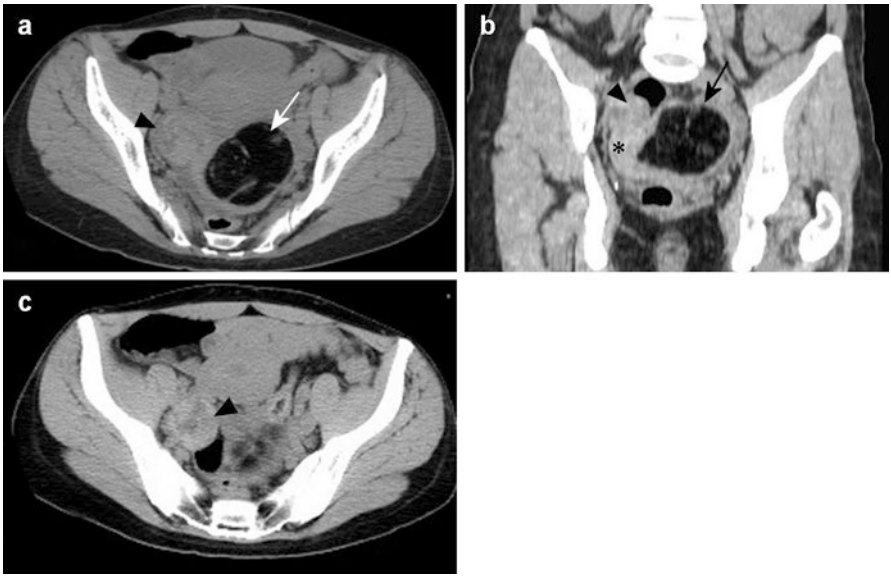

Fig. 17.14 Differential diagnosis of PID. (**a**) Unenhanced CT scan (axial), (**b**) coronal reconstruction, (**c**) axial reconstruction in 34-year-old women shows right ovary torsion (*arrowhead*), twisted pedicle (*asterix*), and dermoid cyst (*arrows*)

Conclusion

PID is a common condition among women and one of the main causes of acute abdominal pain. CT imaging spectrum in PID may vary from normal or subtle findings in early PID, and as the disease progresses, changes may progress to tubo-ovarian or pelvic abscess. CT is important imaging modality for establishment of timely diagnosis and treatment of PID [6].

References

1. Soper DE. Pelvic inflammatory disease. Infect Dis Clin N Am. 1994;8:821–40.
2. Sutton MY, Sternberg M, Zaidi A, et al. Trends in pelvic inflammatory disease hospital discharges and ambulatory visits, United States, 1985-2001. Sex Transm Dis. 2005;32:778–84.
3. Bender N, Herrmann B, Andersen B, et al. Chlamydia infection, pelvic inflammatory disease, ectopic pregnancy and infertility: cross-national study. Sex Transm Infect. 2011;87:601–8.
4. French CE, Hughes G, Nicholson A, et al. Estimation of the rate of pelvic inflammatory disease diagnoses: trends in England, 2000-2008. Sex Transm Dis. 2011;38:158–62.
5. Rekart ML, Gilbert M, Meza R, et al. Chlamydia public health programs and the epidemiology of pelvic inflammatory disease and ectopic pregnancy. J Infect Dis. 2013;207:30–8.
6. Sam JW, Jacobs JE, Birnbaum BA. Spectrum of CT findings in acute pyogenic pelvic inflammatory disease. Radiographics. 2002;22:1327–4.
7. Davis JA, Gosnik BB. Fluid in the female pelvis: cyclic patterns. J Ultrasound Med. 1986;5:75–9.
8. Stevens SK, Hricak H, Stern JL. Ovarian lesions; detection and characterization with gadolinium-enhanced MRI at 1.5 T. Radiology. 1991;181:481–8.
9. Rezvani M, Shaaban AM. Fallopian tube disease in the nonpregnant patient. Radiographics. 2011;31:527–48.
10. Jung SI, Kim YJ, Park HS, Jeon HJ, Jeong KA. Acute pelvic inflammatory disease: diagnostic performance of CT. J Obstet Gynaecol Res. 2011;37:228–35.
11. Birnbaum BA, Jeffrey RB Jr. CT and sonographic evaluation of acute right lower quadrant abdominal pain. Am J Roentgenol. 1998;170:361–71.
12. Quiroz FA. Pelvic inflammatory disease. Appl Radiol. 1999;28:30–5.
13. Ellis JH, Francis IR, Rhodes M, et al. CT findings in tuboovarian abscess. J Comput Assist Tomogr. 1991;15:589–92.
14. Wilbur AC, Aizenstein RI, Napp TE. CT findings in tuboovarian abscess. Am J Roentgenol. 1992;158:575–9.
15. Romo LV, Clarke PD. Fitz-Hugh-Curtis syndrome: pelvic inflammatory disease with an usual CT presentation. J Comput Assist Tomogr. 1992;16:832–3.